Development of Polymer Grafting Technique onto the Surface of Additively Manufactured Titanium Substrate for Improved Hip Arthroplasty Performance

A thesis submitted in fulfilment of the requirements for the degree of Doctor of Philosophy

Subir Kumar Ghosh
M. Eng. Sc. (Biomedical Engg.), University of Malaya
B. Sc. (Mechanical Engg.), Khulna University of Engineering & Technology

School of Engineering
College of Science, Engineering and Health
RMIT University
Melbourne, Australia

May 2019

ORIGINAL LITERARY WORK DECLARATION

I certify that except where due acknowledgement has been made, the work is that of the author alone; the work has not been submitted previously, in whole or in part, to qualify for any other academic award; the content of the thesis is the result of work which has been carried out since the official commencement date of the approved research program; any editorial work, paid or unpaid, carried out by a third party is acknowledged; and, ethics procedures and guidelines have been followed. I acknowledge the support I have received for my research through the provision of an Australian Government Research Training Program Scholarship.

Subir Kumar Ghosh

17th May 2019

DEDICATION

To my grandfather

who taught me honesty, compassion and how to care for people

ACKNOWLEDGEMENTS

I would like to express my heartfelt gratitude to GOD for giving me courage, strength, confidence and good health to accomplish this thesis on time.

My PhD journey was full of opportunities to learn from highly talented individuals at RMIT University. First and foremost, I would like to express my sincere gratitude to my senior supervisor, Professor Sylvester Abanteriba, for accepting me as a PhD student. His suggestions, guidance, trust, and support throughout this tenure were very encouraging. It was a great privilege to work with and be guided by him. I would also like to express my gratitude to my second supervisor, Dr Shadi Houshyar, for her valuable technical advice, support and assistance on this journey.

I am thankful to the RMIT Microscopy and Microanalysis Facility (RMMF) staff members, Dr Edwin Mayes, Dr Matthew Field and Mr Peter Rummel for providing me training and support in solving technical issues that arose in this research. My special appreciation goes to Dr Sherman Wong, for being so helpful during experiments and data analyses.

I would like to acknowledge the facilities within the Advanced Manufacturing Precinct (AMP) for the SLM fabrication process. I hereby acknowledge the chemical and chemistry lab staff members, Ms Zahra Homan, Dr Robert Brkljaca and Ms Nadia Zakhartchouk for assisting me in sample preparation and polymer characterisation experiments. I am also grateful to MicroNano Research Facility (MNRF) staff members, Dr Chenglong Xu & Dr Zeyad Nasa for their technical support. Thanks to Ms Lisa Famularo for assisting in GPC measurements at Commonwealth Scientific and Industrial Research Organisation (CSIRO), Clayton, and Mr Avik Sarker at RMIT University for assisting in cell study. I want to thank my friends, Rana Roy Chowdhury from Bangladesh and Hamza Chouirfa from France for their technical suggestions on my project.

I would like to take the opportunity to express my deepest gratitude to my parents for whom I am here today. They are my inspiration and courage to take any challenge in life. Their countless sacrifice and dedication to build up my career is undoubtedly an example to society. I also want to extend my deep and sincere gratitude to my father-in-law for motivating me during all the challenging moments during my PhD journey. I want to thank you all who directly or indirectly helped me throughout my PhD journey and RMIT University for providing me a full scholarship and financial support for this program.

Last but not least, I am indebted to my wife, Ananya Rani Kundu, who inspired me and provided constant encouragement during the entire degree program, deep thanks for her understanding and patience.

ABSTRACT

Total hip arthroplasty (THA) is one of the common surgical procedures, however, a significant number of the replacements fail permanently due to wear and lack of osseointegration of the implants. In spite of the success of medical procedure, there is not a single implant that can avoid aseptic loosening or prosthetic dislocation during its envisaged operating life. Regardless of tremendous acceptance of additively manufactured (AM) titanium alloys (Ti6Al4V) in the field of biomedical engineering, the high surface roughness due to partially-melted particles (fabricated in selective laser melting (SLM) process), limits their uses as hip implants. Therefore, this project aims to develop cartilage-mimicking poly (2-methacryloyloxyethyl phosphorylcholine) (PMPC) grafting onto the surface of additively manufactured titanium implants, to improve surface properties, wear resistance and lubricating ability of the implant.

Three different grafting techniques; ultraviolet (UV) irradiation and thermal heating both under normal atmosphere and UV irradiation under N_2 gas atmosphere were applied. The energy-dispersive X-ray spectroscopy (EDS) and X-ray photoelectron spectroscopy (XPS) results evidenced the existence of continuous PMPC layer on the Ti6Al4V surface using the UV irradiation under a nitrogen atmosphere, due to the elimination of oxygen from the system. As indicated in the Fourier transform infrared spectroscopy (FTIR) results, one of the advantages of this technique is the presence of phosphorylcholine, mostly on the surface, which demonstrated that the polymer chains had been successfully anchored onto the surface of Ti6Al4V. Filmetric analysis identified the thickest layer of the grafted polymer for the surface grafted using UV irradiation under a nitrogen atmosphere. Therefore, this technique has been considered as optimal grafting technique considering surface morphology, polymer composition onto the top surfaces and film thickness of the grafted polymer.

Three different monomer concentrations, 0.4 M, 0.6 M and 0.8 M were then examined to optimise the monomer concentration for grafting polymer onto the surface of AM Ti6Al4V. The nuclear magnetic resonance (NMR) and gel permeation chromatography (GPC), results revealed that the monomer had been polymerised successfully. Samples grafted with 0.6 M monomer concentration showed more uniform surface and less surface roughness in comparison with other samples and untreated Ti6Al4V surfaces. 0.6 M monomer concentration was found to be the best option for grafting PMPC to the hip implant interfaces due to the improvement in surface morphology, roughness and polymerisation rate. Cell study was performed on the PMPC grafted surface to determine the biological response of PMPC layer. Scanning electron microscopy (SEM) and confocal imaging, results revealed that PMPC grafted surfaces prevent the implant interfaces from uncontrollable cell attachment which is of utmost importance in smoothing the motion of hip implant under cyclic loading.

The thermogravimetric analyser (TGA) and differential scanning calorimetry (DSC), results confirmed the PMPC is thermally stable for implant applications regardless of the monomer concentration and can stand the thermal sterilisation process. Furthermore, the surface grafted with 0.6 M monomer concentration demonstrated improved wettability.

Nanoindentation studies were performed to evaluate the mechanical properties of the implant surface both before and after polymer grafting. Results showed 0.6 M monomer concentration was found to be the optimal concentration for grafting hip implant interfaces with MPC considering their surface properties, penetration depth and hardness results. A significant reduction in Young's modulus of PMPC grafted samples (33.2 - 42.9%), in comparison with untreated Ti6Al4V samples, indicated the capability of PMPC layers in avoiding stress shielding effect under cyclic loadings. The stress-strain curves revealed the improvement in toughness and elasticity behaviour of PMPC grafted surfaces in comparison with the control sample. The nano-scratch test revealed that the PMPC layer protects the

underlying implant substrate from scratching even under high loads. Nano-tribological wear test was performed to investigate the effect of PMPC layer on wear resistance of the implant under loading conditions. The PMPC grafted surface exhibited a significant enhancement in wear resistance compared to the untreated surface even under application of high load. The concomitant improvement of wear resistance proved the potentiality of polymer films for implant applications.

Finally, theoretical modelling was designed to predict the lubricating film formation under different physiological conditions of hip joints. The theoretical model revealed the boundary lubrication mechanism for hip joint conditions even for the polymer grafted surface. The polymer grafted implants showed improved film formation compared to untreated implants. Therefore, the surface grafting with cartilage-mimicking PMPC layer could play a significant role in boundary lubrication by protecting the underlying metallic implant and thus help to reduce surgical recurrence and to increase implant lifetime.

Keywords: additive manufacturing, surface modification, texturing, coating, polymer grafting, hip arthroplasty, Ti-6Al-4V alloy, selective laser melting, MPC polymer, grafting thickness, mechanical properties, nano-indentation, topography, morphology, wettability, roughness, scratch test, wear resistance, cell attachment, film formation, durability

AUTHORS PUBLICATIONS

Journal articles:

[1] **Subir Ghosh,** Sylvester Abanteriba, Sherman Wong, and Shadi Houshyar **(2018)**. Selective laser melted titanium alloys for hip implant applications: Surface modification with new method of polymer grafting. *Journal of the mechanical behaviour of biomedical materials*, 87, 312-324.

[2] **Subir Ghosh**, Sylvester Abanteriba **(2016)**. Status of surface modification techniques for artificial hip implants. *Science and Technology of Advanced Materials*, 17(1), 715-735.

[3] **Subir Ghosh,** Sylvester Abanteriba, Sherman Wong, Robert Brkljača, and Shadi Houshyar **(2019)**. Optimisation of Grafted Phosphorylcholine-based Polymer on Additively Manufactured Titanium Substrate for Hip Arthroplasty, *Materials Science and Engineering:C,* 101, 696-706.

[4] **Subir Ghosh,** Sylvester Abanteriba, Sherman Wong, and Shadi Houshyar, Performance analysis of grafted poly (2-methacryloyloxyethyl phosphorylcholine) on additively manufactured titanium substrate concerning thermal stability and mechanical properties for hip implant applications, *Journal of the mechanical behaviour of biomedical materials* (under review)

Conferences:

[1] **Subir Ghosh**, Sylvester Abanteriba, and Shadi Houshyar (2018); A novel approach of polymer grafting on selective laser melted titanium alloy hip implants for improved lubricity and biocompatibility; *TMS 2018 Annual Meeting & Exhibition*, Phoenix convention centre, Arizona, USA

[2] **Subir Ghosh**, Sylvester Abanteriba, Zahra Homan, and Shadi Houshyar (2017); An investigation into the development of polymer grafting on a 3D printed titanium alloy for implant applications; *Emerging polymer technologies summit (EPTS) 2017,* Melbourne, Australia

This page is left intentionally blank

TABLE OF CONTENTS

ORIGINAL LITERARY WORK DECLARATION ..... *I*

DEDICATION ..... *II*

ACKNOWLEDGEMENTS ..... *III*

ABSTRACT ..... *V*

AUTHORS PUBLICATIONS ..... *VIII*

TABLE OF CONTENTS ..... *X*

LIST OF FIGURES ..... *XVI*

LIST OF TABLES ..... *XX*

CHAPTER ONE: INTRODUCTION *1*

1.1 Problem statement 1

1.2 Motivation and scope 3

1.3 Rationale of this research 4

1.4 Research questions 9

1.5 Research objectives 9

1.6 Thesis outline 9

1.7 References 12

CHAPTER TWO: LITERATURE REVIEW *15*

Chapter Overview 15

2.1 Introduction 16

2.2 Artificial hip joint prostheses 19

2.2.1 MoP hip implants 20

2.2.2 CoP hip implants 21

2.2.3 CoC hip implants....22
2.2.4 CoM and MoC hip implants....23
2.2.5 MoM hip implants....23
2.3 Surface modification techniques and their recent developments....24
2.3.1 Surface texturing....24
2.3.2 Surface coating....31
2.3.3 Surface grafting....37
2.4 Concepts of additively manufactured Ti6Al4V implants and associated challenges....43
2.5 Summary and future perspective....47
2.6 References....49
CHAPTER THREE: MATERIALS AND METHODS....55
3.1 Introduction....55
3.2 Materials....55
3.2.1 Ti6Al4V powder....55
3.2.2 MPC monomer....56
3.2.3 Chemicals....56
3.3 Sample fabrication and polymer grafting process....56
3.3.1 SLM Ti6Al4V implant....56
3.3.2 Polymer grafting process....57
3.4 Surface characterisation....58
3.4.1 Surface morphology....58
3.4.2 Surface roughness....58
3.4.3 Energy-dispersive X-ray spectroscopy (EDS)....59

3.4.4 X-ray photoelectron spectroscopy (XPS) 59
3.4.5 Fourier transform infrared spectroscopy (FTIR) 60
3.4.6 Water contact angle measurement 60
3.4.7 Thickness measurement of polymer grafted layer 60
3.5 Polymer characterisation 61
3.5.1 Nuclear magnetic resonance (NMR) spectroscopy analysis 61
3.5.2 Gel permeation chromatography (GPC) analysis 61
3.5.3 Thermogravimetric (TGA) analysis 61
3.5.4 Differential scanning calorimetry (DSC) analysis 62
3.6 Biological response evaluation 63
3.7 Mechanical and tribological properties evaluation 63
3.7.1 Mechanical properties evaluation 63
3.7.2 Scratch test 65
3.7.3 Tribological properties evaluation 65
3.8 Statistical analysis 65
3.9 References 66
CHAPTER FOUR: DEVELOPMENT OF POLYMER GRAFTING TECHNIQUE ONTO THE SURFACE OF TITANIUM SUBSTRATE *67*
4.1 Chapter overview 67
4.2 Experimental procedure 68
4.3 Results and discussion 72
4.3.1 Surface characterisation 72
4.3.2 Wettability 83

4.3.3 Thickness of grafted polymer layer....86

4.4 Summary....88

4.5 References....89

CHAPTER FIVE: THE EFFECT OF MONOMER CONCENTRATIONS ON POLYMERISATION RATE AND SURFACE PROPERTIES....91

5.1 Chapter overview....91

5.2 Experimental procedure....92

5.3 Results and discussion....93

5.3.1 Structural analysis of polymers....93

5.3.2 Effect of polymer grafting on surface morphology and roughness....97

5.3.3 Effect of PMPC layer on cell adhesion resistance....101

5.4 Summary....104

5.5 References....106

CHAPTER SIX: THE IMPACT OF PMPC LAYER ON THERMAL STABILITY AND MECHANICAL PROPERTIES OF THE IMPLANT....108

6.1 Chapter overview....108

6.2 Experimental procedure....109

6.3 Results and discussion....110

6.3.1 Thermal stability of PMPC....110

6.3.2 Surface properties of PMPC grafted implants....113

6.3.3 Effects of polymer grafting on mechanical properties of the implants....116

6.3.4 Effect of PMPC layer on scratch resistance....124

6.3.5 Effect of PMPC layer on wear resistance....125

6.4 Summary 127

6.5 References 129

CHAPTER SEVEN: THEORETICAL PREDICTION OF LUBRICATING FILM FORMATION UNDER DIFFERENT PHYSIOLOGICAL HIP JOINT CONDITIONS *131*

7.1 Chapter Overview 131

7.2 Lubrication model: main characteristics 132

7.3 Results and discussion 133

7.4 Summary 137

7.5 References 139

CHAPTER EIGHT: SUMMARY AND FUTURE WORK *140*

8.1 Summary 140

8.2 Conclusion 140

8.3 Recommendations for future work 142

REFERENCES *143*

APPENDICES *154*

This page is left intentionally blank

LIST OF FIGURES

Fig. 1.1 (a) Basic principles of selective laser melting [25], (b) polymer grafting under UV irradiation and (c) prospective applications of polymer grafting for hip implants. 4

Fig. 2.1 a)The application of Surface texturing technique on femoral head surface [98] and b) surface morphology of different types of fabricated textured surface [60]. 26

Fig. 2.2 Wear mechanism for a) non-dimpled surfaces, b) low depth dimpled surfaces and c) high depth dimpled surfaces [118].....30

Fig. 2.3 Cross-sectional SEM images of deposited (a) a-C:H and (b) Ta-C on stainless steel [1]. 33

Fig. 2.4 Friction coefficient results for different prosthesis heads [1].....34

Fig. 2.5 SEM images showing (a) as-deposited DLC-coated surface, (b) formation of film transfer due to load, (c) full delamination of coated materials at higher loads, and (d) wear track on dimpled area [114]. 35

Fig. 2.6 Cross-sectional schematic view of the wear mechanism model for (a) DLC-smooth, (b) DLC with high density (c) DLC with suitable density (d) DLC with low density [117]...36

Fig. 2.7 Schema of a THA with the PMPC-grafted CLPE liner. A transmission electron microscope (TEM) image of the surface is shown on the right. Orange and blue lines indicate the PMPC layer and the liner surface, respectively [33]. 38

Fig. 2.8 Graft polymer conformation at various densities of polymer chains [26].....39

Fig. 2.9 Coefficient of dynamic friction of polyelectrolyte-grafted CLPE samples under various lubrication conditions. Data are expressed as means ± standard deviations. * Indicates $p < 0.05$, ** indicates $p < 0.01$, and N.S. indicates no statistical difference [26]. 41

Fig. 2.10 Porous surfaces of implants for (a) acetabular cup, and ((b) tibial tray with zoomed in images of uncontrolled porosity [149].....44

Fig. 4.1 Graphical representation of polymer grafting process onto the surface of SLM Ti6Al4V. 69
Fig. 4.2 Graphical representation of N_2 gas bubbling (degassing) for method 3. 70
Fig. 4.3 Surface morphology of a) as-built, b) UVNP-M1, c) THNP-M2 and d) UVNP-M3 surfaces. 73
Fig. 4.4 Surface morphology of a) polished, b) UVP-M1, c) THP-M2 and d) UVP-M3 surfaces. 74
Fig. 4.5 Surface topography of a) as-built, b) UVNP-M1, c) THNP-M2, and d) UVNP-M3 surfaces. 75
Fig. 4.6 Surface topography of a) polished, b) UVP-M1, c) THP-M2 and d) UVP-M3 surfaces. 76
Fig. 4.7 EDS spectra of (a) untreated and (b) polymer treated surfaces. Inset is the SEM image of the scanned area and corresponding elemental distribution of major element of Ti and C for (c) untreated and (d) polymer treated surfaces. The line mapping results of weight percentages over the distance for (e) untreated and (f) polymer treated surfaces. 78
Fig. 4.8 Surface analysis of the PMPC grafted Ti6Al4V by XPS, The disappearance Ti_{2p}, Al_{2p} peaks and the appearance strong N_{1s}, Si_{2p} and P_{2p} peaks specific to the PMPC, after polymer grafting imply the PMPC was grafted successfully onto the surface of SLM Ti6Al4V. 79
Fig. 4.9 XPS high-resolution Ti_{2p} spectra after grafting with different methods, (a) as-built, surface grafted by (b) method 1, (c) method 2, and (d) method 3. 80
Fig. 4.10 FTIR spectra of polymer grafted surface under different grafting methods (a) non-polished polymer grafted surfaces and (b) polished polymer grafted surfaces. 82
Fig. 4.11 Water-surface interaction for (a) untreated and (b) PMPC treated surface. 84
Fig. 4.12 Filmetrics spectra of polymer grafted layer for (a) non-polished polymer grafted surfaces and (b) polished polymer grafted surfaces. 86

Fig. 5.1 NMR peaks for (a) MPC monomer and (b) PMPC. The NMR peaks changed significantly after monomer being converted into polymer. 94
Fig. 5.2 FTIR spectra for different polymer grafted samples. The presence of $–N+(CH_3)^3$ and P=O bonding confirms the existence of phosphorylcholine in the grafted surface. 96
Fig. 5.3 Surface morphology of untreated and PMPC treated surfaces. 98
Fig. 5.4 Surface topography for untreated and different PMPC grafted samples. 99
Fig. 5.5 Confocal microscopic images of cultured cells onto the untreated and polymer treated surfaces. 102
Fig. 5.6 Cell morphology on as-built surfaces at different magnification after 24 hours and 72 hours of cell growth. 103
Fig. 5.7 Cell morphology on polished surfaces at different magnification after 24 hours and 72 hours of cell growth. 104
Fig. 6.1 Weight loss versus temperature for PMPC with various monomer concentration... 111
Fig. 6.2 DSC curves for polymers with different monomer concentration. 112
Fig. 6.3 Surface morphology of untreated and treated polymer surface with various monomer concentrations. 114
Fig. 6.4 Average water contact angle measurements for untreated (control) and polymer treated samples. 115
Fig. 6.5 Load vs Displacement curve for different samples. 117
Fig. 6.6 Hardness profiles for untreated and treated surfaces with various monomer concentration. 118
Fig. 6.7 Average Young's modulus of grafted polymer with various monomer concentrations. 121
Fig. 6.8 Modulus mapping results for untreated and PMPC grafted surfaces for various monomer concentrations. 122

Fig. 6.9 Stress-strain diagrams for PMPC grafted samples with different monomer concentration. The arrow indicates the elasticity limits of the samples. 123
Fig. 6.10 Surface topography of untreated (a & c) and treated surfaces with MPC (b & d) after scratch test under various applied loads. Wear track data was taken from about half way through the scratch, indicated by the white box. The depths of each scratch are (a) 50 nm (b) 5 nm (c) 100 nm (d) 30 nm.....125
Fig. 6.11 Wear marks under different loading conditions for untreated surface and PMPC treated surface with various monomer concentrations.....127
Fig. 7.1 The minimum film thickness as a function of frequency for untreated and polymer treated implants under (a) 50 N, (b) 100 N, and (c) 150 N Load. *The film thickness values overlap each other for untreated and polymer treated implants where $p > 0.05$.....134
Fig. 7.2 The minimum film thickness as a function of the anatomical orientation of cup angle for untreated and polymer treated implants under (a) 1 Hz, (b) 5 Hz, and (c) 10 Hz frequency. 136
Fig. 7.3 The minimum film thickness as a function of load for untreated and polymer treated implants under (a) 1 Hz, (b) 5 Hz, and (c) 10 Hz frequency. 137

LIST OF TABLES

Table 3.1 The chemical composition of ELI Ti6Al4V powder. 55

Table 3.2 Process parameters for SLM-used to fabricate Ti6Al4V implant. 56

Table 4.1 The experimental condition of all samples. 71

Table 4.2 Average surface roughness measured by Tencor profilometer. 76

Table 4.3 Relative atomic percentages of elements determined using XPS for untreated and treated samples. 81

Table 4.4 Average contact angle for untreated and polymer treated samples by different grafting methods. 83

Table 4.5 Thickness of PMPC grafted layer for different grafting methods. 87

Table 5.1 Degree of polymerisation for different monomers' concentration. 95

Table 5.2 GPC results for the average molecular weight of different polymer samples. 96

Table 5.3 Surface roughness for untreated and treated surfaces. 99

The page is left intentionally blank

CHAPTER ONE: INTRODUCTION

1.1 Problem statement

The patients suffering from osteoarthritis and rheumatoid arthritis require artificial hip replacements due to the affected bone surfaces. Furthermore, the demand for total hip arthroplasty (THA) procedure is increasing with continuing aging of the population as the number of patients are increasing. Unfortunately, these patients experience surgical recurrence due to the shorter functional life of the hip implants compared to the ever-increasing life expectancy of a patient especially younger. THA treatments have been improved significantly in the last two decades to minimise the number of revision surgeries. Nevertheless, revision surgery requires after 20-25 years of implantation [1]. One of the major difficulties of THA is aseptic loosening, which limits their clinical success and durability [2]. High friction and consequent wear cause aseptic loosening, dislocation of the implant [3]. Moreover, abundant protein adsorption and consequent cell adhesion induce the infection, which hinders the functionality of the implant [4-6]. Thus the inability to mimic the host response under various physiological conditions is the critical issue of the implant failure. Therefore, there is a need for quality improvement of hip implant as the developments of implant materials are yet challenging to meet the expectation of the patient's lifetime.

The selection of implant material is the key issue in minimising the revision rate. The quest for specialised materials that respond both to the mechanical and chemical solicitations of the human body could promise a proper host response. Titanium and in particular the titanium alloy (Ti6Al4V) is of high interest as orthopaedic implants because it offers excellent mechanical strength, chemical inertness and good biocompatibility [7-9]. Ti6Al4V has received attention due to its relatively low modulus of elasticity, which is closer to the properties of cortical bone, compared to other metals, resulted in preventing stress shielding

effect after implantation [3, 10]. Still, the elastic modulus is comparatively 10 times higher than cortical bone, which could be a reason for aseptic loosening and premature implant failure [11]. The development of new titanium β alloys is a unique approach to address this problem. Although several studies reported new systems with much lower stiffness, yet these are not identical with the bone [12, 13].

Machining, casting and forging are the traditional manufacturing techniques for fabricating orthopaedic implants. While these techniques are proven and certified industry standard to fabricate the implants safely, the fabrication of customised implants by additive manufacturing (AM) technique is slowly gaining attention due to its numerous advantages. AM, especially selective laser melting (SLM) technique provides controlled and interconnected pores, which play crucial roles in creating a strong bond between the powder particles [14]. This technique has a rapid production rate with high utilisation of materials, and the microstructure can be graded in a controlled manner. By this technique, any complex shape, such as hip implants can be manufactured from direct production, based on computer-aided design (CAD) model which results in saving both cost and time [15].

Though the SLM technique has improved significantly in the last few years, still it has some limitations on long-term use of the product in a biological environment. The product of this technique has a high surface roughness that causes higher friction and consequent wear of the implant. High surface roughness increases unfavourable protein adsorption, bacterial adhesion and uncontrollable cell attachment [16]. Therefore, the long-term success of the 3D printed Ti6Al4V implant is affected as bio-implant. It is crucial to control the osseointegration problems that arise as a result of the introduction of implant in the biological environment. Since the biological response to implanted biomaterials is influenced by the surface properties of the materials, tailoring the physical/chemical properties of the implant surfaces could be useful to control the interaction between an implant and the surrounding tissue. Noteworthy,

Ti6Al4V alloys are not commonly used nowadays as head materials due to its low wear resistance properties. However, significant researches have been undertaken to improve the mechanical and wear resistance properties of Ti6Al4V femoral heads applying various surface coatings [17-22].

1.2 Motivation and scope

To meet the demands of longer human life and implantation in younger patients, improvement of surface properties is imperative. Surface modification technique improves wettability, biocompatibility and mechanical properties of materials surface [23]. The bearing surfaces of natural hip joints are shielded with articular cartilage which protects the joint interface from mechanical wear and assists a smooth motion of joints during daily activity [24]. Therefore, it is crucial to develop cartilage-mimicking layer between implant interfaces. Previous studies revealed that the poly(2-methacryloyloxyethyl phosphorylcholine) [MPC]) (PMPC) carries phosphorylcholine group in their side chains, which provides phospholipid like layer during sliding motion, and thus mimics the articular cartilage of natural hip joints. It is well known that highly cross-linked polyethylene (CLPE) cup/liner is coupled with metallic or composite head materials in artificial hip implants. Based on a comprehensive investigation on the present status of surface modification techniques, it has been realised that the long-term response of metallic implants could be accomplished by grafting phosphorylcholine bearing polymers onto their surfaces. Nevertheless, it is still a great challenge to develop polymer grafting on the metal surface.

In this project, SLM Ti6Al4V samples were chosen due to its potential biomedical applications. Fig. 1.1(a) presents basic principle of selective laser melting process. PMPC grafting process under UV irradiation is presented in Fig. 1.1(b). Fig. 1.1(c) illustrates the interface of Ti6Al4V implant grafted with PMPC.

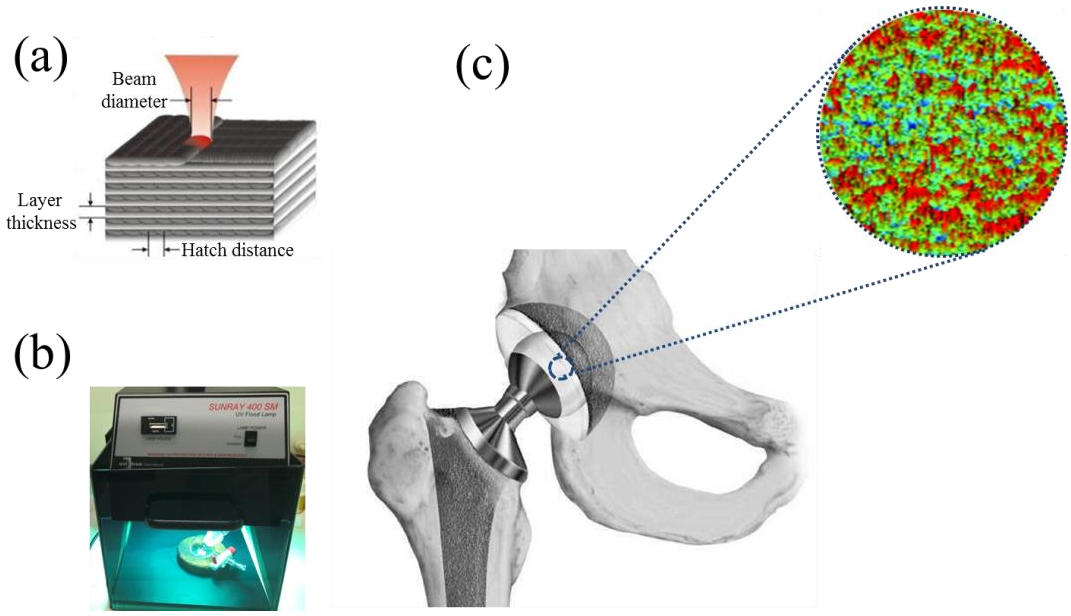

Fig. 1.1 (a) Basic principles of selective laser melting [25], (b) polymer grafting under UV irradiation and (c) prospective applications of polymer grafting for hip implants.

1.3 Rationale of this research

Some surface modification techniques, such as surface texturing and surface coating have been developed to enhance the useful life of joint prostheses. Surface modification techniques are usually applied to femoral head surfaces. Surface texturing improves the lubricating ability of the implant interfaces. However, the wear rate is still higher for the textured surfaces due to the wear debris generation under sliding motion. Surface coating technique has become the most reasonable approach since the last decades, to engineer the bearing surfaces of artificial joints due to its highly wear-resistant coating. Surface coating increases the mechanical properties of the contacting surface, resulted in enhancing wear and corrosion resistance. However, the earlier delamination of coated materials due to poor adhesion between coated materials and substrate limits the uses of this technique for load-bearing applications. Another surface modification technique known as surface grafting on acetabular liner has a significant influence on friction and wear reduction for joint implants

[26]. PMPC has become the attractive choice for grafting acetabular liner due to its unique properties. It possesses excellent biocompatibility and anti-biofouling ability [27], provides unique surface properties, such as high lubricity, low friction, anti-protein adsorption and cell adhesion resistance [28], forms a hydrated lubricating layer, and hence increases wear resistance [29]. Therefore, PMPC could provide host response in artificial hip implant applications.

Recent studies only investigated the effect of PMPC grafting on CLPE substrates for its application on acetabular liner surface [29-34]. Though other surface modifications technique, such as surface texturing and coating focussed on femoral head surface, no study considered polymer grafting on femoral head surfaces. No study reported polymer grafting onto additively manufactured titanium (AM Ti6Al4V) substrate. In fact, the concept of grafting a bioactive polymer on metallic surfaces is relatively new. The formation of covalent bonding between polymer and metal substrate is complex. The radical polymerisation method could be useful to generate free radical onto a metal substrate. These free radicals interact with the monomers in solution under controlled environmental conditions [35].

This PhD research will look into developing a highly lubricated polymer layer onto the surface of the AM Ti6Al4V substrate to improve hip arthroplasty performance. Different from previous studies, this research aims to develop polymer grafting onto the surface of a metallic substrate, which is novel and more complex and challenging. This project will investigate the different techniques to graft the PMPC onto the surface of the AM Ti6Al4V substrate through radical polymerisation. The polymerisation parameters are crucial factors to tailor the surface properties of the implant. The degree of polymerisation and chain length are important parameters that affect the surface morphology, roughness and uniformity of the polymer layer. Therefore, the optimisation of polymerisation parameters is an important aspect of this research. Unmodified Ti-based materials can gradually stimulate the formation of a fibrous

layer even after several years of implantation. Therefore, the fibrous layer interacts with the living tissue and leading to a progressive loss of osseointegration [35, 36]. Sometimes implant surface itself creates a preferential site for bacterial adhesion and leads to inflammatory disease. The gradual loss of supporting bone due to inflammatory disease is one of the major reasons for implant failure. It is obvious that untreated SLM Ti6Al4V surfaces are not able to establish good interaction with the surrounding biological tissues. Proper osseointegration of the joint could increase the useful life of the hip implants.

Various surface modification techniques such as plasma treatment, heat treatment and surface coating are usually applied on SLM fabricated sample to improve the physical properties of the surface. Controlled surface modification on SLM manufactured sample is very complicated. As a result, commonly used mechanical methods, such as sandblasting and grinding or physical methods, such as thermal spraying and ion implantation might not be effective due to inhomogeneous surface treatment [37, 38]. However, chemical etching (CHE) and electrochemical polishing (ECP) could be applied to obtain a controlled and homogeneous roughness of the treated surface. Pyka *et al*. [39] showed a significant reduction in surface roughness using a combination of CHE and ECP with HF-based solutions. Moreover, the HF-based solution helps to remove weakly attached partially-melted particles from the surfaces by chemical etching. Few studies on biochemical modification aim to obtain faster osseointegration and bone adhesion [5, 40]. Surface modification incorporating bioactive biomolecules and/or biocompatible polymers could be the pertinent solution to enhancing the osseointegration and wear resistance of the SLM fabricated implant. However, polymer coating arises poor adhesion between the substrate and the coated materials resulted in early delamination of the coating. Thus, it decreases the useful life of the implants. Moreover, hip implants can generate heat during the sliding motion under loading condition. This heat generation could affect the useful life of the polymer grafted surface.

Few biocompatible polymers are sensitive to high temperatures leading in controlled contraction or expansion with small changes in the external environmental condition [41, 42]. PMPC contains water molecules resulted in polymer decomposition at high temperature. As this polymer will be used in physiological conditions, analysing the thermal stability of the polymer is an important aspect of this research. The wettability property of the implant surface plays a crucial role under lubrication conditions. The deposition of a thin polymer film on the metal surface could impact the mechanical properties of the bulk surface. As a result, investigating the effect of PMPC layer on mechanical properties is crucial. The mechanical properties of PMPC grafted surface could be altered due to changes in interface from Ti6Al4V alloys to polymer. It is expected that polymer grafting will reduce the mechanical properties of the bulk surface. This reduction is acceptable provided it is not significant and meets the implant criteria. Improvement of wear resistance of the Ti6Al4V surface is required to increase the lifetime of the implants.

It is well known that articular cartilage covers the bone surfaces in the natural hip joint. This articular cartilage contains synovial capsule which can be preserved during hip replacement surgery [43]. Synovial fluid stored in the synovial capsule has an excellent shock absorbing ability [44]. It produces lubricant film and protects the bone surfaces from contacting each other. The hip joint can transmit high dynamic loads (7-8 times the body weight) and accommodate a wide range of movements [45] due to the presence of synovial fluid in articular cartilage. As the synovial capsule can be preserved during surgery, it can be reused in artificial hip implants. This synovial capsule could supply the synovial fluid for lubrication of artificial joints during motion and thus could affect the tribological performance of artificial hip implant providing a lubricating layer under loading conditions. Investigating the lubricating ability of artificial implants is essential to understand the overall tribological performance of the implants.

There is a restriction on conducting the film formation experiments as the facilities for the measurement need special arrangements. However, researchers are trying to predict the film formation behaviour of the implant by theoretical approach. Hamrock-Dowson formula is applicable for ball-on-socket hip implants [46]. Various factors affect the overall lubrication performance of artificial implants. Most importantly, the surface roughness of the implant surfaces plays a crucial role in film formation. Poisson's ratio and Young's modulus also influence film formation [47-49]. It is well known that the load and the speed experienced in hip joints varies with the movements. Therefore, the physiological conditions of the hip joint should be considered in the theoretical model.

In this PhD project, concentrations of polymer grafting process have been optimised, through thermal effect as well as the physical and mechanical properties of the implant and interface. A nanoindentation technique has been used to explore mechanical properties of thin polymer films. Previous researchers have correlated mechanical properties such as hardness and Young's modulus, with tribological properties including coefficient of friction and wear resistance [50-52]. The present study will similarly investigate the correlation between Young's modulus and wear resistance property. As discussed earlier, the PMPC layer acts as cartilage on the surface of implants. Therefore, it is important to have the capacity of carrying sufficient loads. In this study, the effect of PMPC layer on the mechanical strength of the implant surfaces will be investigated through nano-scratch test. The wear test will be performed to evaluate the wear resistance of the PMPC grafted surface. From the nano-scratch and wear test, the withstand ability of untreated and PMPC treated surface will be compared. To the knowledge, no theoretical study of lubricating film formation has been conducted on additively manufactured hip joints. In this study, the viscosity of the synovial fluid will be considered. The theoretical model will predict the impact of PMPC layer on film formation. The theoretical results will be compared both for untreated and PMPC treated surfaces.

1.4 Research questions

Based on a comprehensive literature review, the following research questions have been determined for this project:

1. What is the optimal technique for grafting polymer onto the surface of SLM Ti6Al4V implants?
2. What is the influence of monomer concentration on polymerisation and surface properties of the implant?
3. Can PMPC control unfavourable cell adhesion onto the implant interfaces?
4. What is the effect of PMPC layer on the thermal and mechanical properties of the implant surface?
5. How does polymer grafting affect the wear resistance of the implant surfaces?
6. What is the impact of surface grafting on lubricating film formation between the contact interfaces?

1.5 Research objectives

The main aim of this research is to develop a polymer grafting technique onto the surface of the AM Ti6Al4V substrate to enhance the useful life of the implant. This aim can be accomplished by accumulating the following objectives.

1. To develop and optimise the polymer grafting technique on SLM Ti6Al4V implants
2. To characterise the effect of monomer concentrations on surface properties, such as polymer uniformity, surface roughness and wettability
3. To evaluate the impact of PMPC layer on cell adhesion resistance
4. To investigate the thermal and mechanical properties of the grafted surface with a polymer
5. To predict the lubrication mechanism and lubricating film thickness from experimental results using a theoretical model

1.6 Thesis outline

The research work presented in this thesis is divided into eight chapters. The thesis chapter has been outlined as follows:

Chapter one highlights the significance of surface modification techniques for hip implant applications. The overall research background, problem statement, motivation and scope, the rationale of this project, research questions and research objectives have been presented in this chapter.

Chapter two investigates the conventionally employed surface modification techniques for implant applications. Commonly used hip implants and their limitations along with conventional methods of surface modification techniques to enhance the useful life of implants have been described. This chapter provides a comprehensive review of surface modification techniques, materials and surface properties with a focus on tribological performance. This review helps to identify the most satisfactory surface modifications technique for the longevity of artificial hip implants. The potentiality of AM Ti6Al4V implants and their associated challenges for hip implant application has also been highlighted.

Chapter three presents all experimental procedures and the details of the materials used for this project. This chapter briefly describes the polymer grafting techniques and the details of polymer and mechanical characterisation procedures. The details process of cell study has also been presented. A brief description of the statistical analysis was presented in the final section.

Chapter four compares the different polymer grafting techniques on AM TI6Al4V implants. This chapter investigates the effect of different grafting techniques onto the surface uniformity, roughness and also film thickness of the grafted polymer. This chapter also compares the elemental composition of top surface layers to examine the existence of polymer and at the same time to optimise the polymer grafting techniques.

Chapter five evaluates the influence of monomer concentrations on polymerisation rate and surface properties. Polymer characterisation results reveal that monomer being converted into polymer successfully and the optimal monomer concentration has been

determined by analysing the polymerisation rate, surface properties and chemical bonding. The impact of cell PMPC layer in resistance to cell adhesion has been analysed onto optimised samples.

Chapter six analyses the thermal and mechanical properties of grafted surfaces. The main purpose of thermal stability analysis is to investigate whether this polymer is thermally stable in various physiological conditions and under thermal sterilisation process. The effect of PMPC layer on mechanical properties has been investigated. The scratch tests have been performed using the samples prepared by optimised grafting technique and compared the results with untreated samples. Finally, wear tests have been carried out to evaluate the impact of PMPC layer on wear resistance of the implant.

Chapter seven presents the theoretical modelling to predict the lubrication mechanism and lubricant film formation under different physiological conditions of artificial hip implants. This theoretical model considers the lubricant viscosity of synovial fluid, sliding speed and different angular rotation.

Chapter eight summarises the key findings of this project and indicates the major contribution of this project to the body of knowledge in biomedical research. Finally, the perspective of further investigations in this area is outlined.

1.7 References

[1] Choudhury D, Ay Ching H, Mamat A B, Cizek J, Osman A, Azuan N, Vrbka M, Hartl M and Krupka I 2014 Fabrication and characterization of DLC coated microdimples on hip prosthesis heads *Journal of Biomedical Materials Research Part B: Applied Biomaterials*

[2] Böhler C, Weimann P, Alasti F, Smolen J, Windhager R and Aletaha D 2018 FRI0051 The risk of aseptic arthroplasty loosening in patients with rheumatoid arthritis. BMJ Publishing Group Ltd)

[3] Ghosh S and Abanteriba S 2016 Status of surface modification techniques for artificial hip implants *Science and Technology of Advanced Materials* **17** 715-35

[4] Bačáková L, Filova E, Rypáček F, Švorčík V and Starý V 2004 Cell adhesion on artificial materials for tissue engineering *Physiol res* **53** S35-S45

[5] Puleo D and Nanci A 1999 Understanding and controlling the bone–implant interface *Biomaterials* **20** 2311-21

[6] Raynor J E, Capadona J R, Collard D M, Petrie T A and García A J 2009 Polymer brushes and self-assembled monolayers: versatile platforms to control cell adhesion to biomaterials *Biointerphases* **4** FA3-FA16

[7] Ramakrishnaiah R, Mohammad A, Divakar D D, Kotha S B, Celur S L, Hashem M I, Vallittu P K and Rehman I U 2017 Preliminary fabrication and characterization of electron beam melted Ti–6Al–4V customized dental implant *Saudi Journal of Biological Sciences* **24** 787-96

[8] Kaczorowski W, Szymanski W, Batory D and Niedzielski P 2014 Tribological Properties and Characterization of Diamond Like Carbon Coatings Deposited by MW/RF and RF Plasma-Enhanced CVD Method on Poly (ether-ether-ketone) *Plasma Processes and Polymers* **11** 878-87

[9] Fukuda A, Takemoto M, Tanaka K, Fujibayashi S, Pattanayak D, Matsushita T, Sasaki K, Nishida N, Kokubo T and Nakamura T 2011 Bone ingrowth into pores of lotus stem-type bioactive titanium implants fabricated using rapid prototyping technique *Bioceramics Development and Applications* **1**

[10] Long M and Rack H 1998 Titanium alloys in total joint replacement—a materials science perspective *Biomaterials* **19** 1621-39

[11] Fousová M, Vojtěch D, Kubásek J, Jablonská E and Fojt J 2017 Promising characteristics of gradient porosity Ti-6Al-4V alloy prepared by SLM process *Journal of the Mechanical Behavior of Biomedical Materials* **69** 368-76

[12] Kopova I, Stráský J, Harcuba P, Landa M, Janeček M and Bačákova L 2016 Newly developed Ti–Nb–Zr–Ta–Si–Fe biomedical beta titanium alloys with increased strength and enhanced biocompatibility *Materials Science and Engineering: C* **60** 230-8

[13] Niinomi M, Nakai M and Hieda J 2012 Development of new metallic alloys for biomedical applications *Acta Biomaterialia* **8** 3888-903

[14] Zhang C, Zhang L, Xu H, Li P and Qian B 2019 Performance of pool boiling with 3D grid structure manufactured by selective laser melting technique *International Journal of Heat and Mass Transfer* **128** 570-80

[15] Khorasani A, Gibson I, Goldberg M and Littlefair G 2017 Production of Ti-6Al-4V acetabular shell using selective laser melting: possible limitations in fabrication *Rapid Prototyping Journal* **23**

[16] Dylla-Spears R, Wong L, Shen N, Steele W, Menapace J, Miller P, Feit M and Suratwala T 2017 Adsorption of silica colloids onto like-charged silica surfaces of different roughness *Colloids and Surfaces A: Physicochemical and Engineering Aspects* **520** 85-96

[17] Li J, Li Z, Tu J, Jin G, Li L, Wang K and Wang H 2019 In vitro and in vivo investigations of a-C/a-C:Ti nanomultilayer coated Ti6Al4V alloy as artificial femoral head *Materials Science and Engineering: C* **99** 816-26

[18] Jo S, Lee S, Lim W, Kim D and Lee J 2018 APPLICATION OF PLASMA ELECTROLYTIC OXIDATION COATING ON TITANIUM FEMORAL HEAD. In: *Orthopaedic Proceedings*: The British Editorial Society of Bone & Joint Surgery) pp 1-

[19] Luo Y, Ge S, Liu H and Jin Z 2009 Microstructure analysis and wear behavior of titanium cermet femoral head with hard TiC layer *Journal of Biomechanics* **42** 2708-11

[20] Gutmanas E Y and Gotman I 2004 PIRAC Ti nitride coated Ti–6Al–4V head against UHMWPE acetabular cup–hip wear simulator study *Journal of Materials Science: Materials in Medicine* **15** 327-30

[21] Vamsi Krishna B, Xue W, Bose S and Bandyopadhyay A 2008 Functionally graded Co–Cr–Mo coating on Ti–6Al–4V alloy structures *Acta Biomaterialia* **4** 697-706

[22] Liu C, Bi Q and Matthews A 2003 Tribological and electrochemical performance of PVD TiN coatings on the femoral head of Ti–6Al–4V artificial hip joints *Surface and Coatings Technology* **163-164** 597-604

[23] Ghosh S, Choudhury D, Roy T, Mamat A B, Masjuki H and Pingguan-Murphy B 2016 Tribological investigation of diamond-like carbon coated micro-dimpled surface under bovine serum and osteoarthritis oriented synovial fluid *Science and Technology of Advanced Materials*
[24] Ghosh S, Choudhury D, Das N S and Pingguan-Murphy B 2014 Tribological role of synovial fluid compositions on artificial joints — a systematic review of the last 10 years *Lubrication Science* **26** 387-410
[25] Vilaro T, Abed S and Knapp W 2008 Direct manufacturing of technical parts using selective laser melting: example of automotive application. In: *Proc. of 12th European Forum on Rapid Prototyping,*
[26] Ishihara K 2015 Highly lubricated polymer interfaces for advanced artificial hip joints through biomimetic design *Polymer Journal* **47** 585-97
[27] Moro T, Takatori Y, Kyomoto M, Ishihara K, Saiga K-i, Nakamura K and Kawaguchi H 2010 Surface grafting of biocompatible phospholipid polymer MPC provides wear resistance of tibial polyethylene insert in artificial knee joints *Osteoarthritis and Cartilage* **18** 1174-82
[28] Kyomoto M, Moro T, Saiga K-i, Miyaji F, Kawaguchi H, Takatori Y, Nakamura K and Ishihara K 2010 Lubricity and stability of poly (2-methacryloyloxyethyl phosphorylcholine) polymer layer on Co–Cr–Mo surface for hemi-arthroplasty to prevent degeneration of articular cartilage *Biomaterials* **31** 658-68
[29] Kyomoto M, Moro T, Saiga K, Hashimoto M, Ito H, Kawaguchi H, Takatori Y and Ishihara K 2012 Biomimetic hydration lubrication with various polyelectrolyte layers on cross-linked polyethylene orthopedic bearing materials *Biomaterials* **33** 4451-9
[30] Kyomoto M, Moro T, Yamane S, Takatori Y, Tanaka S and Ishihara K 2017 A hydrated phospholipid polymer-grafted layer prevents lipid-related oxidative degradation of cross-linked polyethylene *Biomaterials* **112** 122-32
[31] Moro T, Kawaguchi H, Ishihara K, Kyomoto M, Karita T, Ito H, Nakamura K and Takatori Y 2009 Wear resistance of artificial hip joints with poly (2-methacryloyloxyethyl phosphorylcholine) grafted polyethylene: comparisons with the effect of polyethylene cross-linking and ceramic femoral heads *Biomaterials* **30** 2995-3001
[32] Kyomoto M, Moro T, Konno T, Takadama H, Yamawaki N, Kawaguchi H, Takatori Y, Nakamura K and Ishihara K 2007 Enhanced wear resistance of modified cross-linked polyethylene by grafting with poly (2-methacryloyloxyethyl phosphorylcholine) *Journal of Biomedical Materials Research Part A* **82** 10-7
[33] Moro T, Takatori Y, Kyomoto M, Ishihara K, Hashimoto M, Ito H, Tanaka T, Oshima H, Tanaka S and Kawaguchi H 2014 Long-term hip simulator testing of the artificial hip joint bearing surface grafted with biocompatible phospholipid polymer *Journal of Orthopaedic Research* **32** 369-76
[34] Yarimitsu S, Moro T, Kyomoto M, Watanabe K, Tanaka S, Ishihara K and Murakami T 2015 Influences of dehydration and rehydration on the lubrication properties of phospholipid polymer-grafted cross-linked polyethylene *Proceedings of the Institution of Mechanical Engineers, Part H: Journal of Engineering in Medicine* 0954411915588969
[35] Chouirfa H, Evans M D, Castner D G, Bean P, Mercier D, Galtayries A, Falentin-Daudré C and Migonney V 2017 Grafting of architecture controlled poly (styrene sodium sulfonate) onto titanium surfaces using bio-adhesive molecules: Surface characterization and biological properties *Biointerphases* **12** 02C418
[36] Roos-Jansåker A M, Renvert S and Egelberg J 2003 Treatment of peri-implant infections: a literature review *Journal of clinical periodontology* **30** 467-85
[37] Liu X, Chu P K and Ding C 2004 Surface modification of titanium, titanium alloys, and related materials for biomedical applications *Materials Science and Engineering: R: Reports* **47** 49-121
[38] Zavareh M A, Sarhan A A D M, Razak B B A and Basirun W J 2014 Plasma thermal spray of ceramic oxide coating on carbon steel with enhanced wear and corrosion resistance for oil and gas applications *Ceramics International* **40** 14267-77
[39] Pyka G, Burakowski A, Kerckhofs G, Moesen M, Van Bael S, Schrooten J and Wevers M 2012 Surface modification of Ti6Al4V open porous structures produced by additive manufacturing *Advanced Engineering Materials* **14** 363-70
[40] Kirmanidou Y, Sidira M, Drosou M-E, Bennani V, Bakopoulou A, Tsouknidas A, Michailidis N and Michalakis K 2016 New Ti-alloys and surface modifications to improve the mechanical properties and the biological response to orthopedic and dental implants: a review *BioMed research international* **2016**
[41] Ci J, Kang H, Liu C, He A and Liu R 2017 Thermal sensitivity and protein anti-adsorption of hydroxypropyl cellulose-g-poly (2-(methacryloyloxy) ethyl phosphorylcholine) *Carbohydrate polymers* **157** 757-65

[42] Gupta N R, Ghute P P and Badiger M V 2011 Synthesis and characterization of thermo-sensitive graft copolymer of carboxymethyl guar and poly (N-isopropylacrylamide) *Carbohydrate polymers* **83** 74-80
[43] Buckwalter J A, Mankin H J and Grodzinsky A J 2005 Articular cartilage and osteoarthritis *Instructional Course Lectures-American Academy of Orthopaedic Surgeons* **54** 465
[44] Balazs E A 1974 The physical properties of synovial fluid and the special role of hyaluronic acid *Disorders of the Knee* **2** 61-74
[45] Mattei L, Di Puccio F, Piccigallo B and Ciulli E 2011 Lubrication and wear modelling of artificial hip joints: A review *Tribology International* **44** 532-49
[46] Liu F, Jin Z, Roberts P and Grigoris P 2006 Importance of head diameter, clearance, and cup wall thickness in elastohydrodynamic lubrication analysis of metal-on-metal hip resurfacing prostheses *Proceedings of the Institution of Mechanical Engineers, Part H: Journal of Engineering in Medicine* **220** 695-704
[47] Jalali-Vahid D, Jagatia M, Jin Z and Dowson D 2001 Prediction of lubricating film thickness in UHMWPE hip joint replacements *Journal of biomechanics* **34** 261-6
[48] Kang L, Galvin A L, Fisher J and Jin Z 2009 Enhanced computational prediction of polyethylene wear in hip joints by incorporating cross-shear and contact pressure in additional to load and sliding distance: effect of head diameter *Journal of biomechanics* **42** 912-8
[49] Wang F, Brockett C, Williams S, Udofia I, Fisher J and Jin Z 2008 Lubrication and friction prediction in metal-on-metal hip implants *Physics in medicine and biology* **53** 1277
[50] Chen Y, Bakshi S R and Agarwal A 2010 Correlation between nanoindentation and nanoscratch properties of carbon nanotube reinforced aluminum composite coatings *Surface and Coatings Technology* **204** 2709-15
[51] Sribalaji M, Rahman O A, Laha T and Keshri A K 2016 Nanoindentation and nanoscratch behavior of electroless deposited nickel-phosphorous coating *Materials Chemistry and Physics* **177** 220-8
[52] Akhtari Zavareh M, Sarhan A A D M, Karimzadeh R and Singh R S A l K 2018 Analysis of corrosion protection behavior of Al2O3-TiO2 oxide ceramic coating on carbon steel pipes for petroleum industry *Ceramics International* **44** 5967-75

CHAPTER TWO: LITERATURE REVIEW

Chapter Overview

This chapter provides a comprehensive literature review on the current status of surface modification techniques for hip implant applications. This chapter is divided into five key sections: Section 2.1 discusses the importance of surface modification techniques to enhance the useful life of hip implants. Section 2.2 presents commonly used artificial hip implants and limitations of the different materials used for hip implant applications. Section 2.3 investigates on the conventional methods of surface modification techniques to enhance the useful life of implants. This section analyses various surface modification techniques, materials and surface properties with a focus on tribological performance. This review helps to identify the most suitable surface modification technique for the longevity of artificial hip implants. Section 2.4 highlights the potential of AM Ti6Al4V implants and its existing challenges for hip implants application. Section 2.5, final section, summarises the outcome from the literature review and outlines the perspective for further improvement. The optimised surface modification technique, after a comprehensive literature review, was applied in this PhD project.

*The part of these research findings have been published in ***Science and Technology of advanced Materials*****.**
Ghosh, Subir, and Abanteriba, Sylvester. "***Status of surface modification techniques for artificial hip implants***." Science and Technology of advanced Materials 17.1 (2016): 715-735.

Surface modification techniques have been developed significantly in the last couple of decades for enhanced tribological performances of artificial hip implants. Surface modification technique improves biological, chemical and mechanical properties of joint contact surfaces. Mostly effective techniques, namely surface texturing, surface coating, and surface grafting; are applied to reduce the friction and the wear of artificial implants.

The literature reveals that appropriately modified surfaces exhibited reduced friction and enhanced wear resistance of the contact surfaces. In case of surface texturing and surface coating, wear rates are still noticeable. In textured surface the associated flow aids to release entrapped wear debris resulted in an increment of the wear particles generation. The earlier delamination of coating materials due to poor adhesion and graphitisation transformation has limited the use of surface coating techniques. Moreover, the produced wear debris has adverse biological reactions with body fluids. Conversely, the surface grafting technique provides phospholipid like layer that exhibited lower friction and almost zero wear rates even after a more extended period of friction test. These findings suggest that further investigations are needed to identify the role of surface grafting on film formation, and heat resistance under various physiological hip joint conditions for improved arthroplasty performance and longevity of hip implants.

2.1 Introduction

THA is one of the most successful treatments for patients with severe hip osteoarthritis and rheumatoid arthritis. This treatment has improved the quality of life (QOL) by introducing a solution to the affected joints. On the other hand, demand for THA treatments has been increased steadily because of the rise in the population of elderly [53]. Approximately one of every four adults is affected by some form of arthritis in the United States [54]. According to leading researcher Access Economics, current trends suggest that 7 million Australians will

suffer from some form of arthritis by 2050 [55]. Improvements in the THA treatments are in high demand due to implant wear, dislocation, fracture, and aseptic loosening. However, aseptic loosening resulted in periprosthetic osteolysis remains a serious problem, which degrades prosthetic joint survival and clinical success. Up to 20% of patients implanted with conventional polyethylene (PE) suffer from aseptic loosening within 10 years of implantation, and some of them become disabled due to pain and lack of functionality [56]. The revision rate would be higher for younger patients due to their longer life expectancy. This number would be estimated to be double by the year 2026, which would lead to a cumulative social and economic impact if some preventive mechanisms could not be successfully implemented to avoid the revision surgery [57]. The high friction and consequent wear of artificial hip implants are the major issues to avoid the revision surgery after 10-15 years of implantation [24, 58]. Therefore, surface modification techniques can be developed to improve the implant quality considering the lifespan of younger patients.

Various surface modification techniques have been developed so far to enhance the useful life of joint prostheses, among them surface texturing (dimpling), and surface coatings are prominent [59, 60]. Surface modification techniques are generally applied to femoral head surfaces. Surface texturing improves the tribological performance of the implant. It increases the film thickness between the mating components by acting as a lubricant reservoir. This film provides additional lift effect by generating hydrodynamic pressure between the converging surfaces. Thus, it protects the surfaces from coming into contact and prevents the generation of solid friction. The dimples produced by surface texturing can trap wear debris in boundary lubrication condition.

Surface texturing technique decreases the contact area and reduces adhesion. Roy *et al.* [58] reported nearly 22% friction and 53% wear reduction for the textured disk surfaces compared to non-textured disk surfaces. They also showed that dimple density and depth have

significant influences on improving tribological performances. Ghosh *et al.* [23] also found similar results and comparatively better wear resistance provided by textured surfaces under body oriented fluids to water lubricants.

Further investigations in a combination of texturing and coating techniques had been reported with improved wear performance [1]. Surface coating technique has become the most promising approach since the last decades, to engineer the bearing surfaces of artificial joints due to its highly wear-resistant coating. This technique increases the mechanical properties of the contacting surface, enhance wear and corrosion resistance of the contact surfaces. The graphite coated surface form protecting layer on the counterparts and act as a solid lubricant. Choudhury *et al.* [1] reported the superior tribological results at diamond-like-carbon (DLC)/polyethylene sliding pairs whereas, a-C:N provided the finest performance at DLC/DLC pairs. Few researchers also focussed on the interlayer of multi-layer coating to improve the friction and wear resistance [61, 62].

Another surface modification technique known as surface grafting on acetabular liner has a significant influence on friction and wear reduction for joint implants [26]. The grafted surface for other medical devices inhibits biological reactions when they are in contact with living organisms and are now clinically used on the surfaces of intravascular stents, soft contact lenses, artificial lungs and hearts under the authorisation of the Food and Drug Administration of the United States [29]. It is recognised that the nano-meter scaled phospholipid layer covers articular cartilage and protects the articulating surface from mechanical wear and facilitates a smooth motion of joint during daily activities [27]. Grafted materials are biologically inert and do not cause consequent bone-resorptive responses, indicating that this technique prevents wear particles production and biological reactions to such materials in THA [63].

Though improvements in implant design and materials have provided many people improved QOL, still, there is a considerable room for further developments. This review

discusses and collates recent findings on detailed surface modification techniques for artificial hip implants. This overview illustrates the tribological aspect of artificial hip interfaces, as well as commonly used implants and their merits and demerits based on useful life and functionality of artificial implants, both *in vivo* and *in vitro* environment. This review aims to identify the most acceptable surface modifications technique for the longevity of artificial hip implants. Finally, the concepts of additive manufactured implants and their existing challenges will be discussed. The possible solution for the long-term success of AM parts will also be outlined.

2.2 Artificial hip joint prostheses

According to the National Joint Replacement annual report in 2015, published by Australian Orthopaedic Association, 43,183 hip replacements were reported to the registry in 2014 which were 6.3% higher than those in 2013 [55]. The number of primary total hip replacement due to severe arthritis has been increased by 72.5% compared to 2003 [55]. The revision in replacement surgery is a foremost problem in THA treatments. The revision rate was an increase of 25.1% compared to 2003. However, the revision burden has been decreased by 2.4% in the last 4 years. The main reason behind the decrease in revision rate is due to the implementation of larger size femoral head. It was found that femoral head size equal to or larger than 32 mm is effective in reducing the revision rate [64]. The most common reasons for revision are loosening/lysis (47.8%), prosthesis dislocation (14.1%), infection (14.1%), and fracture (10.4%) [55]. The loosening possibly caused by an inflammatory reaction is due to the production of small wear particles. Moreover, high friction and consequent wear have a significant effect on the movement of the femoral head. The movement of the femoral head causes the prosthetic dislocation. Hence, the minimisation of friction and wear is desirable to prevent the revision surgery of artificial hip implants. This section will describe different artificial joint interfaces. Commonly used material combinations for hip prostheses are: 1)

metal on polyethylene (MoP), 2) ceramic on polyethylene (CoP), 3) ceramic on ceramic (CoC), 4) ceramic on metal (CoM), 5) metal on ceramic (MoC), and 6) metal on metal (MoM). Generally, two types of femoral head (metal and ceramic) and three types of acetabular cup (metal, ceramic, and polyethylene) are used as a combination of bearing surface for artificial hip implants.

2.2.1 MoP hip implants

The most common THA material combination has been a metal femoral head paired with polyethylene acetabular cup (MoP implants). Metals have been used as implants for more than 100 years ago [65]. Different types of metals are used as femoral components, such as Titanium (Ti), Ti alloys, Cobalt-chromium alloys (CoCrMo) and stainless steel. The use of austenitic stainless steel has been limited due to its poor wear resistance properties. Ti alloys and CoCrMo are frequently used in THA. CoCr has been comprehensively employed to fabricate implants prior to the introduction of AM for biomedical applications. A comparative study showed that the highest linear wear was about 1 micron for Ti6Al4V alloys followed by stainless steel (0.2 micron) and CoCrMo (0.1 micron) after one million cycles [66]. Pure Ti and Ti alloys are now the most attractive metallic materials for hip implant applications owing to their high strength, lightweight, formability and excellent corrosion resistance. In addition, the excellent fatigue strength of Ti6Al4V gives a great advantage for lifetime implantations [65, 67].

Polyethylene as acetabular cup has been a leading material for the last 30 years because of its low friction coefficient property with metallic counterparts. Recently, a newer CLPE has been developed that possesses improved wear resistance properties with enhanced mechanical properties [68]. It had been irradiated with a high dose of (~100 kGy) gamma rays or a electron beam. Cross-linking reduces the degree of molecular orientation, and thus improves the wear

resistance [69]. PolyarylEtherKeton (PEEK) is highly used biomateral in orthopaedic industry, especially for orthopaedic implants due to their desired mechanical properties, biocompatibility and stability at high temperature. However, PEEK fabricated implants are found to be bio-inert and does not allow bone in-growth [70]. Polyethylene counterparts experience maximum wear against hard metal femoral heads in MoP hip implants. The generated wear debris mixture in the lubricant further increase the wear rate. Likewise, the produced wear particles enter into the periprosthetic tissues and react with macrophages and giant cells. Thereafter, the macrophages release pro-inflammatory cytokines leading to osteolysis and subsequent loosening of the prostheses [71]. As a result, surface modification like surface coating and microarchitecture enhancement are applied to improve its bioactive and osseointegration properties.

2.2.2 CoP hip implants

Ceramic and polyethylene constitute a promising implant pair, because both materials exhibit lower friction coefficient, consequently less wear. The CoP implants have better wettability than MoP implants. Currently used ceramic materials for hip implants are alumina (Al_2O_3), zirconia (ZrO_2), and alumina-zirconia composite. The commonly used alumina ceramic has excellent corrosion resistance, excellent biocompatibility, high strength and useful wear resistance ability. The significant advantage of alumina material in implant application is their highly polished (±10 nm) surface that leads to low friction and wear. However, alumina has low fracture toughness, which is the reason for early failure of CoP implants. The failure of alumina due to its high brittleness and slow crack growth could be minimised using the composite material of zirconia and alumina. Zirconia is exceedingly hard with excellent mechanical properties. The clinical success of Al_2O_3 bearing materials was reported in follow-up studies where the low mechanical load is applicable [72]. Ceramic implants have lower

osteoconductivity with surrounding tissues compared to metal implants. This poor interfacial bonding between an implant and tissue could lead to aseptic loosening of the implants and subsequent failure of the device [73]. Therefore, the development of an intermediate layer is essential to improve the osseointegration of the implants.

2.2.3 CoC hip implants

CoC implants provide low friction and wear during sliding motion that is essential for its longevity. In this case, alumina on alumina, zirconia on alumina is usually used as a prosthesis pair. Villermaux *et al.* [74] reported extensively low wear at 0.1 mm^3 per million cycles for zirconia femoral heads paired with alumina that is significantly lower compared to other hip implants. However, one of the major problems associated with CoC implants is squeaking. This event happens because of direct contact of two hard surfaces. Squeaking was found to have a significant effect on wear mechanism of CoC hip implants [75]. It creates vibration in the system during sliding or rolling action.

Fracture toughness of zirconia was about 2 times greater than alumina that increased the crack propagation resistance [76]. It possesses high bending strength. As a consequence, zirconia has opened a new way in implant design. However, zirconia exhibits a progressive aging degradation in presence of fluids [77]. A zirconia-alumina composite could provide a better service considering the limitation of earlier developed ceramics. Researchers found that a material composite combination of 80% tetragonal zirconia poly-crystals and 20% alumina, exhibited outstanding mechanical and tribological performance [78]. Despite the improved friction and wear performance by CoC implants, the stress shielding effect has limited their application in hip implants.

2.2.4 CoM and MoC hip implants

Ceramic heads-metal cups for CoM, and metal heads-ceramic cups for MoC, hip implants, respectively, are used in a small number of THA. Due to the high wear rate of polyethylene, other materials have grown in preference as alternative bearings for hip implants. Ceramic is comparatively harder than the metal substrate. As a result, the wear rate is high for metals while ceramic act as a counterpart. MoC implant has more friction and more wear than that of the CoM implant. When the femoral metal head face high loads and ceramic counterparts move over them, they release more metal ions from the surface. However, the tribological performance of MoC and CoM implants are found to be similar for larger size femoral head.

2.2.5 MoM hip implants

The MoM hip implant had grown in interest due to its improved wear resistance properties. The metal possesses excellent mechanical properties, electrical and thermal conductivity. THA procedures using metal on metal bearing are hardly carried out nowadays. Though the MoM exhibits low wear volume, it generates a high concentration of metal ions. Nanoscale size wear particles of metals are believed to have adverse local tissue reactions comprising metal hypersensitivity and allergic reactions [79]. It causes pseudo-tumour, large effusion and/or periprosthetic bone resorption [79]. Increased metal ion concentrations in organs resulted in osteolysis, patient pain, and corresponding wear and failure of the implant [80]. CoCrMo releases Cr, Mo and Ni metal ions and forms a passive oxide layer in human body environment [81]. The corrosion products of CoCrMo have been identified as toxic to the human body [82]. Therefore, Ti alloys are considered more reliable for hip implants considering the toxicity of other metal bearings.

2.3 Surface modification techniques and their recent developments

Surface modification of biomaterials has improved multi-functionality, tribological and mechanical properties as well as biocompatibility of artificial devices while avoiding the need for substantial development costs in terms of money and time [83]. It changes the physiochemical properties of materials, such as surface charge, energy and composition. Optimal surface, physical and chemical properties could be achieved by altering the functionality of bulk materials. Wear rates of the implants can be reduced by making implant with high wear resistance materials. Researchers have developed new alloy materials in the last two decades that can resist wear [84-87]. Nevertheless, the physiological condition *in vivo* is different from *in vitro* condition. As a result, the success of the implant materials *in vitro* does not always bring success in clinical outcomes. It has been observed that highly resistant materials did not always perform well under physiological body fluids. To improve the implant quality and longevity, friction and wear reduction is the best solution. Surface modification technique is becoming an increasingly popular method due to its improved performance in implant applications [37, 88-90]. However, wear is still inevitable. Therefore, further development in surface modification technique is required to overcome the challenges of high friction and consequent wear. The following section will highlight the detailed description of different surface modification techniques for artificial hip implants. Recent studies and development on surface modification techniques will also be outlined.

2.3.1 Surface texturing

Surface texturing technique has been introduced in implant design to get benefits of the lubricating effect. It was previously utilised on golf ball surfaces to improve their aerodynamic characteristics [91]. The spiral grooves were also produced on bearings to build up the pressure

to separate the bearing surfaces [92]. Surface texturing has now many applications in the field of tribology, optics, physics, energetics, biomedicine, electronics and metrology [93].

Surface texturing is popular in implant design due to its improved friction and tribological performances. This technique produces micro-textures on implant surfaces that comprises number of benefits over smooth surfaces— 1) acts as a lubricant reservoir [94], 2) increases the hydrodynamic pressure under sliding condition [95], 3) stores the produced wear debris or foreign materials in dimples [96], 4) decreases the contact area [97], and finally 5) minimises friction and wear [58]. The textured surface is very effective, especially in boundary and elastohydrodynamic regimes. Micro-dimples provide additional hydrodynamic pressure besides the pressure generated by natural mechanisms. Correct optimisation of its geometrical parameters initially confirms micro-dimples functionality. Nevertheless, the influence of dimples quality is not avoidable. Fig. 2.1 (a) and (b) show the application of surface texturing on articulating femoral head and surface morphology of different types of fabricated textured surfaces respectively.

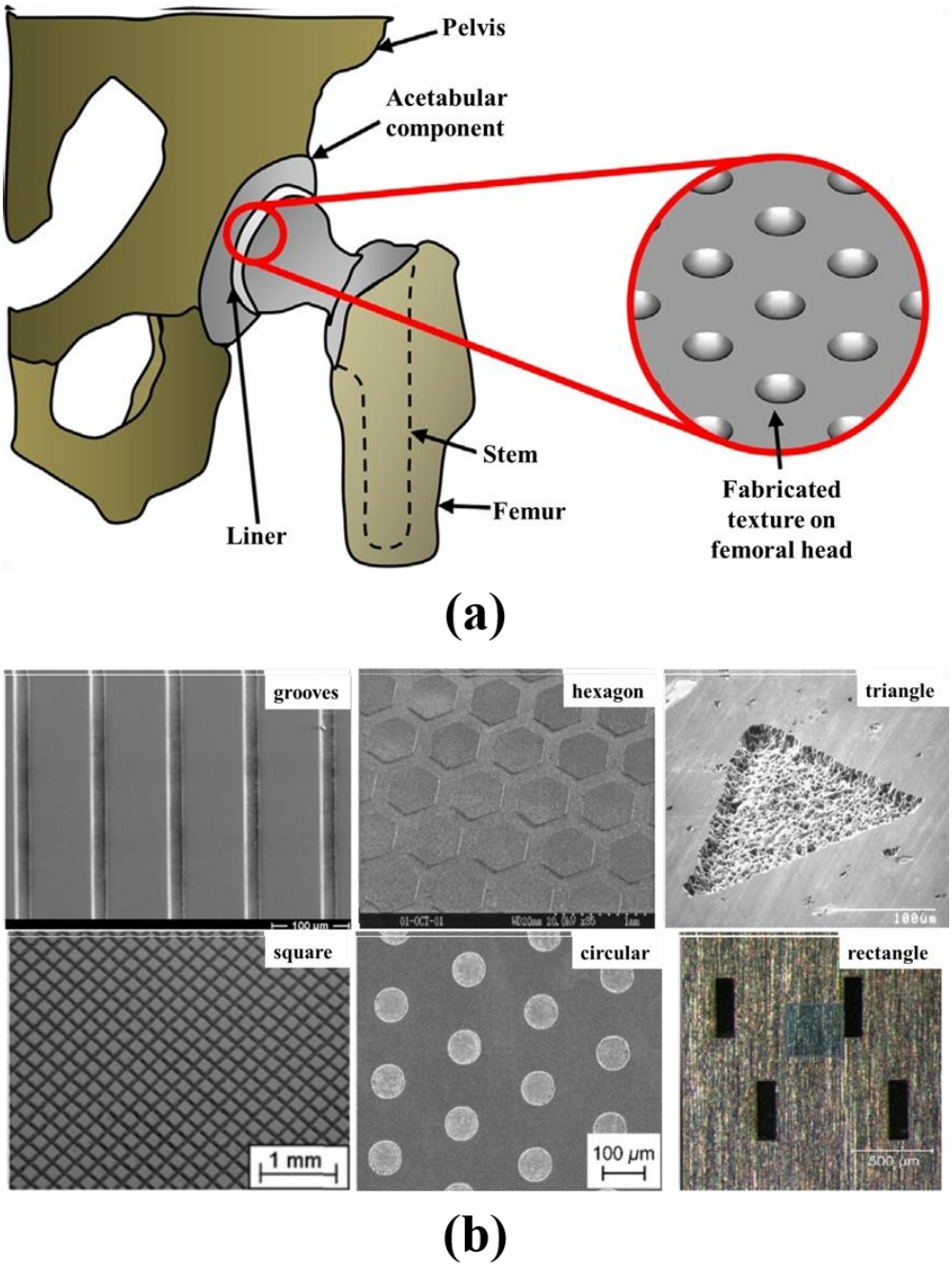

Fig. 2.1 a)The application of Surface texturing technique on femoral head surface [98] and b) surface morphology of different types of fabricated textured surface [60].

2.3.1.1 Recent studies of surface texturing for improved tribological performance

Tribological performance of an implant surface does not depend only on the surface texturing technique but also on the geometrical parameters, such as dimple diameter, depth,

shape, pattern and density [99]. Roy *et al.* [58] revealed that dimple diameter of 400 μm with 15% density showed the enhanced friction and wear performance compared to other geometries (diameter: 300 μm or 400 μm and density: 5% or 10%). They revealed that large-sized dimple with high density reduced friction and wear. Conversely, Huang *et al.* [100] reported the enhanced lubricating effect of the small size dimple with high pore density due to the uniform distribution of lubricant in micro-dimples. The lubricant squeezes out from dimples to minimise the sliding contact under loading conditions. However, surface roughness could be increased with dimple density. As a result, surface defects possibly increased due to the production of more micro-dimples. There is a chance of high friction and fatigue wear if the surface defects increase subsurface stress. Keneta *et al.* [101] observed the reduction in local film thickness due to the increase in dimple depth. Thus, the low film thickness led to high friction coefficient and consequent wear. Circular shaped dimples are commonly applied because it can be easily fabricated with high precision. Ito *et al.* [102] investigated the tribological performance of circular textured Co-Cr-Mo surface and observed a 17% reduction in friction and a 36% polyethylene wear reduction. A regular shape such as ellipse with a round or curved edge was observed to minimise the friction and to enhance load carrying capacity considerably vis-a-vis other shapes.

On the other hand, Shen *et al.* [103] reported significant improvement of tribological performance applying trapezoidal-like dimple during bidirectional hydrodynamic sliding. Researchers are trying to optimise the geometries of dimples using ordinary shape. Unfortunately, no unique approach had been developed to reduce friction and wear in view of geometries of dimples in past decades. Different researchers suggested different optimum geometrical characteristics that do not minimise the gap of understanding the influence of surface texturing for better tribological performances [104-107]. The operating conditions are also influential factors to optimise the surface texturing. The hydrodynamic pressure is

increased at high speed and low load conditions where maximum load is carried out by the operating fluid [108-110]. Textured surface provides additional support due to converging film thickness generated by hydrodynamic pressure at low speed and high load conditions, as a result, the surfaces do not come in contact. The ability to withstand the load, increases with increment of lubricant film pressure [111]. By contrast, the maximum load is carried out by the textured surface under high load and low-speed condition. In this condition, textured surface acts as a lubricant reservoir and a significant portion of the load is carried through the surface bearing contacts [111, 112].

Interestingly, Yan *et al.* [113] reported that dimple density is the dominant factor independent of the different operating conditions. However, Ghosh *et al.* [114] revealed that if the textured surface was not good enough to support high load, then there is a significant increase in friction and wear with an increase in load. The textured surface produced wear particles that act as a third body in wear mechanism. The textured surface showed improved tribological performance under body oriented fluid compared to water lubricant, even at high load. Choudhury *et al.* [115] reported good load bearing capability of a dimpled surface in hip simulator study. They showed that the dimpled surface exhibits higher film thickness compared to the flat surface. The load is supported by the fluid hydrodynamic pressure.

Ghosh *et al.* [3] summarised the recent tribological studies of artificial implants on last 12 years in Table 1 (details are provided in Appendix A) to present the effect of surface texturing for improvement of friction and wear performance. It indicates that laser surface texturing (LST) and computer numerical controlled (CNC) machining is more popular than electro-discharge machining (EDM) as a dimple fabrication technique. Textured surface showed a significant reduction in friction and wear in most literature reviews though the applied load was different in different studies. Hence, it is difficult to optimise the surface texturing by evaluating friction and wear rate under different loading conditions. Few

researchers suggested incorporating coating technique with texturing [114, 115]. The thin film coatings on the textured surface provided very low friction resulted in minimising the problem associated with primary high friction resulted from low contact width and wedge angle for the textured surface due to the line contact [116]. Recent studies revealed that DLC coated textured surface enhanced wear resistance properties of implant materials [1, 117]. He *et al.* [117] observed that DLC coated textured surface with a 24% dimple density exhibited higher friction but lower wear rate in comparison with a 44% dimple density. Both of them provided improved wear rate but higher friction than smooth DLC coated surface. It could be concluded that low friction is not always essential to reduce the wear rate. Choudhury *et al.* [1] showed that the enhanced friction and wear performance were independent on the textured surface. They concluded that DLC coated surfaces exhibited the lowest friction coefficient and it was nearly the same for the dimpled and non-dimpled surface. Choudhury *et al.* [115] mentioned in the different study that DLC coated dimpled surface has dual benefits: DLC coated surface reduces the friction coefficient whereas dimpled surface improves the lubricating effect by enhancing the hydrodynamic lift between the sliding contact.

Overall, the surface texturing technique exhibited a significant reduction of friction coefficient for the implant surfaces. However, the wear rate is still significantly high for the textured surface. Fig. 2.2 shows the wear mechanism of implant surfaces in presence/absence of dimples. The wear debris generated due to the sliding of contact interfaces leads to increase of wear if the surface is not dimpled suitably. Scratch marks observed in Fig. 2.2(a) were due to the presence of wear particles on the contact interfaces and Fig. 2.2(b) shows that dimple depth was not sufficient to trap wear debris inside the dimples [118]. As a result, the wear rate increased with the sliding time as more debris was generated due to friction. Fig. 2.2 (c) shows that the proper dimple depth trapped the wear particles properly and thus reduced friction and wear of the contact interfaces.

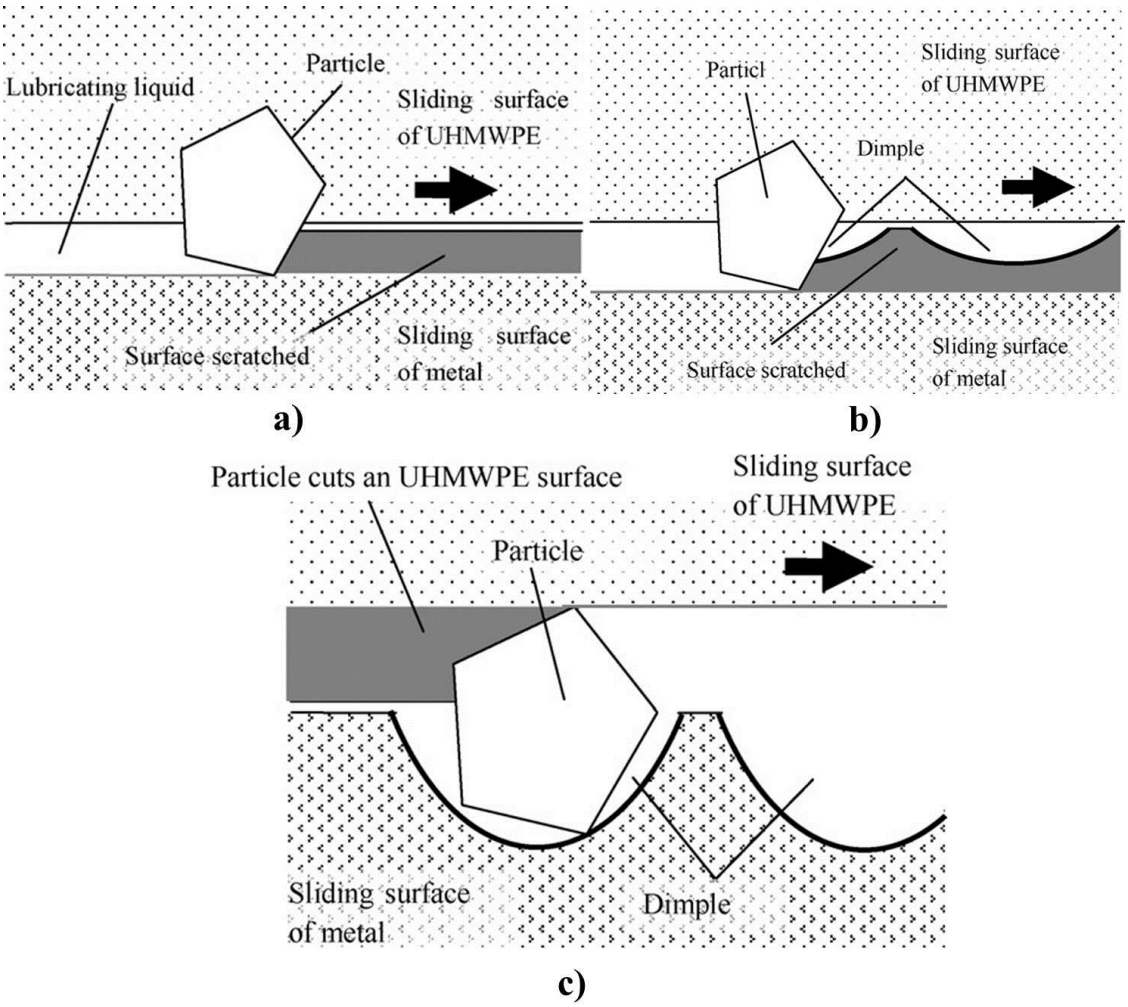

Fig. 2.2 Wear mechanism for a) non-dimpled surfaces, b) low depth dimpled surfaces and c) high depth dimpled surfaces [118].

Meng *et al.* [119] reported that the microscale flow vortex existing in dimple enhanced hydrodynamic pressure that could release the entrapped wear debris from the dimples. The effect of vortex flow could be minimised by increasing the dimple depth. Kai *et al.* [120] concluded that the effect of vortex flow becomes neutral at the deep zone of the high depth dimples and the velocity of the particles approached to zero at the centre of the dimples. Dimple with high depth could have an adverse effect on tribological outcomes by reducing the hydrodynamic pressure at the contact interfaces. In this case, the lubricating effect of the dimple would not be useful.

2.3.2 Surface coating

The application of surface coatings could improve wear resistant to artificial implants. The surface coating provides morphological (topographical design), physiochemical (changes to surface energy, charge, or composition), and biochemical adaptations (how the cells react) to existing bulk materials. It reduces adverse cellular response caused by generated wear particles and improves the useful life of the artificial implant. Various hard and wear resistant coatings, such as metal nitrides, carbides, carbonitrides, and DLC are applied on the surface of artificial implants. These coatings enhance the mechanical and physical properties, such as hardness, elastic strain and wettability of the surface [121, 122]. The improved wettability of the surface leads to low friction and consequently low wear of implant materials. Surface coating prevents the bulk surface from tribo-corrosion [123, 124]. The performance of the coated surface also depends on the coating deposition technique. An ideal deposition process can provide a quality surface with a dense homogenous coating surface and excellent permanent adhesion to the substrate.

2.3.2.1 Recent studies of surface coating for improved tribological performance

Though metal on metal hip bearings reduced the linear wear about 40 times and volumetric wear about 200 times compared to metal on UHMWPE [125], the toxicity of metallic or UHMWPE debris limited their application in hip implants. Therefore, the surface coating has been introduced to avoid the adverse effect of a metallic surface. Coated surface provides a protective layer on the metal surface and improves the mechanical properties of the implant surface. Surface coating reduces surface roughness resulted in a reduction in friction and wear. It was pointed out that Ta coated on Co–Cr–Mo with 5–12 nm surface roughness displayed low wear rate in the range of $4\times10^{-7} – 5\times10^{-7}$ mm^3 $N^{-1}m^{-1}$ [126] whereas Ta coated

on Co-Cr-Mo surface with a surface roughness of 40 nm exhibited a high wear rate in the range of $0.755\times10^{-4} - 1.249\times10^{-4}$ $mm^3N^{-1}m^{-1}$ [127].

Moreover, TiN coating with a high surface roughness of 169 nm exhibited the high wear rate at 6×10^{-4} mm^3 N^{-1} m^{-1}. It suggests that low surface roughness is essential to minimise friction and wear of hip implants. Low surface roughness leads to better surface wettability [128]. The surfaces with good wettability enhance lubrication and perform well even in absence of lubricant. DLC coatings had better wettability compared to GLC, Ta, TiN coatings.

Ghosh *et al.* [3] summarised the recent tribological studies of artificial implants on last 12 years in Table 2 (details are provided in Appendix B). The presented data shows the effect of surface coating on the improvement of friction and wear performance. It is noticed that there was no standardisation in the selection of experimental set-up, such as working load, contact pressure, frequency, testing lubricant, type of simulator, coating technique and thickness. In this situation, it is difficult to compare friction and wear results between different studies. However, the significant reduction in friction and wear value was obtained by the DLC coated surface. Magnetron sputtering method has been widely used in recent tribological studies. Another study conducted by Wang *et al.* [129] pointed out that CrN had better corrosion and wear resistance ability compared to TiN, TiA1N coatings under synovial body fluid.

Overall, DLC coating was superior in tribological performance under body fluid. The DLC (a-C:H /Ta-C) films significantly improved the surface hardness [1]. Fig. 2.3 shows the cross-sectional SEM images of deposited (a) a-C:H and (b)Ta-C DLC films on a stainless-steel substrate.

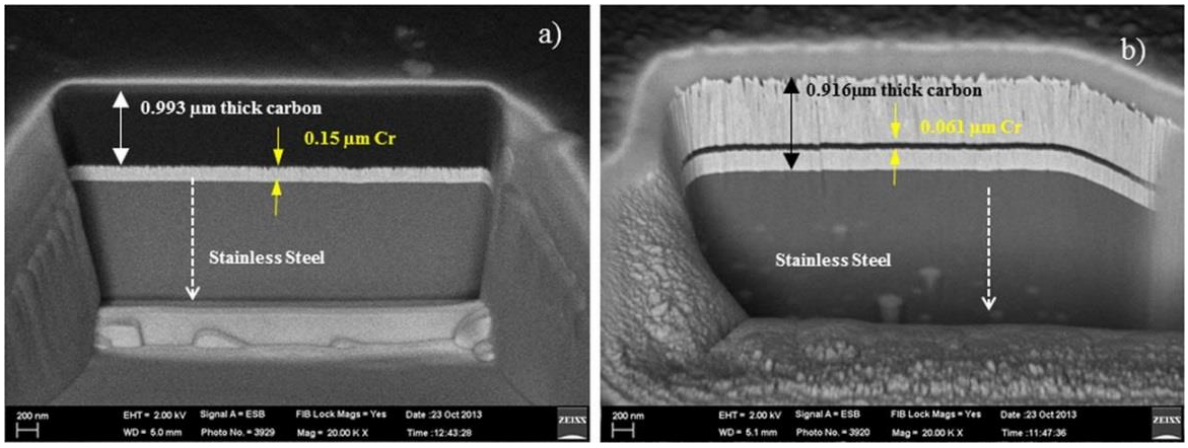

Fig. 2.3 Cross-sectional SEM images of deposited (a) a-C:H and (b) Ta-C on stainless steel [1].

It is observed that Cr was used as an interlayer in both cases to provide strong adhesive strength and bonding between the steel and the carbon layers [130]. Researchers suggest that multilayer coating could improve the wear resistance of implant surface. The intermediate layers, such as chromium nitride (CrN), DLC and titanium nitride (TiN) increased the hardness of the implant surface. CrN increased the bonding strength between the coated material and the substrate [131]. UHMWPE is favourable as a top layer for its better wear resistance properties compared to other polymers [132]. Researchers recommend coating thickness over 1 µm including an interlayer because very thin DLC layers produced pinholes during sliding [61, 133]. The working lubricant can penetrate through these pinholes and consequently, increase the corrosion rate. Thick DLC film associated with interlayer could protect coated surface from corrosion. Adhesion of DLC coated surface can also be improved by changing substrate surface preparation, introducing interlayers, such as CrN, N^+ ion implantation or changing the DLC deposition parameters. It was reported that DLC associated with CrN provided the lowest friction between cemented carbide (WC) and Si(100) wafers because it increased corrosion resistance and adhesion of the coated layer [129]. However, in some cases a slow crack advancement or interlayer dissolution results delaying delamination in corrosive media, such

as body fluid, leading good mechanical adhesion during normal delamination tests [134]. Ghosh *et al.* [114] reported the significant reduction in friction and wear for DLC coated dimpled surface is independent of lubricating environment. The study reported that the dimpled surface acted as a lubricant and wear debris reservoir while DLC coated surface improved the mechanical properties. Therefore, DLC coated dimpled surface exhibited improved tribological performance. Conversely, Choudhury *et al.* [1] found a negligible difference in friction coefficient between dimpled and non-dimpled surfaces, but a-C:H coated surface exhibited the lowest friction coefficient in comparison with dimpled and non-dimpled. Fig. 2.4 summarises friction coefficient results for different prosthesis heads.

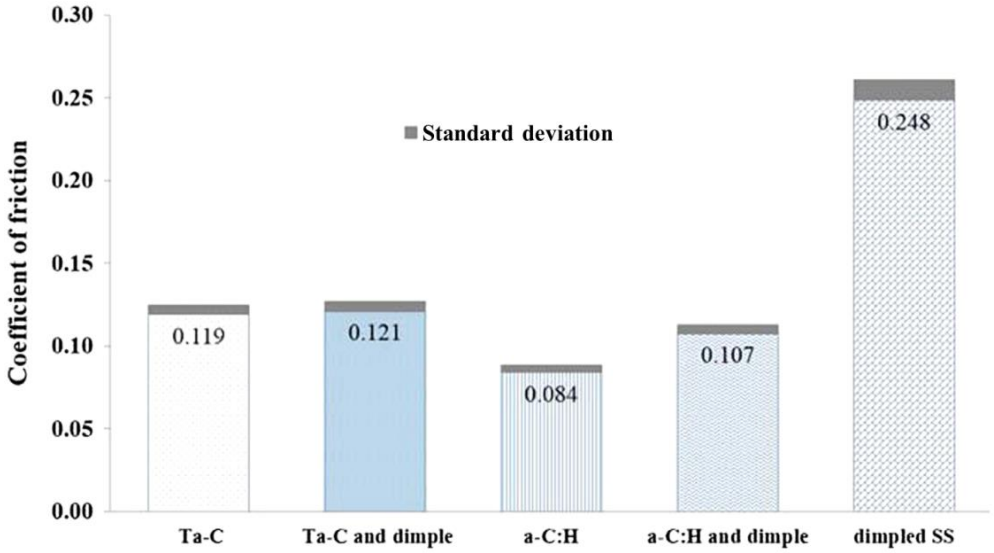

Fig. 2.4 Friction coefficient results for different prosthesis heads [1].

Fig. 2.5 illustrates surface morphology of coated surfaces at different conditions. Major drawbacks of the DLC film was early delamination *in vitro* test due to poor adhesion [23]. Film transfer was observed in Fig. 2.5 (b) due to the graphitisation of the DLC coating, which was caused after a certain period of friction tests. The full delamination of the coated surface was witnessed at high load, Fig. 2.5 (c). The generated wear debris exacerbated the wear rate. The

gain pull out on deposited surfaces were also observed because of generating the large size wear particles under sliding contact (Fig. 2.5 (d)).

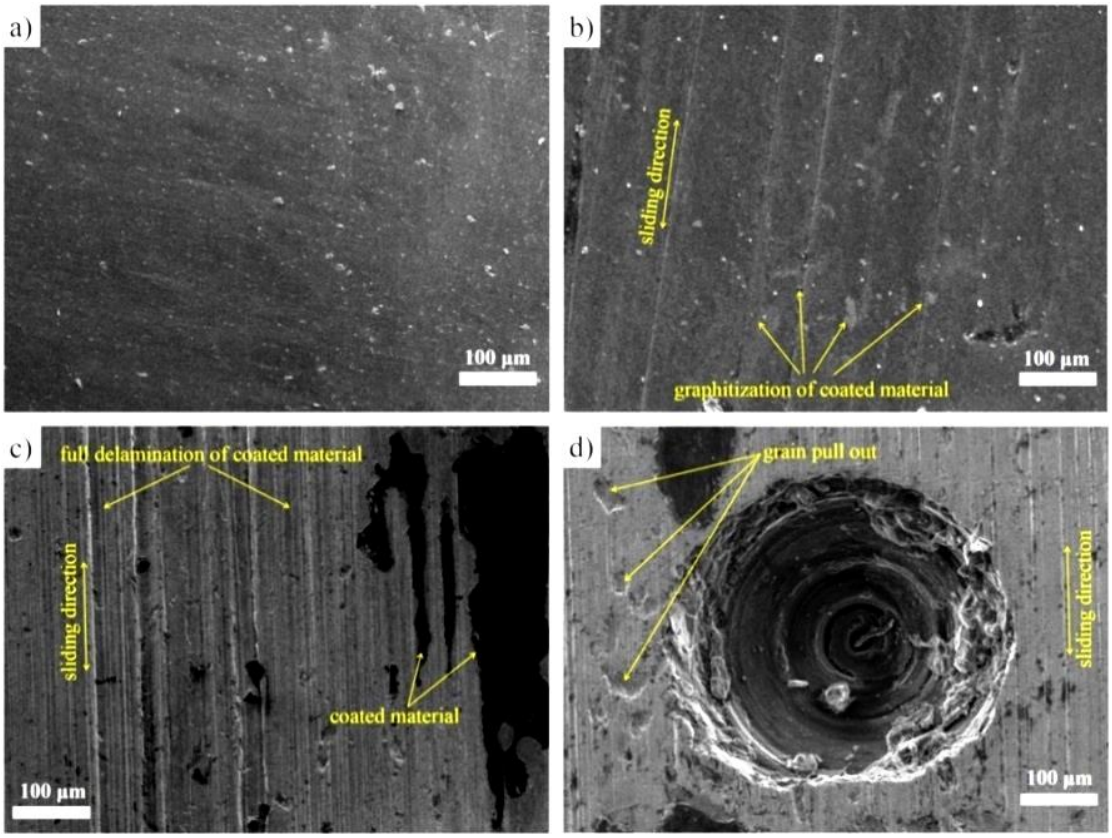

Fig. 2.5 SEM images showing (a) as-deposited DLC-coated surface, (b) formation of film transfer due to load, (c) full delamination of coated materials at higher loads, and (d) wear track on dimpled area [114].

Only a few clinical studies have been published on DLC coated bearing joints. The failure of the DLC coated surface *in vivo* caused by the crevice corrosion (CC) of the silicon-based interlayer [61, 134]. Instability of the interlayer towards the CC leads to the delamination of DLC coating. Hence, selection of interlayer is an essential factor in reducing corrosion under corrosive media. Surface modification by only DLC coating is not good enough to resist wear

of artificial joints nevertheless well-designed structure of DLC coated surface with low residual stress could provide the barrier for corrosion as well as delay the delamination *in vivo*.

The combined effect of surface coating and surface dimpling was also analysed. Continuous sliding motion between contact interfaces generated heat, which lowered the film hardness [117]. The generated wear particles also lowered the graphitisation temperature resulting in adhesive wear by the graphitising transformation. The smooth DLC coated surface directed to increased abrasive wear (Fig. 2.6(a)) that could be minimised with the dimpled coated surface by trapping produced wear particles (Fig. 2.6(b)).

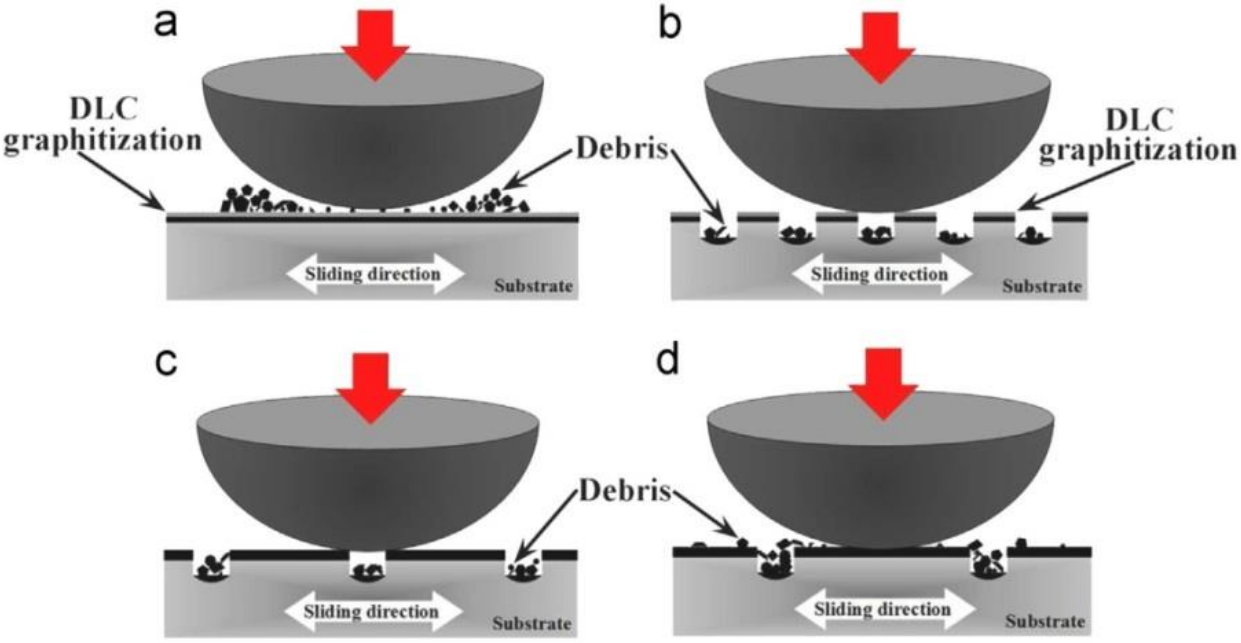

Fig. 2.6 Cross-sectional schematic view of the wear mechanism model for (a) DLC-smooth, (b) DLC with high density (c) DLC with suitable density (d) DLC with low density [117].

However, the dimples with high densities reduced the contact area and resulted in high contact pressure [117]. Dimples with low densities reduced the contact pressure as well as wear particles generation. The suitable dimples with low density and sufficient depth could minimise the graphitisation of coated surfaces (Fig. 2.6(c) & (d). The dimpled with coated surface would

be effective if the graphitisation of the coated surface could be prevented and wear debris generation could be minimised. Despite their significant improvement in friction results, further, wear resistance is expected for the longevity of the implant interfaces. Therefore, surface texturing and coating technique are still under investigation to improve wear performance for implant applications.

2.3.3 Surface grafting

The surface properties and its bulk properties play a significant role in success or failure of implant devices. The surface properties, such as wettability, chemical composition, softness/stiffness, porosity and roughness are vital factors for the performance of a material in a range of biological environment [135]. Nowadays, polymers are used as biomaterials. The bulk properties of polymers, such as conductivity, strength, stiffness and general resistance to deterioration, are considered for selection of polymer in biomedical applications [136]. The low molecular weight proteins start adsorbing on implant surfaces after implantation of biomaterials in a biological environment. The high rate of protein adsorption could result in high friction. However, protein adsorption depends on chemical composition, surface roughness and wettability of the surface.

Noteworthy, surface modification technique, such as polymer grafting is effective to avoid biofilm formation; thus, protects the surface from biofouling. It improves the wettability of the surface and provides an excellent hydrophilic surface. The polymer surfaces possess brush like hydrophilic structure that is assumed to be similar to the articular cartilage. The cartilage surface also shows the hydrophilic nature due to its water-soluble macromolecules [137]. These hydrophilic macromolecules stimulate fluid film formation and reduce the friction of the joints [138]. Fig. 2.7 shows the formation of a hydrated thin layer on polymer grafted CLPE surface.

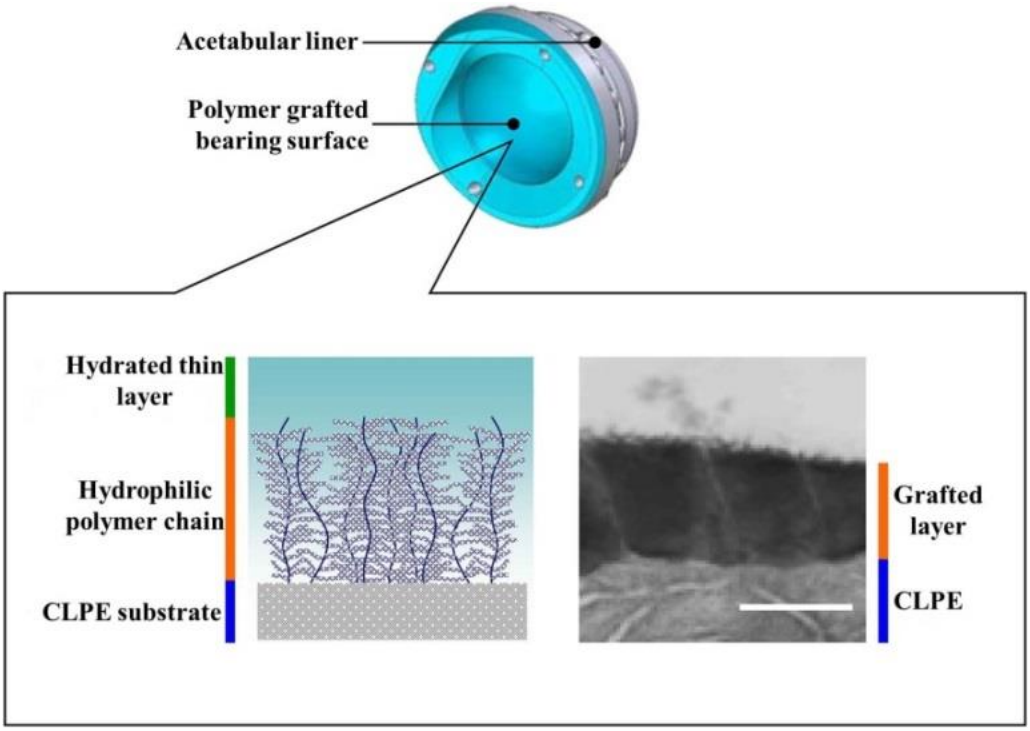

Fig. 2.7 Schema of a THA with the PMPC-grafted CLPE liner. A transmission electron microscope (TEM) image of the surface is shown on the right. Orange and blue lines indicate the PMPC layer and the liner surface, respectively [33].

It demonstrates that the grafted surface is mimicking the articular cartilage in physiological condition. Few researchers reported extremely hydrophilic polyelectrolyte brush surfaces exhibited high lubrication characteristics under water lubricant [139, 140]. Two grafting methods are commonly followed to graft flat surfaces. The "grafting to" approach could be used in physical polymer coatings, such as spin and dip coating [26]. It promotes poor adhesion between the coated materials and the substrate. The coated materials could dissolve in biological environments because the biological fluid acts as a good solvent for coated polymers. Conversely, "grafting from" synthesise high-density polymer brushes. These polymer brushes can change their conformation varying with graft density in solvents [141]. Fig. 2.8 shows that the grafted polymer conformation depends on the density of polymer chains.

The polymer structure seems to be like a mushroom at low graft density, and it turns into a brush-like structure at high graft density. It confirms their high thickness with increasing graft density that can vary from nanometres to micrometres. The polymer thickness for "grafting from" method is comparatively higher than that of "grafting to" method. Moro *et al.* [33] grafted the CLPE using PMPC. This PMPC grafted surface reduced protein adsorption. It exhibited strong covalent bonding between the PMPC and CLPE to improve weight bearing capacity. The low friction coefficient and nearly zero wear rates were reported in recent studies of PMPC grafting on CLPE surfaces [28, 142-144].

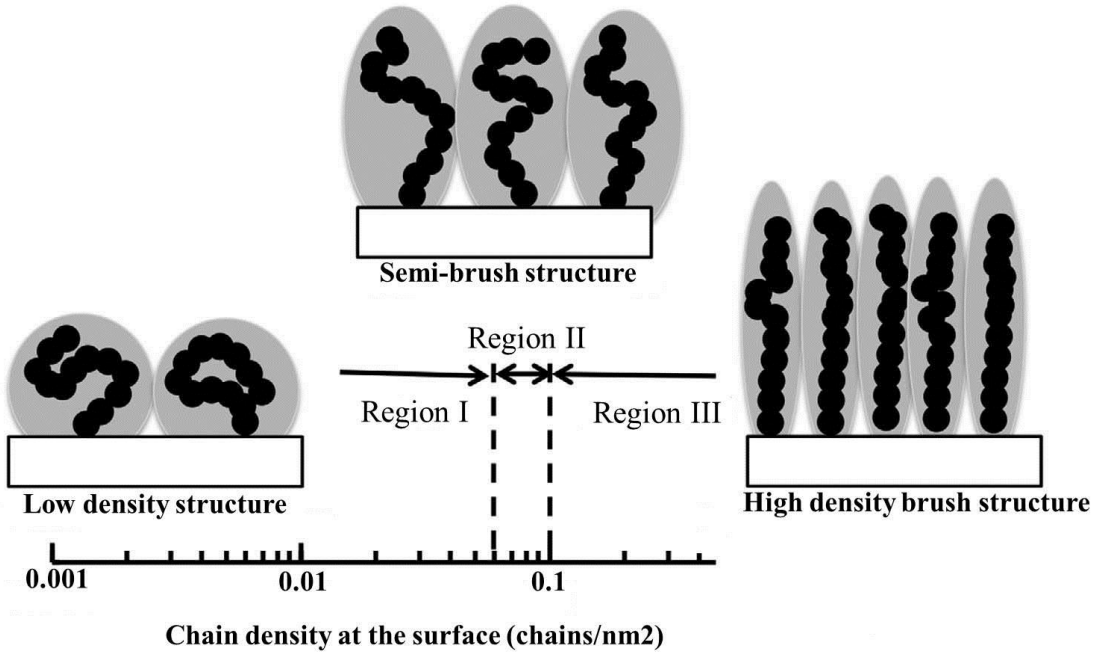

Fig. 2.8 Graft polymer conformation at various densities of polymer chains [26].

2.3.3.1 Recent studies of surface grafting for improved tribological performance

Surface grafting is a new technology developed to graft polymer on to the implant surfaces in order to achieve high lubricity, low friction and consequent wear. Few types of research have been conducted on polymer grafting in the field of joint implants. Ghosh *et al.* [3] summarised the recent tribological studies of artificial implants on the last 12 years in Table

3 (details are provided in Appendix C), this table presents the effect of surface grafting on the improvement of friction and wear performance. Standard experimental set-up, such as working load, contact pressure, frequency, testing lubricant, grafting technique, grafting thickness and type of simulator has been maintained between these studies. Different monomers, such as oligo(ethylene glycol) monomethacrylate (OEGMA), 2-(N, N-dimethylaminoethyl) methacrylate (DMAEMA) and 2-(methacryloylethyl) phosphoric acid (MPA) were used for grafting implant surface to improve tribological performances in previous studies [26, 29]. Kyomoto *et al.* [29] investigated the tribological performance of various polyelectrolyte-grafted CLPE samples under different lubrication conditions. Fig. 2.9 summarises dynamic friction results of various polyelectrolyte-grafted CLPE samples. The polyelectrolyte-grafted CLPE samples exhibited a lower friction coefficient than the untreated CLPE sample in all lubricants. No significant difference was observed between the lubricant for POEGMA-grafted and PMPC-grafted surface where PMPC provided the highest lubricity for the implant. However, the PDMAEMA-grafted surface exhibited a higher coefficient of friction in BS lubricant compared to water and SBF lubricants. Because, positively charged $-NH^{+}(CH_3)_2$ group of PDMAEMA attracted the negatively charged molecules in SBF. It increased the protein adsorption and resistance to motion [145].

Conversely, the negatively charged PMPA attracted the positively charged molecules and deterred negatively charged molecules and resulting shrinkage or bridging of negatively charged polyelectrolyte chains in a solution of positively charged inorganic ions [146]. It reduced the mobility of polymer chains and increased the resistance to sliding motion. Fig. 2.9 illustrates that PMPC grafted CLPE exhibited the lowest friction coefficient in all lubrication conditions. The zwitterionic PMPC-grafted surface attracts the water molecules and resists protein molecules and positively charged inorganic ions. As a result, it reduced protein adsorption as well as adhesive interaction between the implant interfaces.

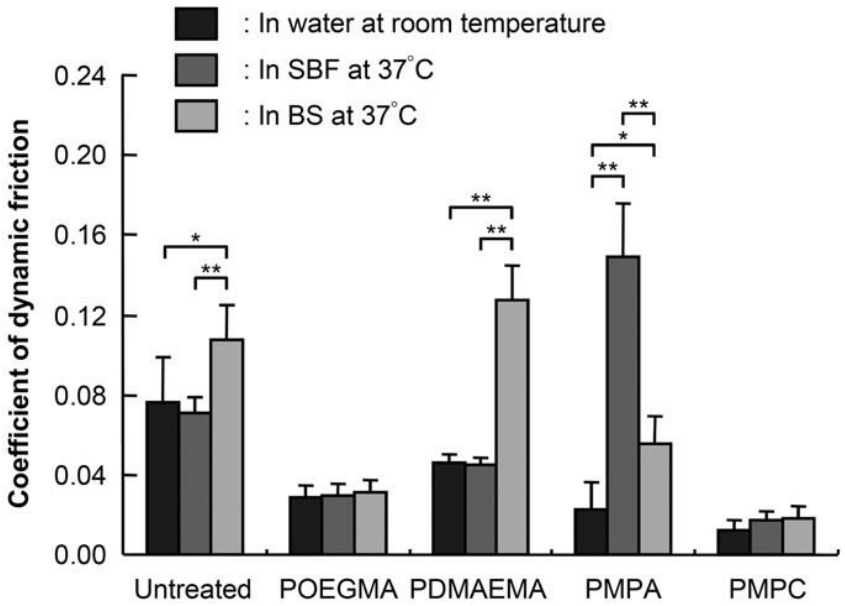

Fig. 2.9 Coefficient of dynamic friction of polyelectrolyte-grafted CLPE samples under various lubrication conditions. Data are expressed as means ± standard deviations. * Indicates $p < 0.05$, ** indicates $p < 0.01$, and N.S. indicates no statistical difference [26].

Recently, Takatori *et al.* [63] investigated a biocompatible and highly hydrophilic surface via nano-meter scaled grafting of PMPC onto CLPE. PMPC-grafted surfaces captured water molecules and reduced the friction between the bearing surfaces via hydration-lubrication mechanism [29]. They revealed that the PMPC grafted layer (100–150 nm in thickness) is mimicking hydrogel structures of articular cartilage and provides hydrophilicity and lubricity without affecting the physical or mechanical properties of the CLPE substrate. Also, they reported that PMPC-grafted particles were biologically inert and did not cause consequent bone-resorptive responses, indicating that this technique prevented wear particle production and biological reactions to these particles in THA [63]. Moro *et al.* [33] reported that PMPC-grafted CLPE surface significantly reduced the wear particles generation and the effect of the PMPC grafting was maintained through 70 million cycles. Yarimitsu *et al.* [34]

investigated the influence of dehydration and rehydration on the tribological performance of the PMPC-grafted CLPE surface and found no significant effect on reducing friction coefficient.

Similarly, vitamin E blending did not make any differences in friction results over the PMPC-grafted surface [142]. PMPC grafted CLPE receiving gamma-ray irradiation showed higher ultimate tensile strength and elongation than those receiving non-extra or plasma irradiation [144]. Conversely, work to failure of PMPC grafted CLPE with gamma-ray irradiation was significantly lower than those receiving non-extra or plasma irradiation. Plasma-irradiated PMPC-grafted CLPE showed significantly higher impact strength than those in the gamma-irradiated sample. Though PMPC-grafted CLPE liner treated with extra irradiation of plasma irradiation or gamma-ray exhibited no significant differences in wettability and wear resistance properties, the plasma irradiation showed improved oxidation resistance as compared to that treated with gamma-ray irradiation after accelerated aging.

Recently Takatori *et al.* [63] reported the clinical success of PMPC grafted liner after 7 years post-surgery. No osteolysis and revision surgery were reported, and no adverse effect related to implanted liner was observed. However, cobalt–chromium (Co–Cr) or cobalt-chromium-molybdenum (Co-Cr-Mo) alloy was used as head material in recent studies against PMPC grafted CLPE liner [27-29, 31, 33, 63, 142-144]. The metal ions such as Cr, released from these types of orthopaedic implant, had been linked to an increased risk of cancer and allergic problems. In addition, the weight gain was observed due to the absorption of water by CLPE material regardless of grafting conditions [143]. Wear debris from CLPE materials could initiate an inflammatory response followed by prosthetic loosening and eventually, cause osteolysis. Therefore, suitable material selection is crucial for an ideal hip implant. More research could be conducted using this surface modification technique that would possibly apply on any polymeric materials, composites, metals and ceramics. This technique provides

good mechanical properties, no toxicity to the body and could also minimise the problem of water absorption by implant material. In most cases, 26-28 mm diameter femoral head had been used. The larger diameter head with small radial clearance should be evaluated to identify the clinical utility of PMPC grafted joint surfaces. Previous researchers [26, 34, 144] only investigated the friction behavior; nevertheless, film thickness measurement could reveal the actual lubrication condition under different dynamic load conditions. The film formation behavior for different lubricants between head and cup material under dynamic loads and lubrication mechanism of polymer-grafted material could be investigated in presence of body-oriented fluid resembling of physiological joint interface.

2.4 Concepts of additively manufactured Ti6Al4V implants and associated challenges

Conventional orthopaedic implants are manufactured through machining metal rods, casting or forging, which usually requires post-processing, to develop stability and to enhance osseointegration [147]. The surface modification techniques, such as surface treatments, texturing, coatings or another porous part are generally applied to improve the stability and to enhance the osseointegration of the implant surface [148]. Conventional techniques, such as casting, vapour deposition plasma sintering, and furnace sintering are commonly used to fabricate another porous layer onto conventional orthopaedic implants. The major issue of these porous layers is random porosity that could not be controlled because of the constraints of the fabrication process. Fig. 2.10 presents some examples of a porous surface on implants for conventionally manufactured implants. Multiple stages of post-processing increase both time and costs in case of conventional implant fabrication techniques. Most importantly, the conventionally fabricated implants do not have the structural characteristics of human bone. In some cases, it might resemble the overall shape of the bone but still unable to represent complex microstructure of human bone. Therefore, the inability to achieve interconnected pores at an

optimal porosity level and controlled porosity of the conventional methods, arises the need for alternatives in implant fabrication technique.

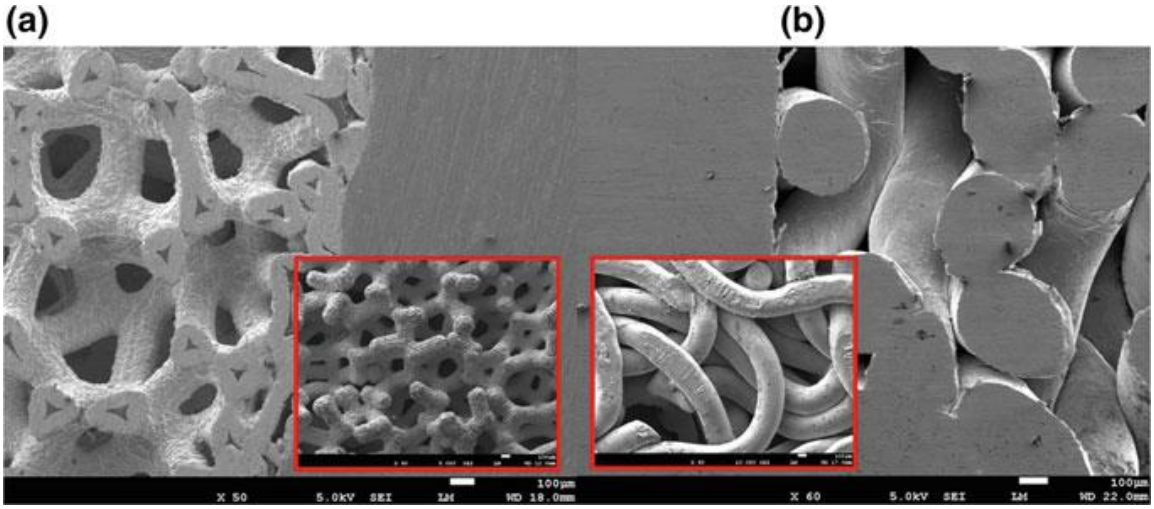

Fig. 2.10 Porous surfaces of implants for (a) acetabular cup, and ((b) tibial tray with zoomed in images of uncontrolled porosity [149].

In recent years, additive manufacturing techniques are introduced to fabricate biomaterials that produce objects in a layer-by-layer approach using CAD models [150, 151]. AM especially SLM technique is performed in an inert gas filled or vacuum chamber which ensures high purity through minimisation of oxygen in the environment and reduction of the risk of hydrogen pickup. SLM technique can control the microstructure of the products by controlling processing parameters. SLM eliminates the expensive tooling and moulds, and as a result, minimise production cost and time. The interconnected pores allow tissue-ingrowth, which prevent implants loosening from surrounding tissues [152]. The major advantage is that SLM can combine different materials, which helps to develop new biomaterials suitable for specific applications. A wide range of materials, such as polymers, metals and ceramics are currently processed using SLM technique [153-157]. Ti6Al4V is widely used for body

prostheses and implants due to its good biocompatibility, superior corrosion resistance and high mechanical strength [9, 158].

The current challenge with the AM process is relatively high surface roughness (> Ra 15 µm) of the parts due to the presence of partially-melted particles left on outer surfaces during fabrication [159, 160]. These outer surfaces experience different cooling rates due to the heat transfer from the melted part straight to the powder bed, and these areas do not undergo re-melting cycles from subsequent layer laser penetration. As a result, partially melted particles exhibit high surface roughness. Adverse biological responses, such as inflammation and osseointegration could be occurred due to high surface roughness [161, 162]. The high surface roughness has a direct adverse effect on the tribological performance of the hip implants. Vaithilingam *et al.*[163] revealed that high surface roughness is responsible for localised osteolysis because partially melted detach from Ti6Al4V surface after implantation if it is applied without surface finishing.

Researchers are trying to improve the surface finish of AM fabricated parts by applying different surface finishing techniques, such as polishing, micro-machining, machining blasting, vibratory grinding, laser ablation and chemical etching [164-169]. Electropolishing and sandblasting are less useful for AM parts as it is difficult to remove finishing products. Moreover, sandblasted parts exhibit impregnated blast media in the form of AlO_x elements, which decrease the oxide layer stability [163]. A combination of sandblasting and chemical etching was found to be effective for SLM Ti6Al4V parts with Ra of approximately 4 µm. Sandblasting removed the partially melted particles, and subsequently, chemical etching removed the blast media from the surface [167]. Bagehorn *et al.* [170] reported smoothest surface finish using milling method compared to vibratory grinding, blasting and micro-machining. It enhanced the fatigue performance of the SLM Ti6Al4V. Mohammad *et al.* [168]

noticed promising results on electron-beam manufacturing (EBM) Ti6Al4V using laser ablation method.

All of these surface finishing techniques are generally line-of-sight dependant, as a result, many difficulties could arise in proper finishing of complicated internal structures, such as pores and lattices. Recently Wangsgard *et al*. [171] reported sterilisation processes could be useful for complicated internal structures. In this study, ethylene oxide gas sterilisation was applied for surface finishing of AM parts. They found the γ irradiation is the most favourable for sterilisation of complex internal structures, voids and intricate geometries without leaving behind by-products. However, the release of Al and V ions are found to be strongly cytotoxic and could cause long-term health problems [172]. Prevention of these adverse metals ions from reacting with biological fluids are paramount importance for the long-term success of AM Ti6Al4V implants.

A thin protective layer on the surface of SLM Ti6Al6V implants could bring a remarkable improvement in implant research. From a comprehensive literature review, it is known that PMPC has numerous advantages for implant applications. PMPC is highly lubricated, and its phospholipid like layer mimics the articular cartilage. Despite the significant advancements in PMPC grafting on CLPE substrate, no study reported the PMPC grafting onto the surface of SLM Ti6Al4V substrates. Polymer grafting to metal substrate is challenging. Polymer can be grafted onto polymer substrate by activating the reaction sites of monomer under UV irradiation [27-30, 33, 142, 143, 173-175], but in case of metal substrate, it is not possible to graft the polymer on metal substrate. Metal substrate requires to produce intermittent media to react with polymer chains. This study will develop the polymer grafting onto metal substrate introducing exothermic reaction on metal substrate to form peroxide radicals that can act as an intermittent media for covalent bonding between polymer and metal substrate. As discussed earlier, Ti6Al4V has numerous advantages as implant materials, but

the problems associated with the SLM fabrication technique are needed to be addressed. Polymer grafting onto AM Ti6Al4V is challenging considering few factors such as high surface roughness, uncontrolled cell attachment due to presence of partially melted particles. These particles may detach from the implant in biological media after implantation, which might have adverse effect on health conditions. The attachment of PMPC on to the surface of SLM Ti6Al4V substrates can prevent the risk of metal ions dissociation. Moreover, polymer grafting techniques using UV irradiation could improve surface finishing of AM parts resulted in minimising the surface roughness of the implants. Controlled cell adhesion is another important factor for smooth motion of hip joint. Therefore, PMPC thin layer could tailor the physical and mechanical properties of the SLM Ti6Al4V implants. To our knowledge, no studies have been carried out to develop polymer grafting onto SLM Ti6Al4V implants. Therefore, the development of polymer grafting, and optimisation of polymerisation parameters is an important aspect in biomedical research, and this remains a significant research gap.

2.5 Summary and future perspective

A literature review of surface modification technique of different implant surfaces has revealed that surface modifications have a significant influence on enhanced tribological performances for different applications and operating conditions. In last two decades substantial developments have been achieved from fundamental understanding, design of new and improved implant surfaces, for both *in vivo* and *in vitro* applications. The literature concludes the following:

- Surface modification technique, such as surface texturing and coating significantly reduced the friction coefficient, and improved the tribological performance of the implants but, the high wear rate limits use of these techniques under loading conditions.

- Another surface modification technique known as surface grafting revealed a significant improvement in tribological performance using PMPC. The PMPC grafted surface layer was found to act as effective lubricants that could mimic the articular cartilage in physiological conditions. It exhibited a significant reduction in friction coefficient in comparison to the textured or coated surfaces and provided almost zero wear rates in hip simulator studies. The recent study reported the clinical success of PMPC-grafted surface. It is now clearly understood from a comprehensive literature review that the polymer grafting technique can be the best surface modification technique considering the tribological performance of hip implants.

- Additively manufactured Ti6Al4V implant is favourable nowadays due to its intrinsic internal structures resemble human bones. However, the high surface roughness is a major drawback for AM parts in the long-term success of the implant.
- PMPC grafting could be a possible solution to enhance the functional life of the AM Ti6Al4V implants. The effects of PMPC layers on the surface and mechanical properties yet to be studied.

In this project, polymer grafting technique will be applied to graft the polymer to the surface of AM Ti6Al4V implants. Different grafting techniques will be examined, and the polymerisation parameters will be optimised. The influence of PMPC layer on cell adhesion resistance will also be evaluated. The effect of PMPC layer on mechanical and thermal stability will be investigated. Finally, a theoretical model will be designed to predict the lubrication mechanism for PMPC grafted SLM Ti6Al4V implants.

2.6 References

[1] Choudhury D, Ay Ching H, Mamat A B, Cizek J, Osman A, Azuan N, Vrbka M, Hartl M and Krupka I 2014 Fabrication and characterization of DLC coated microdimples on hip prosthesis heads *Journal of Biomedical Materials Research Part B: Applied Biomaterials*

[3] Ghosh S and Abanteriba S 2016 Status of surface modification techniques for artificial hip implants *Science and Technology of Advanced Materials* **17** 715-35

[9] Fukuda A, Takemoto M, Tanaka K, Fujibayashi S, Pattanayak D, Matsushita T, Sasaki K, Nishida N, Kokubo T and Nakamura T 2011 Bone ingrowth into pores of lotus stem-type bioactive titanium implants fabricated using rapid prototyping technique *Bioceramics Development and Applications* **1**

[23] Ghosh S, Choudhury D, Roy T, Mamat A B, Masjuki H and Pingguan-Murphy B 2016 Tribological investigation of diamond-like carbon coated micro-dimpled surface under bovine serum and osteoarthritis oriented synovial fluid *Science and Technology of Advanced Materials*

[24] Ghosh S, Choudhury D, Das N S and Pingguan-Murphy B 2014 Tribological role of synovial fluid compositions on artificial joints — a systematic review of the last 10 years *Lubrication Science* **26** 387-410

[26] Ishihara K 2015 Highly lubricated polymer interfaces for advanced artificial hip joints through biomimetic design *Polymer Journal* **47** 585-97

[27] Moro T, Takatori Y, Kyomoto M, Ishihara K, Saiga K-i, Nakamura K and Kawaguchi H 2010 Surface grafting of biocompatible phospholipid polymer MPC provides wear resistance of tibial polyethylene insert in artificial knee joints *Osteoarthritis and Cartilage* **18** 1174-82

[28] Kyomoto M, Moro T, Saiga K-i, Miyaji F, Kawaguchi H, Takatori Y, Nakamura K and Ishihara K 2010 Lubricity and stability of poly (2-methacryloyloxyethyl phosphorylcholine) polymer layer on Co–Cr–Mo surface for hemi-arthroplasty to prevent degeneration of articular cartilage *Biomaterials* **31** 658-68

[29] Kyomoto M, Moro T, Saiga K, Hashimoto M, Ito H, Kawaguchi H, Takatori Y and Ishihara K 2012 Biomimetic hydration lubrication with various polyelectrolyte layers on cross-linked polyethylene orthopedic bearing materials *Biomaterials* **33** 4451-9

[30] Kyomoto M, Moro T, Yamane S, Takatori Y, Tanaka S and Ishihara K 2017 A hydrated phospholipid polymer-grafted layer prevents lipid-related oxidative degradation of cross-linked polyethylene *Biomaterials* **112** 122-32

[31] Moro T, Kawaguchi H, Ishihara K, Kyomoto M, Karita T, Ito H, Nakamura K and Takatori Y 2009 Wear resistance of artificial hip joints with poly (2-methacryloyloxyethyl phosphorylcholine) grafted polyethylene: comparisons with the effect of polyethylene cross-linking and ceramic femoral heads *Biomaterials* **30** 2995-3001

[33] Moro T, Takatori Y, Kyomoto M, Ishihara K, Hashimoto M, Ito H, Tanaka T, Oshima H, Tanaka S and Kawaguchi H 2014 Long-term hip simulator testing of the artificial hip joint bearing surface grafted with biocompatible phospholipid polymer *Journal of Orthopaedic Research* **32** 369-76

[34] Yarimitsu S, Moro T, Kyomoto M, Watanabe K, Tanaka S, Ishihara K and Murakami T 2015 Influences of dehydration and rehydration on the lubrication properties of phospholipid polymer-grafted cross-linked polyethylene *Proceedings of the Institution of Mechanical Engineers, Part H: Journal of Engineering in Medicine* 0954411915588969

[37] Liu X, Chu P K and Ding C 2004 Surface modification of titanium, titanium alloys, and related materials for biomedical applications *Materials Science and Engineering: R: Reports* **47** 49-121

[53] Merx H, Dreinhöfer K, Schräder P, Stürmer T, Puhl W, Günther K and Brenner H 2003 International variation in hip replacement rates *Annals of the rheumatic diseases* **62** 222-6

[54] Bozic K J, Kurtz S M, Lau E, Ong K, Vail T P and Berry D J 2009 The epidemiology of revision total hip arthroplasty in the United States *J Bone Joint Surg Am* **91** 128-33

[55] NJR Annual Report A 2017 Australian Orthopaedic Association National Joint Replacement Annual Report 2017. (The University of Adelaide: Australian Orthopaedic Association)

[56] Malak T, Broomfield J, Palmer A, Hopewell S, Carr A, Brown C, Prieto-Alhambra D and Glyn-Jones S 2016 Surrogate markers of long-term outcome in primary total hip arthroplasty *Bone and Joint Research* **5** 206-14

[57] Kurtz S M, Ong K L, Schmier J, Mowat F, Saleh K, Dybvik E, Kärrholm J, Garellick G, Havelin L I and Furnes O 2007 Future clinical and economic impact of revision total hip and knee arthroplasty *J Bone Joint Surg Am* **89** 144-51

[58] Roy T, Choudhury D, Ghosh S, Mamat A B and Pingguan-Murphy B 2015 Improved friction and wear performance of micro dimpled ceramic-on-ceramic interface for hip joint arthroplasty *Ceramics International* **41** 681-90

[59] Hauert R, Thorwarth K and Thorwarth G 2013 An overview on diamond-like carbon coatings in medical applications *Surface and Coatings Technology* **233** 119-30
[60] Ibatan T, Uddin M and Chowdhury M 2015 Recent development on surface texturing in enhancing tribological performance of bearing sliders *Surface and Coatings Technology* **272** 102-20
[61] Hauert R, Thorwarth G, Müller U, Stiefel M, Falub C, Thorwarth K and Joyce T 2012 Analysis of the in-vivo failure of the adhesive interlayer for a DLC coated articulating metatarsophalangeal joint *Diamond and Related Materials* **25** 34-9
[62] Lackner J M, Waldhauser W, Major L and Kot M 2014 Tribology and Micromechanics of Chromium Nitride Based Multilayer Coatings on Soft and Hard Substrates *Coatings* **4** 121-38
[63] Takatori Y, Moro T, Ishihara K, Kamogawa M, Oda H, Umeyama T, Kim Y T, Ito H, Kyomoto M and Tanaka T 2015 Clinical and radiographic outcomes of total hip replacement with poly (2-methacryloyloxyethyl phosphorylcholine)-grafted highly cross-linked polyethylene liners: Three-year results of a prospective consecutive series *Modern Rheumatology* **25** 286-91
[64] Smith A J, Dieppe P, Howard P W and Blom A W 2012 Failure rates of metal-on-metal hip resurfacings: analysis of data from the National Joint Registry for England and Wales *The Lancet* **380** 1759-66
[65] Leyens C and Peters M 2003 *Titanium and titanium alloys: fundamentals and applications*: John Wiley & Sons)
[66] Davidson J A 1993 Characteristics of metal and ceramic total hip bearing surfaces and their effect on long-term ultra high molecular weight polyethylene wear *Clinical orthopaedics and related research* **294** 361-78
[67] Niinomi M 2008 Mechanical biocompatibilities of titanium alloys for biomedical applications *Journal of the mechanical behavior of biomedical materials* **1** 30-42
[68] Laurent M P, Johnson T S, Crowninshield R D, Blanchard C R, Bhambri S K and Yao J Q 2008 Characterization of a highly cross-linked ultrahigh molecular-weight polyethylene in clinical use in total hip arthroplasty *The Journal of arthroplasty* **23** 751-61
[69] Muratoglu O K, Bragdon C R, O'Connor D O, Jasty M, Harris W H, Gul R and McGarry F 1999 Unified wear model for highly crosslinked ultra-high molecular weight polyethylenes (UHMWPE) *Biomaterials* **20** 1463-70
[70] Kurtz S M 2012 *PEEK Biomaterials Handbook*: Elsevier) pp 1-7
[71] Hatton A, Nevelos J, Nevelos A, Banks R, Fisher J and Ingham E 2002 Alumina–alumina artificial hip joints. Part I: a histological analysis and characterisation of wear debris by laser capture microdissection of tissues retrieved at revision *Biomaterials* **23** 3429-40
[72] Chevalier J and Gremillard L 2009 Ceramics for medical applications: A picture for the next 20 years *Journal of the European Ceramic Society* **29** 1245-55
[73] Campbell A A 2003 Bioceramics for implant coatings *Materials Today* **6** 26-30
[74] Villermaux F 2000 Zirconia-alumina as the new generation of ceramic-ceramic THP: wear performance evaluation including extreme life conditions. In: *Sixth World Biomaterials Congress*, p 2000
[75] Currier J H, Anderson D E and Van Citters D W 2010 A proposed mechanism for squeaking of ceramic-on-ceramic hips *Wear* **269** 782-9
[76] Lee M-C and Ahn J-W 2007 *Bioceramics and Alternative Bearings in Joint Arthroplasty*: Springer) pp 123-32
[77] Kokubo T 2008 *Bioceramics and their clinical applications*: Elsevier)
[78] De Aza A, Chevalier J, Fantozzi G, Schehl M and Torrecillas R 2002 Crack growth resistance of alumina, zirconia and zirconia toughened alumina ceramics for joint prostheses *Biomaterials* **23** 937-45
[79] Goodman S B, Ma T, Chiu R, Ramachandran R and Smith R L 2006 Effects of orthopaedic wear particles on osteoprogenitor cells *Biomaterials* **27** 6096-101
[80] Langton D, Jameson S, Joyce T, Hallab N, Natu S and Nargol A 2010 Early failure of metal-on-metal bearings in hip resurfacing and large-diameter total hip replacement A CONSEQUENCE OF EXCESS WEAR *Journal of Bone & Joint Surgery, British Volume* **92** 38-46
[81] Öztürk O, Türkan U u and Erogˇlu A E 2006 Metal ion release from nitrogen ion implanted CoCrMo orthopedic implant material *Surface and Coatings Technology* **200** 5687-97
[82] Shettlemore M and Bundy K 2001 Examination of in vivo influences on bioluminescent microbial assessment of corrosion product toxicity *Biomaterials* **22** 2215-28
[83] Chu P K 2007 Enhancement of surface properties of biomaterials using plasma-based technologies *Surface and Coatings Technology* **201** 8076-82
[84] Li D 1998 A new type of wear-resistant material: pseudo-elastic TiNi alloy *Wear* **221** 116-23
[85] Hsu C-Y, Yeh J-W, Chen S-K and Shun T-T 2004 Wear resistance and high-temperature compression strength of Fcc CuCoNiCrAl 0.5 Fe alloy with boron addition *Metallurgical and Materials Transactions A* **35** 1465-9

[86] Chuang M-H, Tsai M-H, Wang W-R, Lin S-J and Yeh J-W 2011 Microstructure and wear behavior of AlxCo1. 5CrFeNi1. 5Tiy high-entropy alloys *Acta Materialia* **59** 6308-17
[87] Haftlang F, Hanzaki A Z, Abedi H R, Preisler D and Bartha K 2019 The subsurface frictional hardening: A new approach to improve the high-speed wear performance of Ti-29Nb-14Ta-4.5 Zr alloy against Ti-6Al-4V extra-low interstitial *Wear* **422** 137-50
[88] de Oliveira D P, Toniato T V, Ricci R, Marciano F R, Prokofiev E, Valiev R Z, Lobo A O and Júnior A M J 2019 Biological response of chemically treated surface of the ultrafine-grained Ti–6Al–7Nb alloy for biomedical applications *International journal of nanomedicine* **14** 1725
[89] Lin S-P and Wong P-C 2019 Surface modified structure for improving hemocompatibility of biomedical metallic substrates. Google Patents)
[90] Pippenger B E, Rottmar M, Kopf B S, Stübinger S, Dalla Torre F H, Berner S and Maniura-Weber K 2019 Surface modification of ultrafine-grained titanium: Influence on mechanical properties, cytocompatibility, and osseointegration potential *Clinical oral implants research* **30** 99-110
[91] McGuire K S, Tweddell III R and Hamilton P W 2002 Golf ball with non-circular shaped dimples. Google Patents)
[92] Wang X, Kato K, Adachi K and Aizawa K 2003 Loads carrying capacity map for the surface texture design of SiC thrust bearing sliding in water *Tribology International* **36** 189-97
[93] Coblas D G, Fatu A, Maoui A and Hajjam M 2015 Manufacturing textured surfaces: State of art and recent developments *Proceedings of the Institution of Mechanical Engineers, Part J: Journal of Engineering Tribology* **229** 3-29
[94] Wang X and Kato K 2003 Improving the anti-seizure ability of SiC seal in water with RIE texturing *Tribology Letters* **14** 275-80
[95] Etsion I 2005 State of the art in laser surface texturing *Journal of Tribology* **127** 248-53
[96] Suh N P, Mosleh M and Howard P S 1994 Control of friction *Wear* **175** 151-8
[97] Ranjan R, Lambeth D, Tromel M, Goglia P and Li Y 1991 Laser texturing for low-flying-height media *Journal of Applied Physics* **69** 5745-7
[98] Chyr A, Qiu M, Speltz J W, Jacobsen R L, Sanders A P and Raeymaekers B 2014 A patterned microtexture to reduce friction and increase longevity of prosthetic hip joints *Wear* **315** 51-7
[99] Yu H, Deng H, Huang W and Wang X 2011 The effect of dimple shapes on friction of parallel surfaces *Proceedings of the Institution of Mechanical Engineers, Part J: Journal of Engineering Tribology* **225** 693-703
[100] Huang W and Wang X 2013 Biomimetic design of elastomer surface pattern for friction control under wet conditions *Bioinspiration & biomimetics* **8** 046001
[101] Kaneta M, Kanada T and Nishikawa H 1997 Optical interferometric observations of the effects of a moving dent on point contact EHL *Tribology series* **32** 69-79
[102] Ito H, Kaneda K, Yuhta T, Nishimura I, Yasuda K and Matsuno T 2000 Reduction of polyethylene wear by concave dimples on the frictional surface in artificial hip joints *The Journal of arthroplasty* **15** 332-8
[103] Shen C and Khonsari M 2015 Numerical optimization of texture shape for parallel surfaces under unidirectional and bidirectional sliding *Tribology International* **82** 1-11
[104] Etsion I and Burstein L 1996 A model for mechanical seals with regular microsurface structure *Tribology Transactions* **39** 677-83
[105] Wang X, Adachi K, Otsuka K and Kato K 2006 Optimization of the surface texture for silicon carbide sliding in water *Applied Surface Science* **253** 1282-6
[106] Yu H, Wang X and Zhou F 2010 Geometric shape effects of surface texture on the generation of hydrodynamic pressure between conformal contacting surfaces *Tribology Letters* **37** 123-30
[107] Yan D, Qu N, Li H and Wang X 2010 Significance of dimple parameters on the friction of sliding surfaces investigated by orthogonal experiments *Tribology Transactions* **53** 703-12
[108] Costa H and Hutchings I 2007 Hydrodynamic lubrication of textured steel surfaces under reciprocating sliding conditions *Tribology International* **40** 1227-38
[109] Galda L, Pawlus P and Sep J 2009 Dimples shape and distribution effect on characteristics of Stribeck curve *Tribology International* **42** 1505-12
[110] Shen C and Khonsari M 2013 Effect of dimple's internal structure on hydrodynamic lubrication *Tribology Letters* **52** 415-30
[111] Steinhoff K, Rasp W and Pawelski O 1996 Development of deterministic-stochastic surface structures to improve the tribological conditions of sheet forming processes *Journal of Materials Processing Technology* **60** 355-61
[112] Pettersson U and Jacobson S 2003 Influence of surface texture on boundary lubricated sliding contacts *Tribology International* **36** 857-64

[113] Yan J, Zhang Z, Kuriyagawa T and Gonda H 2010 Fabricating micro-structured surface by using single-crystalline diamond endmill *The International Journal of Advanced Manufacturing Technology* **51** 957-64
[114] Ghosh S, Choudhury D, Roy T, Mamat A B, Masjuki H and Pingguan-Murphy B 2015 Tribological investigation of diamond-like carbon coated micro-dimpled surface under bovine serum and osteoarthritis oriented synovial fluid *Science and Technology of Advanced Materials* **16** 035002
[115] Choudhury D, Urban F, Vrbka M, Hartl M and Krupka I 2015 A novel tribological study on DLC-coated micro-dimpled orthopedics implant interface *Journal of the mechanical behavior of biomedical materials* **45** 121-31
[116] Hao L, Meng Y and Chen C 2014 Experimental investigation on effects of surface texturing on lubrication of initial line contacts *Lubrication Science* **26** 363-73
[117] He D, Zheng S, Pu J, Zhang G and Hu L 2015 Improving tribological properties of titanium alloys by combining laser surface texturing and diamond-like carbon film *Tribology International* **82** 20-7
[118] Sawano H, Warisawa S i and Ishihara S 2009 Study on long life of artificial joints by investigating optimal sliding surface geometry for improvement in wear resistance *Precision engineering* **33** 492-8
[119] Meng F 2013 On influence of cavitation in lubricant upon tribological performances of textured surfaces *Optics & Laser Technology* **48** 422-31
[120] Kai M, Tsuboi R and Sasaki S 2013 A Study on In-situ Observation of the Micro Flow of Lubricant on the Textured Surface *Procedia Engineering* **68** 12-8
[121] Ching H A, Choudhury D, Nine M J and Osman N A A 2014 Effects of surface coating on reducing friction and wear of orthopaedic implants *Science and Technology of Advanced Materials* **15** 014402
[122] Nandakumar N 2018 Experimental Investigation on mechanical properties of Al6061 Hybrid Metal Matrix Composite Reinforced with Silicon Carbide and Graphite
[123] Antunes R A and De Oliveira M C L 2009 Corrosion processes of physical vapor deposition-coated metallic implants *Critical Reviews™ in Biomedical Engineering* **37**
[124] Shao T, Ge F, Dong Y, Li K, Li P, Sun D and Huang F 2018 Microstructural effect on the tribo-corrosion behaviors of magnetron sputtered CrSiN coatings *Wear* **416** 44-53
[125] Rieker C and Kottig P 2008 In vivo tribological performance of 231 metal-on-metal hip articulations *Hip International* **12** 73-6
[126] Balagna C, Faga M and Spriano S 2012 Tantalum-based multilayer coating on cobalt alloys in total hip and knee replacement *Materials Science and Engineering: C* **32** 887-95
[127] Spriano S, Vernè E, Faga M, Bugliosi S and Maina G 2005 Surface treatment on an implant cobalt alloy for high biocompatibility and wear resistance *Wear* **259** 919-25
[128] Ghosh S, Choudhury D and Pingguan-Murphy B 2016 Lubricating ability of albumin and globulin on artificial joint implants: a tribological perspective *International Journal of Surface Science and Engineering* **10** 193-206
[129] Wang Q, Zhou F, Wang C, Yuen M-F, Wang M, Qian T, Matsumoto M and Yan J 2015 Comparison of tribological and electrochemical properties of TiN, CrN, TiAlN and aC: H coatings in simulated body fluid *Materials Chemistry and Physics* **158** 74-81
[130] Love C, Cook R B, Harvey T, Dearnley P and Wood R 2013 Diamond like carbon coatings for potential application in biological implants—a review *Tribology International* **63** 141-50
[131] Choudhury D, Roy T and Krupka I 2015 *Processing Techniques and Tribological Behavior of Composite Materials*: IGI Global) pp 193-217
[132] Chang N, Bellare A, Cohen R and Spector M 2000 Wear behavior of bulk oriented and fiber reinforced UHMWPE *Wear* **241** 109-17
[133] Roy T, Choudhury D, Mamat A B and Pingguan-Murphy B 2014 Fabrication and characterization of micro-dimple array on Al 2 O 3 surfaces by using a micro-tooling *Ceramics International* **40** 2381-8
[134] Hauert R, Falub C, Thorwarth G, Thorwarth K, Affolter C, Stiefel M, Podleska L and Taeger G 2012 Retrospective lifetime estimation of failed and explanted diamond-like carbon coated hip joint balls *Acta biomaterialia* **8** 3170-6
[135] Carré A and Lacarrière V 2010 How substrate properties control cell adhesion. A physical–chemical approach *Journal of Adhesion Science and Technology* **24** 815-30
[136] Goddard J M and Hotchkiss J 2007 Polymer surface modification for the attachment of bioactive compounds *Progress in polymer science* **32** 698-725
[137] Bryant S J, Davis-Arehart K A, Luo N, Shoemaker R K, Arthur J A and Anseth K S 2004 Synthesis and characterization of photopolymerized multifunctional hydrogels: water-soluble poly (vinyl alcohol) and chondroitin sulfate macromers for chondrocyte encapsulation *Macromolecules* **37** 6726-33
[138] Wright V and Dowson D 1976 Lubrication and cartilage *Journal of Anatomy* **121** 107

[139] Kobayashi M, Ishihara K and Takahara A 2014 Neutron reflectivity study of the swollen structure of polyzwitterion and polyeletrolyte brushes in aqueous solution *Journal of Biomaterials Science, Polymer Edition* **25** 1673-86
[140] Chen M, Briscoe W H, Armes S P and Klein J 2009 Lubrication at physiological pressures by polyzwitterionic brushes *science* **323** 1698-701
[141] Edmondson S, Osborne V L and Huck W T 2004 Polymer brushes via surface-initiated polymerizations *Chemical society reviews* **33** 14-22
[142] Kyomoto M, Moro T, Takatori Y, Tanaka S and Ishihara K 2015 Multidirectional Wear and Impact-to-wear Tests of Phospholipid-polymer-grafted and Vitamin E-blended Crosslinked Polyethylene: A Pilot Study *Clinical Orthopaedics and Related Research®* **473** 942-51
[143] Moro T, Takatori Y, Kyomoto M, Ishihara K, Kawaguchi H, Hashimoto M, Tanaka T, Oshima H and Tanaka S 2015 Wear resistance of the biocompatible phospholipid polymer-grafted highly cross-linked polyethylene liner against larger femoral head *Journal of Orthopaedic Research*
[144] Yamane S, Kyomoto M, Moro T, Watanabe K, Hashimoto M, Takatori Y, Tanaka S and Ishihara K 2015 Effects of extra irradiation on surface and bulk properties of PMPC-grafted cross-linked polyethylene *Journal of Biomedical Materials Research Part A*
[145] Crockett R, Roba M, Naka M, Gasser B, Delfosse D, Frauchiger V and Spencer N D 2009 Friction, lubrication, and polymer transfer between UHMWPE and CoCrMo hip-implant materials: A fluorescence microscopy study *Journal of Biomedical Materials Research Part A* **89** 1011-8
[146] Kobayashi M and Takahara A 2010 Tribological properties of hydrophilic polymer brushes under wet conditions *The Chemical Record* **10** 208-16
[147] Affatato S, Goldoni M, Testoni M and Toni A 2001 Mixed oxides prosthetic ceramic ball heads. Part 3: effect of the ZrO 2 fraction on the wear of ceramic on ceramic hip joint prostheses. A long-term in vitro wear study *Biomaterials* **22** 717-23
[148] Sing S L 2019 *Selective laser melting of novel titanium-tantalum alloy as orthopaedic biomaterial*: Springer)
[149] Sing S L 2019 *Selective Laser Melting of Novel Titanium-Tantalum Alloy as Orthopaedic Biomaterial*: Springer) pp 9-36
[150] Mayer J, Borges P V and Simske S J 2018 *Fundamentals and Applications of Hardcopy Communication*: Springer) pp 1-5
[151] Prakash K S, Nancharaih T and Rao V S 2018 Additive Manufacturing Techniques in Manufacturing-An Overview *Materials Today: Proceedings* **5** 3873-82
[152] Habibovic P and de Groot K 2007 Osteoinductive biomaterials—properties and relevance in bone repair *Journal of tissue engineering and regenerative medicine* **1** 25-32
[153] Niendorf T and Brenne F 2013 Steel showing twinning-induced plasticity processed by selective laser melting—An additively manufactured high performance material *Materials Characterization* **85** 57-63
[154] Frazier W E 2014 Metal additive manufacturing: a review *Journal of Materials Engineering and Performance* **23** 1917-28
[155] Eckel Z C, Zhou C, Martin J H, Jacobsen A J, Carter W B and Schaedler T A 2016 Additive manufacturing of polymer-derived ceramics *Science* **351** 58-62
[156] Kumar N, Jain P K, Tandon P and Pandey P M 2018 Additive manufacturing of flexible electrically conductive polymer composites via CNC-assisted fused layer modeling process *Journal of the Brazilian Society of Mechanical Sciences and Engineering* **40** 175
[157] Karandikar P, Watkins M, McCormick A, Givens B, Aghajanian M and Cubed I 2018 Additive Manufacturing (3D Printing) of Ceramics: Microstructure, Properties, and Product Examples. In: *Proceedings of the 41st International Conference on Advanced Ceramics and Composites*: John Wiley & Sons) p 175
[158] Pattanayak D K, Fukuda A, Matsushita T, Takemoto M, Fujibayashi S, Sasaki K, Nishida N, Nakamura T and Kokubo T 2011 Bioactive Ti metal analogous to human cancellous bone: fabrication by selective laser melting and chemical treatments *Acta Biomaterialia* **7** 1398-406
[159] Trevisan F, Calignano F, Aversa A, Marchese G, Lombardi M, Biamino S, Ugues D and Manfredi D 2018 Additive manufacturing of titanium alloys in the biomedical field: Processes, properties and applications *Journal of applied biomaterials & functional materials* **16** 57-67
[160] Ghosh S, Abanteriba S, Wong S and Houshyar S 2018 Selective laser melted titanium alloys for hip implant applications: surface modification with new method of polymer grafting *Journal of the Mechanical Behavior of Biomedical Materials*
[161] Castellani C, Lindtner R A, Hausbrandt P, Tschegg E, Stanzl-Tschegg S E, Zanoni G, Beck S and Weinberg A-M 2011 Bone–implant interface strength and osseointegration: Biodegradable magnesium alloy versus standard titanium control *Acta biomaterialia* **7** 432-40

[162] Pongnarisorn N J, Gemmell E, Tan A E, Henry P J, Marshall R I and Seymour G J 2007 Inflammation associated with implants with different surface types *Clinical oral implants research* **18** 114-25
[163] Vaithilingam J, Prina E, Goodridge R D, Hague R J, Edmondson S, Rose F R and Christie S D 2016 Surface chemistry of Ti6Al4V components fabricated using selective laser melting for biomedical applications *Materials Science and Engineering: C* **67** 294-303
[164] Thomas-Seale L E J, Kirkman-Brown J C, Attallah M M, Espino D M and Shepherd D E T 2018 The barriers to the progression of additive manufacture: Perspectives from UK industry *International Journal of Production Economics* **198** 104-18
[165] Lhuissier P, de Formanoir C, Martin G, Dendievel R and Godet S 2016 Geometrical control of lattice structures produced by EBM through chemical etching: Investigations at the scale of individual struts *Materials & Design* **110** 485-93
[166] Bagehorn S, Wehr J and Maier H J 2017 Application of mechanical surface finishing processes for roughness reduction and fatigue improvement of additively manufactured Ti-6Al-4V parts *International Journal of Fatigue* **102** 135-42
[167] Longhitano G A, Larosa M A, Munhoz A L J, Zavaglia C A d C and Ierardi M C F 2015 Surface finishes for Ti-6Al-4V alloy produced by direct metal laser sintering *Materials Research* **18** 838-42
[168] Mohammad A, Mohammed M K and Alahmari A M 2016 Effect of laser ablation parameters on surface improvement of electron beam melted parts *The International Journal of Advanced Manufacturing Technology* **87** 1033-44
[169] Wang D, Wang Y, Wang J, Song C, Yang Y, Zhang Z, Lin H, Zhen Y and Liao S 2016 Design and fabrication of a precision template for spine surgery using selective laser melting (SLM) *Materials* **9** 608
[170] Bagehorn S, Wehr J and Maier H 2017 Application of mechanical surface finishing processes for roughness reduction and fatigue improvement of additively manufactured Ti-6Al-4V parts *International Journal of Fatigue* **102** 135-42
[171] Wangsgard W and Winters M 2018 Validation of a sterilization dose for products manufactured using a 3D printer *Radiation Physics and Chemistry* **143** 38-40
[172] Murr L, Quinones S, Gaytan S, Lopez M, Rodela A, Martinez E, Hernandez D, Martinez E, Medina F and Wicker R 2009 Microstructure and mechanical behavior of Ti–6Al–4V produced by rapid-layer manufacturing, for biomedical applications *Journal of the mechanical behavior of biomedical materials* **2** 20-32
[173] Kyomoto M, Moro T, Miyaji F, Hashimoto M, Kawaguchi H, Takatori Y, Nakamura K and Ishihara K 2009 Effects of mobility/immobility of surface modification by 2-methacryloyloxyethyl phosphorylcholine polymer on the durability of polyethylene for artificial joints *Journal of Biomedical Materials Research Part A* **90** 362-71
[174] Kyomoto M, Moro T, Takatori Y, Kawaguchi H, Nakamura K and Ishihara K 2010 Self-initiated surface grafting with poly(2-methacryloyloxyethyl phosphorylcholine) on poly(ether-ether-ketone) *Biomaterials* **31** 1017-24
[175] Moro T, Takatori Y, Ishihara K, Konno T, Takigawa Y, Matsushita T, Chung U-i, Nakamura K and Kawaguchi H 2004 Surface grafting of artificial joints with a biocompatible polymer for preventing periprosthetic osteolysis *Nature Materials* **3** 829

CHAPTER THREE: MATERIALS AND METHODS

3.1 Introduction

This chapter describes the materials and the experimental techniques that have been used to characterise the PMPC grafted Ti6Al4V implant surfaces. This chapter is divided into eight key sections. Section 3.1 outlines the chapter overview, introduction. Section 3.2 discusses the details of the materials that have been used in this project. Section 3.3 describes the details of SLM Ti6Al4V samples fabrication process and polymer grafting techniques. Section 3.4 explains the experimental techniques used for characterisation of PMPC grafted surfaces. Section 3.5 highlights the polymer characterisation techniques. Section 3.6 describes biological response evaluation techniques. Section 3.7 explains the mechanical and tribological properties evaluation techniques. Section 3.8 presents the statistical analysis procedure. The characterisation methodologies performed for each study have also been discussed in detail in the relevant chapters.

3.2 Materials

3.2.1 Ti6Al4V powder

Ti6Al4V powder (ASTM Grade 23, ELI, TLS Technik GmbH & Co., Bitterfeld-Wolfen, Germany), size 25-45 µm, was used to fabricate the implants by SLM technique. The composition of Ti6Al4V powder is presented in Table 3.1.

Table 3.1 The chemical composition of ELI Ti6Al4V powder.

Chemical composition (wt.%)							
Ti	Al	V	Fe	C	N	O	H
balanced	6.47	4.08	0.17	0.008	0.009	0.1	0.002

3.2.2 MPC monomer

MPC monomer powder (Product no: 730114-5G) was purchased from Sigma Aldrich. MPC powder contains <= 100 PPM Mono Methyl Ether of Hydroquinone (MEHQ) inhibitor. Therefore, MPC monomer inhibitor removers (Product no.: 306312-12EA) were commercially supplied by Sigma Aldrich to remove inhibitor from the monomer.

3.2.3 Chemicals

Ethanol, Acetone, Cyclohexane and Isopropanol (Sigma-Aldrich, Australia) was used as the dispersant solvent for the sonication of all samples. Kroll's reagent was prepared using 2% hydrofluoric acid (HF), 10% nitric acid (HNO_3) and 88% dH_20. Sulfuric acid (H_2SO_4) (Sigma-Aldrich, Australia) and hydrogen peroxide (H_2O_2) (Sigma-Aldrich, Australia) was used to prepare a piranha solution for exothermic reaction.

3.3 Sample fabrication and polymer grafting process

3.3.1 SLM Ti6Al4V implant

Rectangular Ti6Al4V implants with dimensions of 8 × 6 × 3 mm (XYZ) were fabricated by SLM technique using Ti6Al4V powder. An SLM Solutions (SLM250HL) system was used to fabricate 3D printed implants at Advanced Manufacturing Precinct (AMP) - RMIT University. The powder bed was preheated to 200°C, and the building chamber was purged with argon until the oxygen level was reduced to 100 ppm prior to the SLM process. The selected SLM processing parameters are presented in Table 3.2.

Table 3.2 Process parameters for SLM-used to fabricate Ti6Al4V implant.

Material	Laser power, P (W)	Laser Energy density,γ (J/mm^3)	Focal offset distance (mm)	Hatch spacing h (mm)	Scan speed,v (mm/s)	Layer thickness,t (µm)	Relative density (%)
Ti6Al4V	173	68.5	2	0.12	710	30	99.10

Half of the samples from each batch were polished following standard grinding and polishing procedures to distinguish the effect of surface geometry on different surface properties. At first, grinding was subsequently performed using papers 200, 600, 800, 1200. Then, samples were polished using 1, 6 microns diamond particles with an automatic polishing machine. Finally, OP-S was used at sliding speed of ~50 rpm for at least 10 minutes to achieve the final mirror-polished samples. After polishing, all samples were cleaned using acetone and ethanol.

3.3.2 Polymer grafting process

Prior to the grafting process, all Ti6Al4V implants were cleaned in acetone bath followed by cyclohexane and isopropanol bath, for 10 min. All steps were done in a sonication bath to speed up the cleaning process. Then Kroll's reagent was used to remove the non-uniform oxide layer. The samples were placed in Kroll's reagent for 3 min followed by cleaning with dH_2O for 5 times (10 min for each time) to make sure there is no HF or HNO_3 left on the surface of the sample, then dried under lab environment. A monomer solution with a required concentration was prepared by diluting in dH_20. Hydroquinone and monomethyl ether hydroquinone inhibitor was removed from the monomer solution during the purification process using an inhibitor column [176].

The dried Ti6Al4V samples were immersed in a Piranha solution (sulphuric acid (H_2SO_4)/hydrogen peroxide (H_2O_2) 10:20 v:v) to form functional groups, peroxide radicals, on the surface. First, samples were immersed in 10 mL H_2SO_4 (100%), and stirred for 1 min, followed by addition of 20 mL H_2O_2 (30%) with a further 3 min of stirring. The color of the solution was altered due to an exothermic reaction. In the second step, samples were rinsed with dH_2O prior to immersion in a monomer solution. At last, the samples in the monomer solution bath were exposed to thermal/UV irradiation to start polymerisation by activating the

reaction sites of monomer. The details of the thermal/UV irradiation will be discussed in the experimental section of Chapter four.

3.4 Surface characterisation

Different types of analytical tools were used to characterise the surface of polymer grafted samples. The chemical and physical bonding between PMPC and Ti6Al4V surfaces were evaluated. The surface roughness, chemical composition on the surfaces, wettability and polymer film thickness were also characterised.

3.4.1 Surface morphology

FEI Quanta 200 ESEM (2002) and FEI Nova NanoSEM (2007) was used to compare the morphology of untreated, and PMPC grafted, surface treated by different grafting methods and polymerisation parameters. Prior to analysis, sputter coating was done on non-conducting polymer grafted samples. Samples were mounted on an aluminium stub using carbon tape to attach firmly during imaging. The surface morphology of the control surfaces was compared to treated surfaces to evaluate the changes caused by polymer grafting. Constant acceleration voltage, spot size and magnification were maintained before collecting the image to keep consistency between different sets of samples.

3.4.2 Surface roughness

3D optical profiler (ContourGT-Bruker) was used to measure the surface roughness of all samples. The 3D surface roughness pattern was also obtained for a thin top layer of the sample surface by laser scanning. The in-built software within the 3D optical profiler (ContourGT-Bruker) was used for data processing and acquisition from the equipment. The details of surface topography will be discussed in the relevant chapters.

Tencor profilometer was also used to measure the average surface roughness of the sample. It performs a line scan about 5 mm of the sample. The line scan was performed 5 times on each sample, and the average of surface roughness has been calculated for repetitive measurements. The surface roughness values were compared for the results obtained from 3D optical profiler and Tencor profilometer.

3.4.3 Energy-dispersive X-ray spectroscopy (EDS)

FEI Quanta 200 ESEM (2002) with Oxford X-MaxN 20 EDXS detector (2014) was used to analyse the micro-topography of untreated and polymer treated Ti6Al4V surfaces. The instrument was operated at 5 KV to 15 KV to determine the EDS spectra. The scanning was continued until a stable value was achieved. The mapping procedure was carried out for 30 min on each sample to identify the elemental composition of the micro-level thickness of the surface. The line mapping continued until a stable value was achieved. Each sample was repeated 5 times at different scanning areas for better accuracy in results. The Aztec software was used to analyse the EDS data.

3.4.4 X-ray photoelectron spectroscopy (XPS)

A Thermo K-Alpha XPS instrument was used to analyse the several nanometers of the top surface of all samples. The probing spot size used for these experiments was 400 µm. At least two spots for each sample were analysed for XPS experiments. Survey spectra were obtained in a constant analyser mode at pass energy of 100 eV, and high-resolution spectra were collected at pass energy of 20 eV. Advantage software was used for data acquisition and processing. The compositional analysis was carried out by adding an average peak and peak fitting.

3.4.5 Fourier transform infrared spectroscopy (FTIR)

A Perkin-Elmer 2000 infrared spectrometer was used to analyse the chemical bond between polymer grafting and substrate. The FTIR spectra were obtained for 32 scans at a resolution of 4 cm^{-1} over a range of 400-2000 cm^{-1}. Background spectra were obtained before the actual analysis. Then the inclination angle of the measured surface was adjusted for high energy before scanning the surface. The functional group vibrations and stretches of the untreated and polymer treated surface were analysed at different wavenumbers of FTIR spectra. The inbuilt software was used for processing the acquired spectra. At least three measurements were done for each sample.

3.4.6 Water contact angle measurement

Contact angle instrument (Data Physics OCA20) to measure the contact angle on untreated and polymer treated samples by a sessile drop method [177]. The 2µL drop was used for each measurement. A droplet of 2µL was deposited by a syringe which was positioned above the sample surface. The measurement was done once the stable value was achieved. A high-resolution camera captured the image from the side view. The image was then analysed using image analysis software. Measurements were done on various areas of the samples to confirm the uniformity of the surface.

3.4.7 Thickness measurement of polymer grafted layer

A thin film analyser (F40-Filmetrics) instrument was used to measure the layer of grafted polymer. The instrument was first calibrated using silicon reference wafer plus 18KA SiO_2/Si test wafer. The refractive index was assumed to be 1.50 for MPC polymer [178]. The baseline was selected for untreated surfaces before the film thickness measurement. The reflectance spectrum was obtained in a given wavelength range. The inbuilt software with the instrument can determine the thickness of multiple thin films by analysing the reflectance

spectrum. At least 7 spots were selected for each sample to be measured and the average of 7 data was reported as the thickness of the polymer grafted layer.

3.5 Polymer characterisation

3.5.1 Nuclear magnetic resonance (NMR) spectroscopy analysis

The degree of polymerisation rate was characterised using NMR spectroscopy (Bruker Avance III 300 MHz NMR spectrometer). PMPC were dissolved in D_2O and shaken gently to ensure that all materials had dissolved before the NMR measurement. The NMR tube containing dissolved PMPC was placed in the NMR spectrometer for the measurement. After the NMR measurement, the spectrum was processed and assigned the peaks. The different peaks were correlated to the NMR shifts using a suitable program.

3.5.2 Gel permeation chromatography (GPC) analysis

The molecular weights and polydispersity were examined by GPC experiment. GPC was performed on Water Associates Liquid Chromatograph system (Waters 2695) equipped with a differential refractometer and four micro-Styragel columns (10^5, 10^4, 10^3 and 100 Å). The mobile phase buffer was prepared with Milli-Q water, 200 mM sodium nitrate, 10 mM sodium phosphate and 200 ppm sodium azide. Then it was filtered through a 0.45 µm filter and injected at a flow rate of 1 mL/min at 30°C. The system was calibrated with narrow disperse polyethylene glycol/oxide (PEG/PEO) standards (Polymer Laboratories) ranging from 615 to 1,378,000 g mol^{-1}, and molar masses are reported as PEG/PEO equivalents.

3.5.3 Thermogravimetric (TGA) analysis

Thermal degradation as a function of monomer concentration was investigated using TGA. Perkin Elmer Pyris 1 TGA thermogravimetric analyser (USA) was used for TGA analysis. The inert N_2 gas flow rate of 10 ml/min was set to provide the appropriate

environments for the test. Approximately 5 mg were placed in the specimen holder, and the furnace was raised. Initially, the samples were kept in the furnace until a stable weight reached, and initial weight reading was set to 100%. The temperature was scanned from 25°C to 800°C at 10°C-min^{-1} under a nitrogen purge of 10 ml/min, switched to air with the same flow rate at 700°C. The TGA was calibrated using Curie temperature standard and a references mass. The mass loss after switching to air was due to combustion of carbon residue formed during the scan. The results were represented using Origin software and represented as a mass fraction and its derivative with time as a function of temperature. Three measurements for each set of samples were performed under the same operating conditions. Three measurements for each set of samples were performed under the same operating conditions.

3.5.4 Differential scanning calorimetry (DSC) analysis

DSC (Perkin–Elmer Pyris 1) was used for the analysis of heat generation over increased temperature for pure PMPC. Sample was thoroughly dried, and weighted (approximately ~ 3-5 mg) and placed in a hermetic aluminium pan. The empty pan was used as a reference. The sample pan was placed on a sample slot, and a reference pan was placed on a reference slot before initiating the heating program. The samples were heated from 20°C to 200°C at a rate of 10°C.min^{-1}, under a nitrogen flow of 20 mL/min. The instrument was calibrated for temperature using indium and lead, for enthalpy using indium and a furnace calibration was performed according to the manufacturer recommendation. A baseline with matched empty pan was used to convert the data to heat capacity curves for comparison of curves. DSC experiments were repeated 3 times for each set of samples, and average result was reported.

3.6 Biological response evaluation

The biological response of PMPC grafted surface was evaluated from cell culture study. Cell culture was carried out to investigate the effect of PMPC grafting on cell growth and attachments. Four types of samples were selected: (1) as-built untreated, (2) polished untreated, (3) as-built polymer treated, and (4) polished polymer treated. The cell response of CHO cells was examined on the treated and untreated samples, as they are the most common mammalian cell line used for human applications [179, 180]. These cells allow post-translational modifications to recombinant proteins which can function in humans [181].

In this study, CHO cells were grown in MEMα modification and the media was supplemented with 10% Fetal Bovine Serum, and 1% penicillin and streptomycin. At first, CHO cells were seeded onto the samples at a concentration of 4x104 cells/cm^2. After 24 and 72 hours of incubation at 37 °C, the samples were rinsed with PBS two times and fixed using 4% paraformaldehyde (Sigma-Aldrich) for 30 min at room temperature. The samples were then rinsed twice with PBS and divided into two batches. PBS was employed in the first batch, held at 4°C for later confocal microscopic analysis (N-STORM SuperResolution/Confocal microscope). The second batch was sequentially dehydrated using 50%, 70%, 90% and 95% ethanol solution for 10 min each and then with 100% ethanol for 15 min. After this dehydration was completed, the samples were allowed to dry overnight in a fume hood for subsequent SEM imaging.

3.7 Mechanical and tribological properties evaluation

3.7.1 Mechanical properties evaluation

Nanoindentation studies are useful to evaluate the effect of thin PMPC layer on mechanical properties of polymer grafted surface [182]. The nano-mechanical properties of the fabricated samples such as penetration depth, hardness and reduced elastic modulus were

measured using a Hysitron TI-950 Tribo-indenter (Hysitron Inc., USA) with a diamond Berkovich tip. Penetration depth comparisons were performed by indenting to a maximum load of 500 μN on each sample. Hardness and Young's modulus mapping was also performed by indenting in a 20 x 20 array on each sample, with a separation of 10 μm between each indent (sufficient to avoid any effect of residual stresses from the neighbouring indents). Each indent was loaded over 10 s, held at maximum load for 10 s, then unloaded over 10 s. The maximum load within each array was linearly increased from 5 μN - 1000 μN. The Oliver and Pharr method [183] was used to calculate indentation hardness and Young's modulus, from the load/unload curves.

The relationship between reduced elastic modulus, indenter's contact area and stiffness from unloading curve is given by:

$$E_r = \frac{S\sqrt{\pi}}{2\sqrt{A}} \tag{3.1}$$

where E_r is the reduced elastic modulus.

The Young's modulus (E) of the sample is calculated by the following formula:

$$\frac{1}{E_r} = \frac{1-\vartheta^2}{E} - \frac{1-{\vartheta_i}^2}{E_i} \tag{3.2}$$

Where, ϑ and E are the Poisson's ratio and Young's modulus of indented sample, respectively while ϑ_i and E_i are the corresponding values for indenter. For the diamond indenter tip used in this study, ϑ_i and E_i are 0.07 and 1141 GPa [184], respectively.

Cyclic loading up to a maximum load of 1000 μN was performed using a 5 μm radius spherical tip. Stress-strain curves were calculated from the collected data using the method detailed by Field and Swain [185]. The strain value was calculated for the penetration depth area at maximum load of 1000 μN, and then the stress-strain curve was plotted to compare the elasticity of untreated and polymer treated surfaces.

3.7.2 Scratch test

Nano-scratch tests were carried out to investigate the effect of PMPC film on the scratch resistance of Ti6Al4V substrate. A TI950 Nanoindenter (Hysitron Inc., USA) equipped with a 1 μm diameter spherical tip was used to conduct the nano-scratch test with a progressively increasing load. A 10 μm long scratch was performed over 15 s while the applied load on the tip increased linearly to a maximum load of 0.5 mN (0.033 mN/s) and 2 mN (0.133 mN/s). The displacement of the indenter was constantly monitored during the test. Scanning probe microscopy (SPM) was performed on 12 μm×12 μm square areas to get the topography of the sample after scratch testing.

3.7.3 Tribological properties evaluation

Triboindenter was used to evaluate the nano-tribological performance of PMPC grafted implants. Wear analysis was conducted using a Cube Corner indentation tip under three different loads. Loads were selected based on trial and error nanoindentation method for performance evaluation of polymer grafted samples. The different loads; 20 μN, 60 μN and 100 μN were applied as low, medium and high loads, respectively. Wear tests were carried out at least on 10 different areas of samples with 3 repetitions on each selected area. SPM was performed on affected areas to compare the topography of the sample after wear testing.

3.8 Statistical analysis

The IBM SPSS statistics 21 software was used to perform statistical analysis and determine whether there is any significant difference in the subsets of experimental data. For this purpose, a two-way ANOVA analysis of variance was performed on all subsets of data in each experiment to compare samples. In this project, statistical analyses were performed on surface roughness, polymerisation rate, water contact angle, hardness, Young's modulus and film formation results.

3.9 References

[176] Ghosh S, Abanteriba S, Wong S and Houshyar S 2018 Selective laser melted titanium alloys for hip implant applications: Surface modification with new method of polymer grafting *Journal of the Mechanical Behavior of Biomedical Materials* **87** 312-24

[177] Good R J and Koo M 1979 The effect of drop size on contact angle *Journal of Colloid and Interface Science* **71** 283-92

[178] Chen S, Zheng J, Li L and Jiang S 2005 Strong resistance of phosphorylcholine self-assembled monolayers to protein adsorption: insights into nonfouling properties of zwitterionic materials *Journal of the American Chemical Society* **127** 14473-8

[179] Yamane-Ohnuki N, Kinoshita S, Inoue-Urakubo M, Kusunoki M, Iida S, Nakano R, Wakitani M, Niwa R, Sakurada M and Uchida K 2004 Establishment of FUT8 knockout Chinese hamster ovary cells: An ideal host cell line for producing completely defucosylated antibodies with enhanced antibody-dependent cellular cytotoxicity *Biotechnology and bioengineering* **87** 614-22

[180] Han S and Rhee W J 2018 Inhibition of Apoptosis Using Exosomes in Chinese Hamster Ovary Cell Culture *Biotechnology and bioengineering*

[181] Lai T, Yang Y and Ng S K 2013 Advances in mammalian cell line development technologies for recombinant protein production *Pharmaceuticals* **6** 579-603

[182] Tiwari A and Natarajan S 2017 *Applied Nanoindentation in Advanced Materials*: John Wiley & Sons)

[183] Oliver W C and Pharr G M 1992 An improved technique for determining hardness and elastic modulus using load and displacement sensing indentation experiments *Journal of materials research* **7** 1564-83

[184] Oliver W C and Pharr G M 2004 Measurement of hardness and elastic modulus by instrumented indentation: Advances in understanding and refinements to methodology *Journal of materials research* **19** 3-20

[185] Fielda J and Swain M 1996 The indentation characterisation of the mechanical properties of various carbon materials: Glassy carbon, coke and pyrolytic graphite *Carbon* **34** 1357-66

CHAPTER FOUR: DEVELOPMENT OF POLYMER GRAFTING TECHNIQUE ONTO THE SURFACE OF TITANIUM SUBSTRATE

4.1 Chapter overview

This chapter presents the novel technique of developing polymer grafting onto the surface of a 3D printed metal substrate. In this study, a combination of several relevant surface characterisation techniques such as SEM, surface topography, EDS, XPS, and FTIR analyses were performed to well-understand the production process of different polymer grafting techniques, and finally, it helped in optimising the grafting techniques. Overall, this study fulfils the objective 1 (as stated in section 1.6) and answers the research question 1 (as stated in section 1.5) of this project.

This study aimed to develop a new method of grafting surface of selective laser melted titanium alloy (SLM Ti6Al4V) with PMPC, to improve the surface properties and biocompatibility of the implant. PMPC was grafted onto the surface of SLM Ti6Al4V, through three techniques as follows; ultraviolet (UV) irradiation, thermal heating both under normal atmosphere and UV irradiation under N_2 gas atmosphere.

*This work has been published in ***Journal of the mechanical behaviour of biomedical materials*****.** **Ghosh, Subir**, Abanteriba, Sylvester, Wong, Sherman and Houshyar, Shadi. "***Selective laser melted titanium alloys for hip implant applications: Surface modification with new method of polymer grafting.***" Journal of the mechanical behaviour of biomedical materials 87 (2018): 312-324.

Results demonstrated that a continuous PMPC film on the Ti6Al4V surface was achieved through the UV irradiation under nitrogen atmosphere technique, due to the elimination of oxygen from the system. As indicated in the results, one of the advantages of this technique was the presence of phosphorylcholine, mostly on the surface, which demonstrated that the polymer chains had been successfully anchored onto the surface of Ti6Al4V. Filmetric analysis identified the highest polymer film thickness for the surface grafted using UV irradiation under a nitrogen atmosphere. Therefore, this technique has been considered as optimal grafting technique considering surface morphology, film composition and thickness of the grafted layer.

4.2 Experimental procedure

Ti6Al4V samples were fabricated at 0° inclination with respect to the building direction using the SLM technique. The details of materials and SLM fabrication process were discussed in Chapter three. Prior to the grafting process, multistage of chemical washing and treatments were conducted, details are in Chapter three. 0.4M monomer concentration was used for this study, which was prepared by diluting in dH_2O. Hydroquinone and monomethyl ether hydroquinone were removed from the monomer solution during the purification process using an inhibitor column. The different steps of polymer grafting process onto SLM Ti6Al4V substrate are shown in Fig. 4.1. In this study, three different grafting methods were investigated for the optimisation process. In method 1 (M1), the treated samples were immersed in the monomer solution and kept in a chamber under UV irradiation for 1 hour under a normal atmosphere. In method 2 (M1), the treated samples were immersed in the monomer solution and heated to 60°C under a normal atmosphere for 15 hours. In method 3 (M3), the process

was similar to method one, but the process was carried out under a nitrogen atmosphere to eliminate oxygen.

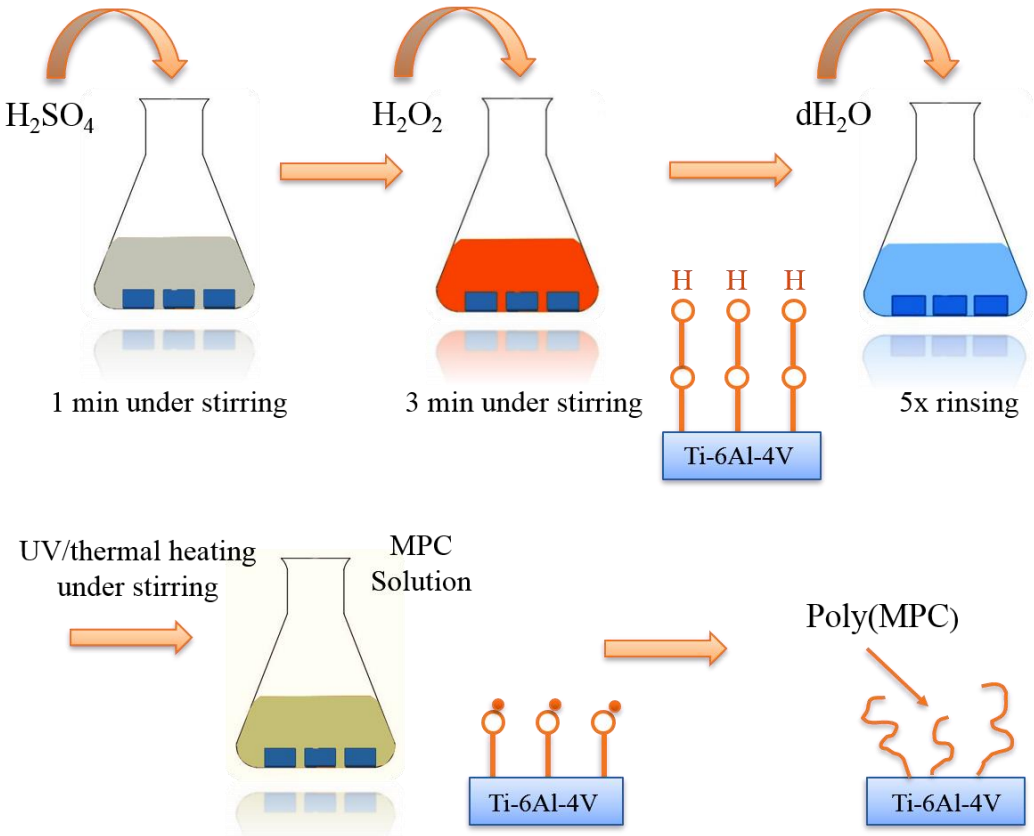

Fig. 4.1 Graphical representation of polymer grafting process onto the surface of SLM Ti6Al4V.

N_2 gas bubbling was carried out for 30 min before immersing the samples and continued for a further 10 min after immersing the samples in the monomer solution, Fig. 4.2.

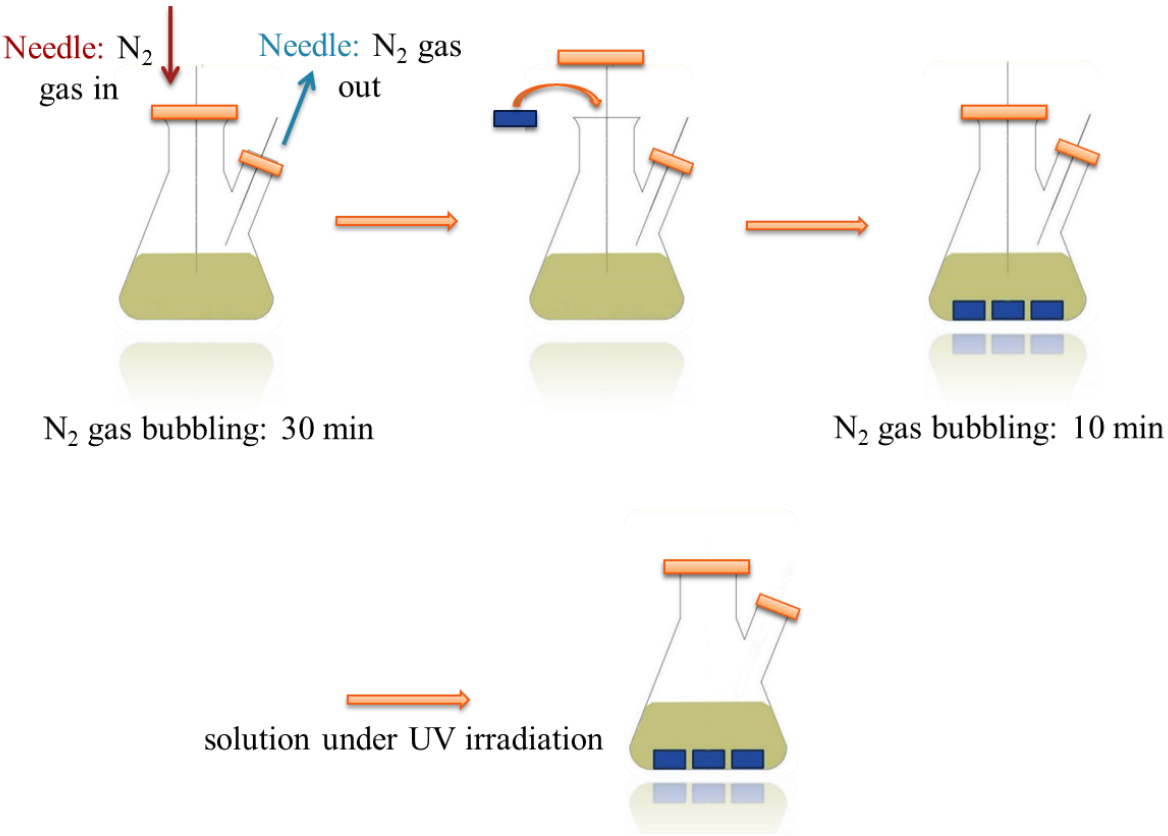

Fig. 4.2 Graphical representation of N_2 gas bubbling (degassing) for method 3.

A closed balloon was used during UV irradiation to ensure the absence of oxygen in the system. UV irradiation and thermal heating were carried out to initiate polymerisation by activating the reaction sites of monomers. A UV curing flood (SUNRAY 400 SM) source with100 mW/cm2 was used for photo-irradiation. Finally, the polymer grafted samples were immersed in distilled water and kept overnight to remove all unpolymerised monomer residues. The washed samples were cleaned in ethanol and dried under nitrogen before storing for further investigation. The samples were labelled as follows: non-polished control surface (as-built), polished surface, non-polished surface treated after polymer grafting method 1 (UVNP-M1), polished surface after polymer grafting method 1 (UVP-M1), non-polished surface after polymer grafting method 2 (THNP-M2), polished surface after polymer grafting method 2 (THP-M2), non-polished surface after polymer grafting method 3 (UVNP-M3), polished

surface after polymer grafting method 3 (UVP-M3). The non-polished untreated Ti6Al4V substrate was used as a control surface in this study. The experimental condition of all samples is summarised in Table 4.1.

Table 4.1 The experimental condition of all samples.

Type of sample	Treated method	Activation method	Polymerisation condition
as-built	untreated	-	-
polished	untreated	-	-
UVNP-M1	method 1	UV irradiation	atmospheric
UVP-M1	method 1	UV irradiation	atmospheric
THNP-M2	method 2	Thermal heating	atmospheric
THP-M2	method 2	Thermal heating	atmospheric
UVNP-M3	method 3	UV irradiation	N_2 gas atmosphere
UVP-M3	method 3	UV irradiation	N_2 gas atmosphere

The SEM machine was operated at a high voltage (HV) power supply of 15 KV under vacuum at spot size 5 for all samples. A Tencor profilometer and 3D optical profiler was used to measure the average surface roughness (R_a) of the samples scanning top surface. Various scanning areas, (~100×130 μm^2) and (~240×320 μm^2) were selected for non-polished and polished surfaces, respectively, to characterise the surface topography for different grafting techniques. The scanning lens has different magnification, and a small area was selected to obtain a 3D surface map from the surface. EDS analysis was carried out to analyse the micro-topography and XPS analysis was performed to analyse the chemical composition of the top 1 to 10 nm of the samples. The surface atomic compositions of the surfaces before and after polymer grafting were determined using XPS. FTIR analysis was undertaken to analyse the chemical bond between the grafted polymer and the substrate. A wettability measurement was carried out to measure the contact angle. The thickness of the polymer grafted layer was measured by Filmetrics analysis. Statistical analysis was performed on all subsets of data in

each experiment to compare samples. The details of the experimental procedure for surface characterisation techniques have been discussed in Chapter three.

4.3 Results and discussion

In this study, MPC monomer was grafted to a surface of SLM Ti6Al4V by radical polymerisation. Covalent bonding formed between the free radicals on the Ti6Al4V surface and the polymer chain when the samples were immersed in a MPC solution [186]. Polymer grafting was not successful in M1 due to the presence of oxygen which inhibited the polymerisation of the MPC monomers. Furthermore, complete polymerisation with M2 technique was achieved after 15 hours of thermal heating while polymerisation was completed after 1 hr of UV irradiation technique in method 3 (M3). Polymerisation under nitrogen atmosphere prevents oxygen from entering the polymerisation vessel during the preparation of the monomer solution. Polymer grafted samples prepared through M3 method was considered for EDS, XPS spectra.

4.3.1 Surface characterisation

4.3.1.1 Surface morphology

The surface morphology of as-built samples after polymer grafting is shown in Fig. 4.3,. Fig. 4.3 (a) shows that the control sample has a rough surface with few partially-melted particles. After grafting the polymer to the surface, the surface looks smooth with small changes. Fig. 4.3(b), (c) and (d) show surface comparisons produced with different methods. Fig. 4.3 (b) shows no significant change in the surface morphology of the control and treated samples using method 1 while Fig. 4.3(c) and (d) show significant modifications in the surface morphology of the treated sample with methods 2 and 3 compared to the control and treated samples with method 1. The surface changes are more visible for the treated sample with

method 2 (Fig. 4.3(c)) than other methods. The grafted polymer in method 3 exhibited the best results (Fig. 4.3(d)), as the grafted layer appears more stable and continuous compared to the surfaces treated by method 1 and 2.

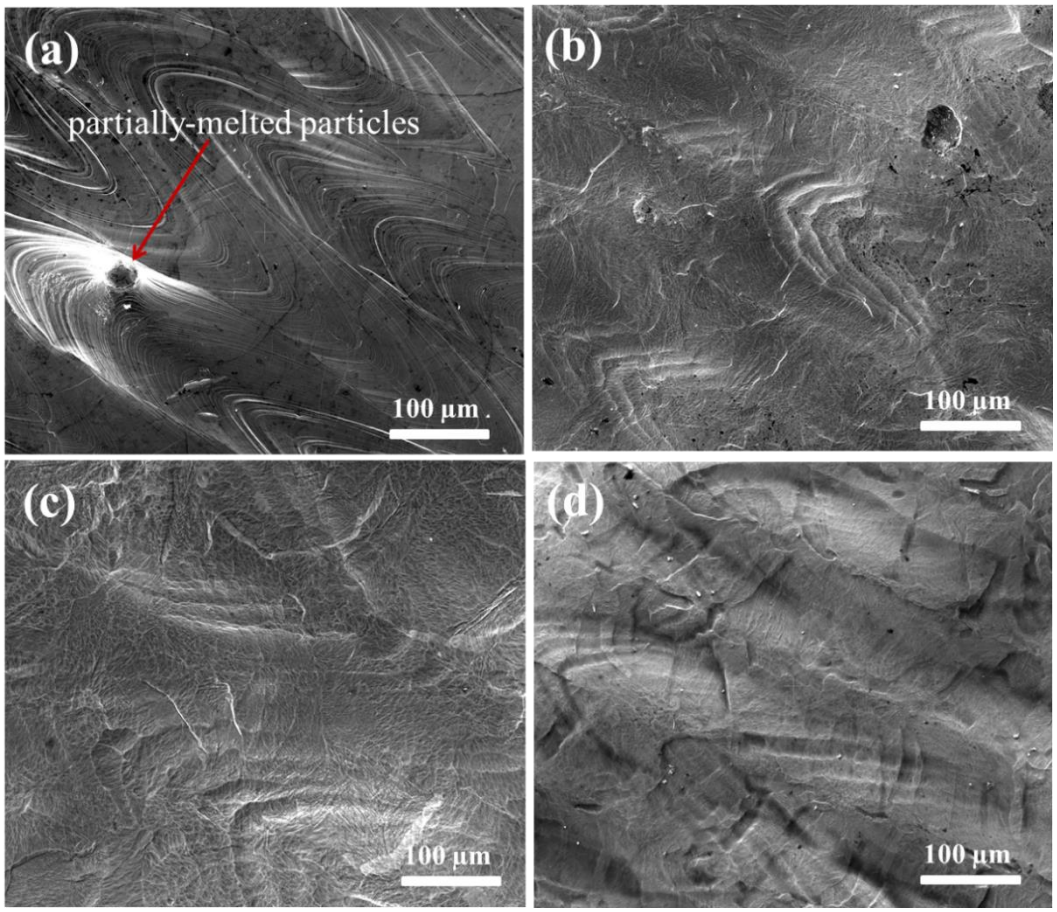

Fig. 4.3 Surface morphology of a) as-built, b) UVNP-M1, c) THNP-M2 and d) UVNP-M3 surfaces.

Fig. 4.4 compares the surface morphology of the polished samples before and after polymerisation. The grafted layer is thick and continuous for the sample treated with method 3, UVP-M3, followed by THP-M2. Fig. 4.4(b) shows that PMPC did not cover most of the Ti6Al4V surface. This outcome suggests that the surface was not properly grafted, and polymerisation was terminated early due to the presence of oxygen during polymerisation.

Oxygen reacts with free radicals and prevents the polymer group to form permanent covalent bonding with functional groups on the surface of the sample [186].

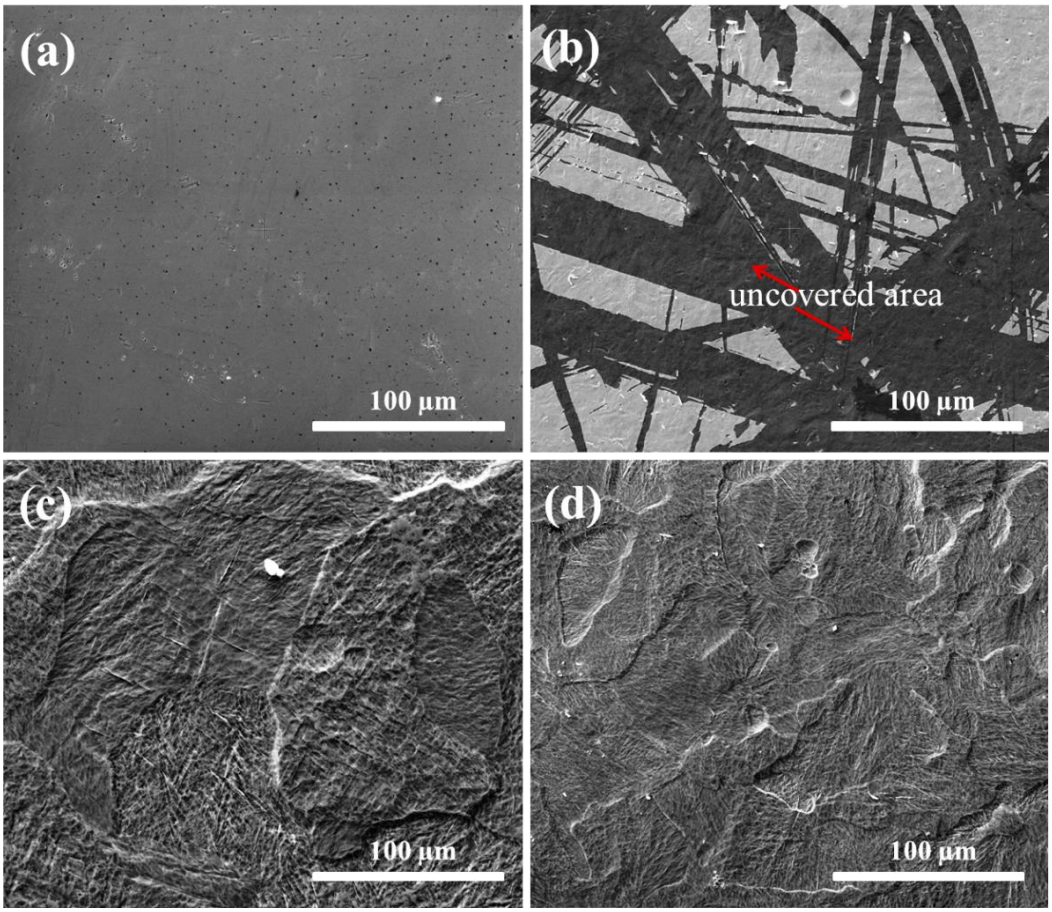

Fig. 4.4 Surface morphology of a) polished, b) UVP-M1, c) THP-M2 and d) UVP-M3 surfaces.

4.3.1.2 Surface topography & roughness

Investigating the surface topography reveals how the polymer is grafted onto the surface of the substrate. A 3D optical profile presents a 3D pattern of the top micrometre area of the surfaces. It facilitates analysis of polymer distribution on the surfaces by measuring the surface roughness of the scanning area. Fig. 4.5 and Fig. 4.6 present the 3D topography for the non-polished and polished surfaces respectively. In Fig. 4.5, both UVNP-M3 (Fig. 4.5(d)) and THNP-M2 (Fig. 4.5(c)) show reduction in surface roughness compared to the control surface

(Fig. 4.5(a)), while UVNP-M1 displays a higher surface roughness compared to the control surface.

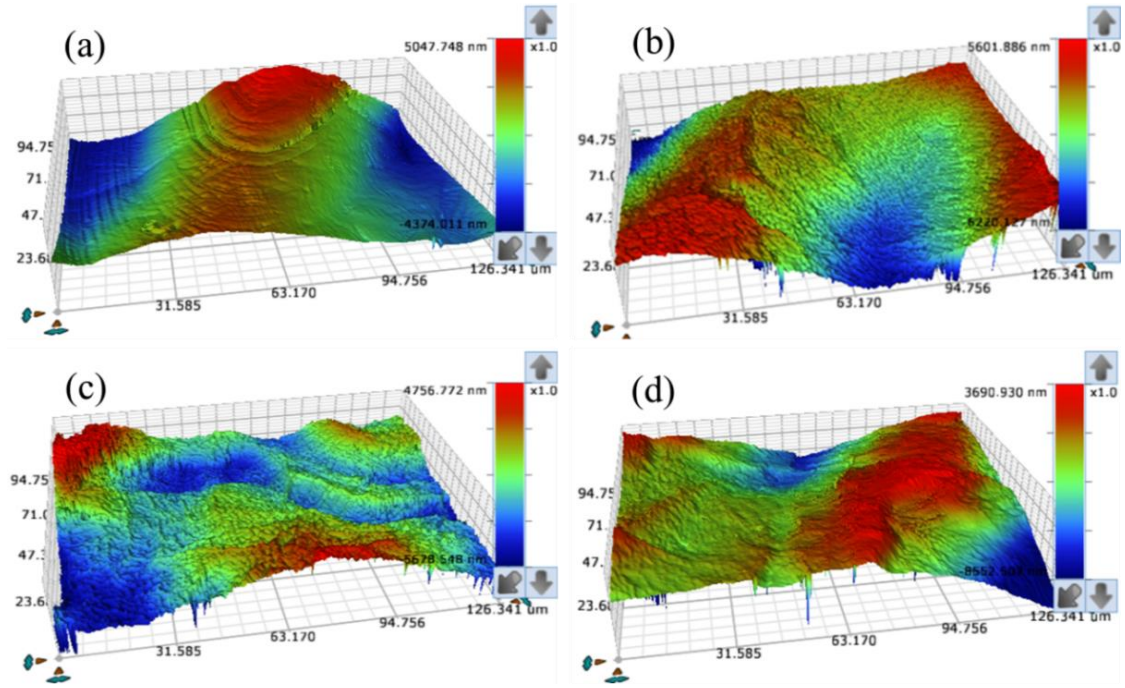

Fig. 4.5 Surface topography of a) as-built, b) UVNP-M1, c) THNP-M2, and d) UVNP-M3 surfaces.

Grafting was not uniform as it seemed that the monomer was merely attached to the surface. The non-uniform film in some areas resulted in higher surface roughness. Previous studies revealed a poorly attached layer delaminated at high loading due to the instability of the coated film [23, 24, 121, 147]. Permanent uniform grafting with low polydispersity is crucial for hip implant longevity. The reduction in surface roughness of UVNP-M3 followed by THNP-M2 confirmed that proper polymer grafting resulted in improved surface roughness for a control surface.

Fig. 4.6 presents different results compared to those found in Fig. 4.5. THP-M2 and UVP-M3 surfaces displayed higher surface roughness than the polished control surface. The polished Ti6Al4V surface had a very low surface roughness (29 ± 5 nm). However, after

polymer grafting, the surface presented a hydrated brush-like structure [26] which led to deposition of PMPC onto the mirror polished surface, increasing roughness. The increased surface roughness, in turn, could impact wettability and other surface properties that will be discussed later.

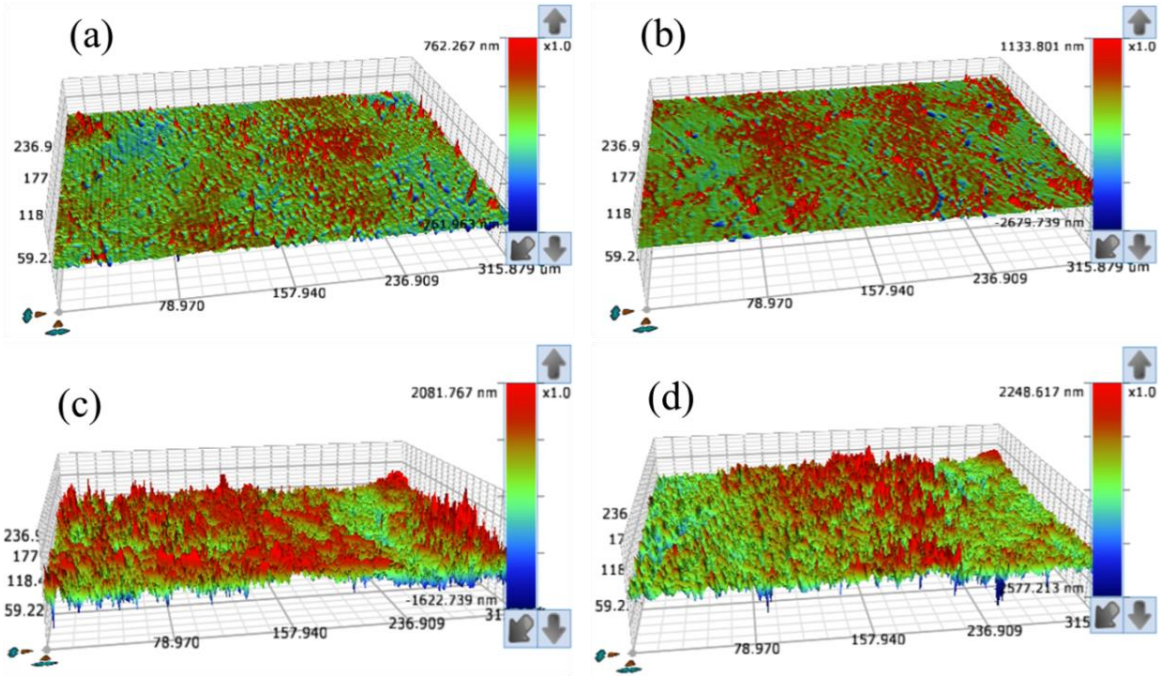

Fig. 4.6 Surface topography of a) polished, b) UVP-M1, c) THP-M2 and d) UVP-M3 surfaces.

Table 4.2 summarises the average surface roughness of all samples measured by the Tencor profilometer; the results followed a similar trend to 3D optical profiler results.

Table 4.2 Average surface roughness measured by Tencor profilometer.

Surface roughness (R_a) in µm							
as-built	**Polished**	**UVNP-M1**	**UVP-M1**	**THNP-M2**	**THP-M2**	**UVNP-M3**	**UVP-M3**
4.755±1.05	0.029±0.01	3.517±0.85	0.226±0.10	2.114±0.75	0.271±0.05	2.306±0.65	0.343±0.25

This surface roughness results indicate that polymer grafting techniques significantly decreased the roughness of coarse surfaces while increased roughness of polished surfaces. It

can be seen from Fig. 4.6 (c) & Fig. 4.6 (d), that the grafted layer was not homogenous. A uniform layer is essential for the reduction of surface roughness and uniform load distribution. The non-uniform grafted layer seen on THP-M2 and UVP-M3 increased surface roughness significantly. Statistical analysis of surface roughness results shows significant ($p<0.05$) differences in average roughness over all samples. However, this variation was still low for the polished surface before and after polymer grafting (<400 nm). It is possible to reduce surface roughness below 400 nm for the polished grafted surface if a homogenous layer can be achieved.

4.3.1.3 Energy-dispersive X-ray spectroscopy (EDS) analysis

EDS is an essential technique for compositional analysis. The main composition of PMPC (C, N, O, H, P, Si) and Ti6Al4V (Ti, Al, V) are different. Fig. 4.7(a-b) shows the EDS spectra for untreated, and PMPC treated surfaces. The peak for the phosphorous element was detected at 2 KeV binding energy for the treated surface, Fig. 4.7(b), due to the presence of a phosphorylcholine group in the PMPC. EDS spectra was obtained using the polymer grafted samples treated by M3 method. Elemental mapping exhibited the presence of Ti was dominant in the untreated surface while C was dominant in the polymer treated surface (Fig. 4.7(c-d)). It confirms that Ti6Al4V surfaces were covered by PMPC layer, therefore, the C composition increased in the treated surface due to the presence of PMPC. The line mapping results justified the previous consequence where a higher percentage of Ti and almost zero percentage of C were identified onto the untreated surface. Ti percentage decreased to almost zero on the polymer treated surface (Fig. 4.7(e-d)). It confirms the PMPC covered the of the surface of Ti substrate. Significant variation in C percentage after grafting proves that the fraction of polymer film was not uniform at different positions of the surfaces.

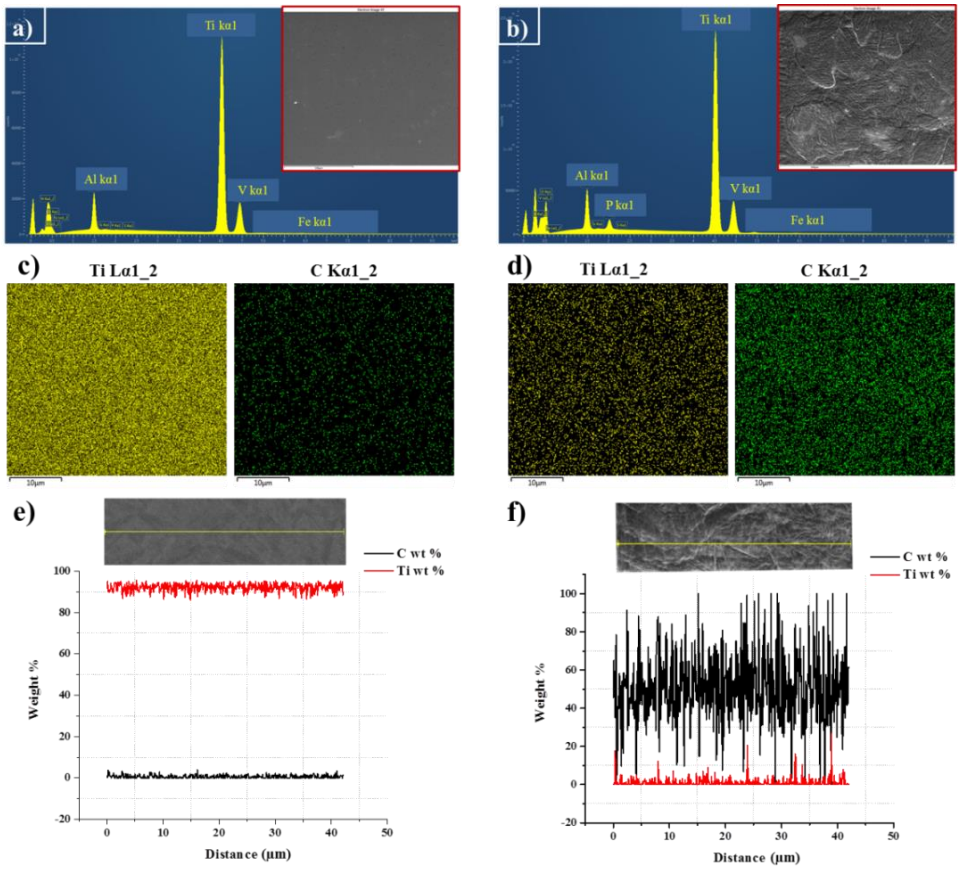

Fig. 4.7 EDS spectra of (a) untreated and (b) polymer treated surfaces. Inset is the SEM image of the scanned area and corresponding elemental distribution of major element of Ti and C for (c) untreated and (d) polymer treated surfaces. The line mapping results of weight percentages over the distance for (e) untreated and (f) polymer treated surfaces.

4.3.1.4 X-ray photoelectron spectroscopy (XPS) analysis

The XPS analysis is a reliable technique in investigating the outermost surface of the polymer grafted layer on a nano-scale. Fig. 4.8 presents XPS spectra for major elemental composition of implant surfaces before and after polymer grafting. XPS spectra was obtained using the polymer grafted samples treated by M3 method. Characteristic peaks of Ti6Al4V were obtained at 458.8 eV and 74.8 eV for Ti_{2p} and Al_{2p} [187-189]. However, these peaks were disappeared after polymer grafting, due to the coverage of the surface with PMPC. New peaks fol all PMPC treated surface was observed at 403 eV, 103 eV, and 134 eV, were observed due

to the presence of N_{1s}, Si_{2p}, and P_{2p} respectively. These peaks are specific to the phosphorylcholine groups in the MPC, which became remarkable for PMPC surface produced by method 3, due to the higher number of phosphorous atoms presented on the surface [190-192]. The peaks in the carbon atom region (C_{1s}) at 286.5eV and 289 eV, indicate the ether bond (C-O-) and the ester bond (C=O) respectively. These findings concurred with the previous studies [174, 175].

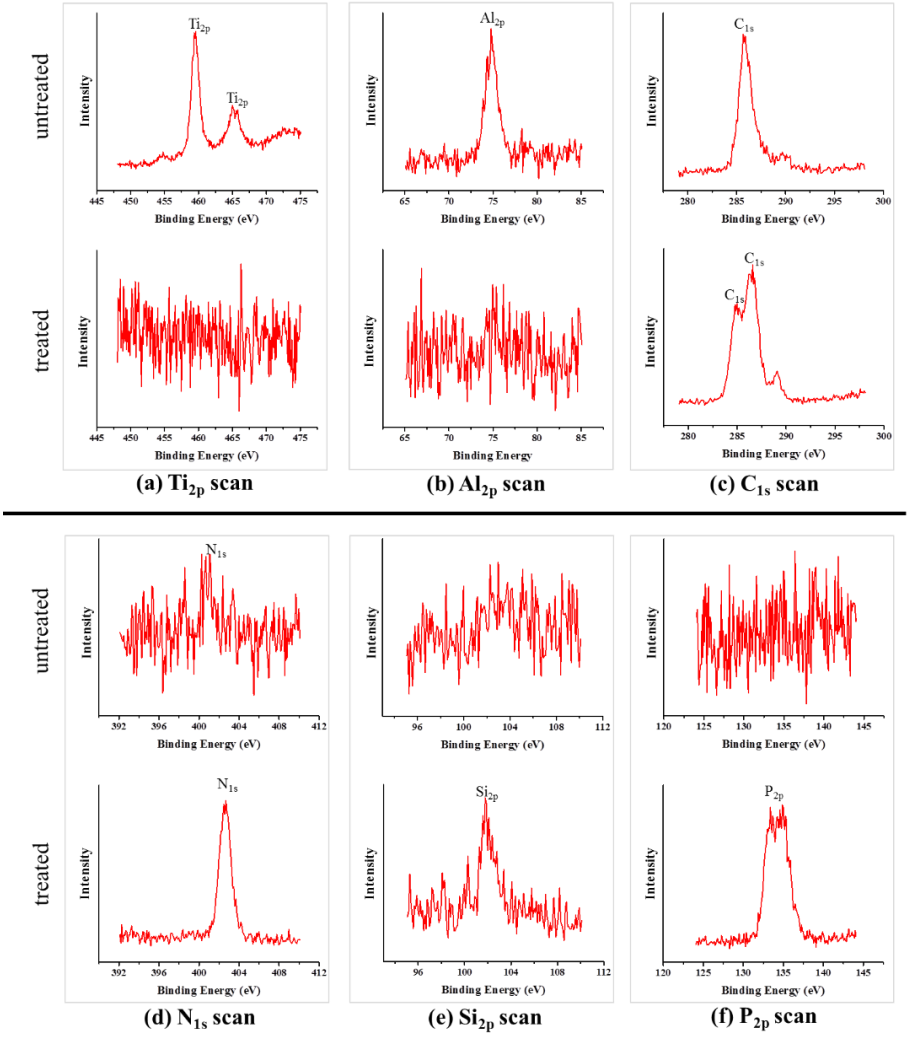

Fig. 4.8 Surface analysis of the PMPC grafted Ti6Al4V by XPS, The disappearance Ti_{2p}, Al_{2p} peaks and the appearance strong N_{1s}, Si_{2p} and P_{2p} peaks specific to the PMPC, after polymer grafting imply the PMPC was grafted successfully onto the surface of SLM Ti6Al4V.

The high-resolution XPS spectra of Ti_{2p} are presented in Fig. 4.9 in order to be able to compare the various grafting methods. The strongest Ti_{2p} peak was detected for the untreated surface followed by the treated surface using method 1 and method 2 respectively. However, no Ti_{2p} peak was detected for the treated surface using method 3, indicating a continuous and thick PMPC layer grafted on to the surface. The elimination of oxygen in this method resulted in high yield polymerisation on the surface of SLM Ti6Al4V implants.

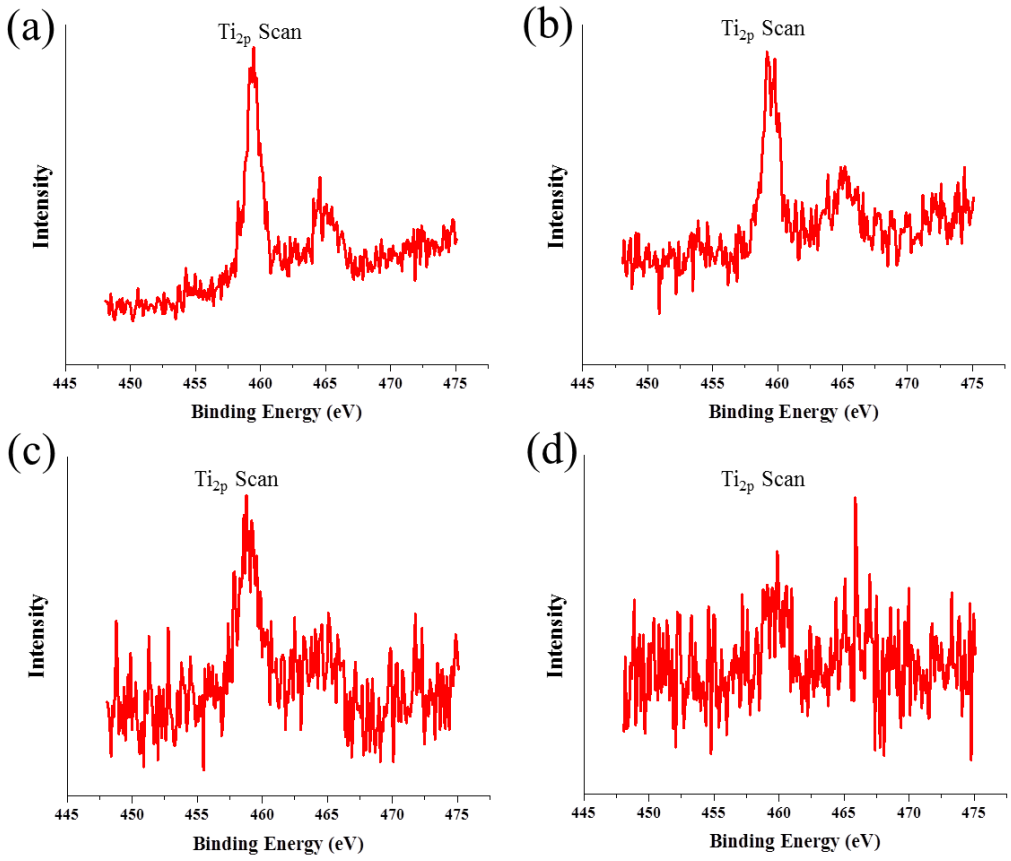

Fig. 4.9 XPS high-resolution Ti_{2p} spectra after grafting with different methods, (a) as-built, surface grafted by (b) method 1, (c) method 2, and (d) method 3.

The relative atomic percentages for elemental compositions are summarised in Table 4.3. A high percentage of C, O is detected for untreated surfaces, because bulk Ti6Al4V reacted with air, forming oxide and carbide depending on the atmospheric conditions [193]. During the

SLM process, the presence of carbon dioxide could not be controlled, resulting in an unknown quantity of carbon in the manufacturing environment. The results from this study concurred with the one obtained by a previous study on SLM Ti6Al4Vs [158, 163]. The lowest amount of Ti was detected for the sample grafted with M3, followed by M2 and M1, respectively.

Table 4.3 Relative atomic percentages of elements determined using XPS for untreated and treated samples.

	Relative atomic (%)							
Type of sample	Al_{2p}	C_{1s}	N_{1s}	O_{1s}	P_{2p}	Si_{2p}	Ti_{2p}	V_{2p}
as-built	5.8±1.5	33.5±3.5	2.6±0.7	38.5±3.9	0.1±0.1	0.5±0.09	15.5±7.8	3.5±1.2
Polished	5.7±1.5	34.5±3.7	3.3±0.1	32.8±3.2	0.1±0.1	0.3±0.05	18.4±4.2	4.9±1.5
UVNP-M1	2.4±0.9	45.5±4.5	4±1.5	37.9±4.5	5.6±1.5	0.6±0.07	3.9±2.4	0.1±0.1
UVP-M1	0.2±0.1	48.4±4.5	4.5±1.5	29.8±3.1	6.7±1.5	0.1±0.09	10.2±3.5	0.1±0.1
THNP-M2	5.6±1.5	45.5±4.3	4.9±1.6	27.2±2.5	4.6±1.5	3.1±1.50	1.4±0.2	7.7±2.5
THP-M2	5.6±1.5	46.6±5.7	4.7±1.4	26.1±2.9	7.1±1.5	1.7±0.07	0.4±0.1	7.8±4.9
UVNP-M3	2.4±0.8	51.3±6.5	6±1.2	22.6±1.8	6.2±1.5	3.8±1.80	0.7±0.1	7±3.5
UVP-M3	1.9±0.7	52.6±3.4	7±1.6	22.1±1.9	8±1.9	1.5±0.80	0.2±0.1	6.7±3.7

These results support previous data obtained by EDS. XPS provided the information at the nanometer scale of the MPC grafted layer. The absence of Ti peak indicates a continuous grafted layer achieved by method 3. The other polymer elements (P, Si, N) were also found in greater amounts using method 3. There was a significant difference ($p<0.05$) in atomic percentages of the elements for various grafting methods, but there is no significant difference ($p>0.05$) between unpolished and polished grafted surfaces in each method.

4.3.1.5 Fourier transform infrared spectroscopy (FTIR) analysis

In a more in-depth analysis, FTIR transmission peaks provide more information about the functional group due to the molecular vibrations. The peaks for nitrogen and phosphate groups were detected only for UVNP-M3 (Fig. 4.10(a)) and UVP-M3 (Fig. 4.10(b)).

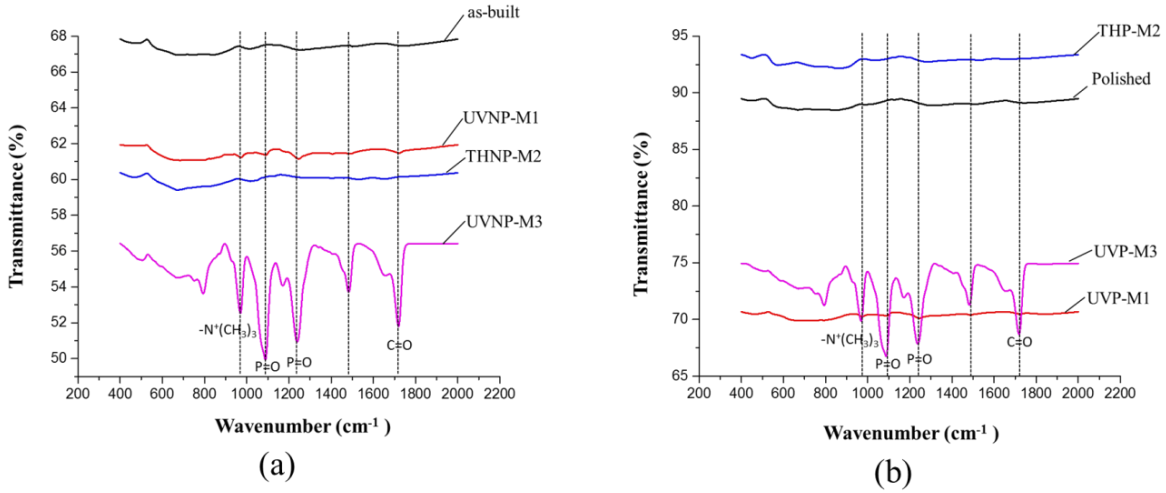

Fig. 4.10 FTIR spectra of polymer grafted surface under different grafting methods (a) non-polished polymer grafted surfaces and (b) polished polymer grafted surfaces.

MPC has phosphorylcholine in its side chains. The strong phosphate (P=O) group spectra for the surface grafted by method 3 confirmed that the polymers were anchored successfully onto the substrate. The presence of $–N+(CH_3)_3$ and P=O bonding confirms the existence of phosphorylcholine in the grafted surface. The phosphorylcholine moiety in the MPC units has a significant effect on reducing unfavourable protein adsorption and inhibiting cell adhesion [194]. High blood compatibility of the MPC polymer was reported in a previous study [195]. The MPC polymer grafting on the surface of Ti6Al4V implants was effectively performed using method 3. Kyomoto *et al.*[30] also reported the strong bonding of phosphate (P=O) and ketone group (C=O) for MPC grafting onto the CLPE. Although thermal heating (method 2) showed significant positive results in the EDS & XPS analysis, no strong polymer peaks for P=O or C=O bonding were detected for THNP-M2 and THP-M2 in FTIR analysis. After PMPC-grafting by method 3, the peaks attributed to the MPC unit were clearly detected in both XPS and FTIR spectra of the PMPC-grafted Ti6Al4V.

4.3.2 Wettability

The water contact angle value indicates the wettability properties of the surface. It was reported that the water contact angle was high for a surface with high roughness and hydrophobic nature [24, 196]. Table 4.4 presents the measured contact angle for all samples. In this table, most of the surfaces displayed hydrophilic nature except for the surface grafted by method 1. It was expected that MPC grafting would improve wettability, but no significant difference ($p>0.05$) was observed between polished and grafted polished surfaces. Nevertheless, the water contact angle was reduced significantly for THNP-M2 and UVNP-M3 compared to the as-built control surface. These results concurred with the surface roughness results in Table 4.2.

Table 4.4 Average contact angle for untreated and polymer treated samples by different grafting methods.

Water contact angle in degree							
as-built	polished	UVNP-M1	UVP-M1	THNP-M2	THP-M2	UVNP-M3	UVP-M3
84.3±5	70.6±4	92.4±5	88.2±4	72.9±4	71.5±3	75.2±05	74.1±4

As-built sample surface showed a relatively high hydrophobic nature compared to the polymer grafted surface using method 2 and 3, due to high surface roughness and non-uniformity of the grafted layer. On the other hand, grafting MPC onto the surface of THNP-M2 and UVNP-M3 reduced surface roughness significantly ($p<0.05$) and resulted in improved surface wettability. However, the surface of polished Ti6Al4V was super-hydrophilic due to its low surface roughness (29±5 nm) and uniformity of the grafted layer. Surface roughness increased significantly for UVNP-M3 followed by THP-M2 after polymer grafting, which could be due to the non-uniformity of the grafted layer. As grafting was conducted by radical polymerisation, there was less control over the length of the grafted chain. Previous researchers have reported a 33 % reduction in contact angle of CLPE grafted surface with MPC in

comparison with untreated one [30]. CLPE is a hydrophobic material, and Ti6Al4V is hydrophilic [23]. Furthermore, the surface roughness of CLPE was found to be a few times higher than that of the Ti6Al4V surfaces. Fig. 4.11 presents the water drops interaction onto the untreated and PMPC treated surface. It shows that better interaction of water and PMPC grafted surface (contact angle~76°) compared to untreated surface (contact angle~ 85°) because of the hydrophilic nature of the PMPC. Therefore, it attracts water molecules and consequently, the proteins present in biological fluids.

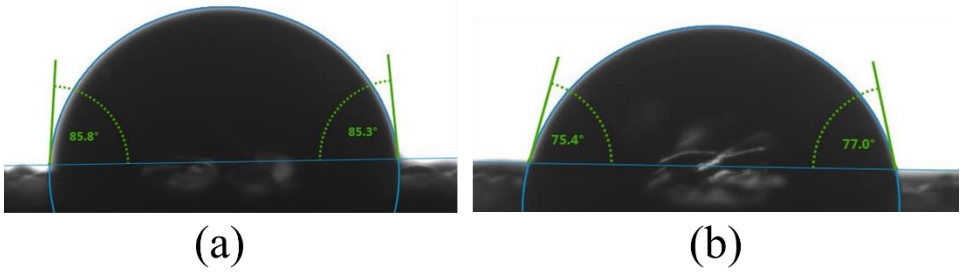

Fig. 4.11 Water-surface interaction for (a) untreated and (b) PMPC treated surface.

Improved wettability properties could be attributed to the homogenous grafted layer. The water molecules of a lubricant in the biological environment could have been attracted by the hydrophobic part of the hydrated MPC polymer. The unfavourable protein adsorption could be controlled if the implant surface is modified using the MPC polymer. Because the water state of the MPC grafted surface is naturally maintained, preventing the protein molecules from releasing the bound water molecules [128, 197, 198]. Therefore, water molecules cannot be interchanged between the polymer grafted implant and protein. The poor interaction is expected between grafted implants and blood components due to the hydration properties of the MPC polymer.

The protein adsorption is the initial indication of implant biocompatibility when the implants come in contact with physiological fluids. These protein adsorptions have both positive and negative effects on implants. The soft protein such as serum albumin can be easily adsorbed on to the metallic interfaces [199]. The adsorbed proteins form a protective layer, between the contacting interfaces, is considered as a driving force to improve the wear resistance of the implant. Favourable protein adsorption assists in improving the tribological behaviour of the implant in a physiological condition. However, these proteins are displaced by larger and unfavourable proteins due to the Vroman effect [200]. These proteins would affect contacting shear stresses changing the native surface behavior of the surface. The larger protein could interact with the implant materials and inhibit their original tribological performances. The larger sized non-specific proteins could increase the friction coefficient and consequently the wear rate of the implant. These proteins can initiate the inflammatory response that leads to platelet adhesion and thrombus formation, which indicates the unfavourable protein adsorption will lead to poor osseointegration of the implant. Controlled protein adsorption is important to maintain the biocompatibility and wear resistance of the implant. The hydrophobic surface is thought to be responsible for adsorbing a higher amount of proteins on the surfaces. The non-specific interaction and adsorption of protein onto the implant interfaces in the biological environment can be controlled by grafting the surface by MPC polymer which is known as a hydrophilic polymer. The MPC grafted surface alters the surface sensitivity and controls the interaction with proteins. Researcher revealed that that the free water fraction is 70% at equilibrium wet state for MPC polymer surfaces whereas; it is 30-40% for orthodox hydrophilic polymers [201]. The water faction is very important to repel the undesired proteins in contact with the implant. Since, the MPC grafted surface maintain hydrophilic properties, only soft albumin protein could adsorb on the surface which is crucial for enhanced wear resistance and perfect osseointegration of the implant. In this study, the

wettability results indicated that the MPC grafted surfaces would inhibit adsorption of non-specific proteins and maintain the biocompatibility by adsorbing only limited albumin proteins. The tribological and osseointegration behaviour has been improved after PMPC grafting.

4.3.3 Thickness of grafted polymer layer

The thickness of the grafted polymer layer is important in evaluating uniformity. The thickness of the grafted polymer was measured from the reflectance of the surface over wavelength. The polished grafted surface exhibited higher reflectance, Fig. 4.12(b), compared to the as-built grafted surface, Fig. 4.12(a), due to its mirror-polished characteristics.

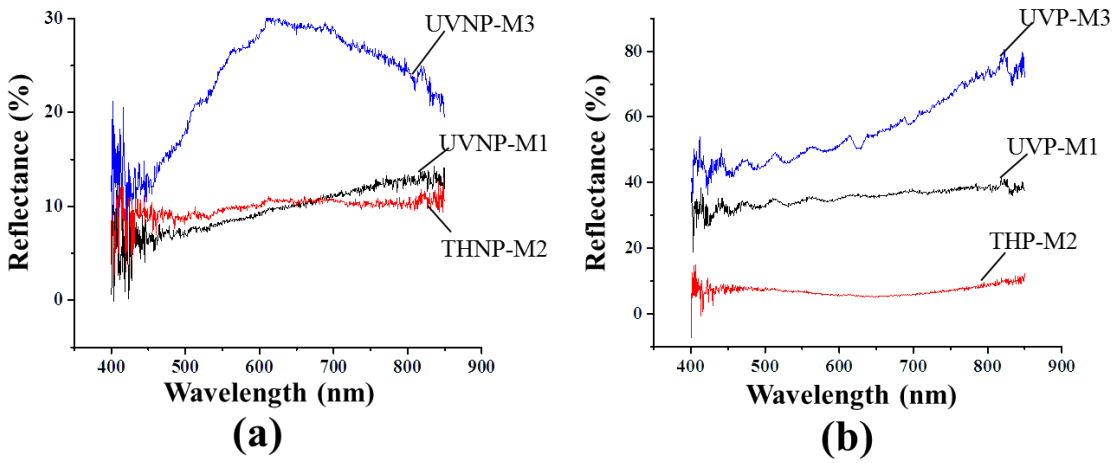

Fig. 4.12 Filmetrics spectra of polymer grafted layer for (a) non-polished polymer grafted surfaces and (b) polished polymer grafted surfaces.

The high thickness of the grafted layer was achieved using method 3, Table 4.5. A similar grafting thickness (100-200 nm) was reported on the CLPE substrate [27, 173]. Table 4.5 illustrates that grafting on a rough surface (as-SLM surface) tends to generate thick grafted layer. The surface is comparatively more inhomogeneous for rougher surfaces than polished surfaces. As a result, the surface area is higher for non-polished surfaces than polished surfaces.

More polymer chain can attach to the rough surface during polymerisation. Therefore, the non-polished surface has comparatively higher polymer thickness surface than the polished surface.

Table 4.5 Thickness of PMPC grafted layer for different grafting methods.

Type of sample	Grafting Thickness (nm)
UVNP-M1	65 ± 20
UVP-M1	60 ± 15
THNP-M2	125 ± 30
THP-M2	105 ± 20
UVNP-M3	221 ± 80
UVP-M3	175 ± 60

The thickest layer (221 ± 80 nm) of the grafted polymer was achieved by non-polished grafted surface using method 3. It is well known that PMPC has brush-like structures which facilitate smooth motion during contacting of two interfaces due to its hydrophilic properties. The thicker polymer layer has several benefits for tribological performance, such as preventing the implant interfaces from boundary contacts and minimising the coefficient of friction. However, the homogenous layer is also important to achieve low friction and high wear resistance of polymer grafted surface because the homogenous surface could lead to uniform load distribution on the surface resulted in higher wear resistance. Though the thickest grafting layer was achieved using grafting method 3, followed by method 2 and method 1, respectively, the grafted layer was not homogeneous. Variation in grafting thickness was maximum in method 3. Further study should be conducted to optimise monomer concentration and irradiation time. The homogeneity of the grafted layer is essential for good wettability and high biocompatibility.

4.4 Summary

In this study, a novel approach for grafting PMPC to the surface of SLM Ti6Al4V implants was investigated using diverse grafting techniques. Key findings are summarised as follows:

- The surface morphology confirmed that the best and most uniform grafted layer was achieved by polymerising using UV irradiation technique under a nitrogen atmosphere to prevent early termination due to present of oxygen.

- The hydrated PMPC layer minimised the surface roughness significantly on the as-built control surface, though a certain rise was observed on the polished surface due to its very low surface roughness.

- XPS and EDS spectroscopy confirmed a continuous PMPC layer on the surface of Ti6Al4V. The FTIR analysis demonstrated that the polymer chains had been successfully anchored onto the surface of Ti6Al4V using method 3, as there were strong peaks for P=O and C=O groups in FTIR analysis.

- There was no significant difference in atomic compositions of non-polished and polished grafted surfaces.

- The thickest layer (221 ± 80 nm) of the grafted polymer was achieved on the surface of the non-polished implant using method 3. However, the homogeneity of the grafted layer should be optimised for better wettability.

A homogenous and uniform hydrated layer of PMPC layer on the surface of SLM Ti6Al4V hip implants could minimise unfavourable protein adsorption and improve resistance to bacterial adhesion and cell attachment.

4.5 References

[23] Ghosh S, Choudhury D, Roy T, Mamat A B, Masjuki H and Pingguan-Murphy B 2016 Tribological investigation of diamond-like carbon coated micro-dimpled surface under bovine serum and osteoarthritis oriented synovial fluid *Science and Technology of Advanced Materials*

[24] Ghosh S, Choudhury D, Das N S and Pingguan-Murphy B 2014 Tribological role of synovial fluid compositions on artificial joints — a systematic review of the last 10 years *Lubrication Science* **26** 387-410

[26] Ishihara K 2015 Highly lubricated polymer interfaces for advanced artificial hip joints through biomimetic design *Polymer Journal* **47** 585-97

[27] Moro T, Takatori Y, Kyomoto M, Ishihara K, Saiga K-i, Nakamura K and Kawaguchi H 2010 Surface grafting of biocompatible phospholipid polymer MPC provides wear resistance of tibial polyethylene insert in artificial knee joints *Osteoarthritis and Cartilage* **18** 1174-82

[30] Kyomoto M, Moro T, Yamane S, Takatori Y, Tanaka S and Ishihara K 2017 A hydrated phospholipid polymer-grafted layer prevents lipid-related oxidative degradation of cross-linked polyethylene *Biomaterials* **112** 122-32

[121] Ching H A, Choudhury D, Nine M J and Osman N A A 2014 Effects of surface coating on reducing friction and wear of orthopaedic implants *Science and Technology of Advanced Materials* **15** 014402

[128] Ghosh S, Choudhury D and Pingguan-Murphy B 2016 Lubricating ability of albumin and globulin on artificial joint implants: a tribological perspective *International Journal of Surface Science and Engineering* **10** 193-206

[147] Affatato S, Goldoni M, Testoni M and Toni A 2001 Mixed oxides prosthetic ceramic ball heads. Part 3: effect of the ZrO 2 fraction on the wear of ceramic on ceramic hip joint prostheses. A long-term in vitro wear study *Biomaterials* **22** 717-23

[158] Pattanayak D K, Fukuda A, Matsushita T, Takemoto M, Fujibayashi S, Sasaki K, Nishida N, Nakamura T and Kokubo T 2011 Bioactive Ti metal analogous to human cancellous bone: fabrication by selective laser melting and chemical treatments *Acta Biomaterialia* **7** 1398-406

[163] Vaithilingam J, Prina E, Goodridge R D, Hague R J, Edmondson S, Rose F R and Christie S D 2016 Surface chemistry of Ti6Al4V components fabricated using selective laser melting for biomedical applications *Materials Science and Engineering: C* **67** 294-303

[173] Kyomoto M, Moro T, Miyaji F, Hashimoto M, Kawaguchi H, Takatori Y, Nakamura K and Ishihara K 2009 Effects of mobility/immobility of surface modification by 2-methacryloyloxyethyl phosphorylcholine polymer on the durability of polyethylene for artificial joints *Journal of Biomedical Materials Research Part A* **90** 362-71

[174] Kyomoto M, Moro T, Takatori Y, Kawaguchi H, Nakamura K and Ishihara K 2010 Self-initiated surface grafting with poly(2-methacryloyloxyethyl phosphorylcholine) on poly(ether-ether-ketone) *Biomaterials* **31** 1017-24

[175] Moro T, Takatori Y, Ishihara K, Konno T, Takigawa Y, Matsushita T, Chung U-i, Nakamura K and Kawaguchi H 2004 Surface grafting of artificial joints with a biocompatible polymer for preventing periprosthetic osteolysis *Nature Materials* **3** 829

[186] Chouirfa H, Migonney V and Falentin-Daudré C 2016 Grafting bioactive polymers onto titanium implants by UV irradiation *RSC Advances* **6** 13766-71

[187] Lin N, Liu Q, Zou J, Li D, Yuan S, Wang Z and Tang B 2017 Surface damage mitigation of Ti6Al4V alloy via thermal oxidation for oil and gas exploitation application: characterization of the microstructure and evaluation of the surface performance *RSC Advances* **7** 13517-35

[188] Znad H, Ang M H and Tade M O 2012 Ta/TiO2-and Nb/TiO2-mixed oxides as efficient solar photocatalysts: preparation, characterization, and photocatalytic activity *International Journal of Photoenergy* **2012**

[189] Nie L, Meng A, Yu J and Jaroniec M 2013 Hierarchically macro-mesoporous Pt/γ-Al 2 O 3 composite microspheres for efficient formaldehyde oxidation at room temperature *Scientific reports* **3** 3215

[190] Xu J, Yuan Y, Shan B, Shen J and Lin S 2003 Ozone-induced grafting phosphorylcholine polymer onto silicone film grafting 2-methacryloyloxyethyl phosphorylcholine onto silicone film to improve hemocompatibility *Colloids and Surfaces B: Biointerfaces* **30** 215-23

[191] Iwasaki Y, Sawada S-i, Ishihara K, Khang G and Lee H B 2002 Reduction of surface-induced inflammatory reaction on PLGA/MPC polymer blend *Biomaterials* **23** 3897-903

[192] Wei F, John B and Shiping Z 2004 Atom-transfer radical grafting polymerization of 2-methacryloyloxyethyl phosphorylcholine from silicon wafer surfaces *Journal of Polymer Science Part A: Polymer Chemistry* **42** 2931-42

[193] Ask M, Lausmaa J and Kasemo B 1989 Preparation and surface spectroscopic characterization of oxide films on Ti6Al4V *Applied surface science* **35** 283-301
[194] Konno T, Kurita K, Iwasaki Y, Nakabayashi N and Ishihara K 2001 Preparation of nanoparticles composed with bioinspired 2-methacryloyloxyethyl phosphorylcholine polymer *Biomaterials* **22** 1883-9
[195] Iwasaki Y, Kurita K, Ishihara K and Nakabayashi N 1997 Effect of reduced protein adsorption on platelet adhesion at the phospholipid polymer surfaces *Journal of Biomaterials Science, Polymer Edition* **8** 151-63
[196] Letchmanan K, Shen S-C, Ng W K, Kingshuk P, Shi Z, Wang W and Tan R B 2017 Mechanical properties and antibiotic release characteristics of poly (methyl methacrylate)-based bone cement formulated with mesoporous silica nanoparticles *Journal of the Mechanical Behavior of Biomedical Materials* **72** 163-70
[197] Ghosh S, Choudhury D, Roy T, Moradi A, Masjuki H H and Pingguan-Murphy B 2015 Tribological performance of the biological components of synovial fluid in artificial joint implants *Science and Technology of Advanced Materials* **16** 045002
[198] Ishihara K, Nomura H, Mihara T, Kurita K, Iwasaki Y and Nakabayashi N 1998 Why do phospholipid polymers reduce protein adsorption? *Journal of biomedical materials research* **39** 323-30
[199] Norde W and Lyklema J 1989 Protein adsorption and bacterial adhesion to solid surfaces: a colloid-chemical approach *Colloids and surfaces* **38** 1-13
[200] Wang M S, Palmer L B, Schwartz J D and Razatos A 2004 Evaluating protein attraction and adhesion to biomaterials with the atomic force microscope *Langmuir* **20** 7753-9
[201] NORDE W 2003 Driving forces for protein adsorption at solid surfaces *Surfactant science series* **110** 21-43

CHAPTER FIVE: THE EFFECT OF MONOMER CONCENTRATIONS ON POLYMERISATION RATE AND SURFACE PROPERTIES

5.1 Chapter overview

This chapter discusses the effect of MPC concentrations on polymerisation rate, polymer chain length and other surface properties of PMPC. Different characterisation techniques were applied to optimise the polymerisation parameters. In this study, a combination of several relevant surface characterisation techniques, such as SEM, NMR, surface topography, GPC and FTIR were performed to evaluate the effect of polymer grafting on the surface of Ti6Al4V and optimising the polymerisation parameters. The effect of PMPC layer on resistance to cell adhesion was also analysed. Overall, this research fulfils the objective 2 and 3 (as stated in section 1.6) and answers the research question 2 and 3 (as stated in section 1.5) of this project.

The objective of this study was to optimise the polymerisation parameters considering polymerisation rate, chain length and surface properties. Previous studies used monomer concentration at 0.5 M for grafting PMPC onto CLPE substrate [27, 28, 30, 173-175]. Other group used it at 0.7 M for grafting poly(sodium styrene sulfonate) (polyNaSS) onto titanium substrate [35, 186].

*This work has been published in ***Materials Science and Engineering C.***
Ghosh, Subir, Abanteriba, Sylvester, Wong, Sherman, Brkljača, Robert and Houshyar, Shadi. "***Optimisation of Grafted Phosphorylcholine-based Polymer on Additively Manufactured Titanium Substrate for Hip Arthroplasty***" Materials Science and Engineering C (published)

No study investigated whether the monomer concentrations have any effect on the physical and mechanical properties of the surface. Therefore, three different concentrations of MPC monomer, 0.4 M, 0.6 M and 0.8 M were examined to determine the influence of monomer concentrations on polymerisation rate, chain length, and surface properties of the implants. Samples grafted with 0.6 M monomer concentration showed more uniform surface and less surface roughness in comparison with other samples and untreated Ti6Al4V surfaces. 0.6 M concentration was found to be the optimal concentration for grafting PMPC to the hip implant interfaces considering their polymerisation rate, surface properties and the existence of polymers onto the grafted surface.

Moreover, cell study on optimal surfaces revealed that PMPC grafted surfaces prevent the implant interfaces from uncontrollable cell attachment which is of utmost importance in smoothing the motion of the hip implant under cyclic loading. Overall, the PMPC grafting demonstrated the potentiality of its application onto the surface of the SLM Ti6Al4V substrate for improved hip arthroplasty performance.

5.2 Experimental procedure

SLM technique was used to fabricate the Ti6Al4V implants. The building direction was 90° for the SLM process. The conversion of monomer to polymer was characterised by NMR spectroscopy. FTIR analysis identified chemical bonds and functional groups in the structure of both untreated and PMPC treated implant. The PMPC curve for 0.6 M concentration has been used in the FTIR results to compare with the grafted polymers. The polymerised PMPC was collected after polymer grafting and dried at 60° C in the oven. The dried PMPC was used as control PMPC in FTIR results. GPC examined the molecular weights and polydispersity. SEM imaging was performed at an acceleration voltage of 10 kV in a low vacuum mode with a spot size of 5. A 3D optical profiler was used to evaluate the surface roughness of PMPC

grafted surfaces. The green illumination was used, which is helpful when measuring very rough surfaces (it is easier to find the height from a longer signal when the data is noisy). Vertical Scanning Interferometry (VSI) was performed with 5X speeds. VSI measurements were set at increased parameters for back scan (~180 μm) and scan length (~150 μm) to account for the longer fringe envelopes. The stitching procedure was applied to scan the whole surfaces with 20% overlapping for each area. To determine the surface roughness of the specimen, 3D optical profiler scanned the top surface and 3D surface topography was obtained from in-built software (Vision64). The tilt position was corrected for plane fit followed by S parameters - height calculations [202]. The average surface roughness was calculated for the measurements of 5 samples. The statistical analysis was performed to determine whether there are any significant differences regarding surface roughness amongst a different group of samples. Cell was cultured on untreated and PMPC treated samples to investigate the influence of PMPC layer on resistance to cell attachment. The details experimental procedures have been presented in Chapter three.

5.3 Results and discussion

5.3.1 Structural analysis of polymers

NMR analysis was carried out to confirm that monomers were being polymerised successfully. Fig. 5.1 shows the ^{1}H NMR spectra of the MPC monomer and polymer. NMR was used to confirm polymerisation. The peaks are labelled to corresponding hydrogen atoms on the MPC structures. The MPC monomer displayed signals at δ_H 5.66 and δ_H 6.09 which are characteristic of the terminal alkene hydrogen atoms (labelled 1 on structure) [203]. Once the MPC monomer polymerised, the terminal alkene signals decreased significantly in size, which was the point of polymerisation (Fig. 5.1). This is due to the alkene hydrogen atoms in

monomer being converted to a methylene group in the polymer. This change to a methylene group gave the hydrogen atoms a new chemical shift which appeared approximately at δ_H 1.88.

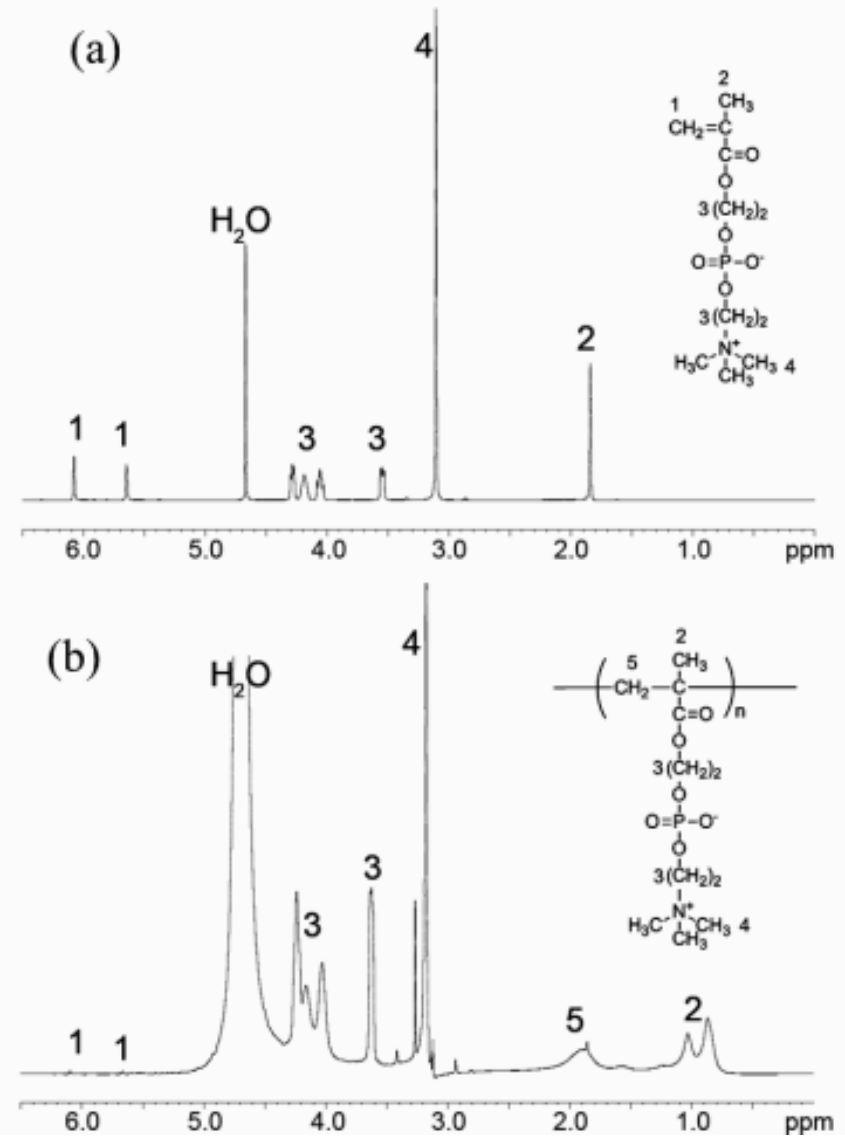

Fig. 5.1 NMR peaks for (a) MPC monomer and (b) PMPC. The NMR peaks changed significantly after monomer being converted into polymer.

Comparison of the areas of the alkene and methylene type hydrogens was used to calculate the degree of polymerisation using the following equation:

$$\text{Degree of polymerisation (\%)} = \frac{\text{area of methylene protons}}{\sum \text{areas of alkene and methylene protons}} \times 100 \qquad (5.1)$$

The degree of polymerisation for each sample is summarised in Table 5.1. The polymerisation rates of more than 95% indicate that monomer was being converted into polymer successfully. The results also show that despite the changes in the concentration of MPC, there was no significant ($p > 0.05$) change in the degree of polymerisation.

Table 5.1 Degree of polymerisation for different monomers' concentration.

Monomer concentration	**Degree of polymerisation (%)**
0.4 M	97
0.6 M	97
0.8 M	95

The FTIR spectra for different monomer concentrations are shown in Fig. 5.2, and agreed with the NMR observations. The polymer grafted samples for different monomer concentrations exhibited similar bonding to control PMPC. The shift for C-H in methylene and methyl groups in alkanes was intense, which confirmed the change of the alkene to alkane during polymerisation. The peak for P=O groups at 1285 cm^{-1} confirmed the presence of the phosphorylcholine group on the surface of SLM Ti6Al4V substrate which is essential for preventing unfavourable protein adsorption and uncontrollable cell adhesion [194]. The peak for C-O groups at 1190 cm^{-1} indicated the ester group in polymer chain [204]. The stronger FTIR peaks (P=O and C=O) for 0.6 M samples compared to the grafted samples indicate that more polymer chains were anchored onto the substrate than the other two samples. This result could be attributed by the uniform distribution of the polymer layer on a metallic substrate.

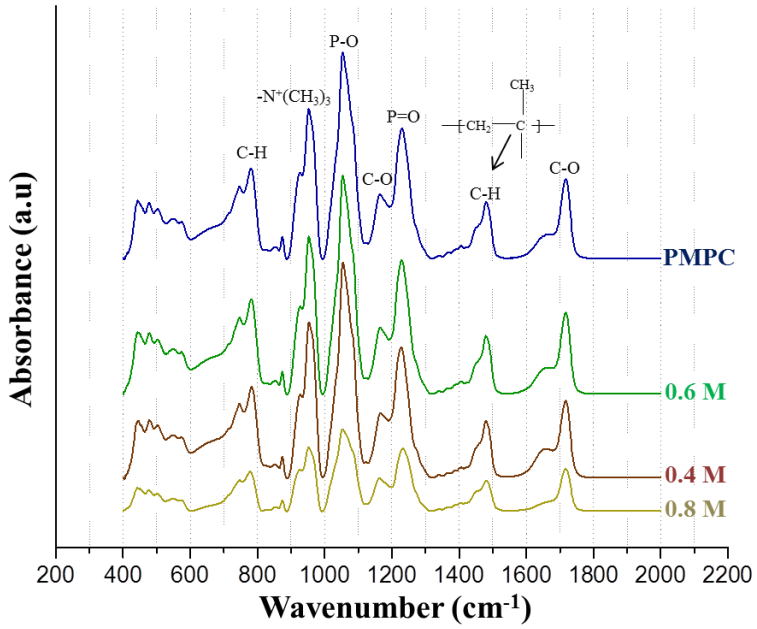

Fig. 5.2 FTIR spectra for different polymer grafted samples. The presence of $–N+(CH_3)^3$ and P=O bonding confirms the existence of phosphorylcholine in the grafted surface.

The GPC results for the different monomer concentrations are presented in Table 5.2. It is clear that the molecular weight of the grafted polymer increased with the increase in the monomer concentration. The highest monomer concentration achieved the longest polymer chain with the maximum molecular weight, 0.8 M, followed by 0.6 M and 0.4 M respectively. The surface with the higher number of polymer chain attached to the implant surface is more favourable for this application than longer polymer chain, as it has more surface coverage.

Table 5.2 GPC results for the average molecular weight of different polymer samples.

Sample	Molecular Weight-Number Average (Mn)	Molecular Weight-Weight Average (Mw)	Polydispersity (Mw/Mn)
0.4 M	75551	308449	4.082674
0.6 M	82081	342295	4.170216
0.8 M	122426	469831	3.837683

5.3.2 Effect of polymer grafting on surface morphology and roughness

Fig. 5.3 presents the surface morphology of untreated and PMPC treated surfaces. The partially-melted particles were clearly visible on untreated surfaces while the surface with grafted polymer showed less partially-melted particles. The best and uniform surface coverage was achieved for the 0.6 M samples followed by 0.8 M and 0.4 M samples. 0.6 M concentration provided full coverage of partially-melted particles. Conversely, coating the surface with 0.4 M and 0.8 M monomer concentration resulted in partial coverage of the partially melted particles. Surface of the implant did not cover completely with polymer for the sample treated with 0.4 M monomer due to insufficient monomer and other hand, sample treated with high amount of monomer (0.8 M) was covered with long polymer chains, and the number of polymer chains did not increase in compared with 0.6 M sample. Our previous study also showed the non-uniform layers on the surface of Ti6Al4V for 0.4 M concentration due to low concentrations of monomer which failed to cover the whole area. When UV irradiation exposed on peroxide formed on the surface of Ti6Al4V in a monomer solution bath under nitrogen, makes the chemical bonding between surface and polymer, due to radial formation and polymerisation [35, 186]. FTIR spectra also exhibited stronger peaks (P=O and C=O) for 0.6 M samples than other samples. Therefore, it can be concluded that 0.6 M is the optimal concentration considering their polymerisation rate, existence of polymers and surface uniformity. It is crucial to achieving a uniform and homogenous layer on the surface of the implant (or on the interface) to minimise friction and wear impact caused by high surface roughness of SLM printed Ti6Al4V implants.

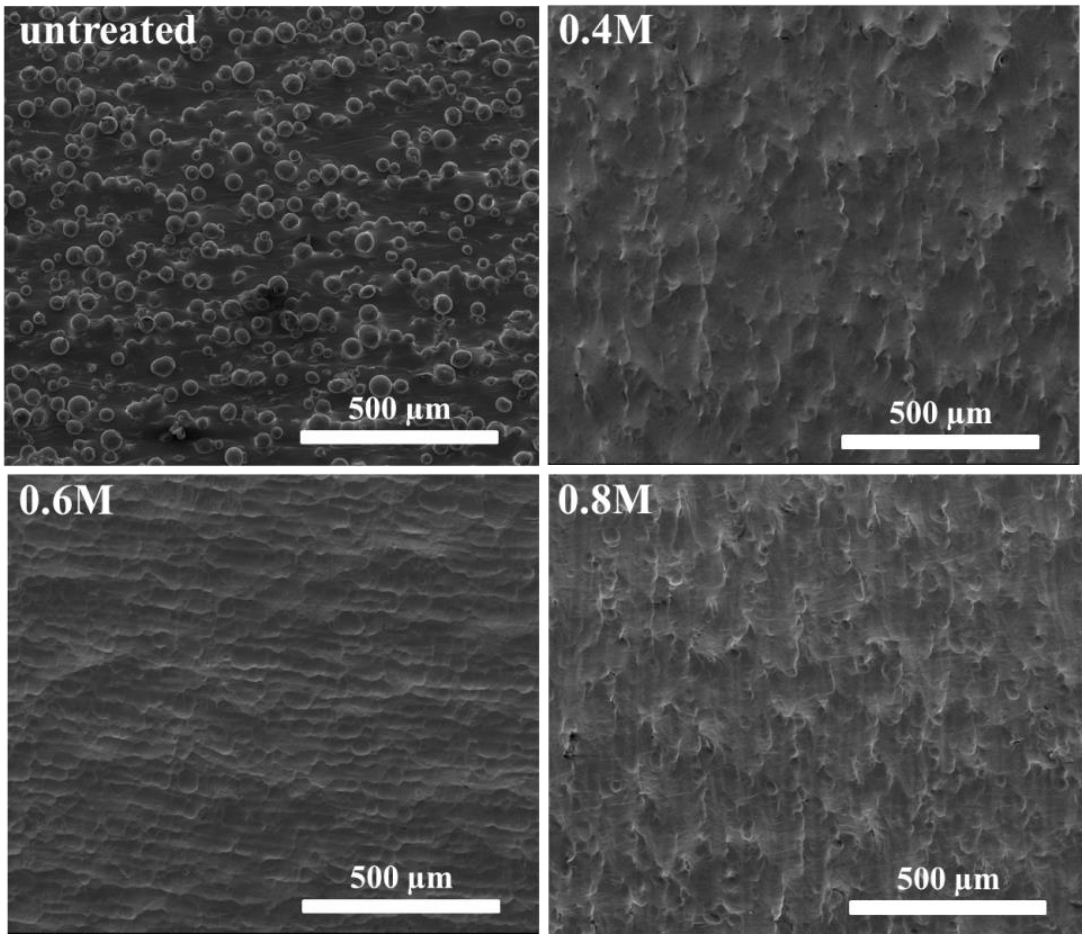

Fig. 5.3 Surface morphology of untreated and PMPC treated surfaces.

The surface topography of untreated and treated surfaces is presented in Fig. 5.4. The untreated surface exhibited rougher surface (more red areas) than the polymer grafted surface. The 0.8 M treated surface showed dominant red areas resulted in high roughness among polymer grafted surfaces (Fig. 5.4(a)). The 0.6 M treated surface exhibited the surface is rough in few areas, but overall, the 0.6 M treated surfaces were found to be smoother compared to other surfaces. Surface morphology results also demonstrated consistent polymer layer for the 0.6 M treated surfaces. The homogeneity in the polymer layer could improve the surface roughness and other surface properties of the implant.

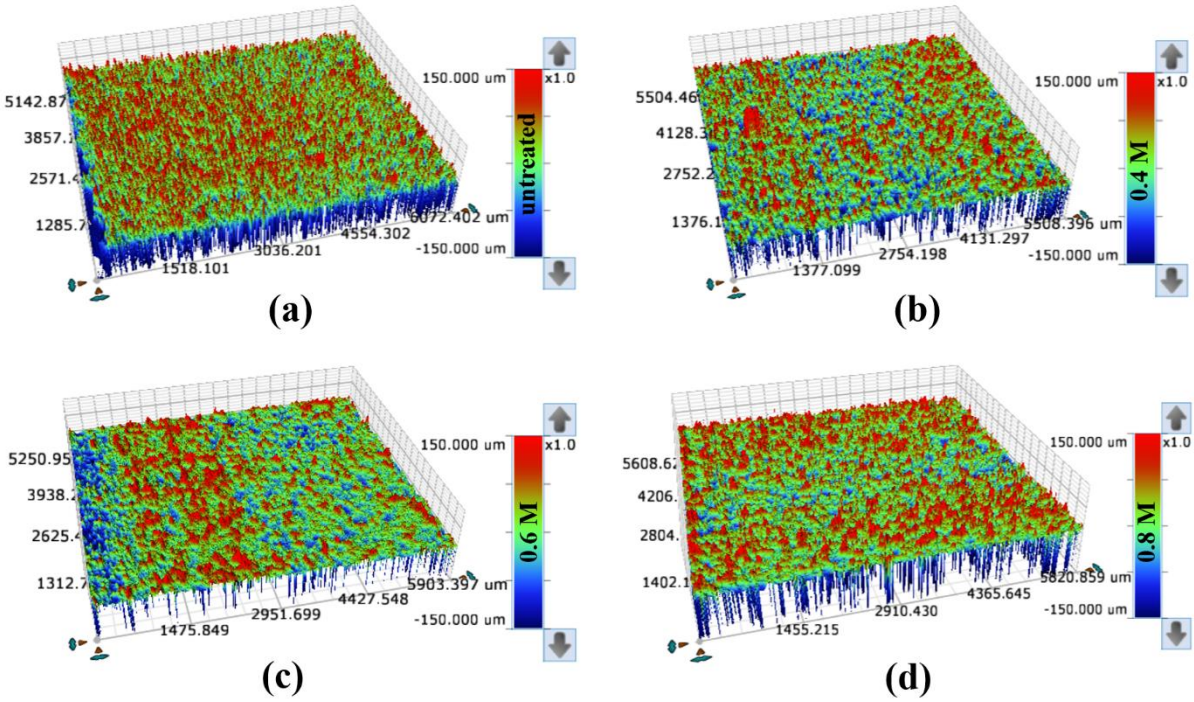

Fig. 5.4 Surface topography for untreated and different PMPC grafted samples.

The arithmetical mean height (Sa) and root mean square height (Sq) of the untreated and treated surface is presented in Table 5.3. Sa value indicates the difference in the height of each point compared to the arithmetical mean of the surface. The surface roughness results in Table 5.3 are the average of 5 samples.

Table 5.3 Surface roughness for untreated and treated surfaces.

Sample	Arithmetical mean height (Sa) (µm)	Root mean square height (Sq) (µm)
Ti6Al4V	13±1.50	20±3.00
0.4 M	7.0±0.55	9.5±1.25
0.6 M	6.0±0.35	8.0±0.65
0.8 M	7.5±0.75	10.0±1.50

The high surface roughness (S_a = 13 ± 1.6 µm) was obtained for untreated surfaces due to the presence of partially-melted particles in SLM processing. The high surface roughness has an adverse effect on the tribological properties of the implant. High surface roughness

induces high friction between the contact surfaces during cyclic loading and results in significant wear. The wear of the implant generates a larger number of wear particles which could even exacerbate wear and have an adverse reaction on biological conditions. The continuous wear of implant surfaces could lead to implant failure. Significant reduction in surface roughness was observed after polymer grafting. It could prove the potentiality of PMPC grafted samples to minimise friction and wear of the implant.

The lowest surface roughness (S_a= 6.0±0.6 µm) was achieved for the treated surface with 0.6 M concentration followed by 0.4 M and 0.8 M concentration. These results indicate that the PMPC layer on the surface of Ti6A14V reduced surface roughness by 53.85%, 46.15% and 42.30% for 0.6 M, 0.4 M and 0.8 M samples, respectively, which is significant. The statistical analysis revealed that the surface roughness results have a statistically significant difference ($p < 0.05$) among.4 M, 0.6 M and 0.8 M samples. Low concentrations result in less grafted polymer and less coverage of partially melted particles, as a result, exhibited more roughness. High concentrations result in grafting long chain to the surface and less grafting distribution on the surface.

The surface roughness result is consistent with the SEM images which show that the uniform and homogenous polymer layers attributed to the surface grafted with 0.6 M monomer concentration. Though polymer layer covered the partially-melted particles for all groups still the 0.4 and 0.8 surfaces exhibited inconsistence coverage of the partially-melted particles. This inconsistency could be caused if not enough polymer chains are grafted on to the implant surfaces. More monomer attached to the grafted polymer chain instead of surface, resulted in longer polymer chain with low and inconsistence surface coverage of partially melted particles. These results are confirmed with GPS results which exhibited the longer polymer chain in the case of high monomer concentration (0.8 M). The FTIR spectra also identified the more polymer chains existence for 0.6 M samples attributed to the more uniform layer of polymer

presence onto the implant surfaces compared to the 0.4 M and 0.8 M samples. Therefore, it can be concluded that 0.6 M exhibited the best surface morphology due to the attachment of a maximum number of polymer chains homogenously onto the Ti6Al4V surfaces resulted in lowest surface roughness.

5.3.3 Effect of PMPC layer on cell adhesion resistance

Fig. 5.5 shows the confocal microscope images of the untreated and polymer treated surfaces after 24 hours and 72 hours culture of mammalian CHO cells. Large amounts of mammalian cell growth were observed on the untreated, as-built Ti6Al4V surfaces after 24 hours of incubation. Conversely, small numbers of cell growth were observed on polymer grafted surfaces. Cell proliferation for as-built untreated surfaces was higher compared to polished untreated surfaces, which could be explained by the presence of large number of partially-melted particles onto as-built surfaces. These partially-melted particles increased the surface area as well as the hydrophobicity of the surface and, as a result, a large number of cells were attached to the surfaces. The same trend was also observed after 72 hours of incubation on both polished and as-built untreated surfaces. Previous studies have also reported the rapid proliferation of cells on Ti substrates [205-208]. Interestingly, cell adhesion was suppressed on the PMPC-treated surfaces regardless of the type of surface after 24 hours of cell culture. Though cell growth increased after 72 hours, cell culture onto the polymer treated surfaces was limited. In this case, cells were less elongated in shape compared to the untreated surfaces. Zwitterionic phosphorylcholine surfaces are known to reduce nonspecific protein adsorption [209, 210]. Proteins hardly adsorb onto PMPC brush surfaces due to unique hydration state of PMPC. The protein adsorption induces the cell adhesion onto the surface [211, 212] that was observed at the interface. If implant interfaces are prevented from cell attachment, a smooth

motion under cyclic loading will be achieved for hip implants. At the same time, it is expected to play a significant role in reducing friction and wear.

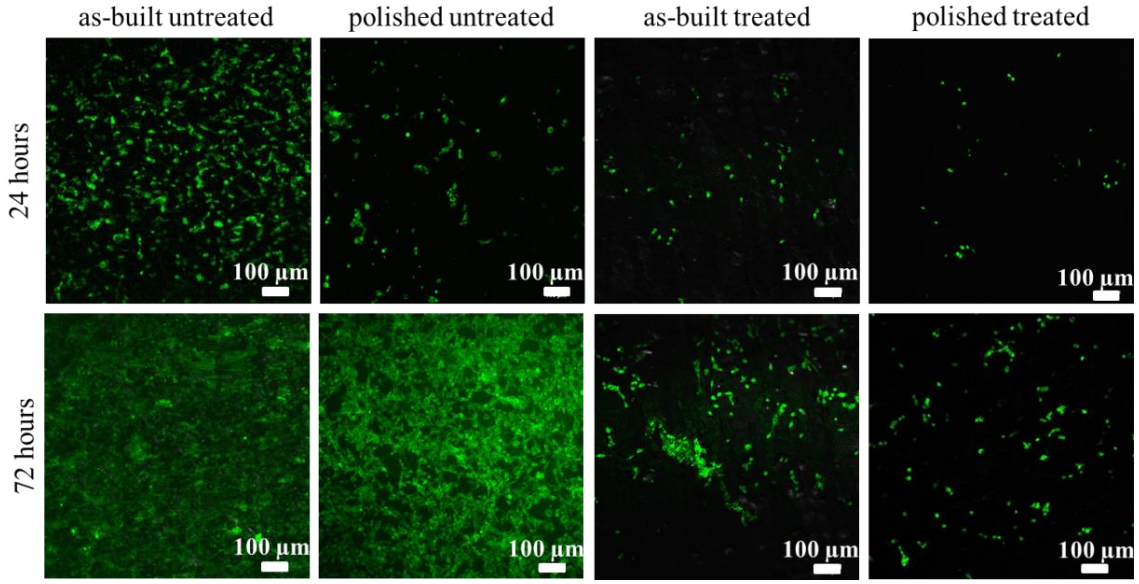

Fig. 5.5 Confocal microscopic images of cultured cells onto the untreated and polymer treated surfaces.

Fig. 5.6 shows the cell morphology onto the as-built surfaces. The arrow marks indicate the cells. It indicates that cells well adhered to partially-melted particles onto as-built surfaces and cells were more elongated in shape after 72 hours of incubation compared to 24 hours. As-built surfaces have a high number of anchorage points due to partially-melted particles, thus encouraging cell attachment on implant interfaces [213-215]. Moreover, high surface roughness resulted in hydrophobic behaviour which triggers more protein adsorption onto implant surfaces. Protein adsorption is considered a biophysical precursor to cell adhesion [198]. Increased protein adsorption promotes cell proliferation and results in increasing the surface roughness of the implants which impacts the smooth motion of the interfaces.

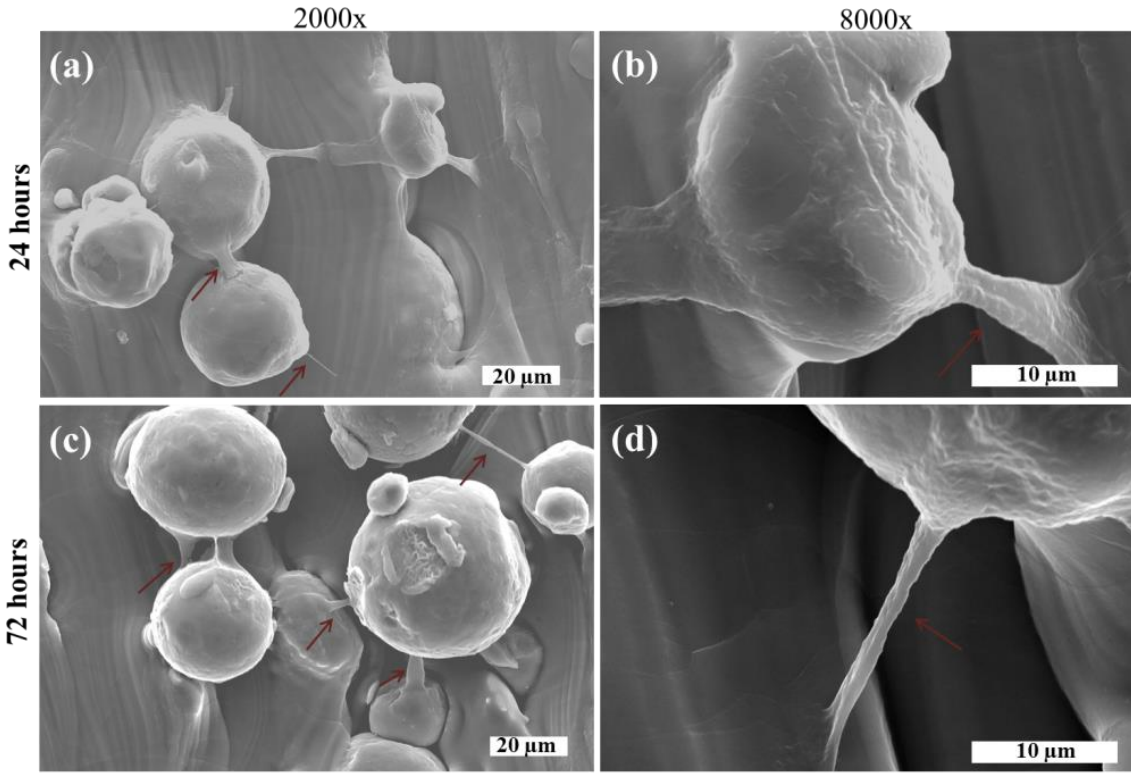

Fig. 5.6 Cell morphology on as-built surfaces at different magnification after 24 hours and 72 hours of cell growth.

Fig. 5.7 shows the cells are attached to the surface after 24 hours but spread significantly after 72 hours onto polished surfaces. The cells were most spherical in shape onto polished surfaces. Surprisingly, no cells were observed on polymer grafted surfaces through SEM imaging. Confocal images also showed a negligible amount of cell attachment onto polymer grafted surfaces. It confirms the PMPC prevented cell attachments onto the surface. PMPC layers covered the partially-melted particles, inhibiting the cell from spreading out to attach to the surface. Hydrophilic moieties of PMPC resulted in preventing of non-specific interactions with biological molecules and cells. Other studies have also reported that MPC units in the polymer can effectively restrain the protein adsorption [216-219], and thus prevents the cell growth onto polymer grafted surface.

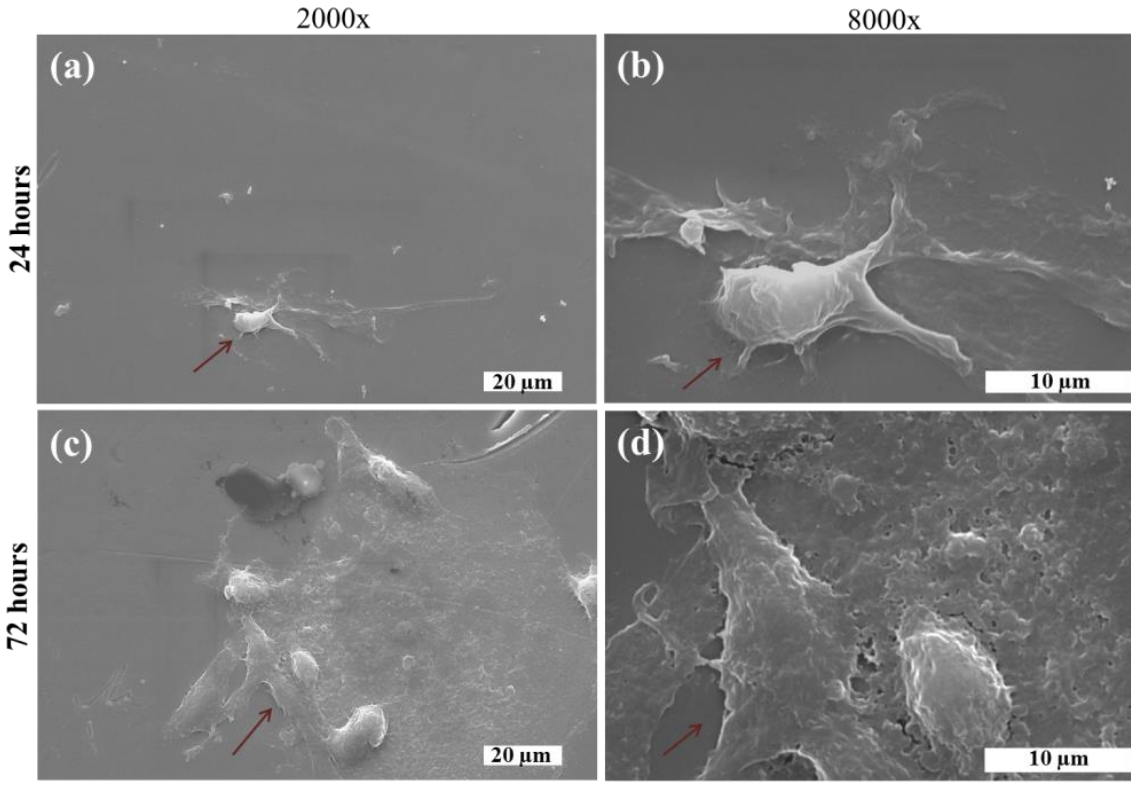

Fig. 5.7 Cell morphology on polished surfaces at different magnification after 24 hours and 72 hours of cell growth.

Controlled cell adhesion will yield several advantages, including protection of the interfaces from high friction and wear, and prevention of the uncontrollable cell attachment to the surfaces.

5.4 Summary

The purpose of this study was to develop a thin polymer layer on the surface of hip implant to produce the surface with optimal properties. The results showed grafting with PMPC improved the surface properties of the additively manufactured implant. Key findings of this study are summarised below:

- NMR results revealed that the degree of polymerisation was higher than 95% regardless of the monomer concentration. NMR peaks confirmed the successful polymerisation onto Ti6Al4Vsubstrate.
- FTIR Spectra exhibited that the alkene group changed to alkane group during polymerisation. Moreover, the presence of phosphorylcholine group on polymer grafted surfaces was confirmed which is crucial for preventing unfavourable protein and cell attachment.
- GPC analysis revealed that the length of the polymer chain increased with the increase in monomer concentration.
- The surface morphology of the samples with 0.6 M monomer concentration exhibited the best and uniform surface coverage followed by 0.8 M and 0.4 M. A significant reduction in surface roughness was demonstrated for PMPC grafted surface in comparison with an untreated surface.
- The PMPC grafted surface dramatically reduced mammalian cell attachment to the implant surfaces. The polymer layer covered the partially melted particles which act as an anchorage for cells. Moreover, the presence of the phosphorylcholine group in the side chains of PMPC inhibits the protein adsorption, and thus prevents the cell attachments to the implant surfaces.

5.5 References

[27] Moro T, Takatori Y, Kyomoto M, Ishihara K, Saiga K-i, Nakamura K and Kawaguchi H 2010 Surface grafting of biocompatible phospholipid polymer MPC provides wear resistance of tibial polyethylene insert in artificial knee joints *Osteoarthritis and Cartilage* **18** 1174-82

[28] Kyomoto M, Moro T, Saiga K-i, Miyaji F, Kawaguchi H, Takatori Y, Nakamura K and Ishihara K 2010 Lubricity and stability of poly (2-methacryloyloxyethyl phosphorylcholine) polymer layer on Co–Cr–Mo surface for hemi-arthroplasty to prevent degeneration of articular cartilage *Biomaterials* **31** 658-68

[30] Kyomoto M, Moro T, Yamane S, Takatori Y, Tanaka S and Ishihara K 2017 A hydrated phospholipid polymer-grafted layer prevents lipid-related oxidative degradation of cross-linked polyethylene *Biomaterials* **112** 122-32

[35] Chouirfa H, Evans M D, Castner D G, Bean P, Mercier D, Galtayries A, Falentin-Daudré C and Migonney V 2017 Grafting of architecture controlled poly (styrene sodium sulfonate) onto titanium surfaces using bio-adhesive molecules: Surface characterization and biological properties *Biointerphases* **12** 02C418

[173] Kyomoto M, Moro T, Miyaji F, Hashimoto M, Kawaguchi H, Takatori Y, Nakamura K and Ishihara K 2009 Effects of mobility/immobility of surface modification by 2-methacryloyloxyethyl phosphorylcholine polymer on the durability of polyethylene for artificial joints *Journal of Biomedical Materials Research Part A* **90** 362-71

[174] Kyomoto M, Moro T, Takatori Y, Kawaguchi H, Nakamura K and Ishihara K 2010 Self-initiated surface grafting with poly(2-methacryloyloxyethyl phosphorylcholine) on poly(ether-ether-ketone) *Biomaterials* **31** 1017-24

[175] Moro T, Takatori Y, Ishihara K, Konno T, Takigawa Y, Matsushita T, Chung U-i, Nakamura K and Kawaguchi H 2004 Surface grafting of artificial joints with a biocompatible polymer for preventing periprosthetic osteolysis *Nature Materials* **3** 829

[186] Chouirfa H, Migonney V and Falentin-Daudré C 2016 Grafting bioactive polymers onto titanium implants by UV irradiation *RSC Advances* **6** 13766-71

[194] Konno T, Kurita K, Iwasaki Y, Nakabayashi N and Ishihara K 2001 Preparation of nanoparticles composed with bioinspired 2-methacryloyloxyethyl phosphorylcholine polymer *Biomaterials* **22** 1883-9

[198] Ishihara K, Nomura H, Mihara T, Kurita K, Iwasaki Y and Nakabayashi N 1998 Why do phospholipid polymers reduce protein adsorption? *Journal of biomedical materials research* **39** 323-30

[202] Ghosh S, Abanteriba S, Wong S, Brkljača R and Houshyar S 2019 Optimisation of grafted phosphorylcholine-based polymer on additively manufactured titanium substrate for hip arthroplasty *Materials Science and Engineering: C* **101** 696-706

[203] Camerano J A, Sämann C, Wadepohl H and Gade L H 2011 Bis (pyridylimino) isoindolato− Iridium Complexes as Epoxidation Catalysts for Alkenes *Organometallics* **30** 379-82

[204] Alberts A, Chen J, Kuron G, Hunt V, Huff J, Hoffman C, Rothrock J, Lopez M, Joshua H and Harris E 1980 Mevinolin: a highly potent competitive inhibitor of hydroxymethylglutaryl-coenzyme A reductase and a cholesterol-lowering agent *Proceedings of the National Academy of Sciences* **77** 3957-61

[205] Sobolčiak P, Popelka A, Mičušík M, Sláviková M, Krupa I, Mosnáček J, Tkáč J, Lacík I and Kasák P 2017 Photoimmobilization of zwitterionic polymers on surfaces to reduce cell adhesion *Journal of colloid and interface science* **500** 294-303

[206] Vilardell A, Cinca N, Garcia-Giralt N, Dosta S, Cano I, Nogués X and Guilemany J 2018 Osteoblastic cell response on high-rough titanium coatings by cold spray *Journal of Materials Science: Materials in Medicine* **29** 19

[207] Oh S, Daraio C, Chen L H, Pisanic T R, Finones R R and Jin S 2006 Significantly accelerated osteoblast cell growth on aligned TiO2 nanotubes *Journal of Biomedical Materials Research Part A* **78** 97-103

[208] Xiang Y, Liu X, Mao C, Liu X, Cui Z, Yang X, Yeung K W K, Zheng Y and Wu S 2018 Infection-prevention on Ti implants by controlled drug release from folic acid/ZnO quantum dots sealed titania nanotubes *Materials Science and Engineering: C* **85** 214-24

[209] Ladd J, Zhang Z, Chen S, Hower J C and Jiang S 2008 Zwitterionic polymers exhibiting high resistance to nonspecific protein adsorption from human serum and plasma *Biomacromolecules* **9** 1357-61

[210] Schlenoff J B 2014 Zwitteration: coating surfaces with zwitterionic functionality to reduce nonspecific adsorption *Langmuir* **30** 9625-36

[211] Ishihara K, Mu M, Konno T, Inoue Y and Fukazawa K 2017 The unique hydration state of poly (2-methacryloyloxyethyl phosphorylcholine) *Journal of Biomaterials Science, Polymer Edition* **28** 884-99

[212] Deligianni D D, Katsala N, Ladas S, Sotiropoulou D, Amedee J and Missirlis Y 2001 Effect of surface roughness of the titanium alloy Ti–6Al–4V on human bone marrow cell response and on protein adsorption *Biomaterials* **22** 1241-51
[213] Boga J C, Miguel S P, de Melo-Diogo D, Mendonça A G, Louro R O and Correia I J 2018 In vitro characterization of 3D printed scaffolds aimed at bone tissue regeneration *Colloids and Surfaces B: Biointerfaces* **165** 207-18
[214] Rechendorff K, Hovgaard M B, Foss M, Zhdanov V P and Besenbacher F 2006 Enhancement of Protein Adsorption Induced by Surface Roughness *Langmuir* **22** 10885-8
[215] Deligianni D D, Katsala N D, Koutsoukos P G and Missirlis Y F 2000 Effect of surface roughness of hydroxyapatite on human bone marrow cell adhesion, proliferation, differentiation and detachment strength *Biomaterials* **22** 87-96
[216] Yuan B, Chen Q, Ding W-Q, Liu P-S, Wu S-S, Lin S-C, Shen J and Gai Y 2012 Copolymer coatings consisting of 2-methacryloyloxyethyl phosphorylcholine and 3-methacryloxypropyl trimethoxysilane via ATRP to improve cellulose biocompatibility *ACS applied materials & interfaces* **4** 4031-9
[217] Wen Y, Zhang Z and Li J 2014 Highly Efficient Multifunctional Supramolecular Gene Carrier System Self-Assembled from Redox-Sensitive and Zwitterionic Polymer Blocks *Advanced Functional Materials* **24** 3874-84
[218] Sibarani J, Takai M and Ishihara K 2007 Surface modification on microfluidic devices with 2-methacryloyloxyethyl phosphorylcholine polymers for reducing unfavorable protein adsorption *Colloids and Surfaces B: Biointerfaces* **54** 88-93
[219] Ishihara K and Iwasaki Y 1998 Reduced protein adsorption on novel phospholipid polymers *Journal of biomaterials applications* **13** 111-27

CHAPTER SIX: THE IMPACT OF PMPC LAYER ON THERMAL STABILITY AND MECHANICAL PROPERTIES OF THE IMPLANT

6.1 Chapter overview

This chapter presents an experimental investigation on thermal stability and mechanical properties of PMPC grafted surface. In this study TGA, DSC and nanoindentation analyses were carried out to evaluate the effect of PMPC layer on implant surfaces. Overall, this study fulfils the objective 4 (as stated in section 1.6) and thus answers the research question 4 & 5 (as stated in section 1.5) of this project.

Investigating thermal stability and mechanical properties of the grafted polymer is extremely important as these properties define the failure mechanism of implants. This study focuses on optimising monomer concentration to achieve the best physical, thermal and mechanical properties of grafted AM Ti6Al4V implants. Three different concentration of monomers, 0.4 M, 0.6 M and 0.8 M were investigated to optimise the monomer concentration based on surface properties, polymerisation rate and mechanical properties of the implant surface. The results from thermal analysis confirmed the PMPC is thermally stable for implant applications regardless of the monomers' concentration. A significant reduction in Young's modulus of polymer grafted samples (33.2 - 42.9%), in comparison with untreated Ti6Al4V samples and the concomitant improvement in elasticity behaviour, proved the potentiality of polymer films for implant applications.

---

*This work is under review in ***Journal of the Mechanical Behavior of Biomedical Materials***.
Ghosh, Subir, Abanteriba, Sylvester, Wong, Sherman and Houshyar, Shadi. "***Performance analysis of grafted poly (2-methacryloyloxyethyl phosphorylcholine) on additively manufactured titanium substrate for hip implant applications*** " Journal of the Mechanical Behavior of Biomedical Materials (under review)

In summary, polymer grafted implant prepared with 0.6 M monomer concentration showed the optimal thermal, physical and mechanical properties. The nano-scratch test revealed that the PMPC layer protects the underlying implant substrate from scratching even under high loads. Nano-tribological wear test was performed to investigate the effect of PMPC layer on wear resistance of the implant under loading conditions. The PMPC grafted surface exhibited a significant enhancement in wear resistance compared to untreated surface despite the increase of the loads. The consequent improvement of wear resistance proved the potentiality of polymer films for implant applications.

6.2 Experimental procedure

The standard process parameters were maintained for Ti6Al4V implant printing [220]. The building direction of the SLM process was inclined at 90° with respect to the fabricated samples. Standard polishing procedures were applied on as-built Ti6Al4V surfaces prior to polymer grafting as nanoindentation analysis was not possible to perform on non-uniform high roughness surfaces.

The details of TGA and DSC analyses were described in Chapter three. SEM imaging was performed to compare the surface morphology of the untreated and polymer treated samples fabricated at different monomer concentrations. The FEI quanta machine was operated at a high voltage (HV) power supply of 10 KV under vacuum at spot size 5 for all samples. The water contact angle measurement was carried out using 2µL water drop in sessile drop method for each measurement, and the measurements were carried out once the stable value was achieved.

Nanoindentation studies are useful to evaluate the effect of thin PMPC layer on mechanical properties of polymer grafted surface [182]. The nano-mechanical properties of the fabricated samples such as penetration depth, hardness and Young’s modulus were measured

using a Hysitron TI-950 Tribo-indenter with a diamond Berkovich tip. Penetration depth was measured by indenting to a maximum load of 500 μN on each sample. The details of nanoindentation studies have been discussed in Chapter three. Nano-scratch analysis was performed to investigate the effect of polymer grafted layer on scratch resistance in the nano-scale size. The wear track was measured to compare the scratch depth for untreated and treated surfaces under different loads. The details of the scratch test are presented in Chapter three. Wear analysis was conducted using a Cube Corner indentation tip under three different loads. 20 μN, 60 μN and 100 μN loads were applied as low, medium and high loads, respectively.

6.3 Results and discussion

6.3.1 Thermal stability of PMPC

6.3.1.1 TGA analysis

Thermal stabilities of the grafted polymers were tested by analysing the changes in weight of the sample as a function of temperature. Fig. 6.1 shows the TGA curves of grafted polymers with various monomer concentrations. Weight loss started around 120°C to 150°C, mainly due to volatilisation of absorbed and bonded water. The second stage of weight loss occurred at 150°C, due to the dehydration and decomposition caused by heat as the temperature reached 200°C, ester would be thermolysis in a polymer chain containing phosphorous-copolymer [221]. The decomposition of ester groups continued to 350°C due to the existence of ester groups in both phosphonate and carbonate inside the polymer chain. The third stage of weight loss was from 350°C to 430°C, caused by the thermo-oxidative degradation of phosphate, forming phosphoric acid [222-224]. Phosphoric acid act as a protective layer and delayed thermal degradation; this effect is higher for grafted layer produced by a high amount of monomer (longer polymer chain, higher amount of phosphate). Therefore, the corresponding

decomposition temperature of the MPC moved to a higher temperature with the increase in monomer concentration while weight loss was the same.

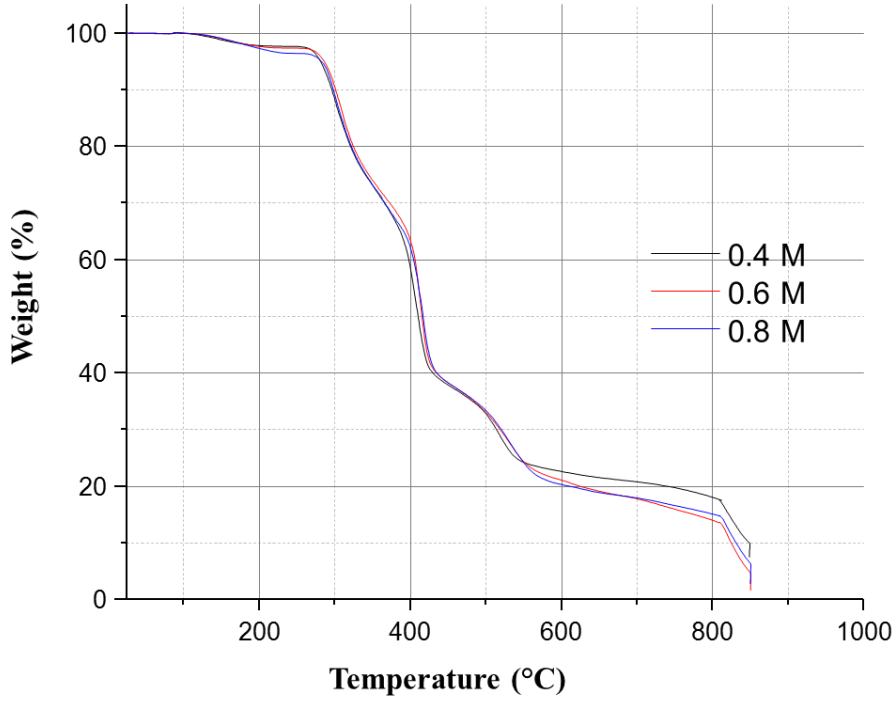

Fig. 6.1 Weight loss versus temperature for PMPC with various monomer concentration.

By switching from nitrogen gas to air at 700°C, carbonaceous residue from polymer, PMPC, oxidized. The human body generally operates at 37°C, and PMPC experienced only 2.6% weight loss that happened above the body temperature, due to a hydration state of polymer. Therefore, it can be concluded that PMPC is thermally stable as an implant material, and a grafted sample can stand thermal sterilisation which is crucial for hip implant application.

6.3.1.2 DSC analysis

The effect of heat flow on polymer structure is an important aspect for analysing the thermal stability of polymers [225-227]. Fig. 6.2 illustrates DSC curves for PMPC with different monomer concentration.

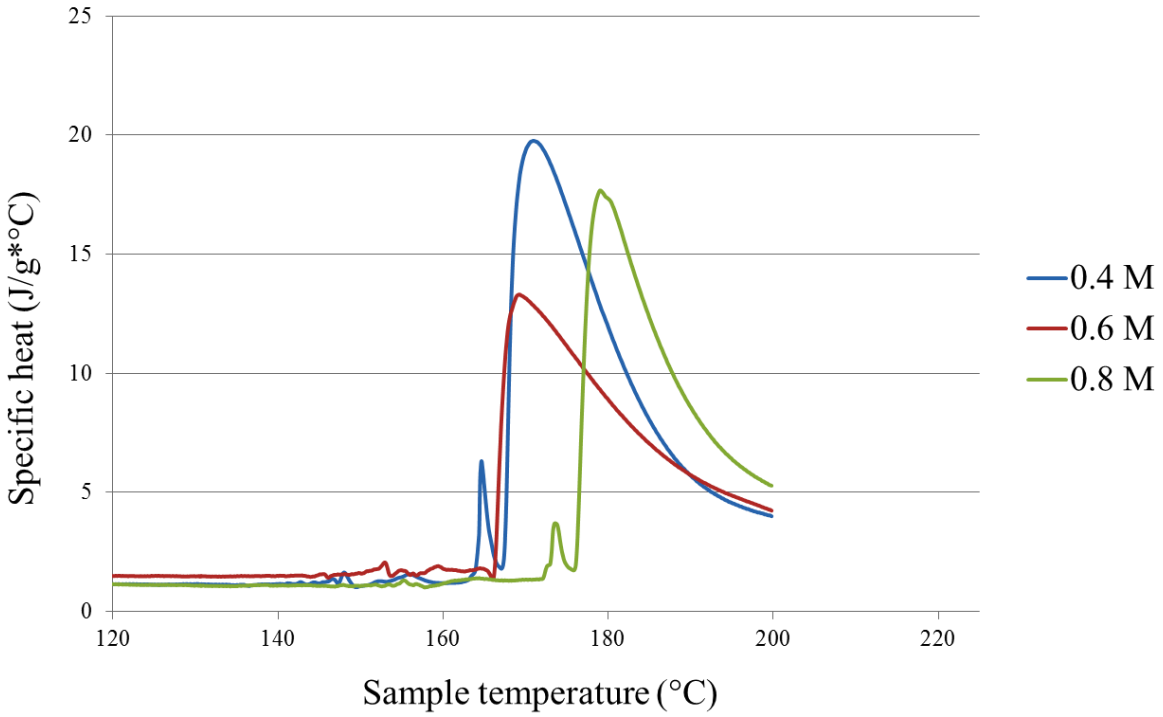

Fig. 6.2 DSC curves for polymers with different monomer concentration.

It shows that temperature rise did not affect PMPC up to 160°C. No heat generation was observed between 20-160°C, which confirmed thermal stability of PMPC in physiological conditions. The heat flows were observed in a temperature range of 160-200°C. The heat generation was not high to affect the surface properties of the implant. The minimum heat flow at 13 J/g*°C was exhibited by 0.6 M samples while 0.4 M showed the maximum heat flow at 20 J/g*°C. Supporting the TGA results, DSC results suggested that thermal stability is better for 0.6 M samples than that of 0.4 M and 0.8 M samples. In this case, sample grafted with 0.6 M PMPC can stand for thermal sterilisation which is an important aspect of the implant preparation for physiological application.

6.3.2 Surface properties of PMPC grafted implants

6.3.2.1 Surface morphology

The surface morphology of grafted polymer was evaluated from the SEM images. Fig. 6.3 illustrates smooth and mirror polished surface for untreated TiAl6V and changes in surface morphology after polymer grafting. It shows that PMPC were attached to metal surfaces and PMPC film deposited on smooth polished surfaces might increase surface roughness on a minor scale. However, uneven surface was observed for 0.4 M and 0.8 M samples, due to the low and high amount of PMPC on the surface which resulted in either not covering the surface or producing congested surface, respectively. 0.6 M treated surface exhibited uniform and evenly distributed PMPC layer on the surface of SLM Ti6Al4V, that means optimal grafted polymer to cover implant surface but not overloaded. The surface treated with 0.6 M exhibited the best surface morphology among all other grafted surfaces due to the attachment of a maximum number of polymer chains homogenously on the surface of implant. Previous study also demonstrated non-uniform surface for the implant grafted with 0.4 M. In the case of 0.4 M monomer concentration, PMPC chain length was too short which did not cover the surface of the implant resulted in an uneven surface. By increasing monomer concentration to 0.6 M, PMPC chian length was just right to be able to cover the surface on implant uniformly, while increasing monomer concentration to 0.8 M resulted in long PMPC chain led to overcrowding implant surface, which did not provide any benefits over 0.6 M monomer concentration. It is, therefore, necessary to maintain optimal monomer concentration during polymer grafting to achieve the best results.

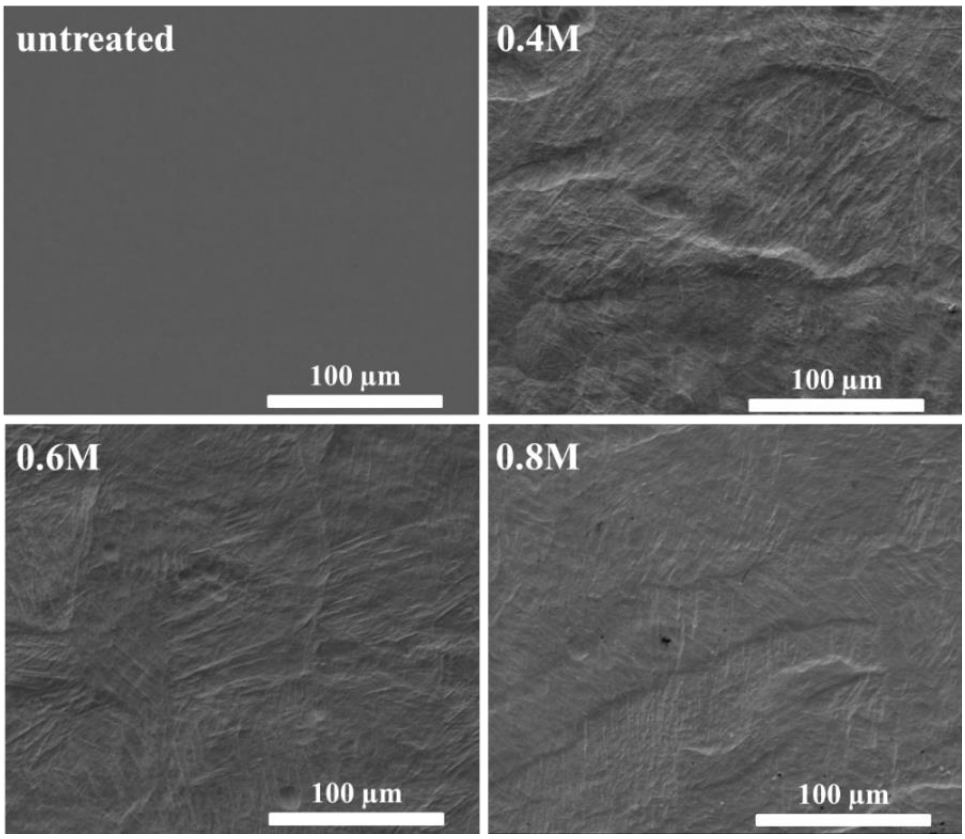

Fig. 6.3 Surface morphology of untreated and treated polymer surface with various monomer concentrations.

6.3.2.2 Surface wettability

Water contact angle is considered to be an indicator to evaluate the wettability of the surface. Surface wettability is an important property which is believed to have an effect on wear resistance. A lower contact angle indicates better wettability, resulting in low friction during cyclic loading of the interfaces [197]. Fig. 6.4 presents the average contact angle for untreated (control) and polymer treated surface. A two-way ANOVA analysis showed a significant difference ($p < 0.05$) in a water contact angle between untreated and polymer treated surfaces, and also between the grafted surface with different monomer concentrations. A hydrophilic nature of PMPC resulted in better grafted surface hydrophilicity and grafted

surface with 0.6 M monomer concentration showed the lowest contact angle and the best wettability in comparison with the rest of grafted surfaces. Therefore, a high performance to wear resistance is expected to achieve by 0.6 M sample due to providing the best wettability. Wettability properties are related to a surface morphology of implants, and PMPC is proven to be highly hydrophilic polymer [228].

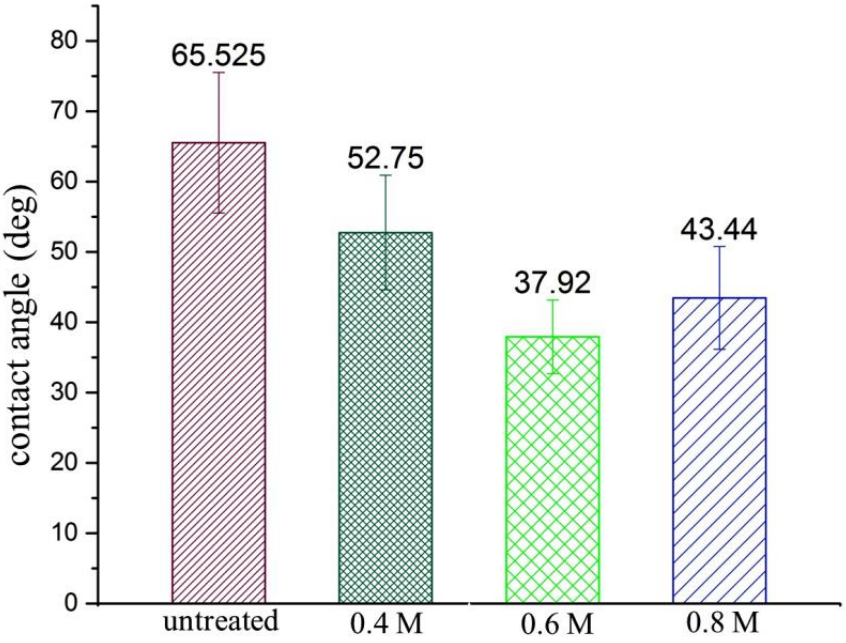

Fig. 6.4 Average water contact angle measurements for untreated (control) and polymer treated samples.

Standard deviations of water contact angles varied significantly due to non-uniform surface behaviour. Interestingly,0.6 M treated surface exhibited less variation in water contact angles resulted in consistent improvement in wettability in comparison to other surfaces. The improvement in wettability results for 0.6 M treated surfaces could be justified by their uniformly distributed polymer layers onto TI6Al4V, which resulted in smooth surfaces. The

improvement in wettability results for 0.6 M treated surfaces could be justified by their uniformly distributed polymer layers onto TI6Al4V, which resulted in smooth surfaces.

Previous studies reported that the mirror polished surface resulted in a reduction of water contact angles and exhibits hydrophilicity behaviour during friction and wear testing [23, 24, 229, 230]. In this study, despite an increase in surface roughness, the PMPC treated surfaces improved wettability property of the implant surface reducing a water contact angle significantly. This results can be attributed to a phosphorylcholine group in side chains of PMPC that acts as hydrophilic moieties [211]. The unique hydration state of PMPC enhances lubricating ability and mimics the articular cartilage of hip joints.

6.3.3 Effects of polymer grafting on mechanical properties of the implants

6.3.3.1 Load vs displacement

The indentation penetration depth was used to evaluate the mechanical strength of polymer grafted surfaces. Some studies have reported that PMPC does not affect the bulk properties of the UHMWPE/PTPE substrate after polymer grafting [142, 143, 173]. Generally, metals have a higher mechanical strength than polymers, and lower penetration depth is expected for Ti6Al4V in compared to polymer grafted surfaces. Fig. 6.5 presents the penetration depth for different surfaces under applied load (maximum load of 500 μN). As expected, all treated samples had a higher penetration depth compared to the untreated sample. Within the treated surfaces, the 0.6 M sample had the lowest penetration depth. It should be noted that the untreated Ti6Al4V surfaces exhibited better mechanical strength compared to the treated sample which questions the necessity of polymer grafting on a metal substrate. Improved mechanical strength is important, however, there are other important physical properties of the implant surface, including wettability, surface morphology and biocompatibility, that should be considered. PMPC contains water molecules, and in the

hydration state, these layers maintain a fluid-like manner at the interfaces (cushion). As a result, PMPC layers enhance the lubrication in the contact region. The better lubrication results in low friction and prevents the surface from wear under cyclic loading and hereafter, enhancing the useful life of the implant.

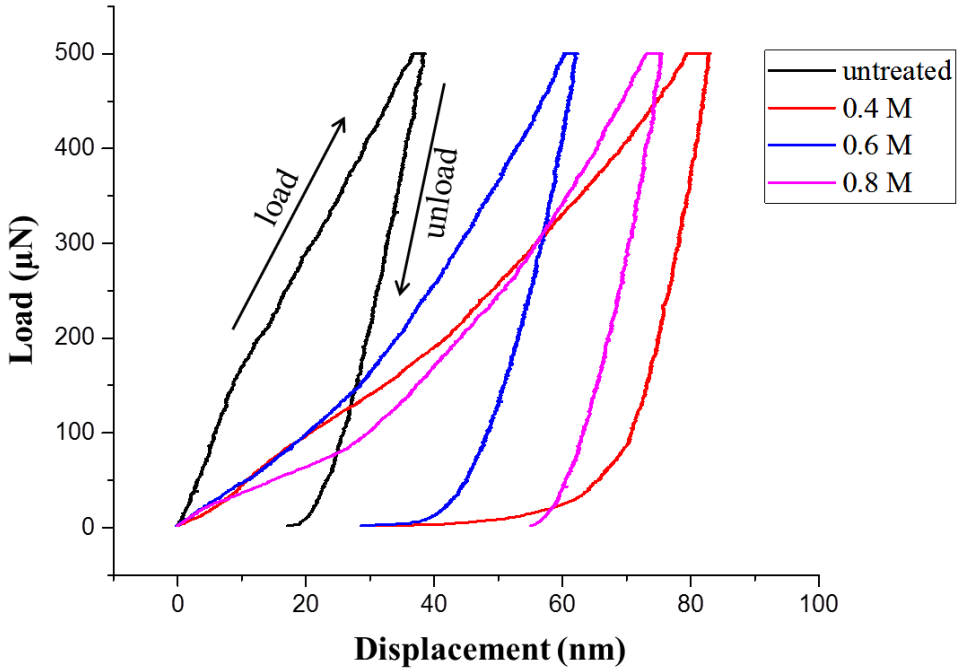

Fig. 6.5 Load vs Displacement curve for different samples.

6.3.3.2 Hardness

The results from penetration depth tests could be justified from indentation hardness results. Indentation hardness is an important property to evaluate the deformation resistance of PMPC grafted samples. It defines permanent material deformation due to a constant compression load from a sharp object. The hardness of materials depends on many important factors, including strength, ductility, elastic stiffness, plasticity, strain, toughness, viscoelasticity, and viscosity [52, 231-233]. Therefore, the useful life of the implant can be

prolonged if the interface has an optimal hardness value. The purpose of PMPC grafting was to tailor the surface of Ti6Al4V implant with cartilage mimicking highly hydrophilic PMPC to minimise the friction forces between hip joint interfaces. Ideally, this thin layer should not affect the mechanical properties of Ti6Al4V implants. Fig. 6.6 presents the 2D and 3D surface map (2D map was projected along the bottom) for hardness values of untreated and treated surface with various monomer concentrations. It shows that hardness was high at 6.28±0.66 GPa for untreated Ti6Al4V surfaces (which is similar to a previous study [234]) while 0.4 M and 0.8 M samples exhibited very low hardness (<2.5 GPa).

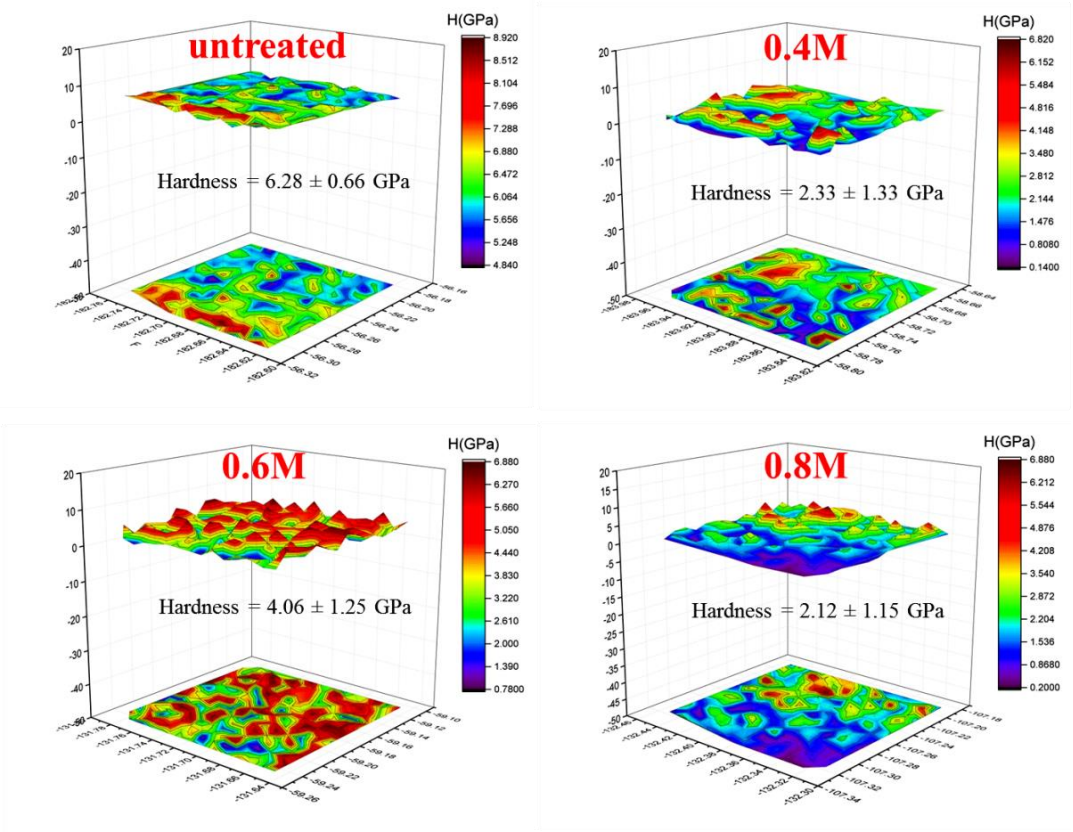

Fig. 6.6 Hardness profiles for untreated and treated surfaces with various monomer concentration.

Sample with 0.6 M showed noticeably higher hardness values, 4.06±1.25 GPa, in comparison with other PMPC treated surface. In the case of 0.4 M and 0.8 M samples, more weak points (hardness < 2 GPa) were visible in the PMPC layer on the surface, which resulted

in lower hardness than 0.6 M samples. Conversely, 0.6 M sample exhibited the uniform layer of PMPC which led to the comparatively higher hardness (> 4 GPa) than other polymer samples. Comparing the hardness results for different monomer concentration, the 0.6 M concentration could be the optimal concentration for polymer grafting. Both indentation hardness and penetration depth results displayed the best mechanical properties for the 0.6 M treated surfaces among the treated surfaces.

Polymers are comparatively softer than the metallic substrates, therefore, a decrease of the mechanical properties of all polymer grafted surfaces compared to untreated surfaces is expected. The PMPC layer was thin (200-400nm), however is able to withstand the low loads [160]. Therefore, nano-indentation experiments were performed at a certain range of loads so that the effect of different polymer grafted surfaces could be compared. The 0.6 M treated surfaces exhibited comparatively better mechanical properties than other polymer grafted surfaces, which could be attributed by its surface uniformity, improved existence of polymers on the implant and surface roughness properties. Higher number of polymer chains were attached and grafted to the implant surface in case of 0.6 M monomer concentration (optimal) while the number of attached polymer chain was lower and longer (GPC) for the sample with high monomer concentration (0.8 M). Similarly, there was not enough monomer to attach to the surface for the sample with low concentration (0.4 M) and did not cover the whole surface. This can describe the better mechanical and surface properties of the 0.6 M treated surface. Previous studies investigated the effect of polymer grafting on the bulk properties of cross-linked polyethylene (CLPE) and reported that the polymer grafted layers did not affect the mechanical properties of the substrate [142, 143, 173]. This study revealed that the polymer grafted layer reduced the hardness and increased penetration depth. Therefore, polymer grafting has a significant effect on mechanical properties of the substrate if the grafting is applied on a metallic substrate.

6.3.3.3 Young's modulus

Young's modulus (also known as elastic modulus) determines an object or substance's resistance to being deformed elastically (i.e., non-permanently) under applied stress [235-237]. Generally, Young's modulus for human cortical bones is very low and, conversely, it is very high for metal implants. The large gaps between an elastic modulus of artificial implant and human bone could cause a mismatch for its application as hip implants. High elastic modulus provides a stress shielding effect which resulted in a possible reduction (fracture) in a useful life of implant [238-240]. As a consequence, researchers attempt to minimise Young's modulus to match human joints. However, it is quite impossible to reduce the elasticity at a scale to a natural bone without compromising the other mechanical properties. This study brought a breakthrough in possibility of significantly minimising Young's modulus. Fig. 6.7 summarises average Young's modulus for different samples. A statistically significant difference ($p < 0.05$) was identified between an untreated and PMPC treated surfaces, but only Young's modulus value for 0.6 M samples was statistically significant from 0.4 M and 0.8 M samples. There was no significant difference ($p > 0.05$) was observed between 0.4 M and 0.8 M samples in Young's modulus value. A modulus was decreased by 42.9% for 0.8 M samples followed by 40.3% for 0.4 M samples and 33.0% for 0.6 M samples, compared to untreated Ti6Al4V implants. The reason for lower Young's modulus achieved by polymer grafted samples might be explained by an effect of a thin polymer layer on the surface. Thin polymer layer on the surface of implant tailored the mechanical properties of the implant surface. This study demonstrated that PMPC grafted surface minimises the "stress shielding" problem of the Ti6Al4V implant. Monomer concentrations have impacted the uniformity of PMPC grafted layer significantly. Higher uniformity resulted in a higher Young's modulus. SEM images confirmed improved uniformity of the film made by 0.6 M monomer concentration. This uniformity can lead to higher Young's modulus which was achieved by 0.6 M samples in comparison to other PMPC grafted samples.

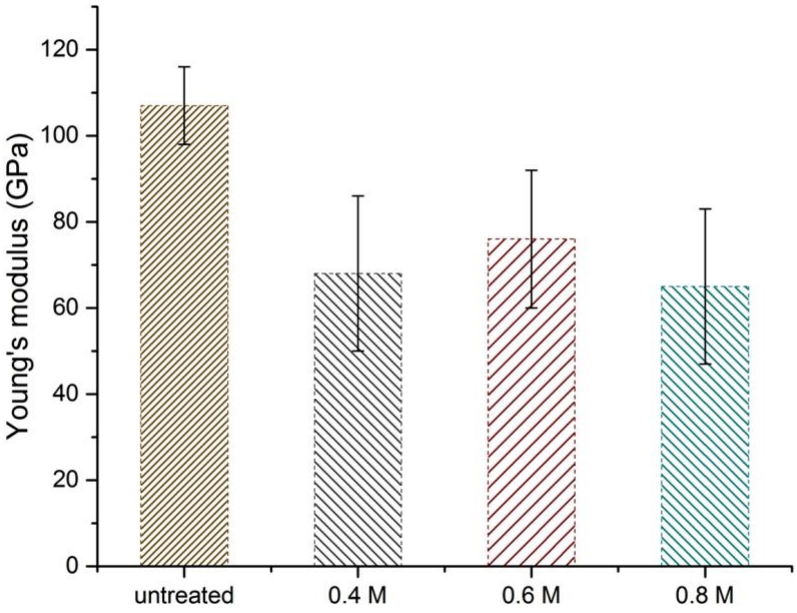

Fig. 6.7 Average Young's modulus of grafted polymer with various monomer concentrations.

Young's modulus was measured to investigate an effect of monomer concentration on the mechanical properties of PMPC grafted surface. Young's modulus value of the samples with various monomer concentrations is presented in surface mapping across a range of loads and surface conditions (Fig. 6.8). This figure presents indentation maps showing Young's modulus. It showed a similar relationship between modulus and monomer concentration as the hardness results. 3D surface maps (together with 2D maps below) are presented for a 20×20 array of indents for each sample. The Young's modulus values were consistent in different areas for untreated Ti6Al4V surfaces while they significantly differed for PMPC grafted surfaces. This is most likely due to inhomogeneous polymer thickness and uniformity, but it could also be explained by the way the polymerisation process works. It is interesting that there were no indications of a relationship between modulus and maximum load.

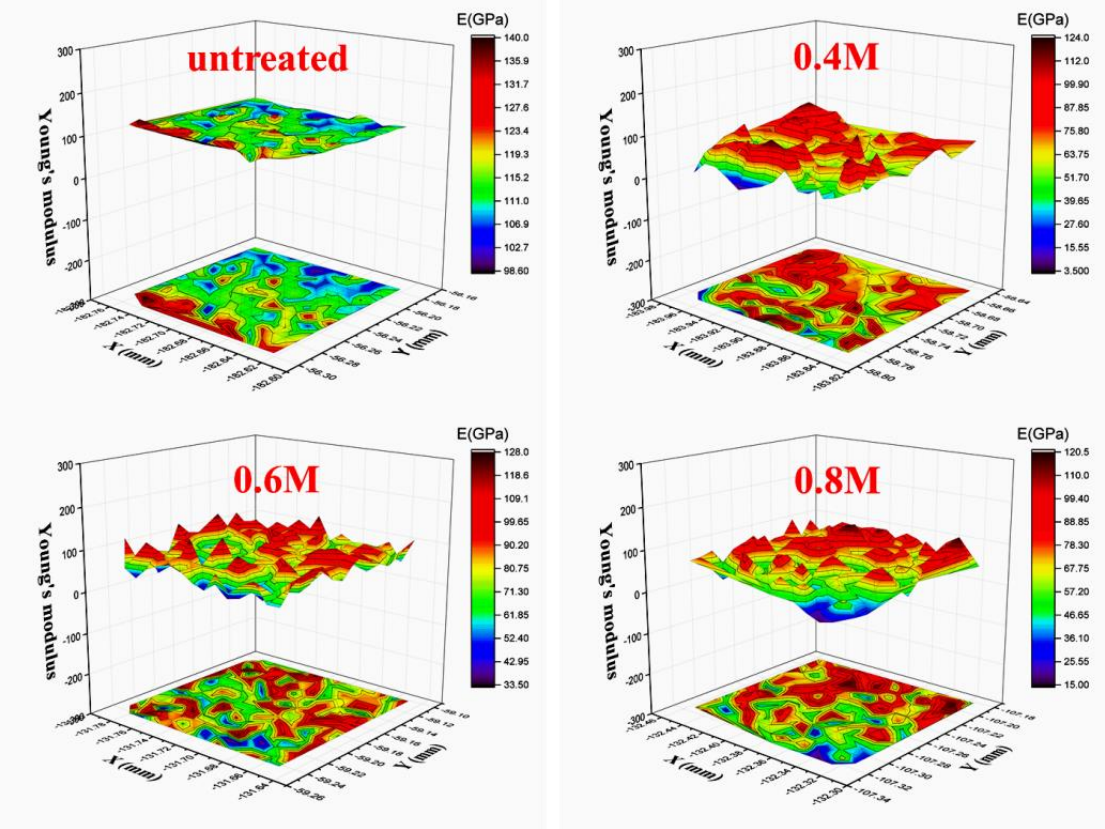

Fig. 6.8 Modulus mapping results for untreated and PMPC grafted surfaces for various monomer concentrations.

These results suggested that PMPC eliminated some surface effects that Ti6Al4V applied over the load. The elastic behaviour of polymer grafted surfaces is also dependent on the structure of PMPC chains and density. Ishihara *et al.* [26] revealed that PMPC exhibits a mushroom-like structure at low load and also semi-brush and high-density brush structure for medium and high load, depends on the concentration of polymerised samples, respectively. 0.6 M monomer concentration showed more stable and higher Young's modulus compared to other polymer surfaces. As a result, it is expected that 0.6 M sample could provide better mechanical strength in comparison with the rest of the surfaces. However, deviations in Young's modulus values on different areas were attributed to differences in the length of PMPC chains, surface uniformity, grafting density and stress distribution.

6.3.3.4 Stress-strain diagram

A stress-strain diagram is presented in Fig. 6.9. Nanoindentation results were plotted for applied load in a range of 5 - 1000 µN, to compare elasticity of different samples. The arrow marks indicate a yield point of the sample and a high strain limit indicates high elasticity. Fig. 6.9 shows that all PMPC grafted sample exhibited greater elasticity (higher strain limit) than untreated Ti6Al4V implant surface.

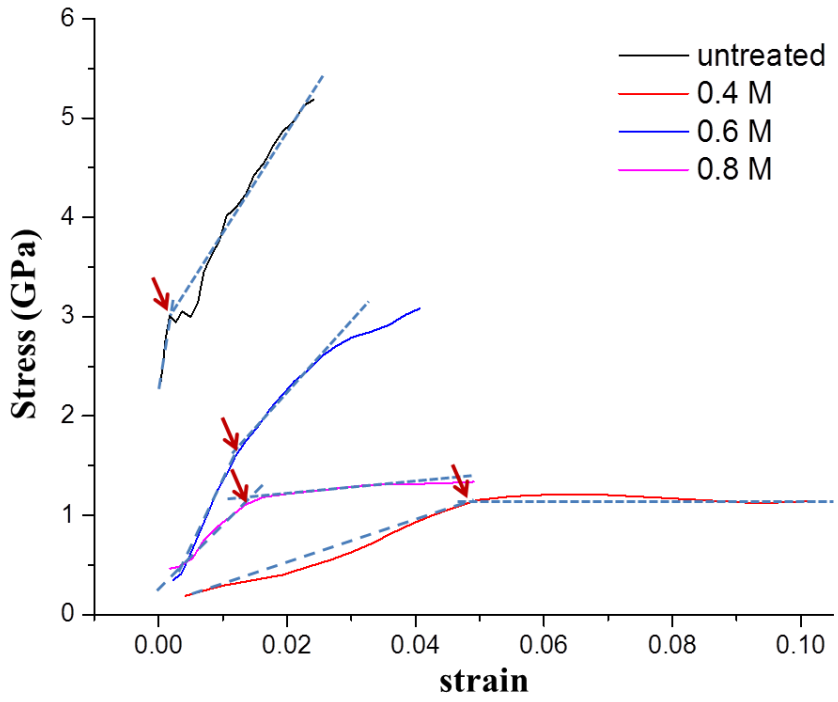

Fig. 6.9 Stress-strain diagrams for PMPC grafted samples with different monomer concentration. The arrow indicates the elasticity limits of the samples.

This means that PMPC grafted sample can stand more force in a elastic region before passing to a viscoelastic region or permanent deformation [241, 242]. As is shown in Fig. 6.9, among all PMPC grafted samples, 0.4 M treated samples had the best elasticity while 0.6 M treated

samples had greater resilience to wear and more desirable Young's modulus than others. It could, therefore, be concluded that the surface of the PMPC grafted sample prepared with 0.6 M monomer concentration exhibit the optimal properties. However, more investigation is required to understand elasticity behaviour of PMPC grafted samples without sacrificing mechanical properties of PMPC grafted surfaces.

6.3.4 Effect of PMPC layer on scratch resistance

The scratch test was performed to compare the mechanical strength of the polymer treated samples with untreated samples. The optimised polymer grafted samples from the previous study were considered for scratch test. The surface topography of untreated and polymer grafted samples was presented in Fig. 6.10. A visible scratch (scratch depth ~ 50 nm) was noticed on the untreated surface (Fig. 6.10(a)) for 0.5 mN load while almost no scratch (scratch depth ~ 5 nm) was observed on the grafted surface (Fig. 6.10(b)). However, for the high load, 2 mN, there is a minor scratch,~ 30 nm, on the grafted surface, Fig. 6.10(d), in comparison with the untreated surface,~ 100 nm, Fig. 6.10 (c). It indicates that PMPC grafted surface can sustain under higher load in comparison with an untreated surface. The absence of spallation and buckling defects suggests that plastic deformation has occurred in the substrate rather than the polymer coating [243, 244]. Deformation recovery shows the flexibility and elasticity of the polymer grafted layer. The other benefit of polymer grafting is to prevent the underlying metallic substrate from scratching under high loads. The measured value (not shown) indicated that the residual depths were higher for a deeper scratch on untreated samples comparing with treated one. The residual depths were much lower than penetration depths due to the deformation recovery of the polymer layers. It means that polymer grafting improved the mechanical strength of the surface by protecting the implant surface from scratching, which leads to a significant effect on enhancement of tribological outcomes of hip implants.

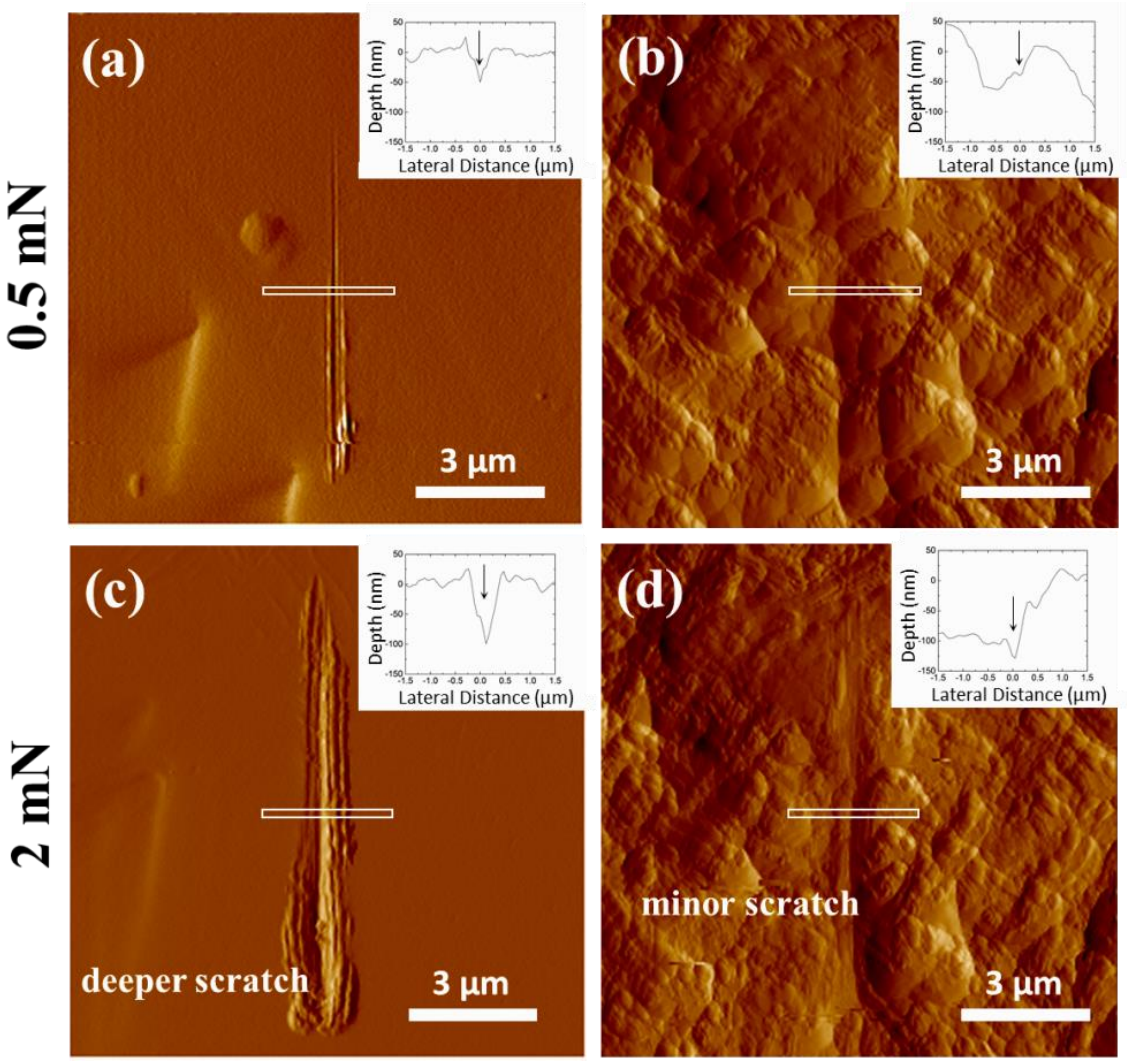

Fig. 6.10 Surface topography of untreated (a & c) and treated surfaces with MPC (b & d) after scratch test under various applied loads. Wear track data was taken from about half way through the scratch, indicated by the white box. The depths of each scratch are (a) 50 nm (b) 5 nm (c) 100 nm (d) 30 nm.

6.3.5 Effect of PMPC layer on wear resistance

Wear of hip implants is a complex mechanism and heavily influenced by mechanical properties such as hardness and Young's modulus of the materials [10, 245]. Wear in hip joints is caused by cyclic loading [23, 246]. However, the good mechanical properties of the material

are subjected to improve wear resistance, due to increasing the elasticity of the surface before permanent deformation of the implant surface. Fig. 6.11 illustrates wear behaviour of untreated and PMPC grafted surface under low to high loads. Fig. 6.11(a) reveals that 20 µN load had no impact on PMPC grafted surfaces while minor wear marks were noticed on untreated Ti6Al4V alloy surfaces, although Young's modulus was highest in value for untreated Ti6Al4V alloy surfaces. This was caused by direct contact and high friction between hard diamond tip and surface of Ti6Al4V substrate. Thin layer of PMPC film prevented direct contact and, as a result, protected surfaces of the implant from wear. However, wear marks became more visible with high load. Even minor wear was so noticeable for 0.4 M, and 0.8 M PMPC grafted surfaces (Fig. 6.11(b)) and, interestingly, no wear was noticed for 0.6 M surfaces at medium load, 60 µN. Differences between surface topography of untreated and 0.6 M treated surfaces justified how PMPC layers contributed to an improvement in wear resistance. A soft PMPC layer can absorb loads and dissipate energy through polymer layer and acts like cartilage in human joint [247]. Wear resistance of 0.6 M PMPC treated surfaces is high under low to medium load, while caused a plastic deformation at high load, 100 µN. Fig. 6.11 (c) shows major wear marks for untreated Ti6Al4V surfaces followed by 0.4 M and 0.8 M surfaces, while 0.6M showed minor plastic deformation, which indicated PMPC layer protected the substrate from wear. PMPC layer can restore its previous position when unloaded because of its structure. Overall, 0.6 M PMPC treated surfaces performed better than 0.4 M and 0.8 M PMPC treated surfaces and significant improvement in wear resistance of PMPC treated surface in comparison with untreated Ti6Al4V surfaces. Wear result was also concurrent to surface morphology and wettability results, where 0.6 M PMPC treated surfaces showed improved performance in all perspective.

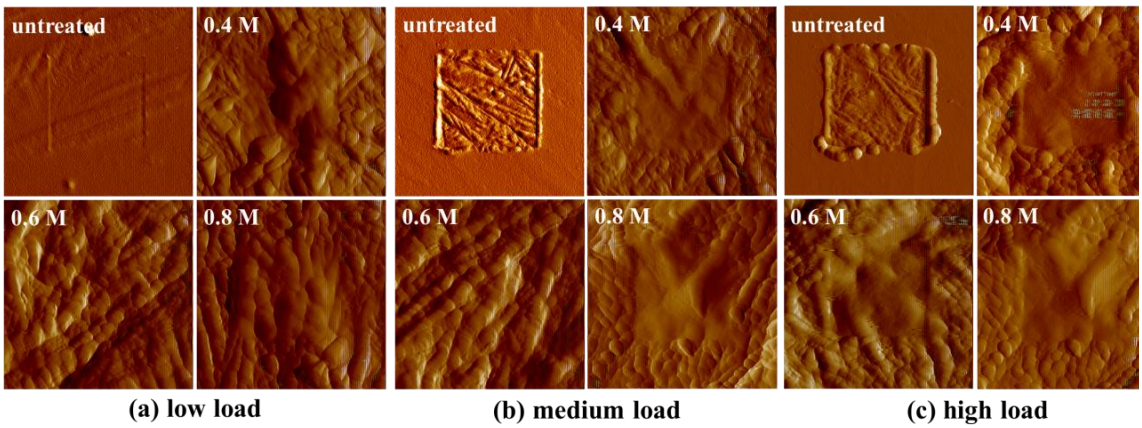

Fig. 6.11 Wear marks under different loading conditions for untreated surface and PMPC treated surface with various monomer concentrations.

This study concluded that despite a decrease in Young's modulus of PMPC grafted surfaces, resistance to wear had been improved in comparison to untreated Ti6Al4V surfaces. Conversely, a PMPC grafted sample treated with 0.6 M monomer concentration exhibited the best wear resistance, and its Young's modulus value was comparatively higher than other PMPC grafted surfaces. Therefore, no specific correlation was possible to draw between Young's modulus and wear resistance property.

6.4 Summary

This work investigated the effect of different monomer concentrations on thermal, mechanical and surface properties of polymer grafted Ti6Al4V implants. The key findings are summarised as follows:

- TGA and DSC analysis revealed excellent thermal stability of PMPC grafted samples for implant applications and thermal sterilisation.
- PMPC treated surface revealed improved wettability property which resulted in enhanced lubricity behaviour during sliding motion.

- 0.6 M samples demonstrated lower penetration depth and higher resistance to permanent deformation than 0.4 M and 0.8 M samples. It suggests that the sample with 0.6 M coating has the greatest potentiality for applications that undergo cyclic loading. Further, it indicates that such samples will have a greater ability to resist wear.
- PMPC grafted samples minimised Young's modulus value by 33.3-42.9 % compared to untreated surface, leading in preventing a stress shielding effect under loading conditions.
- There was a significant improvement in the elasticity behaviour of polymer grafted samples.
- The nano-scratch test exhibited that the polymer grafted layer prevents the Ti6Al4V substrate from scratching at high loads which indicates the better mechanical strength of polymer grafted implants compared to the untreated surface.
- 0.6 M showed the best wear resistance in all loads among all samples. Thin PMPC layer prevented direct contact and, as a result, protected the surfaces from wear.

However, the correlation between the elasticity and other mechanical properties is yet to be investigated to understand the failure mechanism of implants.

6.5 References

[10] Long M and Rack H 1998 Titanium alloys in total joint replacement—a materials science perspective *Biomaterials* **19** 1621-39

[23] Ghosh S, Choudhury D, Roy T, Mamat A B, Masjuki H and Pingguan-Murphy B 2016 Tribological investigation of diamond-like carbon coated micro-dimpled surface under bovine serum and osteoarthritis oriented synovial fluid *Science and Technology of Advanced Materials*

[24] Ghosh S, Choudhury D, Das N S and Pingguan-Murphy B 2014 Tribological role of synovial fluid compositions on artificial joints — a systematic review of the last 10 years *Lubrication Science* **26** 387-410

[26] Ishihara K 2015 Highly lubricated polymer interfaces for advanced artificial hip joints through biomimetic design *Polymer Journal* **47** 585-97

[52] Akhtari Zavareh M, Sarhan A A D M, Karimzadeh R and Singh R S A l K 2018 Analysis of corrosion protection behavior of Al2O3-TiO2 oxide ceramic coating on carbon steel pipes for petroleum industry *Ceramics International* **44** 5967-75

[142] Kyomoto M, Moro T, Takatori Y, Tanaka S and Ishihara K 2015 Multidirectional Wear and Impact-to-wear Tests of Phospholipid-polymer-grafted and Vitamin E-blended Crosslinked Polyethylene: A Pilot Study *Clinical Orthopaedics and Related Research®* **473** 942-51

[143] Moro T, Takatori Y, Kyomoto M, Ishihara K, Kawaguchi H, Hashimoto M, Tanaka T, Oshima H and Tanaka S 2015 Wear resistance of the biocompatible phospholipid polymer-grafted highly cross-linked polyethylene liner against larger femoral head *Journal of Orthopaedic Research*

[160] Ghosh S, Abanteriba S, Wong S and Houshyar S 2018 Selective laser melted titanium alloys for hip implant applications: surface modification with new method of polymer grafting *Journal of the Mechanical Behavior of Biomedical Materials*

[173] Kyomoto M, Moro T, Miyaji F, Hashimoto M, Kawaguchi H, Takatori Y, Nakamura K and Ishihara K 2009 Effects of mobility/immobility of surface modification by 2-methacryloyloxyethyl phosphorylcholine polymer on the durability of polyethylene for artificial joints *Journal of Biomedical Materials Research Part A* **90** 362-71

[182] Tiwari A and Natarajan S 2017 *Applied Nanoindentation in Advanced Materials*: John Wiley & Sons)

[197] Ghosh S, Choudhury D, Roy T, Moradi A, Masjuki H H and Pingguan-Murphy B 2015 Tribological performance of the biological components of synovial fluid in artificial joint implants *Science and Technology of Advanced Materials* **16** 045002

[211] Ishihara K, Mu M, Konno T, Inoue Y and Fukazawa K 2017 The unique hydration state of poly (2-methacryloyloxyethyl phosphorylcholine) *Journal of Biomaterials Science, Polymer Edition* **28** 884-99

[220] Ghosh S A, Sylvester; Wong, Sherman; Houshyar, Shadi 2018 Selective laser melted titanium alloys for hip implant applications: surface modification with new method of polymer grafting *Journal of the Mechanical Behaviour of Biomedical Materials*

[221] Huang J and Matyjaszewski K 2005 Atom transfer radical polymerization of dimethyl (1-ethoxycarbonyl) vinyl phosphate and corresponding block copolymers *Macromolecules* **38** 3577-83

[222] Pan L, Li G, Su Y and Lian J 2012 Fire retardant mechanism analysis between ammonium polyphosphate and triphenyl phosphate in unsaturated polyester resin *Polymer degradation and stability* **97** 1801-6

[223] Vyazovkin S, Dranca I, Fan X and Advincula R 2004 Kinetics of the thermal and thermo-oxidative degradation of a polystyrene–clay nanocomposite *Macromolecular rapid communications* **25** 498-503

[224] Kim M, Ko H and Park S-M 2019 Synergistic effects of amine-modified ammonium polyphosphate on curing behaviors and flame retardation properties of epoxy composites *Composites Part B: Engineering*

[225] Ishihara K, Nomura H, Mihara T, Kurita K, Iwasaki Y and Nakabayashi N 1998 Why do phospholipid polymers reduce protein adsorption? *Journal of Biomedical Materials Research: An Official Journal of The Society for Biomaterials, The Japanese Society for Biomaterials, and the Australian Society for Biomaterials* **39** 323-30

[226] Morisaku T, Watanabe J, Konno T, Takai M and Ishihara K 2008 Hydration of phosphorylcholine groups attached to highly swollen polymer hydrogels studied by thermal analysis *Polymer* **49** 4652-7

[227] Ishihara K, Iwasaki Y, Ebihara S, Shindo Y and Nakabayashi N 2000 Photoinduced graft polymerization of 2-methacryloyloxyethyl phosphorylcholine on polyethylene membrane surface for obtaining blood cell adhesion resistance *Colloids and Surfaces B: biointerfaces* **18** 325-35

[228] Madsen J, Armes S P and Lewis A L 2006 Preparation and aqueous solution properties of new thermoresponsive biocompatible ABA triblock copolymer gelators *Macromolecules* **39** 7455-7

[229] Gates C, Perfect E, Lokitz B, Brabazon J, McKay L and Tyner J 2018 TRANSIENT ANALYSIS OF ADVANCING CONTACT ANGLE MEASUREMENTS ON POLISHED ROCK SURFACES *Advances in Water Resources*
[230] Zhang X, Zhang G, Li J, He X, Wang Y, Hang R, Huang X, Tang B and Chu P K 2018 Cellular response to nano-structured Zr and ZrO2 alloyed layers on Ti-6Al-4V *Materials Science and Engineering: C* **90** 523-30
[231] Marković G, Marinović-Cincović M, Jovanović V, Samaržija-Jovanović S and Budinski-Simendić J Polymer characterization (II)
[232] Giammanco I M, Brown T M, Grant R G, Dewey D L, Hodel J D and Stumpf R A 2015 Evaluating the hardness characteristics of hail through compressive strength measurements *Journal of Atmospheric and Oceanic Technology* **32** 2100-13
[233] Bartlett R 2002 *Sports biomechanics: reducing injury and improving performance*: Routledge)
[234] Wang X, Gong X and Chou K 2015 Scanning Speed Effect on Mechanical Properties of Ti-6Al-4V Alloy Processed by Electron Beam Additive Manufacturing *Procedia Manufacturing* **1** 287-95
[235] Kaner R B, Gilman J J and Tolbert S H 2005 Designing superhard materials *Science* **308** 1268-9
[236] Ilie N, Hilton T, Heintze S, Hickel R, Watts D, Silikas N, Stansbury J, Cadenaro M and Ferracane J 2017 Academy of dental materials guidance—Resin composites: Part I—Mechanical properties *Dental materials* **33** 880-94
[237] Fischer-Cripps A C 2011 *Nanoindentation*: Springer) pp 21-37
[238] Huiskes R, Weinans H and Van Rietbergen B 1992 The relationship between stress shielding and bone resorption around total hip stems and the effects of flexible materials *Clinical orthopaedics and related research* 124-34
[239] Niinomi M and Nakai M 2011 Titanium-based biomaterials for preventing stress shielding between implant devices and bone *International journal of biomaterials* **2011**
[240] Ridzwan M, Shuib S, Hassan A, Shokri A and Ibrahim M M 2007 Problem of stress shielding and improvement to the hip implant designs: a review *J. Med. Sci* **7** 460-7
[241] Terzopoulos D and Fleischer K 1988 Modeling inelastic deformation: viscolelasticity, plasticity, fracture. In: *ACM Siggraph Computer Graphics*: ACM) pp 269-78
[242] Wainwright S A, Biggs W and Currey J D 1982 *Mechanical design in organisms*: Princeton University Press)
[243] Evans A and Hutchinson J 1984 On the mechanics of delamination and spalling in compressed films *International Journal of Solids and Structures* **20** 455-66
[244] Bull S 1997 Failure mode maps in the thin film scratch adhesion test *Tribology international* **30** 491-8
[245] Moharrami N, Langton D, Sayginer O and Bull S 2013 Why does titanium alloy wear cobalt chrome alloy despite lower bulk hardness: A nanoindentation study? *Thin Solid Films* **549** 79-86
[246] Nasab M B, Hassan M R and Sahari B B 2010 Metallic biomaterials of knee and hip-a review *Trends Biomater. Artif. Organs* **24** 69-82
[247] Jahn S and Klein J 2015 Hydration lubrication: the macromolecular domain *Macromolecules* **48** 5059-75

CHAPTER SEVEN: THEORETICAL PREDICTION OF LUBRICATING FILM FORMATION UNDER DIFFERENT PHYSIOLOGICAL HIP JOINT CONDITIONS

7.1 Chapter Overview

This chapter presents a theoretical approach to investigate the role of the implant surfaces on lubricating film formation of synovial fluid under various physiological conditions. In this study, Hamrock-Dowson formula has been used to predict the lubrication behaviour of the implant surfaces [46]. Overall, this study fulfils the objective 5 (as stated in section 1.6), and thus, answers the research question 6 (as stated in section 1.5) of this project.

An investigation on film formation is an important aspect of the research because synovial fluid acts as a shock absorber providing a film thickness between the implant interfaces under load and sliding motions. Different parameters, such as synovial fluid viscosity, sliding speed, applied load, mechanical and surface properties of the implants were considered in this theoretical model. UHMWPE was considered as acetabular cup material to pair with the untreated Ti6Al4V, or PMPC treated Ti6Al4V as head material. The theoretical results revealed both untreated, and polymer treated implants exhibited boundary lubrication without any significant changes in film formation for the same parameters. However, the PMPC treated implants provided comparatively higher film thickness at high speed than that of untreated surfaces. Therefore, it can be concluded that polymer grafted implants exhibited improved lubricity at high load conditions.

7.2 Lubrication model: main characteristics

Fortran programming language was used to analyse the theoretical model in this study. Intel Parallel Studio XE Composer Edition software was used to execute the program. In this model, untreated or PMPC treated Ti6Al4V implants were considered as head materials and UHMWPE as cup materials. All parameters were assumed considering the physiological condition of hip joints. Standard head diameter 28 mm was considered for femoral head [46]. The lubricant viscosity at 2.5 mPa was considered for synovial fluid [47]. Although human is body subjected to significantly higher loads, e.g. 75-85 kg, total load is not subjected to single hip implant. Other hip implant and body parts also share this body weight. Therefore, average vertical load is expected to be reduced on a single implant. In this study, average vertical load of 50 N -150 N were applied with a wide range of frequency (f) 1 Hz -15 Hz for this model. A certain range of speed were considered to simulate the various moving condition including, walking, fast walking and running. Usually, the inclination angle of the acetabular cup is 45º, but it can vary with the movement of the hip joints [248, 249]. Therefore, the effect of anatomical orientation of the acetabular cup concerning head surface was considered in a range of 0º - 90º. The parameters: femoral head radius (R_1), femoral cup radius (R_2), modulus of elasticity for head (E_1), modulus of elasticity for cup (E_2), Poisson's ratio for head (ν_1), Poisson's ratio for cup (ν_2), average angular velocity ($\omega = 2\,\pi\,f$), average vertical load (W_y), absolute or dynamic viscosity of the lubricant (η) and inclination cup angle(Φ_0) were incorporated to outline the theoretical model.

Equivalent modulus of elasticity (E′) is calculated using the following equation:

$$\frac{2}{E'} = \frac{1-{\nu_1}^2}{E_1} + \frac{1-{\nu_2}^2}{E_2} \tag{8.1}$$

The entraining velocity (U_e) is calculated using the following equation:

$$U_e = \frac{\boldsymbol{\omega} R_1}{2} \tag{8.2}$$

The minimum film thickness $(h_{min})_{b\text{-}p}$ holds for an equivalent ball-on-plane configuration is estimated from the following equation [250, 251].

$$(h_{min})_{b\text{-}p} = 2.8\left(\frac{\eta U_e}{E'R'}\right)^{0.65}\left(\frac{W_y}{E'R'}\right)^{-0.21} \tag{8.3}$$

However, this study focussed on hip joints. Actual hip joint condition can be expressed by ball-on-socket configuration. Jalali-Vahid *et al.* [47] developed an equation for minimum film thickness ($(h_{min})_{b\text{-}s}$) in ball-on-socket configuration, which can be derived from the following equation:

$$\frac{(h_{min})_{b-s}}{(h_{min})_{b-p}} = 1.0191\left(\frac{\Phi_0}{90}\right)^4 - 2.3153\left(\frac{\Phi_0}{90}\right)^3 + 0.8151\left(\frac{\Phi_0}{90}\right)^2 - 0.1133\left(\frac{\Phi_0}{90}\right) + 1 \tag{8.4}$$

The lubrication regeime can be determined by λ ratio from equation 8.5,

$$\lambda = \frac{h_{min}}{R_q} \tag{8.5}$$

Where composite roughness (R_q) = $\sqrt{(R_h{}^2 + R_c{}^2)}$

* R_h and R_c are surface roughness for head and cup, respectively.

Therefore, if λ ratio is in between 0.1 and 1, then the lubrication regime is boundary lubrication. If λ ratio is less than or equal to 3, then the lubrication regime is mixed lubrication, otherwise, if the λ ratio exceeds 3 then the lubrication regime is fluid film lubrication. Theoretical results were plotted in Origin software to compare the results based on applied load, speed and the anatomical orientation of the acetabular cup.

7.3 Results and discussion

Lubrication film formation or viable existence of the lubricant is a vital element in tribology for efficient movements such as sliding or rolling [252, 253]. The lubrication film

formation depends on several factors: sliding speed is one of them. Fig. 7.1 presents the sliding speed dependency of lubrication film formation under three different loads for untreated and polymer treated surfaces. The minimum film thickness was about 150-170 nm at the low speed and increased gradually with sliding speed, which reached up to 1000 nm at 50 N load (Fig. 7.1(a)). Fig. 7.1(b) and Fig. 7.1(c) shows similar trends despite the increase in load. Vrbka *et al.* [254] also revealed from their experimental investigation that the film formation increased with the main speed and reported a maximum of 900 nm film on their next study [255].

In this physiological condition, standard cup inclination angle 45° was considered. The wide ranges of sliding speed (estimated from frequency, f) was considered due to the different modes of hip joints, such as slow walking, fast walking, slow running and fast running. Fig. 7.1 compares the film thickness results for untreated, and PMPC treated samples, but no significant differences ($p > 0.05$) were observed for different samples. Both implants exhibited similar lubrication behaviour with the increase of sliding speed for 50 N, 100 N and 150 N loads.

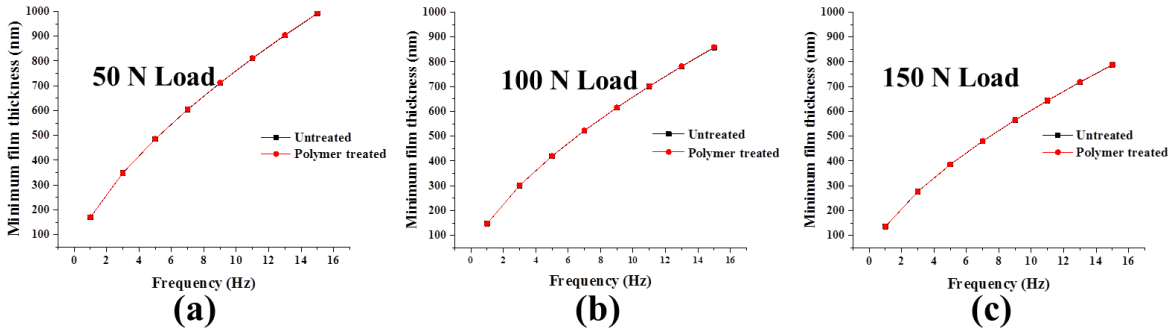

Fig. 7.1 The minimum film thickness as a function of frequency for untreated and polymer treated implants under (a) 50 N, (b) 100 N, and (c) 150 N Load. *The film thickness values overlap each other for untreated and polymer treated implants where $p > 0.05$.

The acetabular orientation varies depending on the anatomical motion of the body. For instance, the extension is the opposite of flexion motion. As a result, the cup inclination angle varies with different anatomical motions. Therefore, it is important to study the impact of anatomical motion on film formation. A wide range of cup inclination angle 0° - 90° was considered to cover all aspect of anatomical motions. Fig. 7.2 demonstrates the changes of film formation with the cup angle under three different speeds for untreated and polymer treated surfaces. The film formation was steady below 35° inclination angle for all speeds while the polymer grafted implants exhibited enhancement in film formation compared to untreated implants which were maximum 40 nm for high speed (Fig. 7.2 (c)), followed by 30 nm for medium speed (Fig. 7.2 (b)) and 10 nm for low speed (Fig. 7.2 (a)). These results could be attributed to the comparatively lower surface roughness of PMPC grafted surface than an untreated surface. A hydrodynamic pressure is developed with speed resulted in high film formation [58]. However, film formation started dropping after 35° regardless of the surface conditions. The reduction in film thickness after 35° inclination angle could be justified due to changes in femoral head and acetabular cup position. At higher angles, the ball and socket joints are expected to come closer, as a result, squeeze out the lubricant from the interface due to its introduction of high forces during shrinkage in area.

No significant variation ($p > 0.05$) was observed in film formation at low speed, but PMPC grafted implants performed well at high speed at all inclination angles. Though experimental conditions were the same in this theoretical model, the surface and mechanical properties were different between the untreated and PMPC treated surfaces. The low surface roughness along with other mechanical properties enhanced the film formation for the polymer grafted substrate. Moreover, improved lubricating performance was expected for PMPC grafted implants *in vivo* conditions because PMPC provides hydrophilic moieties, which could

result better interaction with body-oriented fluids, and thus, helps in the enhancement of film formation.

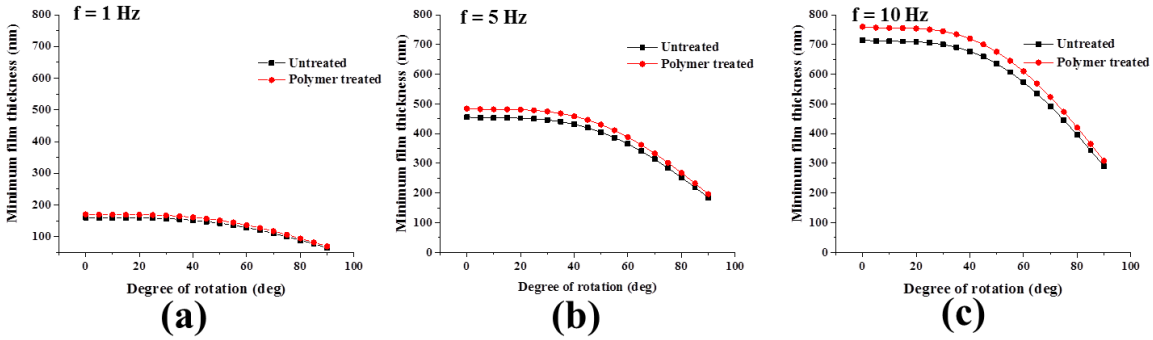

Fig. 7.2 The minimum film thickness as a function of the anatomical orientation of cup angle for untreated and polymer treated implants under (a) 1 Hz, (b) 5 Hz, and (c) 10 Hz frequency.

Fig. 7.3 presents the predicted film thickness of untreated and polymer treated implants as a function of different loads under three sliding speeds. The predicted minimum film thickness was shown to remain remarkably constant at low speed (Fig. 7.3(a)), despite a substantial change with the applied load. The minimum film thickness in a range of 125-175 nm was generated at low speed while 760- 820 nm was generated at low load and high speed. The film thickness tended to decrease with the increase of applied load, Fig. 7.3 (b), and the gradual drop in film thickness was observed with the applied load, Fig. 7.3 (c). Synovial fluid squeezed out at high load resulted in low film thickness. The enhancement in film thickness was noticed for polymer grafted implants with the sliding speed. The film pressure decreases with increasing sliding speeds. Both increasing speed and reducing film pressure, caused a thicker lubricant film [256]. Moreover, synovial fluids can exert pressure to enhance the lubricant film at high speed. The lubrication regime was identified as boundary lubrication due to high surface roughness both for untreated and PMPC treated surfaces. The boundary lubrication was identified in this theoretical model as λ ratio was always found less than 1 in

all physiological conditions. PMPC grafted implants exhibited improved lubrication in comparison to untreated Ti6Al4 implants.

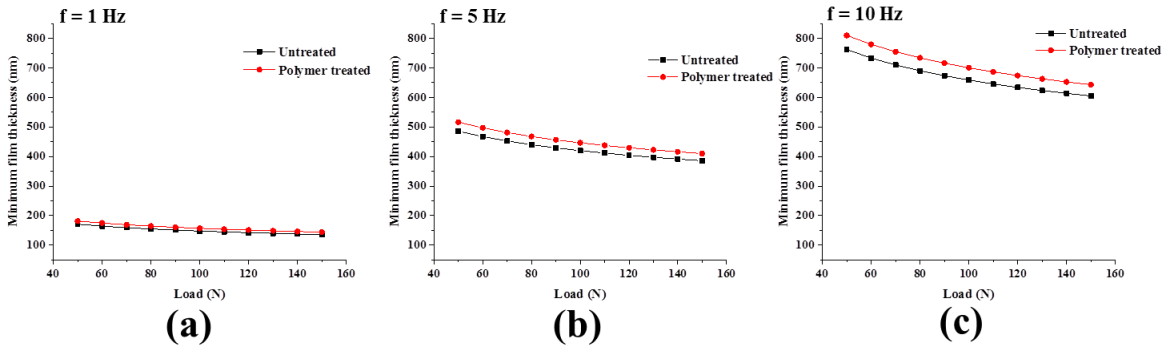

Fig. 7.3 The minimum film thickness as a function of load for untreated and polymer treated implants under (a) 1 Hz, (b) 5 Hz, and (c) 10 Hz frequency.

The PMPC implants are only hoped in enhancing the lubrication performance in boundary lubrication due to their polymer brush-like structure. Otherwise, if the partially melted particles experience the sliding motion, the friction and wear rate would be exacerbated. PMPC thin layer could prevent the AM Ti6Al4V implants from coming in contact with acetabular cup surfaces and thus, could improve the arthroplasty performance.

7.4 Summary

This theoretical investigation predicts the lubrication film thickness considering the physiological condition of artificial hip joints. The following conclusions can be drawn from this study:

- No significant difference in lubricant film formation was identified between untreated and polymer treated implants with increasing sliding speed if the load and inclination angle is constant.
- PMPC grafted implants exhibited the enhancement in film formation with the changes in anatomical orientation of the hip joints.

- Boundary lubrication was identified at all physiological conditions of hip implants in this theoretical model due to the high surface roughness even after polymer grafting.
- PMPC grafted implants showed better performance in lubrication behaviour compared to untreated Ti6Al4V even at high loads and high speeds.
- Improved arthroplasty performance is expected from PMPC treated implants *in vivo* due to their hydrophilic property and good interaction with biological fluids.

7.5 References

[46] Liu F, Jin Z, Roberts P and Grigoris P 2006 Importance of head diameter, clearance, and cup wall thickness in elastohydrodynamic lubrication analysis of metal-on-metal hip resurfacing prostheses *Proceedings of the Institution of Mechanical Engineers, Part H: Journal of Engineering in Medicine* **220** 695-704

[47] Jalali-Vahid D, Jagatia M, Jin Z and Dowson D 2001 Prediction of lubricating film thickness in UHMWPE hip joint replacements *Journal of biomechanics* **34** 261-6

[58] Roy T, Choudhury D, Ghosh S, Mamat A B and Pingguan-Murphy B 2015 Improved friction and wear performance of micro dimpled ceramic-on-ceramic interface for hip joint arthroplasty *Ceramics International* **41** 681-90

[248] Little N J, Busch C A, Gallagher J A, Rorabeck C H and Bourne R B 2009 Acetabular polyethylene wear and acetabular inclination and femoral offset *Clinical Orthopaedics and Related Research®* **467** 2895

[249] Langton D, Jameson S, Joyce T, Webb J and Nargol A 2008 The effect of component size and orientation on the concentrations of metal ions after resurfacing arthroplasty of the hip *The Journal of bone and joint surgery. British volume* **90** 1143-51

[250] Hamrock B J and Dowson D 1978 Elastohydrodynamic lubrication of elliptical contacts for materials of low elastic modulus I—fully flooded conjunction *Journal of Tribology* **100** 236-45

[251] Wang D 1994 Elastohydrodynamic lubrication of point contacts for layers of soft solids and for 'monolithic'hard materials in the transient bouncing ball problem. Ph. D. thesis, University of Leeds)

[252] Stachowiak G and Batchelor A W 2013 *Engineering tribology*: Butterworth-Heinemann)

[253] Stachowiak G and Batchelor A W 2004 *Experimental methods in tribology* vol 44: Elsevier)

[254] Vrbka M, Návrat T, Křupka I, Hartl M, Šperka P and Gallo J 2013 Study of film formation in bovine serum lubricated contacts under rolling/sliding conditions *Proceedings of the Institution of Mechanical Engineers, Part J: Journal of Engineering Tribology* **227** 459-75

[255] Vrbka M, Křupka I, Hartl M, Návrat T, Gallo J and Galandáková A 2014 In situ measurements of thin films in bovine serum lubricated contacts using optical interferometry *Proceedings of the Institution of Mechanical Engineers, Part H: Journal of Engineering in Medicine* **228** 149-58

[256] Harper P, Dwyer-Joyce R, Sjödin U and Olofsson U 2005 *Tribology and Interface Engineering Series*: Elsevier) pp 305-12

CHAPTER EIGHT: SUMMARY AND FUTURE WORK

8.1 Summary

The research presented in this thesis has developed a novel polymer grafting technique on the surface of additively manufactured titanium substrate for improved hip arthroplasty performance. An informative literature review, presented in Chapter two, has discussed the current status of surface modification techniques for improved hip arthroplasty performance. This review has established the research gap and accordingly the research questions and objectives of this project, that presented in detail in Chapter one. The experimental details of this project have been highlighted in Chapter three. Chapter four has addressed the novel technique of PMPC grafting onto the surface of SLM Ti6Al4V implants. Chapter five has discussed the influence of the monomer concentration on polymerisation and surface properties of the implant through an experimental study, and finally, optimised the monomer concentration. Chapter six has highlighted the effect of PMPC layer on the thermal and mechanical properties of the implant. The impact of PMPC layer on scratch and wear resistance has also been analysed. Chapter seven has presented a theoretical approach to predict the lubricating film thickness under physiological hip joint conditions.

8.2 Conclusion

The key findings of this project are summarised as follows:

- PMPC was successfully grafted when UV irradiation was applied under N_2 gas atmosphere to eliminate the O_2 which inhibit the polymerisation. This technique achieved a continuous & uniform PMPC layer with the highest polymer thickness.
- NMR analysis revealed that the degree of polymerisation was higher than 95% and confirmed that monomer had been polymerised successfully. FTIR spectra confirmed the polymerisation by the alkene group conversion to alkane group. The length and the

number of the polymer chain increased with the increase in monomer concentration which was confirmed by GPC analysis.

- The surface morphology of the samples grafted with 0.6 M monomer concentration exhibited the best and uniform surface coverage followed by 0.8 M and 0.4 M.
- The polymer grafted surface dramatically reduced mammalian cell adhesion. Therefore, PMPC grafting could be a suitable solution to resist the uncontrolled cells and facilitate smooth motion of ball-socket joints.
- TGA and DSC analysis revealed the excellent thermal stability of the polymer layer for implant applications. The PMPC treated surface showed better wettability property resulted in better lubricity behaviour during the sliding motion.
- The 0.6 M samples demonstrated the lowest penetration depth and maximum resistance to permanent deformation in compared to 0.4 M and 0.8 M samples.
- Young's modulus was minimised by 33.3-42.9 % for PMPC grafted surfaces compared to an untreated surface, which could help in preventing a stress shielding effect under loading conditions. A significant improvement in the elasticity behaviour of polymer grafted samples was achieved.
- The nano-scratch test exhibited that the polymer grafted layer prevents the surface of Ti6Al4V substrate from scratching at high loads which indicates the improved mechanical strength of polymer grafted implants. Wear resistance of the grafted surface improved due to a reduction in surface roughness.
- Theoretical modelling predicts boundary lubrication occurred in physiological conditions of hip joints. Therefore, surface grafting with PMPC layers could protect the implants from direct contact with cup surfaces leading in minimising the friction and wear.

- Overall, the development of PMPC grafting onto the surface of additively manufactured Ti6Al4V substrate resulted in significant minimisation of Young's modulus and improvement in elasticity behaviour of the implant surface. This would be a significant contribution to a body of knowledge in biomedical research.

8.3 Recommendations for future work

Further studies are needed to address some unresolved issues for the future design of titanium hip implants. These include:

- Tribological investigation is an important aspect of implant research to evaluate the useful life of the implants. Therefore, further studies can be carried out using the hip simulator to investigate the role of PMPC layer on tribological performance.
- Though the newly developed polymer grafting technique minimised the surface roughness of SLM fabricated samples significantly, still, the roughness is not ideal for hip implant applications. Therefore, the optimisation of processing parameters for the SLM technique to reduce the surface roughness of the as-built Ti6Al4V substrate could be an effective way to improve the implant surfaces.
- Further studies are required to evaluate the performance of PMPC layer on cell adhesion. Quantitative analysis can reveal more information in cell adhesion perspective. The performance of PMPC layer on bacterial adhesion could also be investigated to determine the toxicity of the modified implants. Degradation study of PMPC layer in physiological condition is necessary to understand durability of polymer films, mechanism of release, degradation product and bonding strength between the PMPC layer and the implant surface.
- Experimental investigations are required to justify the theoretical model and to evaluate the lubrication performance of polymer grafted implants.

REFERENCES

[1] Choudhury D, Ay Ching H, Mamat A B, Cizek J, Osman A, Azuan N, Vrbka M, Hartl M and Krupka I 2014 Fabrication and characterization of DLC coated microdimples on hip prosthesis heads *Journal of Biomedical Materials Research Part B: Applied Biomaterials*

[2] Böhler C, Weimann P, Alasti F, Smolen J, Windhager R and Aletaha D 2018 FRI0051 The risk of aseptic arthroplasty loosening in patients with rheumatoid arthritis. BMJ Publishing Group Ltd)

[3] Ghosh S and Abanteriba S 2016 Status of surface modification techniques for artificial hip implants *Science and Technology of Advanced Materials* **17** 715-35

[4] Bačáková L, Filova E, Rypáček F, Švorčík V and Starý V 2004 Cell adhesion on artificial materials for tissue engineering *Physiol res* **53** S35-S45

[5] Puleo D and Nanci A 1999 Understanding and controlling the bone–implant interface *Biomaterials* **20** 2311-21

[6] Raynor J E, Capadona J R, Collard D M, Petrie T A and García A J 2009 Polymer brushes and self-assembled monolayers: versatile platforms to control cell adhesion to biomaterials *Biointerphases* **4** FA3-FA16

[7] Ramakrishnaiah R, Mohammad A, Divakar D D, Kotha S B, Celur S L, Hashem M I, Vallittu P K and Rehman I U 2017 Preliminary fabrication and characterization of electron beam melted Ti–6Al–4V customized dental implant *Saudi Journal of Biological Sciences* **24** 787-96

[8] Kaczorowski W, Szymanski W, Batory D and Niedzielski P 2014 Tribological Properties and Characterization of Diamond Like Carbon Coatings Deposited by MW/RF and RF Plasma-Enhanced CVD Method on Poly (ether-ether-ketone) *Plasma Processes and Polymers* **11** 878-87

[9] Fukuda A, Takemoto M, Tanaka K, Fujibayashi S, Pattanayak D, Matsushita T, Sasaki K, Nishida N, Kokubo T and Nakamura T 2011 Bone ingrowth into pores of lotus stem-type bioactive titanium implants fabricated using rapid prototyping technique *Bioceramics Development and Applications* **1**

[10] Long M and Rack H 1998 Titanium alloys in total joint replacement—a materials science perspective *Biomaterials* **19** 1621-39

[11] Fousová M, Vojtěch D, Kubásek J, Jablonská E and Fojt J 2017 Promising characteristics of gradient porosity Ti-6Al-4V alloy prepared by SLM process *Journal of the Mechanical Behavior of Biomedical Materials* **69** 368-76

[12] Kopova I, Stráský J, Harcuba P, Landa M, Janeček M and Bačákova L 2016 Newly developed Ti–Nb–Zr–Ta–Si–Fe biomedical beta titanium alloys with increased strength and enhanced biocompatibility *Materials Science and Engineering: C* **60** 230-8

[13] Niinomi M, Nakai M and Hieda J 2012 Development of new metallic alloys for biomedical applications *Acta Biomaterialia* **8** 3888-903

[14] Zhang C, Zhang L, Xu H, Li P and Qian B 2019 Performance of pool boiling with 3D grid structure manufactured by selective laser melting technique *International Journal of Heat and Mass Transfer* **128** 570-80

[15] Khorasani A, Gibson I, Goldberg M and Littlefair G 2017 Production of Ti-6Al-4V acetabular shell using selective laser melting: possible limitations in fabrication *Rapid Prototyping Journal* **23**

[16] Dylla-Spears R, Wong L, Shen N, Steele W, Menapace J, Miller P, Feit M and Suratwala T 2017 Adsorption of silica colloids onto like-charged silica surfaces of different roughness *Colloids and Surfaces A: Physicochemical and Engineering Aspects* **520** 85-96

[17] Li J, Li Z, Tu J, Jin G, Li L, Wang K and Wang H 2019 In vitro and in vivo investigations of a-C/a-C:Ti nanomultilayer coated Ti6Al4V alloy as artificial femoral head *Materials Science and Engineering: C* **99** 816-26

[18] Jo S, Lee S, Lim W, Kim D and Lee J 2018 APPLICATION OF PLASMA ELECTROLYTIC OXIDATION COATING ON TITANIUM FEMORAL HEAD. In: *Orthopaedic Proceedings*: The British Editorial Society of Bone & Joint Surgery) pp 1-

[19] Luo Y, Ge S, Liu H and Jin Z 2009 Microstructure analysis and wear behavior of titanium cermet femoral head with hard TiC layer *Journal of Biomechanics* **42** 2708-11

[20] Gutmanas E Y and Gotman I 2004 PIRAC Ti nitride coated Ti–6Al–4V head against UHMWPE acetabular cup–hip wear simulator study *Journal of Materials Science: Materials in Medicine* **15** 327-30

[21] Vamsi Krishna B, Xue W, Bose S and Bandyopadhyay A 2008 Functionally graded Co–Cr–Mo coating on Ti–6Al–4V alloy structures *Acta Biomaterialia* **4** 697-706

[22] Liu C, Bi Q and Matthews A 2003 Tribological and electrochemical performance of PVD TiN coatings on the femoral head of Ti–6Al–4V artificial hip joints *Surface and Coatings Technology* **163-164** 597-604

[23] Ghosh S, Choudhury D, Roy T, Mamat A B, Masjuki H and Pingguan-Murphy B 2016 Tribological investigation of diamond-like carbon coated micro-dimpled surface under bovine serum and osteoarthritis oriented synovial fluid *Science and Technology of Advanced Materials*

[24] Ghosh S, Choudhury D, Das N S and Pingguan-Murphy B 2014 Tribological role of synovial fluid compositions on artificial joints — a systematic review of the last 10 years *Lubrication Science* **26** 387-410

[25] Vilaro T, Abed S and Knapp W 2008 Direct manufacturing of technical parts using selective laser melting: example of automotive application. In: *Proc. of 12th European Forum on Rapid Prototyping,*

[26] Ishihara K 2015 Highly lubricated polymer interfaces for advanced artificial hip joints through biomimetic design *Polymer Journal* **47** 585-97

[27] Moro T, Takatori Y, Kyomoto M, Ishihara K, Saiga K-i, Nakamura K and Kawaguchi H 2010 Surface grafting of biocompatible phospholipid polymer MPC provides wear resistance of tibial polyethylene insert in artificial knee joints *Osteoarthritis and Cartilage* **18** 1174-82

[28] Kyomoto M, Moro T, Saiga K-i, Miyaji F, Kawaguchi H, Takatori Y, Nakamura K and Ishihara K 2010 Lubricity and stability of poly (2-methacryloyloxyethyl phosphorylcholine) polymer layer on Co–Cr–Mo surface for hemi-arthroplasty to prevent degeneration of articular cartilage *Biomaterials* **31** 658-68

[29] Kyomoto M, Moro T, Saiga K, Hashimoto M, Ito H, Kawaguchi H, Takatori Y and Ishihara K 2012 Biomimetic hydration lubrication with various polyelectrolyte layers on cross-linked polyethylene orthopedic bearing materials *Biomaterials* **33** 4451-9

[30] Kyomoto M, Moro T, Yamane S, Takatori Y, Tanaka S and Ishihara K 2017 A hydrated phospholipid polymer-grafted layer prevents lipid-related oxidative degradation of cross-linked polyethylene *Biomaterials* **112** 122-32

[31] Moro T, Kawaguchi H, Ishihara K, Kyomoto M, Karita T, Ito H, Nakamura K and Takatori Y 2009 Wear resistance of artificial hip joints with poly (2-methacryloyloxyethyl phosphorylcholine) grafted polyethylene: comparisons with the effect of polyethylene cross-linking and ceramic femoral heads *Biomaterials* **30** 2995-3001

[32] Kyomoto M, Moro T, Konno T, Takadama H, Yamawaki N, Kawaguchi H, Takatori Y, Nakamura K and Ishihara K 2007 Enhanced wear resistance of modified cross-linked polyethylene by grafting with poly (2-methacryloyloxyethyl phosphorylcholine) *Journal of Biomedical Materials Research Part A* **82** 10-7

[33] Moro T, Takatori Y, Kyomoto M, Ishihara K, Hashimoto M, Ito H, Tanaka T, Oshima H, Tanaka S and Kawaguchi H 2014 Long-term hip simulator testing of the artificial hip joint bearing surface grafted with biocompatible phospholipid polymer *Journal of Orthopaedic Research* **32** 369-76

[34] Yarimitsu S, Moro T, Kyomoto M, Watanabe K, Tanaka S, Ishihara K and Murakami T 2015 Influences of dehydration and rehydration on the lubrication properties of phospholipid polymer-grafted cross-linked polyethylene *Proceedings of the Institution of Mechanical Engineers, Part H: Journal of Engineering in Medicine* 0954411915588969

[35] Chouirfa H, Evans M D, Castner D G, Bean P, Mercier D, Galtayries A, Falentin-Daudré C and Migonney V 2017 Grafting of architecture controlled poly (styrene sodium sulfonate) onto titanium surfaces using bio-adhesive molecules: Surface characterization and biological properties *Biointerphases* **12** 02C418

[36] Roos-Jansåker A M, Renvert S and Egelberg J 2003 Treatment of peri-implant infections: a literature review *Journal of clinical periodontology* **30** 467-85

[37] Liu X, Chu P K and Ding C 2004 Surface modification of titanium, titanium alloys, and related materials for biomedical applications *Materials Science and Engineering: R: Reports* **47** 49-121

[38] Zavareh M A, Sarhan A A D M, Razak B B A and Basirun W J 2014 Plasma thermal spray of ceramic oxide coating on carbon steel with enhanced wear and corrosion resistance for oil and gas applications *Ceramics International* **40** 14267-77

[39] Pyka G, Burakowski A, Kerckhofs G, Moesen M, Van Bael S, Schrooten J and Wevers M 2012 Surface modification of Ti6Al4V open porous structures produced by additive manufacturing *Advanced Engineering Materials* **14** 363-70

[40] Kirmanidou Y, Sidira M, Drosou M-E, Bennani V, Bakopoulou A, Tsouknidas A, Michailidis N and Michalakis K 2016 New Ti-alloys and surface modifications to improve the mechanical properties and the biological response to orthopedic and dental implants: a review *BioMed research international* **2016**

[41] Ci J, Kang H, Liu C, He A and Liu R 2017 Thermal sensitivity and protein anti-adsorption of hydroxypropyl cellulose-g-poly (2-(methacryloyloxy) ethyl phosphorylcholine) *Carbohydrate polymers* **157** 757-65

[42] Gupta N R, Ghute P P and Badiger M V 2011 Synthesis and characterization of thermo-sensitive graft copolymer of carboxymethyl guar and poly (N-isopropylacrylamide) *Carbohydrate polymers* **83** 74-80
[43] Buckwalter J A, Mankin H J and Grodzinsky A J 2005 Articular cartilage and osteoarthritis *Instructional Course Lectures-American Academy of Orthopaedic Surgeons* **54** 465
[44] Balazs E A 1974 The physical properties of synovial fluid and the special role of hyaluronic acid *Disorders of the Knee* **2** 61-74
[45] Mattei L, Di Puccio F, Piccigallo B and Ciulli E 2011 Lubrication and wear modelling of artificial hip joints: A review *Tribology International* **44** 532-49
[46] Liu F, Jin Z, Roberts P and Grigoris P 2006 Importance of head diameter, clearance, and cup wall thickness in elastohydrodynamic lubrication analysis of metal-on-metal hip resurfacing prostheses *Proceedings of the Institution of Mechanical Engineers, Part H: Journal of Engineering in Medicine* **220** 695-704
[47] Jalali-Vahid D, Jagatia M, Jin Z and Dowson D 2001 Prediction of lubricating film thickness in UHMWPE hip joint replacements *Journal of biomechanics* **34** 261-6
[48] Kang L, Galvin A L, Fisher J and Jin Z 2009 Enhanced computational prediction of polyethylene wear in hip joints by incorporating cross-shear and contact pressure in additional to load and sliding distance: effect of head diameter *Journal of biomechanics* **42** 912-8
[49] Wang F, Brockett C, Williams S, Udofia I, Fisher J and Jin Z 2008 Lubrication and friction prediction in metal-on-metal hip implants *Physics in medicine and biology* **53** 1277
[50] Chen Y, Bakshi S R and Agarwal A 2010 Correlation between nanoindentation and nanoscratch properties of carbon nanotube reinforced aluminum composite coatings *Surface and Coatings Technology* **204** 2709-15
[51] Sribalaji M, Rahman O A, Laha T and Keshri A K 2016 Nanoindentation and nanoscratch behavior of electroless deposited nickel-phosphorous coating *Materials Chemistry and Physics* **177** 220-8
[52] Akhtari Zavareh M, Sarhan A A D M, Karimzadeh R and Singh R S A l K 2018 Analysis of corrosion protection behavior of Al2O3-TiO2 oxide ceramic coating on carbon steel pipes for petroleum industry *Ceramics International* **44** 5967-75
[53] Merx H, Dreinhöfer K, Schräder P, Stürmer T, Puhl W, Günther K and Brenner H 2003 International variation in hip replacement rates *Annals of the rheumatic diseases* **62** 222-6
[54] Bozic K J, Kurtz S M, Lau E, Ong K, Vail T P and Berry D J 2009 The epidemiology of revision total hip arthroplasty in the United States *J Bone Joint Surg Am* **91** 128-33
[55] NJR Annual Report A 2017 Australian Orthopaedic Association National Joint Replacement Annual Report 2017. (The University of Adelaide: Australian Orthopaedic Association)
[56] Malak T, Broomfield J, Palmer A, Hopewell S, Carr A, Brown C, Prieto-Alhambra D and Glyn-Jones S 2016 Surrogate markers of long-term outcome in primary total hip arthroplasty *Bone and Joint Research* **5** 206-14
[57] Kurtz S M, Ong K L, Schmier J, Mowat F, Saleh K, Dybvik E, Kärrholm J, Garellick G, Havelin L I and Furnes O 2007 Future clinical and economic impact of revision total hip and knee arthroplasty *J Bone Joint Surg Am* **89** 144-51
[58] Roy T, Choudhury D, Ghosh S, Mamat A B and Pingguan-Murphy B 2015 Improved friction and wear performance of micro dimpled ceramic-on-ceramic interface for hip joint arthroplasty *Ceramics International* **41** 681-90
[59] Hauert R, Thorwarth K and Thorwarth G 2013 An overview on diamond-like carbon coatings in medical applications *Surface and Coatings Technology* **233** 119-30
[60] Ibatan T, Uddin M and Chowdhury M 2015 Recent development on surface texturing in enhancing tribological performance of bearing sliders *Surface and Coatings Technology* **272** 102-20
[61] Hauert R, Thorwarth G, Müller U, Stiefel M, Falub C, Thorwarth K and Joyce T 2012 Analysis of the in-vivo failure of the adhesive interlayer for a DLC coated articulating metatarsophalangeal joint *Diamond and Related Materials* **25** 34-9
[62] Lackner J M, Waldhauser W, Major L and Kot M 2014 Tribology and Micromechanics of Chromium Nitride Based Multilayer Coatings on Soft and Hard Substrates *Coatings* **4** 121-38
[63] Takatori Y, Moro T, Ishihara K, Kamogawa M, Oda H, Umeyama T, Kim Y T, Ito H, Kyomoto M and Tanaka T 2015 Clinical and radiographic outcomes of total hip replacement with poly (2-methacryloyloxyethyl phosphorylcholine)-grafted highly cross-linked polyethylene liners: Three-year results of a prospective consecutive series *Modern Rheumatology* **25** 286-91
[64] Smith A J, Dieppe P, Howard P W and Blom A W 2012 Failure rates of metal-on-metal hip resurfacings: analysis of data from the National Joint Registry for England and Wales *The Lancet* **380** 1759-66
[65] Leyens C and Peters M 2003 *Titanium and titanium alloys: fundamentals and applications*: John Wiley & Sons)

[66] Davidson J A 1993 Characteristics of metal and ceramic total hip bearing surfaces and their effect on long-term ultra high molecular weight polyethylene wear *Clinical orthopaedics and related research* **294** 361-78
[67] Niinomi M 2008 Mechanical biocompatibilities of titanium alloys for biomedical applications *Journal of the mechanical behavior of biomedical materials* **1** 30-42
[68] Laurent M P, Johnson T S, Crowninshield R D, Blanchard C R, Bhambri S K and Yao J Q 2008 Characterization of a highly cross-linked ultrahigh molecular-weight polyethylene in clinical use in total hip arthroplasty *The Journal of arthroplasty* **23** 751-61
[69] Muratoglu O K, Bragdon C R, O'Connor D O, Jasty M, Harris W H, Gul R and McGarry F 1999 Unified wear model for highly crosslinked ultra-high molecular weight polyethylenes (UHMWPE) *Biomaterials* **20** 1463-70
[70] Kurtz S M 2012 *PEEK Biomaterials Handbook*: Elsevier) pp 1-7
[71] Hatton A, Nevelos J, Nevelos A, Banks R, Fisher J and Ingham E 2002 Alumina–alumina artificial hip joints. Part I: a histological analysis and characterisation of wear debris by laser capture microdissection of tissues retrieved at revision *Biomaterials* **23** 3429-40
[72] Chevalier J and Gremillard L 2009 Ceramics for medical applications: A picture for the next 20 years *Journal of the European Ceramic Society* **29** 1245-55
[73] Campbell A A 2003 Bioceramics for implant coatings *Materials Today* **6** 26-30
[74] Villermaux F 2000 Zirconia-alumina as the new generation of ceramic-ceramic THP: wear performance evaluation including extreme life conditions. In: *Sixth World Biomaterials Congress*, p 2000
[75] Currier J H, Anderson D E and Van Citters D W 2010 A proposed mechanism for squeaking of ceramic-on-ceramic hips *Wear* **269** 782-9
[76] Lee M-C and Ahn J-W 2007 *Bioceramics and Alternative Bearings in Joint Arthroplasty*: Springer) pp 123-32
[77] Kokubo T 2008 *Bioceramics and their clinical applications*: Elsevier)
[78] De Aza A, Chevalier J, Fantozzi G, Schehl M and Torrecillas R 2002 Crack growth resistance of alumina, zirconia and zirconia toughened alumina ceramics for joint prostheses *Biomaterials* **23** 937-45
[79] Goodman S B, Ma T, Chiu R, Ramachandran R and Smith R L 2006 Effects of orthopaedic wear particles on osteoprogenitor cells *Biomaterials* **27** 6096-101
[80] Langton D, Jameson S, Joyce T, Hallab N, Natu S and Nargol A 2010 Early failure of metal-on-metal bearings in hip resurfacing and large-diameter total hip replacement A CONSEQUENCE OF EXCESS WEAR *Journal of Bone & Joint Surgery, British Volume* **92** 38-46
[81] Öztürk O, Türkan U u and Erogˇlu A E 2006 Metal ion release from nitrogen ion implanted CoCrMo orthopedic implant material *Surface and Coatings Technology* **200** 5687-97
[82] Shettlemore M and Bundy K 2001 Examination of in vivo influences on bioluminescent microbial assessment of corrosion product toxicity *Biomaterials* **22** 2215-28
[83] Chu P K 2007 Enhancement of surface properties of biomaterials using plasma-based technologies *Surface and Coatings Technology* **201** 8076-82
[84] Li D 1998 A new type of wear-resistant material: pseudo-elastic TiNi alloy *Wear* **221** 116-23
[85] Hsu C-Y, Yeh J-W, Chen S-K and Shun T-T 2004 Wear resistance and high-temperature compression strength of Fcc CuCoNiCrAl 0.5 Fe alloy with boron addition *Metallurgical and Materials Transactions A* **35** 1465-9
[86] Chuang M-H, Tsai M-H, Wang W-R, Lin S-J and Yeh J-W 2011 Microstructure and wear behavior of AlxCo1. 5CrFeNi1. 5Tiy high-entropy alloys *Acta Materialia* **59** 6308-17
[87] Haftlang F, Hanzaki A Z, Abedi H R, Preisler D and Bartha K 2019 The subsurface frictional hardening: A new approach to improve the high-speed wear performance of Ti-29Nb-14Ta-4.5 Zr alloy against Ti-6Al-4V extra-low interstitial *Wear* **422** 137-50
[88] de Oliveira D P, Toniato T V, Ricci R, Marciano F R, Prokofiev E, Valiev R Z, Lobo A O and Júnior A M J 2019 Biological response of chemically treated surface of the ultrafine-grained Ti–6Al–7Nb alloy for biomedical applications *International journal of nanomedicine* **14** 1725
[89] Lin S-P and Wong P-C 2019 Surface modified structure for improving hemocompatibility of biomedical metallic substrates. Google Patents)
[90] Pippenger B E, Rottmar M, Kopf B S, Stübinger S, Dalla Torre F H, Berner S and Maniura-Weber K 2019 Surface modification of ultrafine-grained titanium: Influence on mechanical properties, cytocompatibility, and osseointegration potential *Clinical oral implants research* **30** 99-110
[91] McGuire K S, Tweddell III R and Hamilton P W 2002 Golf ball with non-circular shaped dimples. Google Patents)
[92] Wang X, Kato K, Adachi K and Aizawa K 2003 Loads carrying capacity map for the surface texture design of SiC thrust bearing sliding in water *Tribology International* **36** 189-97

[93] Coblas D G, Fatu A, Maoui A and Hajjam M 2015 Manufacturing textured surfaces: State of art and recent developments *Proceedings of the Institution of Mechanical Engineers, Part J: Journal of Engineering Tribology* **229** 3-29
[94] Wang X and Kato K 2003 Improving the anti-seizure ability of SiC seal in water with RIE texturing *Tribology Letters* **14** 275-80
[95] Etsion I 2005 State of the art in laser surface texturing *Journal of Tribology* **127** 248-53
[96] Suh N P, Mosleh M and Howard P S 1994 Control of friction *Wear* **175** 151-8
[97] Ranjan R, Lambeth D, Tromel M, Goglia P and Li Y 1991 Laser texturing for low-flying-height media *Journal of Applied Physics* **69** 5745-7
[98] Chyr A, Qiu M, Speltz J W, Jacobsen R L, Sanders A P and Raeymaekers B 2014 A patterned microtexture to reduce friction and increase longevity of prosthetic hip joints *Wear* **315** 51-7
[99] Yu H, Deng H, Huang W and Wang X 2011 The effect of dimple shapes on friction of parallel surfaces *Proceedings of the Institution of Mechanical Engineers, Part J: Journal of Engineering Tribology* **225** 693-703
[100] Huang W and Wang X 2013 Biomimetic design of elastomer surface pattern for friction control under wet conditions *Bioinspiration & biomimetics* **8** 046001
[101] Kaneta M, Kanada T and Nishikawa H 1997 Optical interferometric observations of the effects of a moving dent on point contact EHL *Tribology series* **32** 69-79
[102] Ito H, Kaneda K, Yuhta T, Nishimura I, Yasuda K and Matsuno T 2000 Reduction of polyethylene wear by concave dimples on the frictional surface in artificial hip joints *The Journal of arthroplasty* **15** 332-8
[103] Shen C and Khonsari M 2015 Numerical optimization of texture shape for parallel surfaces under unidirectional and bidirectional sliding *Tribology International* **82** 1-11
[104] Etsion I and Burstein L 1996 A model for mechanical seals with regular microsurface structure *Tribology Transactions* **39** 677-83
[105] Wang X, Adachi K, Otsuka K and Kato K 2006 Optimization of the surface texture for silicon carbide sliding in water *Applied Surface Science* **253** 1282-6
[106] Yu H, Wang X and Zhou F 2010 Geometric shape effects of surface texture on the generation of hydrodynamic pressure between conformal contacting surfaces *Tribology Letters* **37** 123-30
[107] Yan D, Qu N, Li H and Wang X 2010 Significance of dimple parameters on the friction of sliding surfaces investigated by orthogonal experiments *Tribology Transactions* **53** 703-12
[108] Costa H and Hutchings I 2007 Hydrodynamic lubrication of textured steel surfaces under reciprocating sliding conditions *Tribology International* **40** 1227-38
[109] Galda L, Pawlus P and Sep J 2009 Dimples shape and distribution effect on characteristics of Stribeck curve *Tribology International* **42** 1505-12
[110] Shen C and Khonsari M 2013 Effect of dimple's internal structure on hydrodynamic lubrication *Tribology Letters* **52** 415-30
[111] Steinhoff K, Rasp W and Pawelski O 1996 Development of deterministic-stochastic surface structures to improve the tribological conditions of sheet forming processes *Journal of Materials Processing Technology* **60** 355-61
[112] Pettersson U and Jacobson S 2003 Influence of surface texture on boundary lubricated sliding contacts *Tribology International* **36** 857-64
[113] Yan J, Zhang Z, Kuriyagawa T and Gonda H 2010 Fabricating micro-structured surface by using single-crystalline diamond endmill *The International Journal of Advanced Manufacturing Technology* **51** 957-64
[114] Ghosh S, Choudhury D, Roy T, Mamat A B, Masjuki H and Pingguan-Murphy B 2015 Tribological investigation of diamond-like carbon coated micro-dimpled surface under bovine serum and osteoarthritis oriented synovial fluid *Science and Technology of Advanced Materials* **16** 035002
[115] Choudhury D, Urban F, Vrbka M, Hartl M and Krupka I 2015 A novel tribological study on DLC-coated micro-dimpled orthopedics implant interface *Journal of the mechanical behavior of biomedical materials* **45** 121-31
[116] Hao L, Meng Y and Chen C 2014 Experimental investigation on effects of surface texturing on lubrication of initial line contacts *Lubrication Science* **26** 363-73
[117] He D, Zheng S, Pu J, Zhang G and Hu L 2015 Improving tribological properties of titanium alloys by combining laser surface texturing and diamond-like carbon film *Tribology International* **82** 20-7
[118] Sawano H, Warisawa S i and Ishihara S 2009 Study on long life of artificial joints by investigating optimal sliding surface geometry for improvement in wear resistance *Precision engineering* **33** 492-8
[119] Meng F 2013 On influence of cavitation in lubricant upon tribological performances of textured surfaces *Optics & Laser Technology* **48** 422-31

[120] Kai M, Tsuboi R and Sasaki S 2013 A Study on In-situ Observation of the Micro Flow of Lubricant on the Textured Surface *Procedia Engineering* **68** 12-8
[121] Ching H A, Choudhury D, Nine M J and Osman N A A 2014 Effects of surface coating on reducing friction and wear of orthopaedic implants *Science and Technology of Advanced Materials* **15** 014402
[122] Nandakumar N 2018 Experimental Investigation on mechanical properties of Al6061 Hybrid Metal Matrix Composite Reinforced with Silicon Carbide and Graphite
[123] Antunes R A and De Oliveira M C L 2009 Corrosion processes of physical vapor deposition-coated metallic implants *Critical Reviews™ in Biomedical Engineering* **37**
[124] Shao T, Ge F, Dong Y, Li K, Li P, Sun D and Huang F 2018 Microstructural effect on the tribo-corrosion behaviors of magnetron sputtered CrSiN coatings *Wear* **416** 44-53
[125] Rieker C and Kottig P 2008 In vivo tribological performance of 231 metal-on-metal hip articulations *Hip International* **12** 73-6
[126] Balagna C, Faga M and Spriano S 2012 Tantalum-based multilayer coating on cobalt alloys in total hip and knee replacement *Materials Science and Engineering: C* **32** 887-95
[127] Spriano S, Vernè E, Faga M, Bugliosi S and Maina G 2005 Surface treatment on an implant cobalt alloy for high biocompatibility and wear resistance *Wear* **259** 919-25
[128] Ghosh S, Choudhury D and Pingguan-Murphy B 2016 Lubricating ability of albumin and globulin on artificial joint implants: a tribological perspective *International Journal of Surface Science and Engineering* **10** 193-206
[129] Wang Q, Zhou F, Wang C, Yuen M-F, Wang M, Qian T, Matsumoto M and Yan J 2015 Comparison of tribological and electrochemical properties of TiN, CrN, TiAlN and aC: H coatings in simulated body fluid *Materials Chemistry and Physics* **158** 74-81
[130] Love C, Cook R B, Harvey T, Dearnley P and Wood R 2013 Diamond like carbon coatings for potential application in biological implants—a review *Tribology International* **63** 141-50
[131] Choudhury D, Roy T and Krupka I 2015 *Processing Techniques and Tribological Behavior of Composite Materials*: IGI Global) pp 193-217
[132] Chang N, Bellare A, Cohen R and Spector M 2000 Wear behavior of bulk oriented and fiber reinforced UHMWPE *Wear* **241** 109-17
[133] Roy T, Choudhury D, Mamat A B and Pingguan-Murphy B 2014 Fabrication and characterization of micro-dimple array on Al 2 O 3 surfaces by using a micro-tooling *Ceramics International* **40** 2381-8
[134] Hauert R, Falub C, Thorwarth G, Thorwarth K, Affolter C, Stiefel M, Podleska L and Taeger G 2012 Retrospective lifetime estimation of failed and explanted diamond-like carbon coated hip joint balls *Acta biomaterialia* **8** 3170-6
[135] Carré A and Lacarrière V 2010 How substrate properties control cell adhesion. A physical–chemical approach *Journal of Adhesion Science and Technology* **24** 815-30
[136] Goddard J M and Hotchkiss J 2007 Polymer surface modification for the attachment of bioactive compounds *Progress in polymer science* **32** 698-725
[137] Bryant S J, Davis-Arehart K A, Luo N, Shoemaker R K, Arthur J A and Anseth K S 2004 Synthesis and characterization of photopolymerized multifunctional hydrogels: water-soluble poly (vinyl alcohol) and chondroitin sulfate macromers for chondrocyte encapsulation *Macromolecules* **37** 6726-33
[138] Wright V and Dowson D 1976 Lubrication and cartilage *Journal of Anatomy* **121** 107
[139] Kobayashi M, Ishihara K and Takahara A 2014 Neutron reflectivity study of the swollen structure of polyzwitterion and polyeletrolyte brushes in aqueous solution *Journal of Biomaterials Science, Polymer Edition* **25** 1673-86
[140] Chen M, Briscoe W H, Armes S P and Klein J 2009 Lubrication at physiological pressures by polyzwitterionic brushes *science* **323** 1698-701
[141] Edmondson S, Osborne V L and Huck W T 2004 Polymer brushes via surface-initiated polymerizations *Chemical society reviews* **33** 14-22
[142] Kyomoto M, Moro T, Takatori Y, Tanaka S and Ishihara K 2015 Multidirectional Wear and Impact-to-wear Tests of Phospholipid-polymer-grafted and Vitamin E-blended Crosslinked Polyethylene: A Pilot Study *Clinical Orthopaedics and Related Research®* **473** 942-51
[143] Moro T, Takatori Y, Kyomoto M, Ishihara K, Kawaguchi H, Hashimoto M, Tanaka T, Oshima H and Tanaka S 2015 Wear resistance of the biocompatible phospholipid polymer-grafted highly cross-linked polyethylene liner against larger femoral head *Journal of Orthopaedic Research*
[144] Yamane S, Kyomoto M, Moro T, Watanabe K, Hashimoto M, Takatori Y, Tanaka S and Ishihara K 2015 Effects of extra irradiation on surface and bulk properties of PMPC-grafted cross-linked polyethylene *Journal of Biomedical Materials Research Part A*

[145] Crockett R, Roba M, Naka M, Gasser B, Delfosse D, Frauchiger V and Spencer N D 2009 Friction, lubrication, and polymer transfer between UHMWPE and CoCrMo hip-implant materials: A fluorescence microscopy study *Journal of Biomedical Materials Research Part A* **89** 1011-8
[146] Kobayashi M and Takahara A 2010 Tribological properties of hydrophilic polymer brushes under wet conditions *The Chemical Record* **10** 208-16
[147] Affatato S, Goldoni M, Testoni M and Toni A 2001 Mixed oxides prosthetic ceramic ball heads. Part 3: effect of the ZrO 2 fraction on the wear of ceramic on ceramic hip joint prostheses. A long-term in vitro wear study *Biomaterials* **22** 717-23
[148] Sing S L 2019 *Selective laser melting of novel titanium-tantalum alloy as orthopaedic biomaterial*: Springer)
[149] Sing S L 2019 *Selective Laser Melting of Novel Titanium-Tantalum Alloy as Orthopaedic Biomaterial*: Springer) pp 9-36
[150] Mayer J, Borges P V and Simske S J 2018 *Fundamentals and Applications of Hardcopy Communication*: Springer) pp 1-5
[151] Prakash K S, Nancharaih T and Rao V S 2018 Additive Manufacturing Techniques in Manufacturing-An Overview *Materials Today: Proceedings* **5** 3873-82
[152] Habibovic P and de Groot K 2007 Osteoinductive biomaterials—properties and relevance in bone repair *Journal of tissue engineering and regenerative medicine* **1** 25-32
[153] Niendorf T and Brenne F 2013 Steel showing twinning-induced plasticity processed by selective laser melting—An additively manufactured high performance material *Materials Characterization* **85** 57-63
[154] Frazier W E 2014 Metal additive manufacturing: a review *Journal of Materials Engineering and Performance* **23** 1917-28
[155] Eckel Z C, Zhou C, Martin J H, Jacobsen A J, Carter W B and Schaedler T A 2016 Additive manufacturing of polymer-derived ceramics *Science* **351** 58-62
[156] Kumar N, Jain P K, Tandon P and Pandey P M 2018 Additive manufacturing of flexible electrically conductive polymer composites via CNC-assisted fused layer modeling process *Journal of the Brazilian Society of Mechanical Sciences and Engineering* **40** 175
[157] Karandikar P, Watkins M, McCormick A, Givens B, Aghajanian M and Cubed I 2018 Additive Manufacturing (3D Printing) of Ceramics: Microstructure, Properties, and Product Examples. In: *Proceedings of the 41st International Conference on Advanced Ceramics and Composites*: John Wiley & Sons) p 175
[158] Pattanayak D K, Fukuda A, Matsushita T, Takemoto M, Fujibayashi S, Sasaki K, Nishida N, Nakamura T and Kokubo T 2011 Bioactive Ti metal analogous to human cancellous bone: fabrication by selective laser melting and chemical treatments *Acta Biomaterialia* **7** 1398-406
[159] Trevisan F, Calignano F, Aversa A, Marchese G, Lombardi M, Biamino S, Ugues D and Manfredi D 2018 Additive manufacturing of titanium alloys in the biomedical field: Processes, properties and applications *Journal of applied biomaterials & functional materials* **16** 57-67
[160] Ghosh S, Abanteriba S, Wong S and Houshyar S 2018 Selective laser melted titanium alloys for hip implant applications: surface modification with new method of polymer grafting *Journal of the Mechanical Behavior of Biomedical Materials*
[161] Castellani C, Lindtner R A, Hausbrandt P, Tschegg E, Stanzl-Tschegg S E, Zanoni G, Beck S and Weinberg A-M 2011 Bone–implant interface strength and osseointegration: Biodegradable magnesium alloy versus standard titanium control *Acta biomaterialia* **7** 432-40
[162] Pongnarisorn N J, Gemmell E, Tan A E, Henry P J, Marshall R I and Seymour G J 2007 Inflammation associated with implants with different surface types *Clinical oral implants research* **18** 114-25
[163] Vaithilingam J, Prina E, Goodridge R D, Hague R J, Edmondson S, Rose F R and Christie S D 2016 Surface chemistry of Ti6Al4V components fabricated using selective laser melting for biomedical applications *Materials Science and Engineering: C* **67** 294-303
[164] Thomas-Seale L E J, Kirkman-Brown J C, Attallah M M, Espino D M and Shepherd D E T 2018 The barriers to the progression of additive manufacture: Perspectives from UK industry *International Journal of Production Economics* **198** 104-18
[165] Lhuissier P, de Formanoir C, Martin G, Dendievel R and Godet S 2016 Geometrical control of lattice structures produced by EBM through chemical etching: Investigations at the scale of individual struts *Materials & Design* **110** 485-93
[166] Bagehorn S, Wehr J and Maier H J 2017 Application of mechanical surface finishing processes for roughness reduction and fatigue improvement of additively manufactured Ti-6Al-4V parts *International Journal of Fatigue* **102** 135-42
[167] Longhitano G A, Larosa M A, Munhoz A L J, Zavaglia C A d C and Ierardi M C F 2015 Surface finishes for Ti-6Al-4V alloy produced by direct metal laser sintering *Materials Research* **18** 838-42

[168] Mohammad A, Mohammed M K and Alahmari A M 2016 Effect of laser ablation parameters on surface improvement of electron beam melted parts *The International Journal of Advanced Manufacturing Technology* **87** 1033-44
[169] Wang D, Wang Y, Wang J, Song C, Yang Y, Zhang Z, Lin H, Zhen Y and Liao S 2016 Design and fabrication of a precision template for spine surgery using selective laser melting (SLM) *Materials* **9** 608
[170] Bagehorn S, Wehr J and Maier H 2017 Application of mechanical surface finishing processes for roughness reduction and fatigue improvement of additively manufactured Ti-6Al-4V parts *International Journal of Fatigue* **102** 135-42
[171] Wangsgard W and Winters M 2018 Validation of a sterilization dose for products manufactured using a 3D printer *Radiation Physics and Chemistry* **143** 38-40
[172] Murr L, Quinones S, Gaytan S, Lopez M, Rodela A, Martinez E, Hernandez D, Martinez E, Medina F and Wicker R 2009 Microstructure and mechanical behavior of Ti–6Al–4V produced by rapid-layer manufacturing, for biomedical applications *Journal of the mechanical behavior of biomedical materials* **2** 20-32
[173] Kyomoto M, Moro T, Miyaji F, Hashimoto M, Kawaguchi H, Takatori Y, Nakamura K and Ishihara K 2009 Effects of mobility/immobility of surface modification by 2-methacryloyloxyethyl phosphorylcholine polymer on the durability of polyethylene for artificial joints *Journal of Biomedical Materials Research Part A* **90** 362-71
[174] Kyomoto M, Moro T, Takatori Y, Kawaguchi H, Nakamura K and Ishihara K 2010 Self-initiated surface grafting with poly(2-methacryloyloxyethyl phosphorylcholine) on poly(ether-ether-ketone) *Biomaterials* **31** 1017-24
[175] Moro T, Takatori Y, Ishihara K, Konno T, Takigawa Y, Matsushita T, Chung U-i, Nakamura K and Kawaguchi H 2004 Surface grafting of artificial joints with a biocompatible polymer for preventing periprosthetic osteolysis *Nature Materials* **3** 829
[176] Ghosh S, Abanteriba S, Wong S and Houshyar S 2018 Selective laser melted titanium alloys for hip implant applications: Surface modification with new method of polymer grafting *Journal of the Mechanical Behavior of Biomedical Materials* **87** 312-24
[177] Good R J and Koo M 1979 The effect of drop size on contact angle *Journal of Colloid and Interface Science* **71** 283-92
[178] Chen S, Zheng J, Li L and Jiang S 2005 Strong resistance of phosphorylcholine self-assembled monolayers to protein adsorption: insights into nonfouling properties of zwitterionic materials *Journal of the American Chemical Society* **127** 14473-8
[179] Yamane-Ohnuki N, Kinoshita S, Inoue-Urakubo M, Kusunoki M, Iida S, Nakano R, Wakitani M, Niwa R, Sakurada M and Uchida K 2004 Establishment of FUT8 knockout Chinese hamster ovary cells: An ideal host cell line for producing completely defucosylated antibodies with enhanced antibody-dependent cellular cytotoxicity *Biotechnology and bioengineering* **87** 614-22
[180] Han S and Rhee W J 2018 Inhibition of Apoptosis Using Exosomes in Chinese Hamster Ovary Cell Culture *Biotechnology and bioengineering*
[181] Lai T, Yang Y and Ng S K 2013 Advances in mammalian cell line development technologies for recombinant protein production *Pharmaceuticals* **6** 579-603
[182] Tiwari A and Natarajan S 2017 *Applied Nanoindentation in Advanced Materials*: John Wiley & Sons)
[183] Oliver W C and Pharr G M 1992 An improved technique for determining hardness and elastic modulus using load and displacement sensing indentation experiments *Journal of materials research* **7** 1564-83
[184] Oliver W C and Pharr G M 2004 Measurement of hardness and elastic modulus by instrumented indentation: Advances in understanding and refinements to methodology *Journal of materials research* **19** 3-20
[185] Fielda J and Swain M 1996 The indentation characterisation of the mechanical properties of various carbon materials: Glassy carbon, coke and pyrolytic graphite *Carbon* **34** 1357-66
[186] Chouirfa H, Migonney V and Falentin-Daudré C 2016 Grafting bioactive polymers onto titanium implants by UV irradiation *RSC Advances* **6** 13766-71
[187] Lin N, Liu Q, Zou J, Li D, Yuan S, Wang Z and Tang B 2017 Surface damage mitigation of Ti6Al4V alloy via thermal oxidation for oil and gas exploitation application: characterization of the microstructure and evaluation of the surface performance *RSC Advances* **7** 13517-35
[188] Znad H, Ang M H and Tade M O 2012 Ta/TiO2-and Nb/TiO2-mixed oxides as efficient solar photocatalysts: preparation, characterization, and photocatalytic activity *International Journal of Photoenergy* **2012**
[189] Nie L, Meng A, Yu J and Jaroniec M 2013 Hierarchically macro-mesoporous Pt/γ-Al 2 O 3 composite microspheres for efficient formaldehyde oxidation at room temperature *Scientific reports* **3** 3215

[190] Xu J, Yuan Y, Shan B, Shen J and Lin S 2003 Ozone-induced grafting phosphorylcholine polymer onto silicone film grafting 2-methacryloyloxyethyl phosphorylcholine onto silicone film to improve hemocompatibility *Colloids and Surfaces B: Biointerfaces* **30** 215-23
[191] Iwasaki Y, Sawada S-i, Ishihara K, Khang G and Lee H B 2002 Reduction of surface-induced inflammatory reaction on PLGA/MPC polymer blend *Biomaterials* **23** 3897-903
[192] Wei F, John B and Shiping Z 2004 Atom-transfer radical grafting polymerization of 2-methacryloyloxyethyl phosphorylcholine from silicon wafer surfaces *Journal of Polymer Science Part A: Polymer Chemistry* **42** 2931-42
[193] Ask M, Lausmaa J and Kasemo B 1989 Preparation and surface spectroscopic characterization of oxide films on Ti6Al4V *Applied surface science* **35** 283-301
[194] Konno T, Kurita K, Iwasaki Y, Nakabayashi N and Ishihara K 2001 Preparation of nanoparticles composed with bioinspired 2-methacryloyloxyethyl phosphorylcholine polymer *Biomaterials* **22** 1883-9
[195] Iwasaki Y, Kurita K, Ishihara K and Nakabayashi N 1997 Effect of reduced protein adsorption on platelet adhesion at the phospholipid polymer surfaces *Journal of Biomaterials Science, Polymer Edition* **8** 151-63
[196] Letchmanan K, Shen S-C, Ng W K, Kingshuk P, Shi Z, Wang W and Tan R B 2017 Mechanical properties and antibiotic release characteristics of poly (methyl methacrylate)-based bone cement formulated with mesoporous silica nanoparticles *Journal of the Mechanical Behavior of Biomedical Materials* **72** 163-70
[197] Ghosh S, Choudhury D, Roy T, Moradi A, Masjuki H H and Pingguan-Murphy B 2015 Tribological performance of the biological components of synovial fluid in artificial joint implants *Science and Technology of Advanced Materials* **16** 045002
[198] Ishihara K, Nomura H, Mihara T, Kurita K, Iwasaki Y and Nakabayashi N 1998 Why do phospholipid polymers reduce protein adsorption? *Journal of biomedical materials research* **39** 323-30
[199] Norde W and Lyklema J 1989 Protein adsorption and bacterial adhesion to solid surfaces: a colloid-chemical approach *Colloids and surfaces* **38** 1-13
[200] Wang M S, Palmer L B, Schwartz J D and Razatos A 2004 Evaluating protein attraction and adhesion to biomaterials with the atomic force microscope *Langmuir* **20** 7753-9
[201] NORDE W 2003 Driving forces for protein adsorption at solid surfaces *Surfactant science series* **110** 21-43
[202] Ghosh S, Abanteriba S, Wong S, Brkljača R and Houshyar S 2019 Optimisation of grafted phosphorylcholine-based polymer on additively manufactured titanium substrate for hip arthroplasty *Materials Science and Engineering: C* **101** 696-706
[203] Camerano J A, Sämann C, Wadepohl H and Gade L H 2011 Bis (pyridylimino) isoindolato− Iridium Complexes as Epoxidation Catalysts for Alkenes *Organometallics* **30** 379-82
[204] Alberts A, Chen J, Kuron G, Hunt V, Huff J, Hoffman C, Rothrock J, Lopez M, Joshua H and Harris E 1980 Mevinolin: a highly potent competitive inhibitor of hydroxymethylglutaryl-coenzyme A reductase and a cholesterol-lowering agent *Proceedings of the National Academy of Sciences* **77** 3957-61
[205] Sobolčiak P, Popelka A, Mičušík M, Sláviková M, Krupa I, Mosnáček J, Tkáč J, Lacík I and Kasák P 2017 Photoimmobilization of zwitterionic polymers on surfaces to reduce cell adhesion *Journal of colloid and interface science* **500** 294-303
[206] Vilardell A, Cinca N, Garcia-Giralt N, Dosta S, Cano I, Nogués X and Guilemany J 2018 Osteoblastic cell response on high-rough titanium coatings by cold spray *Journal of Materials Science: Materials in Medicine* **29** 19
[207] Oh S, Daraio C, Chen L H, Pisanic T R, Finones R R and Jin S 2006 Significantly accelerated osteoblast cell growth on aligned TiO2 nanotubes *Journal of Biomedical Materials Research Part A* **78** 97-103
[208] Xiang Y, Liu X, Mao C, Liu X, Cui Z, Yang X, Yeung K W K, Zheng Y and Wu S 2018 Infection-prevention on Ti implants by controlled drug release from folic acid/ZnO quantum dots sealed titania nanotubes *Materials Science and Engineering: C* **85** 214-24
[209] Ladd J, Zhang Z, Chen S, Hower J C and Jiang S 2008 Zwitterionic polymers exhibiting high resistance to nonspecific protein adsorption from human serum and plasma *Biomacromolecules* **9** 1357-61
[210] Schlenoff J B 2014 Zwitteration: coating surfaces with zwitterionic functionality to reduce nonspecific adsorption *Langmuir* **30** 9625-36
[211] Ishihara K, Mu M, Konno T, Inoue Y and Fukazawa K 2017 The unique hydration state of poly (2-methacryloyloxyethyl phosphorylcholine) *Journal of Biomaterials Science, Polymer Edition* **28** 884-99
[212] Deligianni D D, Katsala N, Ladas S, Sotiropoulou D, Amedee J and Missirlis Y 2001 Effect of surface roughness of the titanium alloy Ti–6Al–4V on human bone marrow cell response and on protein adsorption *Biomaterials* **22** 1241-51

[213] Boga J C, Miguel S P, de Melo-Diogo D, Mendonça A G, Louro R O and Correia I J 2018 In vitro characterization of 3D printed scaffolds aimed at bone tissue regeneration *Colloids and Surfaces B: Biointerfaces* **165** 207-18
[214] Rechendorff K, Hovgaard M B, Foss M, Zhdanov V P and Besenbacher F 2006 Enhancement of Protein Adsorption Induced by Surface Roughness *Langmuir* **22** 10885-8
[215] Deligianni D D, Katsala N D, Koutsoukos P G and Missirlis Y F 2000 Effect of surface roughness of hydroxyapatite on human bone marrow cell adhesion, proliferation, differentiation and detachment strength *Biomaterials* **22** 87-96
[216] Yuan B, Chen Q, Ding W-Q, Liu P-S, Wu S-S, Lin S-C, Shen J and Gai Y 2012 Copolymer coatings consisting of 2-methacryloyloxyethyl phosphorylcholine and 3-methacryloxypropyl trimethoxysilane via ATRP to improve cellulose biocompatibility *ACS applied materials & interfaces* **4** 4031-9
[217] Wen Y, Zhang Z and Li J 2014 Highly Efficient Multifunctional Supramolecular Gene Carrier System Self-Assembled from Redox-Sensitive and Zwitterionic Polymer Blocks *Advanced Functional Materials* **24** 3874-84
[218] Sibarani J, Takai M and Ishihara K 2007 Surface modification on microfluidic devices with 2-methacryloyloxyethyl phosphorylcholine polymers for reducing unfavorable protein adsorption *Colloids and Surfaces B: Biointerfaces* **54** 88-93
[219] Ishihara K and Iwasaki Y 1998 Reduced protein adsorption on novel phospholipid polymers *Journal of biomaterials applications* **13** 111-27
[220] Ghosh S A, Sylvester; Wong, Sherman; Houshyar, Shadi 2018 Selective laser melted titanium alloys for hip implant applications: surface modification with new method of polymer grafting *Journal of the Mechanical Behaviour of Biomedical Materials*
[221] Huang J and Matyjaszewski K 2005 Atom transfer radical polymerization of dimethyl (1-ethoxycarbonyl) vinyl phosphate and corresponding block copolymers *Macromolecules* **38** 3577-83
[222] Pan L, Li G, Su Y and Lian J 2012 Fire retardant mechanism analysis between ammonium polyphosphate and triphenyl phosphate in unsaturated polyester resin *Polymer degradation and stability* **97** 1801-6
[223] Vyazovkin S, Dranca I, Fan X and Advincula R 2004 Kinetics of the thermal and thermo-oxidative degradation of a polystyrene–clay nanocomposite *Macromolecular rapid communications* **25** 498-503
[224] Kim M, Ko H and Park S-M 2019 Synergistic effects of amine-modified ammonium polyphosphate on curing behaviors and flame retardation properties of epoxy composites *Composites Part B: Engineering*
[225] Ishihara K, Nomura H, Mihara T, Kurita K, Iwasaki Y and Nakabayashi N 1998 Why do phospholipid polymers reduce protein adsorption? *Journal of Biomedical Materials Research: An Official Journal of The Society for Biomaterials, The Japanese Society for Biomaterials, and the Australian Society for Biomaterials* **39** 323-30
[226] Morisaku T, Watanabe J, Konno T, Takai M and Ishihara K 2008 Hydration of phosphorylcholine groups attached to highly swollen polymer hydrogels studied by thermal analysis *Polymer* **49** 4652-7
[227] Ishihara K, Iwasaki Y, Ebihara S, Shindo Y and Nakabayashi N 2000 Photoinduced graft polymerization of 2-methacryloyloxyethyl phosphorylcholine on polyethylene membrane surface for obtaining blood cell adhesion resistance *Colloids and Surfaces B: biointerfaces* **18** 325-35
[228] Madsen J, Armes S P and Lewis A L 2006 Preparation and aqueous solution properties of new thermoresponsive biocompatible ABA triblock copolymer gelators *Macromolecules* **39** 7455-7
[229] Gates C, Perfect E, Lokitz B, Brabazon J, McKay L and Tyner J 2018 TRANSIENT ANALYSIS OF ADVANCING CONTACT ANGLE MEASUREMENTS ON POLISHED ROCK SURFACES *Advances in Water Resources*
[230] Zhang X, Zhang G, Li J, He X, Wang Y, Hang R, Huang X, Tang B and Chu P K 2018 Cellular response to nano-structured Zr and ZrO2 alloyed layers on Ti-6Al-4V *Materials Science and Engineering: C* **90** 523-30
[231] Marković G, Marinović-Cincović M, Jovanović V, Samaržija-Jovanović S and Budinski-Simendić J Polymer characterization (II)
[232] Giammanco I M, Brown T M, Grant R G, Dewey D L, Hodel J D and Stumpf R A 2015 Evaluating the hardness characteristics of hail through compressive strength measurements *Journal of Atmospheric and Oceanic Technology* **32** 2100-13
[233] Bartlett R 2002 *Sports biomechanics: reducing injury and improving performance*: Routledge)
[234] Wang X, Gong X and Chou K 2015 Scanning Speed Effect on Mechanical Properties of Ti-6Al-4V Alloy Processed by Electron Beam Additive Manufacturing *Procedia Manufacturing* **1** 287-95
[235] Kaner R B, Gilman J J and Tolbert S H 2005 Designing superhard materials *Science* **308** 1268-9
[236] Ilie N, Hilton T, Heintze S, Hickel R, Watts D, Silikas N, Stansbury J, Cadenaro M and Ferracane J 2017 Academy of dental materials guidance—Resin composites: Part I—Mechanical properties *Dental materials* **33** 880-94

[237] Fischer-Cripps A C 2011 *Nanoindentation*: Springer) pp 21-37
[238] Huiskes R, Weinans H and Van Rietbergen B 1992 The relationship between stress shielding and bone resorption around total hip stems and the effects of flexible materials *Clinical orthopaedics and related research* 124-34
[239] Niinomi M and Nakai M 2011 Titanium-based biomaterials for preventing stress shielding between implant devices and bone *International journal of biomaterials* **2011**
[240] Ridzwan M, Shuib S, Hassan A, Shokri A and Ibrahim M M 2007 Problem of stress shielding and improvement to the hip implant designs: a review *J. Med. Sci* **7** 460-7
[241] Terzopoulos D and Fleischer K 1988 Modeling inelastic deformation: viscolelasticity, plasticity, fracture. In: *ACM Siggraph Computer Graphics*: ACM) pp 269-78
[242] Wainwright S A, Biggs W and Currey J D 1982 *Mechanical design in organisms*: Princeton University Press)
[243] Evans A and Hutchinson J 1984 On the mechanics of delamination and spalling in compressed films *International Journal of Solids and Structures* **20** 455-66
[244] Bull S 1997 Failure mode maps in the thin film scratch adhesion test *Tribology international* **30** 491-8
[245] Moharrami N, Langton D, Sayginer O and Bull S 2013 Why does titanium alloy wear cobalt chrome alloy despite lower bulk hardness: A nanoindentation study? *Thin Solid Films* **549** 79-86
[246] Nasab M B, Hassan M R and Sahari B B 2010 Metallic biomaterials of knee and hip-a review *Trends Biomater. Artif. Organs* **24** 69-82
[247] Jahn S and Klein J 2015 Hydration lubrication: the macromolecular domain *Macromolecules* **48** 5059-75
[248] Little N J, Busch C A, Gallagher J A, Rorabeck C H and Bourne R B 2009 Acetabular polyethylene wear and acetabular inclination and femoral offset *Clinical Orthopaedics and Related Research®* **467** 2895
[249] Langton D, Jameson S, Joyce T, Webb J and Nargol A 2008 The effect of component size and orientation on the concentrations of metal ions after resurfacing arthroplasty of the hip *The Journal of bone and joint surgery. British volume* **90** 1143-51
[250] Hamrock B J and Dowson D 1978 Elastohydrodynamic lubrication of elliptical contacts for materials of low elastic modulus I—fully flooded conjunction *Journal of Tribology* **100** 236-45
[251] Wang D 1994 Elastohydrodynamic lubrication of point contacts for layers of soft solids and for 'monolithic'hard materials in the transient bouncing ball problem. Ph. D. thesis, University of Leeds)
[252] Stachowiak G and Batchelor A W 2013 *Engineering tribology*: Butterworth-Heinemann)
[253] Stachowiak G and Batchelor A W 2004 *Experimental methods in tribology* vol 44: Elsevier)
[254] Vrbka M, Návrat T, Křupka I, Hartl M, Šperka P and Gallo J 2013 Study of film formation in bovine serum lubricated contacts under rolling/sliding conditions *Proceedings of the Institution of Mechanical Engineers, Part J: Journal of Engineering Tribology* **227** 459-75
[255] Vrbka M, Křupka I, Hartl M, Návrat T, Gallo J and Galandáková A 2014 In situ measurements of thin films in bovine serum lubricated contacts using optical interferometry *Proceedings of the Institution of Mechanical Engineers, Part H: Journal of Engineering in Medicine* **228** 149-58
[256] Harper P, Dwyer-Joyce R, Sjödin U and Olofsson U 2005 *Tribology and Interface Engineering Series*: Elsevier) pp 305-12

APPENDICES

Appendix A. Summary of tribological studies on surface texturing.

Type of simulator	Type of material	Specimens	Operating conditions	Texturing technique	Coating properties	Friction coefficient	Wear rate for different counter surface
Ball-on-disk tribometer [1]	Ti–6Al–4V alloy	Friction test: Disk diameter: 60 mm and thickness 5 mm Ball diameter: 11mm Average roughness, Ra : 0.10 µm	Applied load: 20, 40, 60, 80 and 100 N Rotational speed: 100 rpm Sliding distance: 100 m Lubricant: Tonna oil 32	CNC machining		Ground surface: 0.05-0.09 UNSM-treated surface:0.035-0.065	Ground surface: 0.004-0.012× 10^{-7} mm^3/Nm Textured surface: 0.0015-0.007× 10^{-7} mm^3/Nm
Ball-on-disk tribometer [2]	Cylinder: Co–Cr–Mo Liner: UHMWPE	Cylinder diameter: 50 mm Average roughness, Ra < 50 nm. Liner diameter : 50.75mm	Contact pressure: 0.57–1.13MPa Sliding frequency: 1 Hz Lubricant: BS	LST		Smooth cylinder: 0.30 Textured cylinder: 0.15	
Hip simulator. Ball-on-disk tribometer [3]	Cup: ceramic Head: Co–Cr–Mo and SS	SS head diameter: 25 mm CrCo head diameter: 28 mm Average roughness, Ra: 20–100 nm	Load: 1750KN Starting inclined angle: 16° Sliding frequency: 0.5Hz Lubricant: BS	EDM	PVD process Coating thickness : 1 µm	Non-dimpled a-C:H: 0.084 Dimpled a-C:H: 0.107 Dimpled Ta-C: 0.119 Dimpled Ta-C: 0.121 Non-dimpled Co–Cr–Mo: 0.248	

Pendulum hip joint simulator [4]	Wear test: Cup: UHMWPE Head: Co–Cr–Mo	Wear test: Cylinder diameter: 28 mm Average roughness, Ra: 10 nm. Liner diameter: 28 mm Friction test: Pin: 3 x 3 mm^2	Wear test: Load: 50 N Lubricant: BS Frequency: 0.49 Hz Friction test: Contact pressure: 2.2MPa Sliding distance : 3 mm Frequency:1.12Hz	Vibroroll ing	Plasma carburising treatment	Untreated surface: 0.19 Plasma carburized surface: 0.20-0.21 Untreated textured suface: 0.19 Plasma carburized textured surface: 0.15	
Pin-on-disk tribometer [5]	Pin: ceramic Disk: ceramic	Pin dimension: Ø6.35 mm x L6 mm Disk dimension: 15 x 15 x 6 mm^3 Average roughness, Ra: 0.12±0.02 µm Dimple diameter: 300, 400 µm	Load: 10, 15, 20 N Frequency: 5, 10, 15 and 20 Hz Lubricant: BS	CNC machining		Plain surface: 0.135-0.15 Dimpled surface: 0.1-0.14	Weight loss: Plain surface: 0.77 mg Dimpled surface: 0.36-0.65 mg
Pin-on-disk tribometer [6]	Ti–6Al–4V alloy	Pin dimension: Ø6.35 mm x L6 mm Disk dimension: 15 x 15 x 6 mm^3 Average roughness, Ra: 50±5 nm	Load: 10, 15, 20 N Frequency: 5 Hz Lubricant: BS, Water	CNC machining	PVD	Plane surface: 0.18-0.26 Dimpled surface: 0.16-0.24 DLC coated dimpled surface: 0.13-0.18	% of weight loss: Plane surface: 0.008 % Dimpled surface: 0.005% DLC coated dimpled surface: 0.002%
Ball-on-plate tribometer [7]	Ti–6Al–4V alloy	Friction test: Plate dimension: 3 x 2 cm^2 Ball diameter: 10 mm Ra of substrate ≤ 0.03µm. Ra of coated surface ≤ 0.02 µm.	Amplitude: 5 mm Applied load: 5 N (initial Hertzian contact pressure 820 MPa) Sliding frequency: 5 Hz	LST	PVD Coating thickness : 3.3 µm	DLC-smooth : 0.06 DLC-T13% : 0.065 DLC-T24% : 0.065 DLC-T44% : 0.055	DLC-smooth : 4.3×10^{-7} mm^3/Nm DLC-T13% : 3.2×10^{-7} mm^3/Nm DLC-T24% : 2.75×10^{-7} mm^3/Nm DLC-T44% : 4.8×10^{-7} mm^3/Nm

Abbreviations: EDT stands for electrical discharge texturing, PVD for physical vapour deposition, SS for stainless steel, Ta-C for tetrahedral amorphous carbon and UHMWPE for ultrahigh molecular weight polyethylene.

APPENDICES

Appendix B. Summary of tribological studies on surface coating.

Type of Simulator	Type of Material	Specimens	Experimental conditions	Coating Technique	Coating materials	Coating thickness	Friction coefficient	Wear rate
Pin-on-disk tribometer [8]	Disk: SS, TiN , Micronite, DLC Pin:UHMWPE	Pin: 20 mm length, 8mm diameter Disk: 80mm diameter, 4mm thickness	Applied load: 9 MPa Sliding speed: 100 mm/s Temperature: 37±1°C Lubricant:BS	Magnetron sputtering	Micronite- and TiN-coating	3 µm	316L: 0.088 TiN: 0.139 Micronite: 0.140 DLC: 0.254	316L: 1.39 µm/km TiN: 3.11 µm/km Micronite: 4.12 µm/km DLC: 47.80 µm/km
Hip joint simulator [9]	Cup: UHMWPE Head: Co–Cr–Mo	Head diameter: 28 mm	Applied load: maximum 4500N Temperature: 37°C Cup inclination: 23° Lubricant: BS	Filtered cathodic vacuum arc Plasma immersion ion implantation	DLC coated or N^+ ion implanted	600 nm	Untreated head: 0.01 DLC coated head: 0.05 N^+ implanted head: 0.06	
Ball-on-disk tribometer [10]	Ball:100Cr6 steel Disk: PEEK	Ball diameter: 6 mm Disk diameter: 25 mm Thickness: 3mm	Applied load: 3 N Sliding speed: 10 cm/s Temperature: 22±2°C Lubricant: SBF	Magnetron sputtering	Nb containing GLC	1.4 µm	Uncoated PEEK (air): 0.45 Uncoated PEEK (SBF): 0.25 Nb/GLC coated substrate(air):: 0.15 Nb/GLC coated substrate (SBF): 0.07	Uncoated PEEK (air): 0.87-2.25 × 10^{-15} mm^3/Nm Uncoated PEEK (SBF): 0.15-0.5 × 10^{-15} mm^3/Nm Nb/GLC coated substrate (air): 3.13-5.53 × 10^{-15} mm^3/Nm Nb/GLC coated substrate (SBF): 3.38-3.49 × 10^{-15} mm^3/Nm

Ball-on-disk tribometer [11]	Disk: PEEK Ball: Ceramic (ZrO_2)	Disk diameter: 14.4 mm & thickness: 2.5 mm Ball Diameter: 6.4 mm	Applied load: 5N (Hertzian calculated stresses of 117.23 MPa) Sliding speed: 0.05 m/s Sliding distance: 500-1000 m Temperature: 25°C	CVD	DLC coating Plasma activation: MW and RF Applied process gases: O_2, N_2, and CH_4	200 ± 20 nm	Normal PEEK: 0.38 MW/RF-O_2/CH_4: 0.36 *MW/RF-N_2/CH_4: 0.34 RF-O_2/CH_4: 0.31 RF-N_2/CH_4: 0.21	Normal PEEK: 7.26×10^{-7} mm^3/Nm MW/RF: $2–2.25 \times 10^{-7}$ mm^3/Nm RF-0.03: 0.2×10^{-7} mm^3/Nm
Ball-on-disk tribometer [12]	Ball: ceramic Disk: austenitic steel substrates (AISI 304)	Ball diameter: 6 mm	Applied load: 2 N Sliding speed: 10 m/s Sliding distance: 110-157 m Temperature: 25°C	Magnetron sputtering	Cr-CrN multilayer and Cr-CrN multilayer with DLC top coating	3.94-5.16 µm	Cr, Cr-CrN: >0.6 Cr-CrN with DLC: ~0.2	
Hip simulator [13]	Cup: ceramic Head: SS	Cup diameter: 28 mm Head diameter: 25 mm	Applied load: 1760 N Frequency: 0.5 Hz Temperature: 37°C Lubricant: BS	Magnetron sputtering	DLC coating: 1. a-C:H layers and 2. Ta-C layers	> 1 µm	SS:0.248 Ta-C: 0.119 a-C:H: 0.0.084	
Pin/ball on disk [14]	Test 1: DLC/Polyethylene (disk/pin) Test 2: DLC/DLC (disk/ball:ML1) Test 3: DLC/DLC (disk/ball:ML1)		Load: Test1: 80 n, Test 2& 3: 4 N Lubricant: Test1&2: BS plus y-globulin and test 3: water Speed: 20 mm/s Temperature: 37°C	Magnetron sputtering	Cr doped DLC (a-C:H:Cr) N doped DLC (a-C:N)	0.6 µm	GL3 and #GL4: 0.25 ML1 and #GL1: 0.12 ML3: 0.16	SS on UHMWPE: 42.3×10^{-7} mm^3/Nm GL1 on UHMWPE: 36.3×10^{-7} mm^3/Nm ML1 on UHWMPE: 6×10^{-7} mm^3/Nm

wear simulato r machine [15]	Head & cup: silicon nitride (Si_3N_4)ceramic	Cup and head diameter: 27.96 mm and 27.88 mm Clearance: 78 μm	Applied load: Minimum 300N and maximum 3000 N Frequency: 1 Hz Temperature: 37°C	CVD	Nanocrystalline diamond coatings	0 10 μm		0.022 mm^3/Mc
Ball-on-disk tribometer [16]	Disc: cemented carbide (WC) Ball: ceramic (Al_2O_3)	Ball diameter : 8mm Disk dimension: Ø30×4 mm3	Applied load: 2 N Sliding speed: 0.2 m/s Temperature: 37°C Lubricant:SBF	Arc magnetron sputtering	TiN, CrN, TiAlN and a-C:H coatings	TiAlN: 1.89 μm a-C:H: 1.79 μm a-C:H: 0.76 μm CrN: 2.05 μm	CrN: 0.241 TiAlN: 0.222 TiN: 0.139 a-C:H: 0.097	TiAlN: 1.78×10^{-7} mm^3/Nm a-C:H: 1.64×10^{-7} mm^3/Nm TiN: 0.319×10^{-7} mm^3/Nm CrN: 0.088×10^{-7} mm^3/Nm

Abbreviations: TiN stands for titanium nitride, CVD stands for chemical vapour deposition, MW for microwave, PEEK for poly(etheretherketone), RF for radio frequency and SBF for simulated body fluid.

Appendix C. Summary of tribological studies on surface grafting.

Type of Simulator	Type of Material	Specimens	Experimental Conditions	Thickness	Friction coefficient	Wear rate
12-station hip simulator for wear test [17]	Femoral head: Co–Cr–Mo Liner:polymer-grafted CLPE	Wear test: *Head dia: 26 mm Liner inner dia:26 mm Liner outer dia: 52 mm	Wear test: Load: (Paul-type) with double peaks at 1793 and 2744 N with a multidirectional (biaxial and orbital) motion Frequency:1 Hz	100–200 nm		CLPE: -1.42 to 4.64 mg/ 10^6 cycles PMPC-grafted CLPE: -3.74 to 0.48 mg/ 10^6 cycles
Friction test:ball-on-plate machine Hip simulator for wear test [18]	Pin: Co–Cr–Mo Plate:polymer-grafted CLPE Femoral head: Co–Cr–Mo Liner: polymer-grafted CLPE	Friction test: Pin diameter: 9 mm Wear test: Head dia: 26 mm Liner inner dia:26 mm Liner outer dia: 52 mm Lubricant: water Ra=> 0.01 µm	Friction test: Load: 0.98 N Sliding distance: 25 mm Frequency: 1 Hz Temperature: 37ºC Wear test: Load: (Paul-type) with double peaks at 1793 and 2744 N with a multidirectional (biaxial and orbital) motion Frequency:1 Hz.	100-150 nm	CLPE (untreated): 0.07 *PMB30 coated CLPE: 0.06 PMSi90 coated CLPE: 0.05 PMPC-grafted CLPE: 0.01	CLPE (untreated): 6.1 mg/ 10^6 cycles PMB30 coated CLPE: 5.9 mg/ 10^6 cycles PMSi90 coated CLPE: 4.5 mg/ 10^6 cycles PMPC-grafted CLPE : -1.5 mg/ 10^6 cycles
Friction test:ball-on-plate machine Hip simulator for wear test [19]	Pin: Co–Cr–Mo & ceramic Plate: untreated and polymer-grafted PE & CLPE Femoral head: Co–Cr–Mo & ceramic Liner: untreated and polymer-grafted PE & CLPE	Friction test: Pin diameter: 9 mm Wear test: Head dia: 26 mm *liner inner dia:26 mm *liner outer dia: 52 mm *lubricant: water *Ra<0.01 µm *lubricant: water	Friction test: Load: 0.98 N Sliding distance: 25 mm Frequency: 1 Hz Temperature: 37ºC Wear test: Load: (Paul-type) with double peaks at 1793 and 2744 N with a multidirectional (biaxial and orbital) motion Frequency:1 Hz.	100-150 nm	Co–Cr–Mo as head : PE: 0.07 PMPC-grafted PE: 0.015 CLPE: 0.08 PMPC-grafted CLPE: 0.01 Ceramic as head : CLPE: 0.05 *PMPC-grafted CLPE: 0.01	PE: 0-80 mg/ 10^6 cycles PMPC-grafted PE: << 0 CLPE: 0-10 mg/ 10^6 cycles PMPC-grafted CLPE: <<0

Friction test by ball-on-plate machine [20]	Pin-: Co–Cr–Mo Disk: Co–Cr–Mo	Friction test: Pin diameter: 9 mm Ra<0.01 µm	Friction test: Load:0.49 to 0.98 N Sliding distance: 25 mm Frequency: 1 Hz Temperature: 37ºC	PMB3: 50 nm PMSi90:130nm, PMPC-grafting: 200 nm	Co–Cr–Mo surface: 0.15 PMPC-grafted Co–Cr–Mo surface << 0.01	
Friction test:ball-on-plate machine Hip simulator for wear test [21]	Pin: Co–Cr–Mo *plate: polymer-grafted CLPE Femoral head: Co–Cr–Mo Liner:polymer-grafted CLPE	Friction test: Pin diameter: 9 mm Wear test: Head dia: 26 mm Liner inner dia:26 mm Liner outer dia: 52 mm Ra<0.01 µm Lubricant: water	Friction test: Load: 0.98 N Sliding distance: 25 mm Frequency: 1 Hz Temperature: 37ºC Wear test: Load: (Paul-type) with double peaks at 1793 and 2744 N with a multidirectional (biaxial and orbital) motion Frequency:1 Hz.	100-150 nm	Untreated surface : 0.07-0.11 POEGMA-grafted surface: 0.03-0.035 PDMAEMA- grafted surface: 0.04-0.13 PMPA- grafted surface: 0.02-0.15 PMPC- grafted surface: 0.01-0.015	
12-station hip simulator for wear test [22]	Femoral head: Co–Cr–Mo Liner: polymer-grafted CLPE	Wear test: Head diameter:r 26 mm Inner and outer diameters of liner are 26 and 52 mm, respectively	Wear test: Load: (Paul-type) with double peaks at 1793 and 2744 N with a multidirectional (biaxial and orbital) motion Frequency:1 Hz. Inclined angle of +23º.	100-150 nm		CLPE: 0-60 mg/ 10^6 cycles PMPC-grafted CLPE <<0
Friction test: ball-on-disk tribometer [23]	Ball: Al_2O_3 Plate:UHMWPE	Ball diameter: 6 mm Plate diameter: 49 mm Height: 6 mm Ra ≤ 0.2 m Lubricant: distilled and saline water	Friction test:* Load: 2.5 N ~25 MPa Angular speed: 84 rpm Temperature: 37ºC Wear test: Load: (Paul-type) with double peaks at 1793 and 2744 N with a multidirectional (biaxial and orbital) motion Frequency:1 Hz.		No grafting, saline: 0.07-0.06 No grtafting, water: 0.07-0.055 PMPC , saline: 0.045-0.055 PMPC, water: 0.04-0.005	No grafting, saline: 0.45×10^{-7} mm3/Nm No grtafting, water: 0.42×10^{-7} mm3/Nm PMPC grafting, saline: 0.25×10^{-7} mm3/Nm PMPC grtafting, water: 0.24×10^{-7} mm3/Nm

Reciprocating friction tester [24]	Pin: Co–Cr–Mo Plate: polymer-grafted CLPE	Pin geometry: flat-ended diameter: 9 mm Height: 6 mm Pin,Ra:0.04 µm Plate, Ra: 0.05 µm	Reciprocating Friction test: Vertical load-7.84N (mean contact pressure was 2.50MPa) Sliding speed: 10mm/s Total sliding distance: 2 m. Temperature: 37ºC		CLPE-rehydration: 0.12 CLPE without rehydration: 0.15 PMPC- CLPE with rehydration: 0.068 PMPC-CLPE without rehydration: 0.07	
Friction test:ball-on-plate machine Wear test: POD machine [25]	Disk: Titanium alloy Pins: Co–Cr–Mo with 30 mm surface curvature	Friction test: Pin diameter: 9 mm Wear test: Surface curvature radius of Co–Cr–Mo: 30 mm Ra<0.01 µm	Friction test: Load: 0.98 N Sliding distance: 25 mm Frequency: 1 Hz Temperature: 37ºC Wear test: Static load: 213 N Sliding distance: 30 mm Frequency: 1Hz.			Untreated CLPE without vitamin E blending: 0.22 mg/ 10^6 cycles PMPC-grafted CLPE without vitamin E blending: 0.05 mg/ 10^6 cycles Untreated CLPE with vitamin E blending: 0.1 mg/ 10^6 cycles PMPC-grafted CLPE with vitamin E blending <<0
Friction test:ball-on-plate machine Hip simulator for wear test [26]	Pin: Co–Cr–Mo Plate-polymer-grafted CLPE Femoral head: Co–Cr–Mo Liner: polymer-grafted CLPE	Friction test: Pin diameter: 9 mm Wear test: Head diameter: 26 mm or 40 mm Liner diameters: 26 mm or 400 mm Liner thickness: 10 mm and 6 mm Lubricant: water	Friction test: Load: 2.5 N ~25 MPa Angular speed: 84 rpm Temperature: 37ºC Wear test: Load: (Paul-type) with double peaks at 1793 and 2744 N with a multidirectional (biaxial and orbital) motion Frequency:1 Hz.	100-150 nm		CLPE 26 mm: 20 mg/ 10^6 cycles CLPE 40 mm: 45 mg/ 10^6 cycles PMPC-CLPE 26 mm <<0 PMPC-CLPE 40 mm <<0

Friction test:ball-on-plate machine Hip simulator for wear test [27]	Pin: Co–Cr–Mo Plate: polymer-grafted CLPE Femoral head: Co–Cr–Mo Liner: polymer-grafted CLPE	Friction test: Pin diameter: 9 mm Wear test: Head diameter: 26 mm Inner and outer diameters of liner are 26 and 52 mm, respectively Ra<0.01 μm Lubricant: water	Friction test: Load: 2.5 N ~25 MPa Angular speed: 84 rpm Temperature: 37ºC Wear test: Load: (Paul-type) with double peaks at 1793 and 2744 N with a multidirectional (biaxial and orbital) motion Frequency:1 Hz.	100-150 nm	CLPE-Gamma-ray irradiation:15 mg/ 10^6 cycles CLPE-Plasma-ray irradiation:15 mg/ 10^6 cycles PMPC-grafted CLPE-Gamma-ray irradiation <<0 PMPC-graftedCLPE-Plasma-ray irradiation<<0

Abbreviations: PDMAEMA stands for poly(2-(N,Ndimethylaminoethyl) methacrylate), POEGMA for poly(oligo(ethylene glycol) monomethacrylate) and PMPA for poly(2-(methacryloylethyl) phosphoric acid).

References:

[1] Amanov A, Cho I, Pyoun Y, Lee C and Park I 2012 Micro-dimpled surface by ultrasonic nanocrystal surface modification and its tribological effects *Wear* **286** 136-44

[2] Chyr A, Qiu M, Speltz J W, Jacobsen R L, Sanders A P and Raeymaekers B 2014 A patterned microtexture to reduce friction and increase longevity of prosthetic hip joints *Wear* **315** 51-7

[3] Choudhury D, Ay Ching H, Mamat A B, Cizek J, Osman A, Azuan N, Vrbka M, Hartl M and Krupka I 2014 Fabrication and characterization of DLC coated microdimples on hip prosthesis heads *Journal of Biomedical Materials Research Part B: Applied Biomaterials*

[4] Dong Y, Svoboda P, Vrbka M, Kostal D, Urban F, Cizek J, Roupcova P, Dong H, Krupka I and Hartl M 2015 Towards near-permanent CoCrMo prosthesis surface by combining micro-texturing and low temperature plasma carburising *Journal of the mechanical behavior of biomedical materials* **55** 215-27

[5] Roy T, Choudhury D, Ghosh S, Mamat A B and Pingguan-Murphy B 2015 Improved friction and wear performance of micro dimpled ceramic-on-ceramic interface for hip joint arthroplasty *Ceramics International* **41** 681-90

[6] Ghosh S, Choudhury D, Roy T, Mamat A B, Masjuki H and Pingguan-Murphy B 2016 Tribological investigation of diamond-like carbon coated micro-dimpled surface under bovine serum and osteoarthritis oriented synovial fluid *Science and Technology of Advanced Materials*

[7] He D, Zheng S, Pu J, Zhang G and Hu L 2015 Improving tribological properties of titanium alloys by combining laser surface texturing and diamond-like carbon film *Tribology International* **82** 20-7

[8] Hoseini M, Jedenmalm A and Boldizar A 2008 Tribological investigation of coatings for artificial joints *Wear* **264** 958-66

[9] Liu H, Leng Y, Tang J, Wang S, Xie D, Sun H and Huang N 2012 Tribological performance of ultra-high-molecular-weight polyethylene sliding against DLC-coated and nitrogen ion implanted CoCrMo alloy measured in a hip joint simulator *Surface and Coatings Technology* **206** 4907-14

[10] Huang W and Wang X 2013 Biomimetic design of elastomer surface pattern for friction control under wet conditions *Bioinspiration & biomimetics* **8** 046001

[11] Kaczorowski W, Szymanski W, Batory D and Niedzielski P 2014 Tribological Properties and Characterization of Diamond Like Carbon Coatings Deposited by MW/RF and RF Plasma-Enhanced CVD Method on Poly (ether-ether-ketone) *Plasma Processes and Polymers* **11** 878-87

[12] Lackner J M, Waldhauser W, Major L and Kot M 2014 Tribology and Micromechanics of Chromium Nitride Based Multilayer Coatings on Soft and Hard Substrates *Coatings* **4** 121-38

[13] Choudhury D, Urban F, Vrbka M, Hartl M and Krupka I 2014 Tribological investigation of DLC coated micro dimpled femoral head on acetabular ceramic cup. In: *2nd International Conference on BioTribology*,

[14] Choudhury D, Urban F, Vrbka M, Hartl M and Krupka I 2015 A novel tribological study on DLC-coated micro-dimpled orthopedics implant interface *Journal of the mechanical behavior of biomedical materials* **45** 121-31

[15] Maru M, Amaral M, Rodrigues S, Santos R, Gouvea C, Archanjo B, Trommer R, Oliveira F, Silva R and Achete C 2015 The High performance of nanocrystalline CVD diamond coated hip joints in wear simulator test *Journal of the mechanical behavior of biomedical materials* **49** 175-85

[16] Wang Q, Zhou F, Wang C, Yuen M-F, Wang M, Qian T, Matsumoto M and Yan J 2015 Comparison of tribological and electrochemical properties of TiN, CrN, TiAlN and aC: H coatings in simulated body fluid *Materials Chemistry and Physics* **158** 74-81

[17] Kyomoto M, Moro T, Konno T, Takadama H, Yamawaki N, Kawaguchi H, Takatori Y, Nakamura K and Ishihara K 2007 Enhanced wear resistance of modified cross-linked polyethylene by grafting with poly (2-methacryloyloxyethyl phosphorylcholine) *Journal of Biomedical Materials Research Part A* **82** 10-7

[18] Kyomoto M, Moro T, Miyaji F, Hashimoto M, Kawaguchi H, Takatori Y, Nakamura K and Ishihara K 2009 Effects of mobility/immobility of surface modification by 2-methacryloyloxyethyl phosphorylcholine polymer on the durability of polyethylene for artificial joints *Journal of Biomedical Materials Research Part A* **90** 362-71

[19] Moro T, Kawaguchi H, Ishihara K, Kyomoto M, Karita T, Ito H, Nakamura K and Takatori Y 2009 Wear resistance of artificial hip joints with poly (2-methacryloyloxyethyl phosphorylcholine) grafted polyethylene: comparisons with the effect of polyethylene cross-linking and ceramic femoral heads *Biomaterials* **30** 2995-3001

[20] Kyomoto M, Moro T, Saiga K-i, Miyaji F, Kawaguchi H, Takatori Y, Nakamura K and Ishihara K 2010 Lubricity and stability of poly (2-methacryloyloxyethyl phosphorylcholine) polymer layer on Co–Cr–Mo surface for hemi-arthroplasty to prevent degeneration of articular cartilage *Biomaterials* **31** 658-68

[21] Kyomoto M, Moro T, Saiga K, Hashimoto M, Ito H, Kawaguchi H, Takatori Y and Ishihara K 2012 Biomimetic hydration lubrication with various polyelectrolyte layers on cross-linked polyethylene orthopedic bearing materials *Biomaterials* **33** 4451-9

[22] Moro T, Takatori Y, Kyomoto M, Ishihara K, Hashimoto M, Ito H, Tanaka T, Oshima H, Tanaka S and Kawaguchi H 2014 Long-term hip simulator testing of the artificial hip joint bearing surface grafted with biocompatible phospholipid polymer *Journal of Orthopaedic Research* **32** 369-76

[23] Xiong D, Deng Y, Wang N and Yang Y 2014 Influence of surface PMPC brushes on tribological and biocompatibility properties of UHMWPE *Applied Surface Science* **298** 56-61

[24] Yarimitsu S, Moro T, Kyomoto M, Watanabe K, Tanaka S, Ishihara K and Murakami T 2015 Influences of dehydration and rehydration on the lubrication properties of

phospholipid polymer-grafted cross-linked polyethylene *Proceedings of the Institution of Mechanical Engineers, Part H: Journal of Engineering in Medicine* 0954411915588969

[25] Kyomoto M, Moro T, Takatori Y, Tanaka S and Ishihara K 2015 Multidirectional Wear and Impact-to-wear Tests of Phospholipid-polymer-grafted and Vitamin E-blended Crosslinked Polyethylene: A Pilot Study *Clinical Orthopaedics and Related Research*® **473** 942-51

[26] Moro T, Takatori Y, Kyomoto M, Ishihara K, Kawaguchi H, Hashimoto M, Tanaka T, Oshima H and Tanaka S 2015 Wear resistance of the biocompatible phospholipid polymer-grafted highly cross-linked polyethylene liner against larger femoral head *Journal of Orthopaedic Research*

[27] Yamane S, Kyomoto M, Moro T, Watanabe K, Hashimoto M, Takatori Y, Tanaka S and Ishihara K 2015 Effects of extra irradiation on surface and bulk properties of PMPC-grafted cross-linked polyethylene *Journal of Biomedical Materials Research Part A*